Universidade do Minho
Escola de Medicina

Cláudia Filipa Cunha Antunes

Role of TET3 enzyme in brain function

Tese de Doutoramento
Doutoramento em Envelhecimento e Doenças Crónicas

Trabalho efetuado sob a orientação de
Doutora Cristina Joana Moreira Marques
Doutora Luísa Alexandra Meireles Pinto
Doutora Rita Oliveira Teodoro

Julho de 2020

DIREITOS DE AUTOR E CONDIÇÕES DE UTILIZAÇÃO DO TRABALHO POR TERCEIROS

Este é um trabalho académico que pode ser utilizado por terceiros desde que respeitadas as regras e boas práticas internacionalmente aceites, no que concerne aos direitos de autor e direitos conexos.

Assim, o presente trabalho pode ser utilizado nos termos previstos na licença abaixo indicada.

Caso o utilizador necessite de permissão para poder fazer um uso do trabalho em condições não previstas no licenciamento indicado, deverá contactar o autor, através do RepositóriUM da Universidade do Minho.

Licença concedida aos utilizadores deste trabalho

Atribuição 4.0
CC BY

https://creativecommons.org/licenses/by/4.0/

Agradecimentos/Acknowledgements

Ao Programa Doutoral Inter-Universitário em Envelhecimento e Doenças Crónicas (PhD OC), em nome da Professora Catarina Resende, Professora Margarida Correia Neves, Professor Duarte Barral e Professor Henrique Girão.

Ao Instituto de Ciências da Vida e da Saúde (ICVS/3B's), em nome do Professor Jorge Correia Pinto, à Escola de Medicina em nome do Professor Nuno Sousa e ao Domínio das Neurociências (NeRD), em nome do Professor João Bessa. A todos os NeRD.

Às minhas orientadoras: Doutora Joana Marques, Doutora Luísa Pinto e Doutora Rita Teodoro.

Aos colegas do programa doutoral, Ana Soares, Anna Pliassova, Carlos Portugal Nunes, Cláudia Pereira, Deolinda Santinha, Joana Gaifém, Rita Silva, Susana Ponte e Tânia Marques. Aos colegas dos grupos onde trabalhei em Braga, Coimbra e Lisboa: Mafalda, Marta, Fábio, Eduardo, Dinis, Patrícia, António, Tiago, Bruna, Joana, Ricardo, Vanessa, João.

Ao Jorge, Francisca, Sónia, Luísa, Vanessa, Dulce, Rita, Cristina e Marina.

À Susana, Francisca, Marta, Silvia e Zé.

Aos meus pais e irmã.

The work presented in this thesis was funded by:

The author was financial supported by the Portuguese Foundation for Science and Technology (FCT) with a fellowship granted to Cláudia Antunes (PD/BD/106049/2015) via Inter-University Doctoral Programme in Ageing and Chronic Diseases – PhDOC.

This work was supported by FCT project grant (PTDC/BIA-BCM/121276/2010), by EpiGeneSys Small Collaborative project, by BIAL Foundation Grant 427/14, by FEDER funds through the Operational Programme Competitiveness Factors - COMPETE and National Funds through FCT under the project POCI-01-0145-FEDER-007038; and by the project NORTE-01-0145-FEDER-000013, supported by Norte Portugal Regional Operational Programme (NORTE 2020), under the PORTUGAL 2020 Partnership Agreement, through the European Regional Development Fund (ERDF).

Statement of integrity

I hereby declare having conducted my thesis with integrity. I confirm that I have not used plagiarism or any form of undue use of information or falsification of results in the process leading to its elaboration.
I further declare that I have fully acknowledged the Code of Ethical Conduct of the University of Minho.

O papel da enzima TET3 na função cerebral

Resumo

A familia de enzimas "Ten Eleven Translocation" (TET) consiste em três dioxigenases envolvidadas na desmetilação do DNA, convertendo 5-metilcitosina (5-mC) em 5-hidroximetilcitosina (5hmC), 5-formilcitosina (5fC) e 5-carboxilcitosina (5caC). Níveis elevados de 5hmC estão correlacionados positivamente com a transcrição de genes, e são característicos de neurónios pós-mitóticos. Os genes *Tet* são altamente expressos no cérebro, sendo o *Tet3* o mais abundante. Nesta tese demonstramos que os níveis de expressão de *Tet3* aumentam durante a diferenciação neuronal. Além disso, usando um sistema de diferenciação *in vitro*, onde células estaminais embrionárias (ESC) podem ser diferenciadas numa população homogénea de percursores de células neurais (NPCs), verificamos que a *Tet3* é essencial para manter o silenciamento de genes de pluripotência nos NPCs. O descréscimo de expressão de *Tet3* (KD), induzido pela técnica de RNA de interferência (RNAi), em NPCs, resultou num aumento da expressão dos genes de pluripotência *Oct4* e *Nanog*, com células positivas para OCT4 formando agregados celulares. Adicionalmente, o KD de *Tet3* desencadeou uma perda global de metilação no DNA e hiper-metilação de alguns genes relacionados com a neurogénese e regiões controlo de genes "imprinted". Mais, analisamos o impacto da deleção de *Tet3* nos neurónos pós-mitóticos usando um modelo onde a *Tet3* é deletada especificamente em células positivas para *Camk2a,* após administração de tamoxifeno. Caracterizamos o efeito a nível comportamental em ratinhos jovens adultos, machos e fêmeas; demonstrando que a deleção da *Tet3* conduz a um aumento do comportamento do tipo ansioso e induz défices cognitivos, nomeadamente na orientação espacial. Demonstramos que nos machos, mas não nas fêmeas, existe um aumento dos níveis de corticosterona e aumento da maturação das espinhas na região ventral hipocampal,CA1. Contrariamente aos machos que não demonstraram qualquer dano na memória a curto prazo, as fêmeas Tet3 cKO apresentaram. Em ambos os géneros, observamos uma expressão aumentada de *Npas4* e *c-fos* no hipocampo. Assim, nesta tese, propomos que a enzima TET3 tem um papel fulcral na manutenção da identidade das células precursoras neurais e funciona como um regulador epigenético no comportamento do tipo ansioso e na orientação espacial.

Palavras-chave: cérebro; neurónios; NPCs; TET3

Role of TET3 enzyme in brain function

Abstract

The Ten eleven translocation (TET) family of enzymes consists of three dioxygenases involved in the DNA demethylation process; they convert 5-methylcytosine base (5mC) into 5-hydroxymethylcytosine (5hmC), 5-formylcytosine (5fC), and 5-carboxylcytosine (5caC). High 5hmC content is positively correlated with gene transcription and is a feature of post-mitotic neurons. *Tet* genes have also been shown to be highly transcribed in the brain, with *Tet3* being the most abundant. Here we showed that *Tet3* is highly upregulated during neuronal differentiation. Importantly, using an *in vitro* differentiation system, where ES cells can be differentiated into a homogeneous population of neural precursor cells (NPCs), we discovered that *Tet3* is required to maintain the silencing of pluripotency-associated genes in neural precursor cells (NPCs). *Tet3* knockdown (KD) in NPCs led to a significant increase in *Oct4* and *Nanog* gene expression, with OCT4-positive cells forming cellular aggregates. Moreover, Tet3 KD triggered a genome-scale loss of DNA methylation and hypermethylation of a small number of neurogenesis-related genes and at imprinting control regions of imprinted genes. We extended the analyses of *Tet3* deletion impact to post-mitotic neurons using a conditional and inducible mouse model where *Tet3* is deleted specifically in *Camk2a*-positive cells after tamoxifen administration. We characterized the impact of *Tet3* deletion on behavior performance in young adult mice, males and females; the absence of *Tet3* led to an increase in anxiety-like behavior and cognitive impairment, namely spatial orientation, in female and male mice. The Tet3 cKO males showed increased corticosterone levels and increased dendritic spine maturation in the ventral CA1 hippocampal subregion, which was not observed in females. Also, contrary to the results in males, Tet3 cKO female mice presented impairment in short-term memory. In both genders, we observed an increase in *Npas4* and *c-fos* gene expression in the hippocampus. Thus, in this thesis, we propose that TET3 plays a pivotal role in maintaining neural precursor cell identity and DNA methylation levels, and has an important function as an epigenetic regulator of anxiety-like behavior and spatial orientation.

Key-words: brain; neurons; NPCs; TET3

Table of contents

List of abbreviations

#

3D – Three-dimensional

5caC – 5-carboxylcytosine

5fC – 5-formylcytosine

5hmC – 5-hydroxymethylcytosine

5hmU – 5-hydroxymethyluracil

5mC – 5-methylcytosine

A

A – Adenine

AID – activation-induced cytidine deaminase

APOBEC – apolipoprotein B mRNA editing enzyme, catalytic polypeptide

B

BER – Base excision repair

BrdU – Bromodeoxyuridne

BSA – Bovine serum albumin

C

C – Cytosine

CA – Cellular aggregates

CA1 – Cornu Ammonis 1

CA2 – Cornu Ammonis 1

CA3 – Cornu Ammonis 1

cDNA – Complementary DNA

CFC – Contextual fear conditioning

CNPase – 2′,3′-cyclic nucleotide-3′-phosphodiesterase

CNS – Central nervous system

CpG – Cytosine-guanine dinucleotide

CFC – Contextual fear conditioning

CTRL – Control

CXXC – cysteine-X-X-cysteine domain

D

dDG – Dorsal Dentate Gyrus

Dcx – Doublecortin

DNMT – DNA methyltransferase

dHip – Dorsal hippocampus

DSBH – Double-stranded β helix domain

E

EB – Embryonic bodies

ELISA – Enzyme-Linked Immunosorbent Assay

ESC – Embryonic stem cells

EPM – Elevated plus maze

F

FBS – Fetal bovine serum

Fgf1 – fibroblast growth factor 1

FST – Forced swimming test

G

G – Guanine

GFAP – Glial fibrillary acidic protein

H

HPA – Hypothalamo-pituitary-adrenocortical

I

ICRs – Imprinting control regions

IEG's – Immediate early genes

iGluR – Ionotropic glutamate receptor

IHC – immunohistochemical

ILPF – Infralimbic prefrontal cortex

i.p. – intraperitoneal

K

Kd –Knockdown

KO – Knockout

L

LTD – Long-term depression

LTP – Long-term potentiation

M

MBD – Methyl-CpG-binding

MeCP2 – Methyl-CpG-binding protein 2

mEPSC – Excitatory synaptic transmission

mGluR – Metabotropic glutamate receptor

mPFC – Medial prefrontal cortex

MWM – Morris water maze

N

NeuN – Neuronal nuclei

NOR – Novel object recognition

NPCs – Neural precursor cells

NSCs – Neural stem cells

O

OE – overexpression

OF – Open field

ON – overnight

oxRRBS – Oxidative Reduced Representation Bisulfite Sequencing

P

PBS – Phosphate-buffered solution

PCR – Polymerase Chain Reaction

PFC – Prefrontal cortex

PI – Propidium Iodide

PSD95 – Postsynaptic density protein of 95 Kd molecular weight

PTSD – Posttraumatic stress disorder

Q

qPCR – Quantitative Real-Time Polymerase Chain Reaction

R

RA – Retinoic Acid

RAWM – Radial arm maze

RT-PCR – Reverse Transcription Polymerase Chain Reaction

RTT – neurological disorder Rett syndrome

S

Scr– Scrambled

shRNA – Short hairpin RNA

SMUG – Strand-selective monofunctional uracil-DNA glycosylase 1

SV – Synaptic vesicle

T

T – Thymine

TET – Ten-Eleven Translocation (enzyme)

TDG – Thymidine-DNA glycosylase

TSS – Transcription Start Sites

TST – Tail suspension test

TTX – Tetrodotoxin

U

U – Uracil

V

vDG – Ventral Dentate Gyrus

vHip – Ventral hippocampus

W

WB – Western blot

WT – Wild-type

List of figures and tables

Chapter 1

Chapter 2

Chapter 3

Chapter 4

Chapter 5

Outline of the thesis

This thesis was divided and ordered in **five** chapters:

In **chapter 1**, a general introduction is given about epigenetics principles, basic knowledge concerning animal behavior, and the identified role of each TET enzyme in brain function.

In **chapter 2** we investigate the effects of TET3 enzyme knockdown in NPCs, using an *in vitro* differentiation system, where NPCs are derived from mouse ES cells.

In **chapter 3** we address the establishment and characterization of the TET3 conditional deletion in post-mitotic neurons in male mice, using a conditional knockout mouse model *Tet3*$^{fl/fl}$; *Camk2a-CreERT2* (Tet3 cKO).

In **chapter 4**, the model mentioned in chapter 3 was used to investigate the effect of TET3 conditional deletion in female mice.

In **chapter 5**, the results we obtained are discussed, addressing the methodological advantages and disadvantages of the techniques and experimental models used, and the contribution of the present work to a comprehensive understanding of the role of TET enzymes in brain function, combined with the upcoming perspectives.

Chapter I

Introduction

INTRODUCTION

1.1. What is epigenetics?

The term epigenetics was introduced by Conrad Waddington in the early 1940s. Waddington defined epigenetics as "the branch of biology which studies the causal interactions between genes and their products, which bring the phenotype into being"(Goldberg et al., 2007). Two-thirds of a century later, Adrien Bird introduced a more mechanistic definition, describing epigenetic as the structural adaptation of chromosomal regions by which cellular memories are stored and perpetuated, without altering the DNA sequence (Bird, 2007). These mechanisms can interfere with gene packaging in cell nucleus, involve changes in chemical groups in the DNA, or modify the interaction of RNA molecules with the DNA. Thus, we can identify three main molecular epigenetic mechanisms: histone post-translational modifications, covalent modifications of DNA and non-coding RNAs (Snijders et al., 2018). In this thesis, more relevance is given to DNA methylation and hydroxymethylation which will be discussed in the next sections of this chapter.

1.1.2. DNA methylation

DNA methylation constitutes one of the most well studied and understood epigenetic modifications. DNA methylation represents an essential epigenetic mark controlling several biological processes such as genomic imprinting, transposon inactivation, stem cell differentiation, transcription repression, and inflammation (Smith and Meissner, 2013). Mechanistically, it is a process by which a methyl group (-CH3) is added to the carbon-5 position of cytosine residues to form 5-methylcytosine (5-mC), and is carried out by DNA methyltransferases (DNMTs) (Okano et al., 1998). Not all cytosines are methylated; predominantly methylation occurs in CpG dinucleotides, but also can occur in other contexts (normally referred as CpH, mainly in CpA and CpT) (Shin et al., 2014), and its function is suggested to be repressive as well (Guo et al., 2014a). 70%–80% of mammalian CpGs are thought to be methylated (Ehrlich et al., 1982). Importantly, most genomic methylation signatures are conserved across tissues and throughout life. The alteration of methylation status is localized in specific contexts and cellular processes to activate or shut down specific genes (Smith and Meissner, 2013). Less than 10% of CpGs occur in regions with a high density of this dinucleotide that are called CpG islands; with the majority being resistant to DNA methylation and frequently found at promoter sites of housekeeping and developmental regulatory genes

(Deaton and Bird, 2011). DNA methylation is singularly enriched at promoter gene regions of oocytes, embryonic stem cells (ESCs) and neurons (Smith and Meissner, 2013).

Two general classes of DNMTs can be identified: maintenance methylation and *de novo* methylation. DNMT1 is the maintenance DNMT, DNMTs 3a and 3b are the *de novo* methyltransferases. DNMT1 has a preference for hemi-methylated DNA, maintaining CpG methylation during DNA replication and DNMT 3a and 3b methylate previously unmethylated CpG sites in the DNA (Okano et al., 1998).

In most cases, DNA methylation is associated with repression of gene transcription, namely when occurring in promoter regions, due to structural chromatin alterations. However, its effect is highly influenced by the location of the methylated CpGs and in certain genomic contexts, namely within gene bodies, DNA methylation may have the opposite effect, i.e., an increase in transcriptional activity (Deaton and Bird, 2011). The molecular processes underlying this effect are complex and under intense study at present. However, the repressive outcome of DNA methylation at gene promoters is well described and it is the result of the binding of several proteins (MeCP2, MBD1, MBD2, MBD4 and Kaiso) to methylated CpG sites (Hendrich and Bird, 1998; Prokhortchouk et al., 2001). Mechanistically, the methylation of DNA triggers the association with histone proteins, which interacts with the DNA and results in a higher affinity between DNA and histone core, and consequent transcriptional repression (Smith and Meissner, 2013).

1.1.2.1 DNA methylation in the brain

Similarly to all other parts of the body, DNA in the brain is methylated throughout life and presents methyltransferase activity. In the brain, 4.2% of all cytosines are methylated (Lister et al., 2013). Neuronal cells are the main contributors to this global enrichment in methylation, since glial cells present sparse levels of this DNA modification (Lister et al., 2013). This epigenetic mark plays an important role in brain development and neuronal function. Indeed, a rapid increase in mammalian brain methylation levels coincides with synaptogenesis (Lister et al., 2013). Evidence that DNA methylation has a critical role in the brain arose with the discovery of methyl-CpG-binding protein 2 (MeCP2) and its implication in the X-linked neurological disorder Rett syndrome (RTT) (Amir et al., 1999). Indeed, MeCP2 is important to regulate mature neuronal functions, since MeCP2 deletion results in reduced spontaneous excitatory synaptic transmission (mEPSC). Moreover, MeCP2 knock-out (KO) brains have a reduced size, retraction

of dendritic arbours and reduction of dendritic spinal density, potentially triggered by post-translational dysregulation of a number of synaptic proteins (Derecki et al., 2012).

Rett syndrome could also reflect a certain sensitivity of neurons to methylation-dependent transcriptional suppression. In fact, mutations in DNA methyltransferases were associated with neurodevelopmental disorders (Tatton-Brown et al., 2014), suggesting that both the enzymatic "writers" of DNA methylation patterns and the "readers" of these marks are crucial regulators of brain function. Regarding the "writers", both maintenance and *de novo* DNMTs are expressed in most brain cells with a differential expression profile. DNMT1 is highly expressed in neurons from embryogenesis through adulthood (Goto et al., 1994). DNMT3b expression is observed in neural progenitors during early embryogenesis and tends to be low in the adult stage. DNMT3a is expressed from late embryogenesis to adulthood with a peak during the early postnatal period, remaining present in the adult brain (Feng et al., 2005). The high levels of DNMT1 and DNMT3a in post-mitotic neurons indicate a specific role for these enzymes in the adult brain beyond the classic view of *de novo* and maintenance DNMT. Despite, the high transcription level, single depletion of DNMT1 or DNMT3a in post-mitotic neurons did not affect behavior and synaptic plasticity. However, the double knockout (DKO) showed abnormal hippocampal long-term plasticity and deficits of learning and memory. Additionally, a significant decrease in DNA methylation levels was observed in DKO neurons (Feng et al., 2010). The function of these enzymes was shown to be detrimental in distinct processes involving neuronal plasticity at the adult stage, such as contextual fear conditioning memory formation (Miller and Sweatt, 2007), cocaine addiction and chronic social defeat stress (LaPlant et al., 2010) and cognitive decline associated with aging (Oliveira et al., 2012).

Interestingly, the modulation of DNMT expression influences methylation on the promoters of plasticity-related genes. For example, neuronal depolarization leads to a loss of methylation at regulatory regions of the *Bdnf* gene, which is correlated with higher transcription. Mechanistically, this regulation is explained by dissociation of MeCP2-histone deacetylase-mSin3A repression complex from the promoter of *Bdnf* (Martinowich et al., 2003).

The methylation status of *Bdnf* was also implicated in the regulation of fear memory. The contextual fear learning-induced differential regulation of *Bdnf* mRNAs, associated with decreased methylation in the exon IV promoter and altered local chromatin structure (Lubin et al., 2008). Also, the GADD45b is implicated in activity-dependent DNA demethylation of Bdnf exon IX and fibroblast growth factor 1 (Fgf1) promoters (Ma et al., 2009a).

Strikingly, in the adult mouse and human brain genome, high levels of methylation in non-CpG cytosines (mCH, where H stands for A, T or C) have been observed. This is still under intense study; however, it

was suggested that mCH has the same repressive function of mCG in differentiated cells (Guo et al., 2014a; Lister et al., 2013).

Altogether, these studies support the idea that DNA methylation is a key epigenetic mark regulating brain function.

1.1.3. Active DNA demethylation- a focus on DNA hydroxymethylation

Despite the chemical and genetic stability of 5mC due to chemical carbon-carbon bond and the action of DNMT enzymes, the methyl group of this base can be passively or actively lost during DNA replication or through enzymatic DNA demethylation, respectively (Wu and Zhang, 2017). During mammalian development, active DNA demethylation occurs during specific stages: during early embryogenesis, shortly after fertilization, before DNA replication occurs, in the paternal pronucleus (Mayer et al., 2000) (Oswald et al., 2000), and in primordial germ cells that includes demethylation of imprinted genes (Hajkova et al., 2002; Yamazaki et al., 2003). Active DNA demethylation is thought to occur when cytosine hydroxymethylation (5hmC) is formed by the oxidation of 5-methylcytosine, a reaction catalyzed by the TET (Ten Eleven Translocation) family of enzymes (Tahiliani et al., 2009a). TETs also intermediate oxidation of 5hmC to formylcytosine (5fC) and then to 5-carboxylcytosine (5caC), which are suggested to be intermediates in the DNA demethylation process. Subsequently, the 5fC and 5caC can be subject to deamination, glycosylase-dependent excision by thymine DNA glycosylase (TDG) and DNA base-excision repair (BER) pathway, removing the methylated cytosine (Ito et al., 2011) Additionally, 5mC and 5hmC can be deaminated by AID/APOBEC, giving rise to T and 5hmU respectively, that are recognized by DNA glycosylases, producing an abasic site that is then repaired by the BER machinery (**Figure1**).

DNA hydroxymethylation is called the sixth base of the genome and it has been described as a fundamental epigenetic mark, not only as an intermediate during 5mC demethylation but also playing important roles such as maintenance of pluripotency in ESCs (Thomson and Meehan, 2017). In these cells, 5hmC is the most predominant oxidative base and it is found mainly at gene promoters and CpG islands, regions commonly depleted of 5mC, accompanying the increase in gene transcriptional level (Ficz et al., 2011). The 5hmC base is also enriched in gene bodies of genes actively transcribed (Wu et al., 2011a). 5hmC is particularly relevant in the function of the neural system, as it will be detailed next.

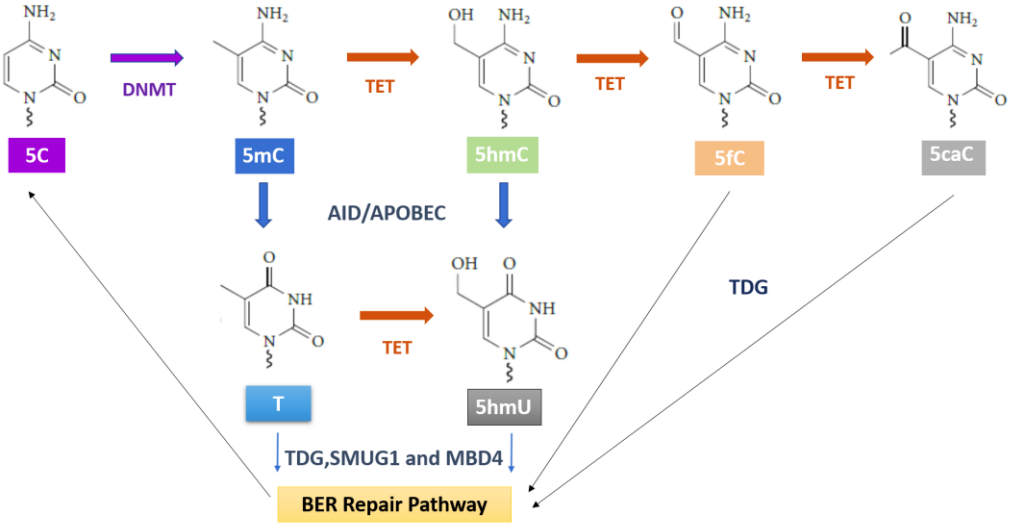

Figure 1 Potential pathways for TET-mediated active DNA demethylation cycle.
DNMTs convert unmodified C to 5mC. 5mC can be converted back to unmodified cytosine by TET-mediated oxidation to 5hmC, 5fC and 5caC, followed by excision of 5fC or 5caC mediated by TDG coupled with BER. 5mC and 5hmC can be deaminated by AID/APOBEC, giving rise to T and 5hmU respectively, that are recognized by DNA glycosylases, producing an abasic site that is then repaired by the BER machinery. C, cytosine; 5-mC, 5-methylcytosine; 5-hmC, 5-hydroxymethylcytosine; 5fC, 5-formylcytosine; 5-caC, 5-carboxylcytosine; 5hmU, 5-hydroxymethyluracil; T, Thymine; DNMT, DNA methyltransferase; TET, Ten-eleven translocation enzyme; TDG, thymine glycosylase; BER, base excision repair; AID/APOBEC, activation-induced cytidine deaminase/ apolipoprotein B mRNA editing enzyme, catalytic polypeptide-like; SMUG1, strand-selective monofunctional uracil-DNA glycosylase 1; MBD4, methyl-CpG- binding domain protein 4. Adapted from (Antunes et al., 2019).

1.1.3.1. DNA hydroxymethylation in the brain

5hmC base is detected in all mammalian tissues and cell types analysed to date. Contrary to the relatively constant levels of 5mC in different somatic tissues of the organism, this base is up to ten times enriched in the central nervous system, constituting between 0.4 and 0.7% of all cytosines (Kriaucionis and Heintz, 2009; Munzel et al., 2010). 5hmC derivatives, 5caC and 5fC, have also been detected, although at much lower levels than 5hmC (a ratio of ~10000:11:1 in human brain and ~4700:12:1 in mouse brain, for 5hmC, 5fC and 5caC respectively was reported (Liu et al., 2013b) with their relevance still being largely unknown. In the brain, 5hmC is particularly enriched in the hypothalamus, cortex, hippocampus and cerebellum (Munzel et al., 2010; Szwagierczak et al., 2010). Immunostaining analysis revealed that the highest levels of 5hmC are found in fully differentiated neurons; in the cells located in the subgranular zone between the dentate gyrus and hilus (the region containing the neural progenitors), a clear reduction in the 5hmC levels was found (Chen et al., 2012). Additionally, the distribution of 5hmC is associated with gene expression in neurons (Mellen et al., 2012; Tahiliani et al., 2009a). Within the neuronal population, 5hmC content seems to be heterogeneous, since in the Purkinje cells is two times more

abundant than in granular cells (Kriaucionis and Heintz, 2009). The 5hmC levels increase in the brain significantly after birth, with no concomitant 5mC decrease, when synaptogenesis and neuronal maturation occur (Song et al., 2011; Szulwach et al., 2011). During aging this pattern of increase is also maintained, suggesting that 5hmC can represent a stable epigenetic mark throughout life (Chen et al., 2012). Regarding the genomic distribution of 5hmC, genome-wide analysis of the brain and neuronal cells have given us a progressively clearer perspective of this DNA base patterns. Although the Transcription Start Sites (TSS) sites are largely depleted in 5hmC marker; in actively transcribed and expressed genes, an enrichment of 5hmC on gene bodies and in proximal upstream and downstream regions relative to the TSS was demonstrated (Lister et al., 2013; Mellen et al., 2012; Song et al., 2011; Szulwach et al., 2011). In exons, both 5hmC and 5mC are scarce but abundant at the exon-intron boundary (Khare et al., 2012). As it happens in ESCs, also in the brain a 5hmC abundance at distal regulatory elements is found, and this is more evident at poised than active enhancers, suggesting that a hydroxymethylation is an upstream event in enhancer activation (Guy et al., 2011; Wen et al., 2014). Contrary to ESCs, in which 5hmC is frequently found in the promoter CpGs, in the brain they are depleted (Song et al., 2011; Szulwach et al., 2011; Wen et al., 2014). Regarding 5hmC readers, the methyl-CpG-binding protein MeCP2 was identified as the major 5hmC-binding protein in the brain (Mellen et al., 2012). Although surprising, since it was initially identified by selective binding at 5mC DNA modification promoting gene repression, MeCP2 is highly abundant in mature neurons, with evidence arising that suggests it can act as a transcriptional activator (Chahrour et al., 2008; Guy et al., 2011). Additionally, Wdr76, Thy28 (Thyn1) and Neil1 proteins were commonly described as 5hmC readers in ESCs, NPC and brain (Spruijt et al., 2013). However, our understanding of the function of 5hmC in the brain is very incomplete, and new studies addressing the relevance of this base are still required.

1.1.4. Methodologies to identify 5mC and 5hmC DNA modifications

Global 5mC and 5hmC levels can be examined by immunohistochemical (IHC) staining, enzyme-linked immunosorbent assay (ELISA) and restriction enzyme-depend methods associated with polymerase chain reaction (PCR) (Snijders et al., 2018). The site resolution is the main limitation using these methodologies, allowing only to determine the global methylation or hydroxymethylation levels. To determine the gene-specific DNA modifications, three main techniques can be used: pyrosequencing, quantitative reverse transcription PCR (qRT-PCR) and methylation-specific PCR (Snijders et al., 2018).

Regarding the mapping of genome-wide DNA methylation distribution, during the last years, various methods have been developed. Globally, all methods involve the fragmentation of the genomic DNA (by

restriction enzymes or sonication), methyl-CpG-binding (MBD) or antibody enrichment (MeDIP), bisulfite conversion or TET oxidation and next-generation sequencing (NGS) or microarray analysis (Yong et al., 2016).

Bisulfite conversion of genomic DNA is the gold standard approach for DNA methylation analysis, since it allows distinguishing between methylated and unmethylated C residues, and between 5-mC and 5hmC when an oxidation step is combined. It consists in the treatment of genomic DNA with sodium bisulfite which deaminates Cytosine (C) base to Uracil (U), while the methylated C remain unaffected. The U is converted to T (Thymine) in a following PCR (Booth et al., 2013; Frommer et al., 1992). This methodology is used in both, whole-genome bisulfite (WGBS) and reduced-representation bisulfite sequencing (RRBS) technique. The WGBS is considered the best methodology to provide the coverage of all cytosines information. However, the high amount of data generated and the high sequencing costs are the major disadvantages. To decrease these, RRBS technique emerged as a valuable tool to study the methylome at a lower cost, which integrates the digestion of DNA by MspI restriction enzyme with bisulfite conversion and NGS (Snijders et al., 2018).

Since the conventional bisulfite sequencing cannot distinguish 5mC from 5hmC, a modified bisulfite approach - oxidative bisulfite sequencing (ox-BS) - including an oxidation step prior to bisulfite treatment, has been described. This step allows to discriminate the 5mC and 5hmC base, since 5hmC is chemically oxidized to 5fC, which after bisulfite treatment becomes U. The last step is to calculate the 5hmC level by subtracting the BS-seq (5mC+5hmC detection) and the ox-BS-seq (5hmC detection) outcomes (Booth et al., 2013) (**Figure 2**).

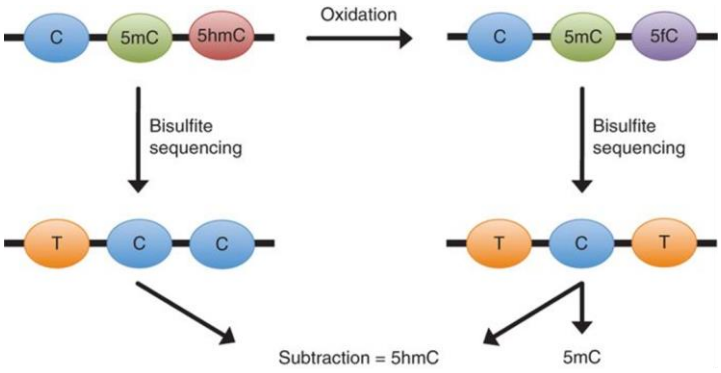

Base	Sequence	BS Sequence	oxBS Sequence
C	C	T	T
5mC	C	C	C
5hmC	C	C	T

Figure 2 Oxidative Bisulfite Sequencing.
After bisulfite treatment of DNA, C is read as T, and 5mC and 5hmC are read as C. With the oxidation of 5hmC to 5fC followed by bisulfite treatment, C and 5hmC are read as T and only 5mC as C. Thus, 5hmC profile is determined by the subtraction of both processes. C, cytosine; 5-mC, 5-methylcytosine; 5-hmC, 5-hydroxymethylcytosine. Adapted from (Booth et al., 2013).

1.1.5. TET enzymes

The molecular mechanism underlying the conversion of 5mC to 5hmC was discovered in 2009 when two distinct groups described 5hmC accumulation in neurons and ESCs (Kriaucionis and Heintz, 2009; Tahiliani et al., 2009a). This conversion was firstly verified by the action of TET1 enzyme (Tahiliani et al., 2009a) and later by TET2 and TET3 (Ito et al., 2010). Thus, the TET enzyme family comprises a cluster of three dioxygenases which share the capacity to convert 5mC to 5hmC and subsequent products, all dependent on α-ketoglutarate (α-KG) and Fe(II) (Tahiliani et al., 2009a). Structurally, the three TET enzymes share a less conserved N-terminal region and a conserved C-terminal catalytic domain, which is composed of a double-stranded β helix domain (DSBH) and a cysteine-rich region preceding the DSBH (**Figure 3**). This domain contains the metal-binding residues for α-KG and Fe(II), indispensable for the oxidation reaction (Tahiliani et al., 2009a), while the N-terminal zinc finger cysteine-X-X-cysteine (CXXC) domain is implicated in the binding of unmethylated CpGs (Long et al., 2013).

While for TET2 enzyme, only one isoform is known, for TET1 and TET3 multiple splicing isoforms have been described. Both have a full-length isoform with the CXXC domain; however, TET2 does not contain a CXXC domain but partners with IDAX, an independent CXXC-containing protein (Ko et al., 2013b). For TET1, a N-terminus-truncated form (TET1s) was identified in somatic tissues, while the full-length (TET1FL

or TETe) was found in early embryos, ESCs and primordial germ cells (PGCs). The shorter version, TET1s, presents weaker demethylation activity compared with the full version, TET1FL (Zhang et al., 2016b). Regarding TET3, three isoforms were described, including two without the CXXC domain, TET3s and TET3o (Liu et al., 2013a) (Jin et al., 2016) and one full version (TET3FL). TET3o is exclusively found in oocytes, while TET3s and TET3FL were shown to be upregulated with neuronal differentiation (Jin et al., 2016). Contrarily to TET1, TET3 isoforms without the CXXC domain show higher demethylation capacity (Jin et al., 2016).

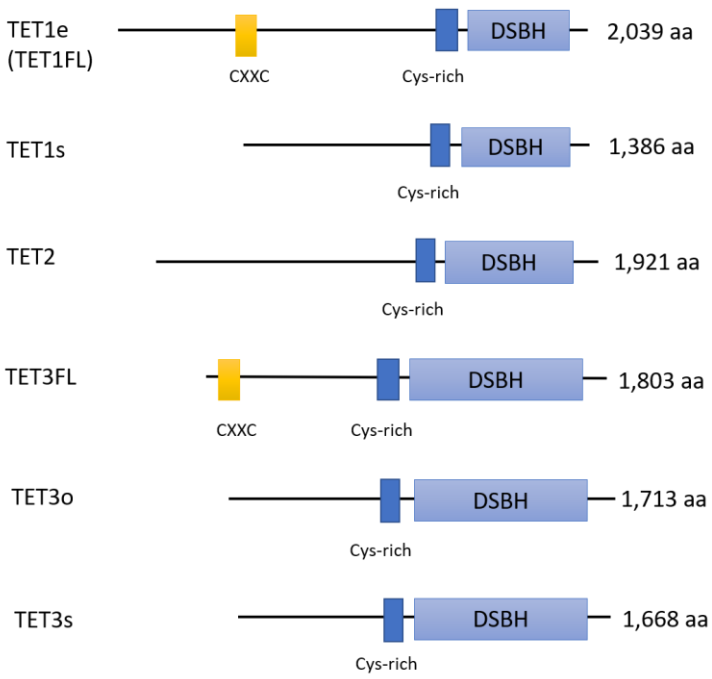

Figure 3 Structure of mouse TET proteins.
All TET isoforms share the conserved Cysteine-rich and double-stranded β-helix (DSBH) domains at the carboxyl terminus, which constitute the catalytic structure. Full-length TET1 (TET1FL) and TET3 have a CXXC domain at the amino terminus, while TET2 does not. Multiple splicing isoforms have been reported for TET1 (Zhang et al., 2016b) and TET3 (Liu et al., 2013a) (Jin et al., 2016). Adapted from (Wu and Zhang, 2017).

1.1.5.1. TET Enzymes in pluripotency and in neural progenitors derived from ESCs

Both TET1 and TET2 enzymes are highly expressed in mouse ES cells with a critical role in self-renewal and lineage specification (Ficz et al., 2011; Ito et al., 2010; Koh et al., 2011). Indeed, the single or double Tet1/Tet2 KO decreases 5hmC levels and impacts the ESC transcriptional signature (Ito et al., 2010). Importantly, TET1 and TET2 have distinct roles at gene-specific regulatory regions: TET1 regulates 5hmC levels at gene promoters and transcription start sites, while TET2 mainly regulates 5hmC levels in gene bodies and exon boundaries of highly-expressed genes and exons, respectively (Huang et al., 2014). On

the contrary, and consistently with the low TET3 levels detected in ESC, its depletion does not affect pluripotency (Li et al., 2015a).

In mouse ES cells, TET1 was the first enzyme implicated in the conversion of 5mC into 5hmC and its deletion results in decreased levels of 5hmC (Tahiliani et al., 2009a). Nevertheless, Tet1 KO ES cells do not lose pluripotency, expressing Nanog, Oct4 and Sox2 at comparable levels to control cells (Dawlaty et al., 2011). TET1 preferentially binds to CpG-rich sequences at promoters and gene bodies, promoting DNA demethylation and transcription, while it also binds to Polycomb group target genes and participates in transcriptional repression (Ficz et al., 2011; Wu et al., 2011b). TET1 KD in ESCs modifies gene expression and normal cell differentiation by negative regulation of key trophectoderm regulators and positive regulation of neuroectoderm factors (Pastor et al., 2013). Its knockdown increases the methylation at the promoters of pluripotency-related genes, such as Esrrb, Klf2, Tcl1 and Zfp42, downregulating its expression (Ficz et al., 2011). Even so, TET1-null cells are pluripotent. Moreover, TET1 depleted embryoid bodies can be differentiated into neural precursor cells (Dawlaty et al., 2011), and both $TET1^{-/-}$ and $TET2^{-/-}$ mice develop all three germ layers and survive, suggesting that both enzymes do not have a crucial role in differentiation (Dawlaty et al., 2011; Ko et al., 2011).

In ES cells, TET1 and TET2 physically interact with Nanog, and both proteins facilitate the reprogramming process, which is dependent of their catalytic activity (Costa et al., 2013). In neural stem cells (NSCs) the co-transfection of Nanog with either TET1 or TET2 increased the expression of pluripotency markers such as Oct4, suggesting that TET1 or TET2 are recruited by Nanog to enhance the expression of a subgroup of crucial reprogramming target genes (Costa et al., 2013).

During neural differentiation, a decrease in TET1 and TET2 levels was observed (Li et al., 2015a). Contrarily, although TET3 is almost undetectable in ESCs, a strong upregulation during neuronal differentiation has been observed. However, the percentage of nestin-positive cells generated from Tet3 KO ESCs is not affected, suggesting that Tet3 is not essential for the commitment of the NPCs. Yet, during the differentiation from NPCs to differentiated neurons, the nestin-positive NPCs from Tet3 KO ES cells declined much faster than NPCs derived from WT cells, indicating that Tet3 is important for NPC maintenance. Importantly, neuronal maturation is reduced with Tet3 deletion, since MAP2 expression is strongly reduced in these cells, triggered by significant apoptotic cell death of NPCs (Li et al., 2015a).

However, how TET3 is regulated in the process of neuronal differentiation needs a deeper examination.

1.2. Emotion and Cognition- the bases of animal behavior

Emotion and cognition represent central processes in brain function. During the last decades, animal research has contributed immensely to our current knowledge of human physiology, providing essential insights in the neurosciences field. The mammalian brain presents a similar structure and function across species becoming easier to map the circuits of the human brain. Consequently, the use of rodent models is a suitable and helpful tool to study different behavior dimensions. In fact, the extensive knowledge of the mouse genome and the vast number of genetically modified strains have been essential for the current knowledge in the neuroscience field. Nowadays, it is possible to target any gene and regulate its expression spatially and temporally. The opportunity to use mouse models mimicking human brain diseases has become an essential tool to improve the knowledge about the molecular bases of brain dysfunction. In this context, behavior assessment is frequently used to evaluate either mood, motor or cognitive funtions. Behavioral studies imply control for variable parameters such as environment, handling and the paradigm itself. Importantly, different behaviors will adress particular functions of a certain brain region or a specific association of a circuit integrating different brain regions. In this thesis, a special focus will be given to the hippocampal function and its dependent behaviors namely anxiety and cognition.

1.2.1 Assessment of anxiety-like behavior

Fear is an essential adaptive mechanism of alarm for the organism; however, it can also become deleterious when the anxious sensation continues, implicating an undesirable effect on daily life. When fear appears, in an inappropriate situation or chronically, is called anxiety. Thus, anxiety is a mood disorder characterized by a sensation of discomfort and apprehension in response to undefined diffuse signals. Anxiety disorder spectrum includes phobias, panic disorder, posttraumatic stress disorder (PTSD) and general anxiety disorder (Lang and McTeague, 2009). Anxious behavior can be studied using specific behavioral paradigms (**Figure 4**). In rodents, the most commonly used is the elevated plus maze (EPM) test. The EPM paradigm consists of two opposite open arms and two closed arms that produce a conflict between the rodent's tendency to explore dark and enclosed spaces, and their natural fear of bright light and open spaces. Thus, a reduced ratio between time spent on open and closed arms is an indicator of anxiety (Walf and Frye, 2007). Similar to EPM's principle, the light-dark box (LDB) test is based on the innate aversion of rodents to places with bright light. In this test, a box is divided into two sections: a minimally lit side with black walls (dark side) and a brightly lit side with white walls (light side). Each animal is placed at the center of the arena facing the lateral wall and allowed to explore it. Longer latencies

to enter and/or greater amounts of time spent in the black side of the box are interpreted as indicating more anxiety-like behavior (Bourin and Hascoet, 2003). Another test frequently used to examine anxiety is the open field (OF). This test consists in placing an animal in an unfamiliar environment surrounded by walls and enables to investigate a variety of behavior patterns such as thigmotaxis – the tendency to rely on the periphery of the arena avoiding the center. Importantly, higher levels of anxiety should mainly lead to a decrease in the ratio 'time in centre/time on periphery' (Bourin et al., 2007). Another model using the OF apparatus is the novelty suppressed feeding (NSF), which is frequently used to assess anxiety-like phenotype as it is also based on rodents' innate fear of novel spaces. However, the NSF test introduces an additional component of motivation, as the food-deprived animal's drive to eat conflicts with its fear of novel open spaces. Thus, the NSF explores the natural apprehension of rodents to consume food after a period of starvation. In this test, animals under food deprivation are placed in the corner of the OF arena, and the latency to approach and to begin eating a food pellet located in the center of the arena is measured (Blasco-Serra et al., 2017), being a measure of anxiety like-behavior.

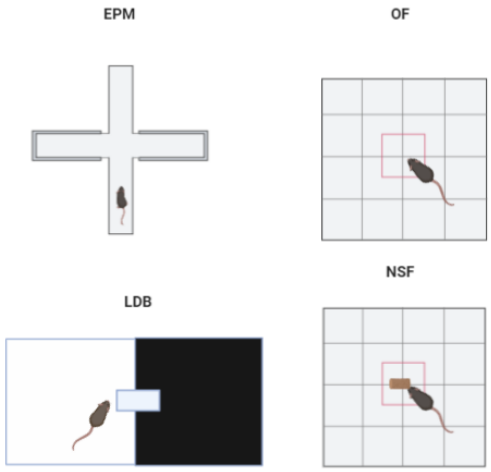

Figure 4 Anxiety-like behavior paradigms.
Some examples of anxiety-like behavior tests are represented: elevated plus maze (EPM), open field (OF), the light-dark box (LDB), and novelty suppressed feeding (NSF) tests.

1.2.2. Assessment of depressive-like behavior

Major depressive disorder (MDD) is a highly prevalent chronic psychiatric disorder and commonly associated with significant morbidity and mortality. MDD symptoms include depressed mood and anhedonia (i.e., a relative lack of pleasure in response to a formerly rewarding stimulus), both

considered fundamental features of depression (Nelson and Charney, 1981). There are several behavioral tests used to study these symptoms, such as the sucrose preference test (SPT) to study anhedonia and the tail suspension test (TST) and the forced swimming test (FST, also known as Porsolt's test (Porsolt et al., 1977) being used to study depressive-like behavior (**Figure 5**).

During the FST, the animal is placed in a container filled with water from which it cannot escape. The animal will first try to escape, but eventually will exhibit immobility (i.e. floating with the absence of any movement) (Porsolt et al., 1977). Similarly, during the TST, a rodent is subjected to the short term inescapable stress of being suspended in the air and will develop an immobile posture (i.e., when the animal doesn't want to put in the effort to try to escape) (Can et al., 2012). The immobility time is a measure of learned-helplessness (a hallmark of depressive-like behavior) since it refers to a deficit in escaping from an aversive situation after exposure to uncontrollable stress (Chourbaji et al., 2005).

Anhedonia is commonly measured by a sucrose preference test (SPT) based on a two-bottle choice paradigm. In this test, preference for a sweetened solution, in relation to water, is assessed. A decrease in the sucrose preference ratio is indicative of anhedonic-like behavior in rodents (Liu et al., 2018).

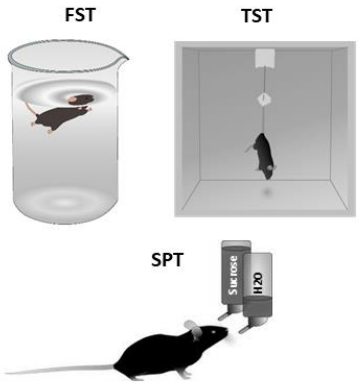

Figure 5 Examples of mood behavioral tests.
Some examples of behavior tests to evaluate the mood dimension: forced swimming test (FST), tail suspension test (TST) and sucrose preference test (SPT).

1.2.3. Stress-induced behaviors – link to the Hypothalamo-Pituitary-Adrenocortical (HPA) axis function

One biological system of major interest in depressed and anxious individuals is brain neuroendocrine function. The involvement of the HPA axis in the modulation of behavior is well known (**Figure 6**). Importantly, the persistent HPA axis activation and glucocorticoids (GCs) feedback resistance, are

frequently found in depressed patients (Lucassen et al., 2014). The HPA axis is one of the biological systems involved in the stress response. The first phase of the stress response is considered the ”alarme reaction”, which involves the activation of the autonomic nervous system (ANS) that stimulates the adrenal medulla to produce cathecolamines (adrenaline and noradrenaline). These hormones will intermediate physiological alterations, such as elevated basal metabolic rate, blood pressure and respiration, and increased blood flow to the vital organs, allowing the response to the alarm (Lucassen et al., 2014). In turn, HPA axis, a vital neuroendocrine system that interprets an environmental risk or challenge into a sequence of coordinated physiological responses, is activated as well (Herman and Cullinan, 1997). The stress response leads to stimulation of the paraventricular nucleus (PVN) in the hypothalamus, inducing the secretion of corticotropin-releasing hormone (CRH) and arginine-vasopressin (AVP). This leads to the secretion of adrenocorticotropic hormone (ACTH) from the pituitary into the bloodstream. Finally, this hormone stimulates glucocorticoids (GCs) hormones (cortisol in humans and corticosterone in rodents) release from the adrenal cortex. Regulation of HPA axis occurs through negative feedback after GC binding to mineralocorticoid (MR) and GRs, which apply a negative feedback control on the hypothalamus and pituitary, as well as in specif brain areas. Indeed, the huge number of GRs in the brain, and principally in the hippocampus, making it susceptible to elevated GC levels (Lucassen et al., 2014). The GR is particularly relevant to regulate the GC levels, since aberrant GR levels is associated with stress resistance, and anxiety and depression (Ridder et al., 2005; Wei et al., 2004). GC plasma levels follow a circadian rhythm, with a diurnal secretion peak coinciding with the beginning of the active phase (light-phase in human, dark-phase in rodents), after which circulating corticosteroids rapidly decay to basal levels (dark-phase in human, light-phase in rodents) (Yang et al., 2008). When this circadian pattern of activity is interrupted in the context of maladaptive stress, results in deleterious effects in the brain, namely brain disorders such as MDD (Koch et al., 2016).

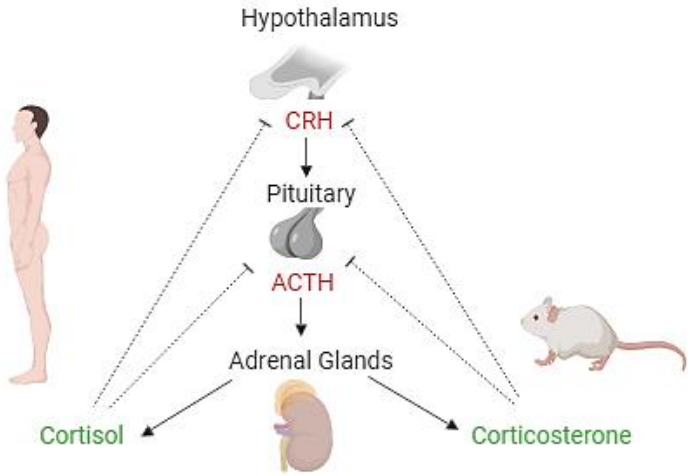

Figura 6 Schematic representation of the hypothalamic-pituitary-adrenal (HPA) axis regulation in humans and rodents.

Hypothalamus releases corticotropin-releasing homone (CRH). Within the pituitary gland, CRF will prompt the secretion of adrenocorticotropic hormone (ACTH), leading to the production of corticosteroids (cortisol-humans; corticosterone-rodents) from adrenal glands. Corticosteroids will impact both peripherally and in the central nervous system, applying a negative feedback control on the hypothalamus and pituitary.

1.2.4. Assessment of learning and memory

Cognitive function is composed by a wide range of domains such as perception, action, motivation, attention, reasoning, learning and memory (Kandel E, 2012). In the present work, we will focus in learning and memory functions. Learning is the ability to process information, whereas memory is the capacity to recall or retrieve that information at a later time (Kandel E, 2012). Memories are created after learning, and are dependent of synaptic plasticity, involving structural modifications on dentritic spines at postsynaptic sites. The magnitude of these modifications are dependent of the types of memories involved. Short-term memory induces reversible and temporary changes in synaptic transmission, while long-term memory implicates persistent structural alterations and requires gene expression and ultimately, synthesis of new proteins (Kandel E, 2012; Mizuno and Giese, 2005).

Numerous paradigms have been used to assess the effects of genetic modifications, brain lesions, or chemical compounds on learning and memory in rodents. A large variety of hippocampal-dependent tasks were already described and are regularly used. A gold standard paradigm for studying learning and memory behavior in rodents is the Morris water maze (MWM), which represents a precise way to assess spatial learning and memory (D'Hooge and De Deyn, 2001). This approach relies on distal cues which

drive the navigation trajectory from start sites around the perimeter of an open swimming arena to find a submerged escape platform (Morris, 1984). MWM test is used to study both spatial/discriminative learning and working memory processes, being currently applied to study cognitive decline characteristic dysfunctions of neurodegenerative disorders such as Alzheimer´s and Parkinson's diseases (Terry, 2009). Another test commonly used to assess memory is the novel object recognition (NOR). This paradigm evaluates the rodents' capacity to identify a novel object in the environment, since the natural predisposition of rodents to explore novel items is well recognized. Considering the amount of time that rodents spend exploring the presented objects, memory performance can be evaluated (Cohen and Stackman, 2015).

In order to assess associative learning and memory a gold standard behavior test is the contextual fear conditioning (CFC), which relies on hippocampal function. Fear conditioning is a form of learning in which an aversive stimulus (e.g. an electrical shock) is associated with a particular impartial context (e.g., a room) or neutral stimulus (e.g., a tone), resulting in the appearance of fear responses to the original stimulus or context. In this paradigm, the animal is placed in a novel environment, providing an aversive stimulus, and then removed. When the animal is returned to the same environment, it will adopt a freezing response if it remembers and associates that environment with the aversive stimulus (Peter Curzon, 2009).

1.2.5. Hippocampal structural organization and dependent behaviors

Research focused on the hippocampus have been supported by two essential evidences: first, lesions of the hippocampus impair the acquisition of new episodic memories; second, activity-dependent synaptic plasticity is a key property of hippocampal synapses (Neves et al., 2008). Indeed, this brain region plays a key role in memory processes such as spatial learning, declarative memory and the establishment of relational representations (Eichenbaum, 2004). Functional studies showed that hippocampal neurons exhibit spatially specific firing, particularly decisive to encode spatial location (Ciocchi et al., 2015). All these processes are strongly regulated by dendritic plasticity and generation of new synapses, induced by long-term potentiation (LTP) or by the weakening of synaptic strength as a result of long-term depression (LTD) (Becker et al., 2008; Raymond, 2007). Therefore, neuroplasticity is a key feature of the hippocampus, allowing to adapt its activity and structure to experience and environmental stimuli.

Structurally, the hippocampus belongs to the limbic system and is located in the medial temporal lobe of the brain (Strange et al., 2014). Although its formation occurs during embryonic development, the main neuronal population is only produced post-natally (Rolando and Taylor, 2014). The basic

hippocampal architecture is preserved between humans and rodents and includes two main areas: the Dentate Gyrus (DG) and the *Cornu Ammonis* (CA) regions. The DG has a characteristic U shape and is one of the few regions of the adult brain where cytogenesis occurs (Kempermann et al.). The CA comprises: CA3, CA2 and CA1 subregions. The DG and CA regions are composed by neurons with different morphology; the DG neurons are granular cells (presenting only apical dentrites) while the CA regions are composed by pyramidal neurons (presenting both apical and basal dendrites) (Bliss, 2007). Strong and complex signal flow is established between these hippocampal subregions. Within the DG, granule neurons project their axons (mossy fibers) to the CA3 pyramidal neurons. These, in turn, send projections to the ipsilateral CA1 (through Schaffer collaterals) or to the contralateral CA3 or still to the CA1 (through commissural connections). The circuit loop is closed with the CA1 axonal projection to the subiculum or to deep layers of the entorhinal cortex (Bliss, 2007) (**Figure 7b**).

The adult mammalian hippocampus presents an elongated C-shape which extends along a dorsal-ventral axis in rodents, corresponding to the posterior and anterior axis in humans (**Figure 7a**). Different circuits arise along the hippocampal axis, with anatomical projections patterns variation along dorsal and the ventral hippocampus, associated with characteristic functions (Strange et al., 2014). Additionally, the molecular signature differs along the hippocampal axis, suggesting that it can be divided into separate structures (Fanselow and Dong, 2010). Functionally, the dorsal hippocampus is associated with spatial navigation and episodic memory, while the ventral hippocampus is related to affective and emotional dimensions, which comprises anxious and motivational behaviors (Fanselow and Dong, 2010; Morris et al., 1982). The dorsal hippocampal region contains a great density of place cells, which are fundamental for spatial memory (Moser et al.) 2018). The ventral hippocampal cells establish intimate connections with the amygdalar and prefrontal cortex. This circuit composed by the vHip, the amygdala and the prefrontal cortex is the neuronal base modulating fear dependent behaviors (Mahan and Ressler, 2012). Interestingly, it was already shown that dorsal and ventral hippocampus can react differently to experience and environmental stimuli. For instance, chronic stress impacts differently the dorsal and ventral hippocampal neurons. While dorsal hippocampal dendrites are shortened, ventral dendrites are enlarged. Importantly, these morphological alterations are reversible after cessation of stress, highlighting the high plasticity of the hippocampus (McEwen, 1999). In fact, the hippocampus is highly experience-dependent with axonal and dendritic structural modifications induced by the environmental stimulus.

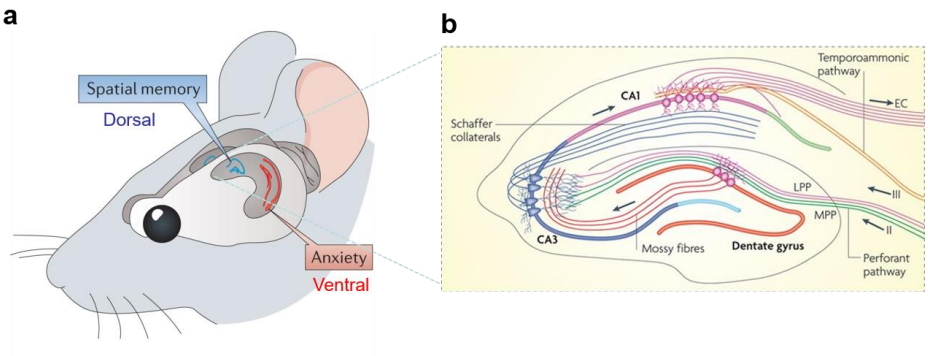

Figura 7 Mouse hippocampal architecture.
a. The rodent hippocampus is an elongated structure with a C-shaped structure, which extends along a dorsal-ventral axis. **b.** Coronary perspective of hippocampus structure which includes DG and CA regions (CA3 and CA1), connected by the Schaffer collateral and Mossy fibers. CA1/CA3- Cornu Ammonis regions 1and 3, DG- dentate gyrus. Adapted from (Bannerman et al., 2014; Deng et al., 2010).

1.2.5.1. Hippocampal cytogenic niche

The development of mammalian brain is a spatial and temporally orchestrated process that involves appropriate gene regulation to allow the NSCs to differentiate into distinct cell types, and ultimately to give rise to brain and spinal cord structures (Okano and Temple, 2009). NSCs reside in the adult mammalian brain and contribute to brain plasticity throughout life (Bond et al., 2015). Notably, not only in the embryonic but also in the postnatal brain, discrete anatomical regions contain a pool of NSCs, which continue differentiating into mature neurons and glia, a process called cytogenesis. Specifically, the transition of proliferative and multipotent NSCs to the three major central nervous system cell types is called neurogenesis (neurons) and gliogenesis (astrocytes, and oligodendrocytes) (Bond et al., 2015). Besides dendritic plasticity, adult hippocampal cytogenesis represents a key form of neuronal plasticity and it has been implicated in different cognitive domains, such as reference memory, behavioral flexibility and pattern separation/completion (Dupret et al., 2008; Nakashiba et al., 2012; Snyder et al., 2005). Indeed, suppression of hippocampal cell proliferation in naive animals through irradiation or the use of transgenic models of cytogenesis ablation has been shown to be related with the development of deficits in different behavioral dimensions (Snyder et al., 2011).

Thus, the proper control of the cytogenic process is crucial for normal brain function. The ability of NSCs to integrate extrinsic and intrinsic signals to control their plasticity is controlled by transcription factors under the regulation of epigenetic mechanisms. A clear example is DNA methylation, impacting multiple aspects of neurogenesis from stem cell maintenance and proliferation, fate specification, neuronal differentiation and maturation, and synaptogenesis (Jobe and Zhao, 2017). Neurogenesis is defined as a process of generating functional neurons from precursors, occurring in embryonic stages and prevailing

throughout life (Ming and Song, 2011). In the adult stage, this process occurs in two specific brain areas: the subgranular zone (SGZ) in the DG of the hippocampus and the subventricular zone (SVZ) lining the lateral ventricles (Gage, 2000). Within the hippocampal DG, newly-born cells are produced in the SGZ, a thin band between the granule cell layer and the hilus, which provides a singular microenvironment for the maintenance of NSCs population. When committed to the neuronal lineage, these cells migrate to the granule cell layer (GCL), where the maturation to granule neurons occurs and the vast majority becomes excitatory glutamatergic neurons (Seri et al., 2004). Adult hippocampal neurogenesis mainly reviews embryonic neurogenesis and consists of 4 main steps: firstly, the quiescent NSC population called radial glia-like cells (RGLs, type 1 cells) is activated and can generate proliferating intermediate progenitor cells (IPCs, type 2 cells). These type 2 cells can generate neuroblasts (type 3) that subsequently differentiate and mature into adult-born dentate granule cells (Ming and Song, 2011) (**Figure 8**). These new functional neurons integrate the pre-existing neuronal circuitry, and modulate local neural plasticity and network (Deng et al., 2010). This incorporation is essential for hippocampal integrity and function, regulating a wide variety of biological processes such as learning, memory, emotion and neurodegeneration (Deng et al., 2010; Horgusluoglu et al., 2017; Santarelli et al., 2003). The coordinated action of transcription factors and epigenetic regulators is critical for the differentiation of embryonic NSCs into the vast diversity of neuronal and glial populations present in the adult brain. Significant developments have been made in our understanding of the regulation of adult hippocampal neurogenesis. Next, the most recent findings on the role of TET enzymes in brain function, namely in neurogenic process will be reviewed.

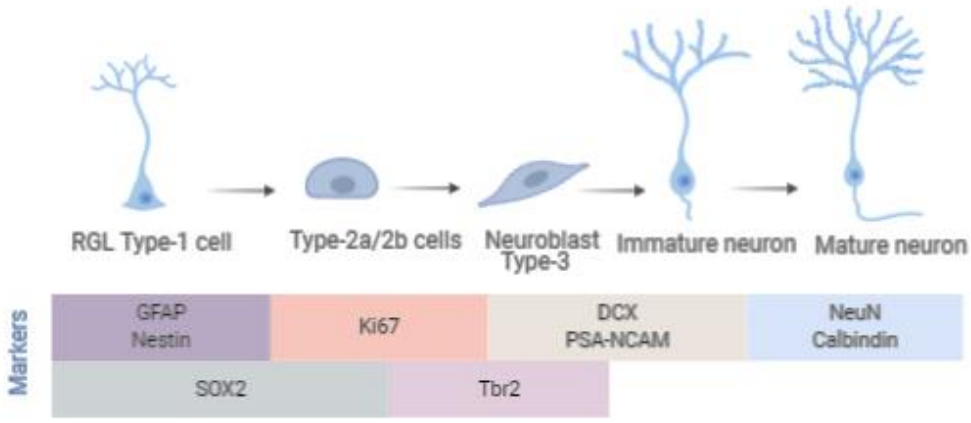

Figura 8 Representation of the adult hippocampal neurogenic process.
The developmental stages and the corresponding stage-specific markers are described.GFAP (glial fibrillary acidic protein); Sox2 (SRY box 2); Tbr2 (T box brain protein 2); PSA-NCAM (Polysialylated-neural cell adhesion molecule); DCX (doublecortin); NeuN (neuronal nuclei).

1.3. TET enzymes in brain function and behavior control

All TETs are expressed in the brain, with TET3 being expressed the highest in the cerebellum, cortex, and hippocampus, followed by TET2 and TET1, which has much lower expression than the other two enzymes (Szwagierczak et al., 2010). All TETs exhibit strong co-localization with the neuronal marker NeuN (Kaas et al., 2013; Li et al., 2014; Mi et al., 2015), which is in line with 5hmC enrichment; it remains unclear what are the levels of expression in other non-neuronal cells in the CNS. To date, there is only one report showing TET1 expression in the soma of glial fibrillary acidic protein (GFAP) positive cells, hence identified as astrocytes, in the adult mouse hippocampus (Kaas et al., 2013). TET2 and TET3 expression has not been addressed in this type of cells, but our results suggest absence of TET3 expression in astrocytes, at least in the adult stage. Regarding oligodendrocytes, expression of all TET enzymes from the embryonic development until P30 was detected in the corpus callosum (Zhao et al., 2014). The expression from that moment until the adult stage remains to be clarified, as well as its expression in other brain regions.

Since 2011, many studies have shown the importance of TET enzymes in neurophysiology and brain function (Antunes et al., 2019; Santiago et al., 2014), which are summarized in **Table 1** and described in detail for each TET, in the following sections.

1.3.1. TET1

TET1, the first enzyme described as being capable of catalyzing the conversion of 5mC into 5hmC (Tahiliani et al., 2009a), is the best-studied TET family member in the brain.

Regarding neurophysiology, two main studies are reporting how TET1 is regulated in basal physiology. Kaas and collaborators observed that *Tet1* transcript levels are downregulated by neuronal activity either *in vitro,* when primary hippocampal neurons were incubated with KCl, resulting in cellular depolarization, or *in vivo,* in the dorsal CA1 subregion, after flurothyl-induced seizures or after fear conditioning (Kaas et al., 2013). All these approaches resulted in a significant reduction in *Tet1* mRNA levels compared to controls, while the transcripts of *Tet2* and *Tet3* did not consistently respond to stimulation using any of these activity-inducing paradigms. On the other hand, Yu and collaborators did not observe changes in *Tet1* (and *Tet2*) transcript levels when hippocampal neurons in culture were treated with bicuculline, a $GABA_A$ receptor antagonist commonly used to induce a robust increase in neuronal firing and synaptic activity, or with Tetrodotoxin (TTX), which decreases global synaptic activity (Yu et al., 2015). Additionally, TET1 KO mice exhibited normal basal synaptic transmission and presynaptic excitability in hippocampal slices (Kumar et al., 2015; Rudenko et al., 2013).

In terms of synaptic plasticity in the Schaffer collateral-CA1 pathway, it was observed that LTD was significantly increased in the TET1 KO mouse (Rudenko et al., 2013), whereas hippocampal LTP remained normal (Kumar et al., 2015; Rudenko et al., 2013). Considering that LTD is regulated by AMPA receptor trafficking and Arc modulates the trafficking of AMPA-type glutamate receptors (AMPARs) (Clem and Huganir, 2010; Liu and Cull-Candy, 2000), the observed downregulation of Arc (Rudenko et al., 2013) may affect proper function of various components of LTD machinery. Additionally, previous studies demonstrated a connection between LTD and memory extinction (Dalton et al., 2008; Kim et al., 2011; Ryu et al., 2008; Tsetsenis et al., 2011). Additionally, overexpression of either the catalytic active or inactive forms of TET1 peptide did not lead to any significant effects in LTP either (Kumar et al., 2015).

In terms of basal electrophysiology findings, *in vitro* work showing that *Tet1* knockdown (KD) in primary hippocampal neurons leads to increased miniature excitatory postsynaptic current (mEPSC) amplitudes (Yu et al., 2015).

The TET1 KO mouse model was used to unravel a potential connection between TET1 protein function and behavior/cognitive processes. In terms of learning and memory, there are conflicting results (Rudenko et al., 2013; Zhang et al., 2013). Zhang and colleagues addressed the putative involvement of TET1 in neural plasticity using hippocampal-dependent cognitive tasks, such as spatial memory (Broadbent et al., 2004). Both WT and Tet1 KO mutants exhibited similar escape latency and swim path to the visible platform, suggesting comparable vision and motivation between the two groups. However, when short term memory retention was tested (24 hours after the 5-day training), the mutant group showed significant deficiency in reaching the virtual platform, measured by both the platform crossing and the time spent in the target quadrant, indicating that *Tet1* deficiency can lead to impairment in spatial learning and short-term memory. The brain structure was analyzed but no obvious morphological or developmental brain abnormalities were observed (Zhang et al., 2013), as reported by other authors (Rudenko et al., 2013). Considering adult neurogenesis implication in spatial learning and memory, a potential link between memory impairment and the lack of TET1 was further explored. Using Nestin-GFP transgenic mice, the authors observed that, when TET1 was ablated in neural precursor cells, the number of GFP-positive cells in the subgranular zone of the hippocampal dentate gyrus (DG) in adult mice was dramatically reduced, by 45%, compared to WT animals (Zhang et al., 2013). NPCs isolated from the DG of Tet1 KO produced fewer and smaller primary neurospheres compared to WT controls. Upon differentiation *in vitro*, the neurospheres from mutant mice were normally tripotent, with similar potential for the generation of neurons, astrocytes, and oligodendrocytes in comparison to WT neurospheres. Analysis of gene expression and methylation changes in TET1 KO mice revealed decreased expression of

a cohort of genes involved in neurogenesis, including Galanin (Gal), Ng2 (Cspg4) and Neuroglobin (Ngb). Methylation analysis using gene-specific bisulfite sequencing showed that the promoter regions of these genes were hypermethylated, suggesting that TET1 positively regulates adult neurogenesis through the oxidation of 5mC to 5hmC in these genes (Zhang et al., 2013).

In contrast to the results by Zhang and collaborators, Rudenko and colleagues reported normal short-term memory and spatial learning, but impaired memory extinction of both contextual fear memory and spatial reference memory (Rudenko et al., 2013). The authors observed normal locomotor behavior and no changes in anxiety and depressive-like behaviors, as well as no difference, was observed in contextual learning and cued fear memory acquisition. However, regarding memory extinction, the authors reported impaired memory extinction in TET1 KO mice, both after contextual fear conditioning and for hippocampus-dependent spatial reference memory, using the Morris water maze (MWM) test. Several neuronal activity-regulated genes were found to be downregulated, namely *Arc*, *Npas4* and *c-Fos*, in the cortex and hippocampus. Hypermethylation of the *Npas4* promoter region was observed in in the cortex and in the hippocampus of both naïve TET1 KO mice and after extinction training. *Npas4* is a transcription factor highly expressed in the brain which regulates the formation and maintenance of inhibitory synapses in response to excitatory synaptic activity; it was shown to be a key regulator of transcriptional programs involving neural activity-regulated genes and essential for contextual memory formation and regulation of cognitive and social functions (Coutellier et al., 2012; Ramamoorthi et al., 2011).

These results might indicate independent epigenetic programs being activated during memory acquisition versus memory extinction. Nonetheless, the discrepancy between TET1 role in spatial learning and memory could also be explained by the differences in the TET1 KO mouse models, with distinct exons being targeted (exon 4 in the study by Rudenko et al., resulting in an unstable truncated form; and exons 11-13 in the study by Zhang et al., which are part of the catalytic domain). Moreover, no other learning and memory tasks were used beyond MWM in the study by Zhang and colleagues, whereas Rudenko and colleagues used Pavlovian fear conditioning showing that TET1 mutant mice have normal memory acquisition.

Additionally, a curious finding was the observation of memory enhancement in TET1 KO animals, namely threat recognition learning, long-term memory and remote memory consolidation (Kumar et al., 2015). Consistent with a previous study (Rudenko et al., 2013), this group found normal threat memory acquisition and short-term fear memory in TET1 KO mice. However, an enhancement in memory consolidation and long-term storage was observed in TET1 KO, using contextual and cued fear conditioning tests. These are apparent opposing results when compared with Zhang and colleagues work,

which showed an impairment in spatial learning (Zhang et al., 2013). Kumar and colleagues suggested that these might be attributed to the behavior test used since MWM and fear conditioning are both hippocampal-dependent tasks, but MWM may involve stronger and more aversive motivational factors than fear conditioning and occur over many more training trials of longer duration (Kumar et al., 2015). These differences might account for differential susceptibilities to effects of Tet1 KO in the water maze versus fear conditioning behavioral tests.

Using a virally mediated knockdown of *Tet1* mRNA in the dorsal hippocampus, they also observed an enhancement in hippocampus-dependent long-term spatial memory for object location (Kumar et al., 2015). Zhang and colleagues reported that TET1 KO impairs hippocampal-dependent spatial short-term memory, using the MWM test (Zhang et al., 2013). Hence, distinct roles for TET1 in different memory types can explain these differences. At the molecular level, Kumar and colleagues also found that TET1 ablation resulted in altered expression of numerous neuronal activity-regulated genes, such as increased expression of *Bdnf* and decreased levels of *Arc*, *Fos* and *Npas4*, as previously observed by others (Rudenko et al., 2013). Interestingly, a compensatory upregulation of *Tet2* and *Tet3* was reported, together with increased transcript levels of other genes involved in the active DNA demethylation pathway, such as *Gadd45b*, *Smug*, *Apobec1* and *Tdg*. Intriguingly, a strong upregulation was also observed for DNA methyltransferases *Dnmt1*, *Dnnmt3a* and *Dnmt3b*, suggesting coordination of the epigenetic regulators transcriptional network in the CNS (Kumar et al., 2015).

In addition to loss-of-function studies, the discovery that TET1 expression is downregulated in the dorsal CA1 of mice after fear learning motivated gain-of-function studies: TET1 overexpression (OE) in the dorsal hippocampus did not affect exploratory or anxiety-like behavior but impaired long-term, but not short-term, memory in the contextual fear conditioning (CFC) test (Kaas et al., 2013). This deficit in long-term memory formation was observed for both catalytically active and inactive forms of TET1, suggesting that TET1's role in memory formation is independent of its catalytic activity but may rely on an allosteric mechanism and contribute to explain non-redundancy between TET enzymes. Importantly, the authors found the same set of genes (*Fos*, *Nr4a2*, *Bdnf*, *Homer1*) upregulated by overexpression of TET1 and TET1m, suggesting that TET1 regulates the expression of these genes, at least in part independently of 5mC to 5hmC conversion, and that these genes might be responsible for the memory dysfunction. Another gain-of-function study has shown that overexpression of either the catalytically active or the catalytically inactive TET1 peptide did not lead to any significant effect on LTP compared with control, and basal synaptic transmission also remained constant (Kumar et al., 2015).

Additionally, TET1 overexpression, but not TET1m, led to an increase in 5hmC levels in the microdissected CA1 area, concomitant with a decrease in global 5mC levels, suggesting an increase in global 5mC to 5hmC conversion (Kaas et al., 2013). Furthermore, TET1 OE resulted in upregulation of many neuronal activity-related genes such as *c-Fos*, *Bdnf*, *Arc*, *Egr1* (Kaas et al., 2013), whereas TET1 KO resulted in downregulation of some of these genes (Rudenko et al., 2013). Therefore, considering the downregulation of IEGs in TET1 KO mice and their upregulation in TET1 OE in hippocampal regions, these studies suggest that *Tet1* bidirectionally regulates IEGs levels. Similarly, Guo and collaborators performed overexpression of TET1, and TET1m, in the adult mouse dentate gyrus and observed that OE of TET1, but not TET1m, led to an increase in the levels of 5hmC by 43% (Guo et al., 2011b). Concerning methylation levels at specific neuronal-genes, namely *Bdnf* and *Fgf1*, the authors reported that overexpression of TET1, but not TET1m, led to significant decreases in CpG methylation levels at promoter IX of Bdnf and brain-specific promoter of Fgf1. On the other hand, *Tet1* knockdown in the adult dentate gyrus completely abolished electroconvulsive stimulation (ECS)-induced demethylation of both Bdnf IX and FGF1B, suggesting that Tet1 is required for neuronal activity-induced, region-specific, active DNA demethylation and gene expression in the adult brain (Guo et al., 2011b).

Together, these findings support that TET1 contributes to basal neuronal 5hmC levels, and this interferes with the regulation of important neuronal regulatory genes. However, the behavioral effects of TET1 should still motivate further investigation, considering the discrepant results in short-term memory and spatial learning.

1.3.2. TET2

TET2 is the least characterized TET enzyme member in the brain, despite its high level of expression (Szwagierczak et al., 2010). Whilst brain defects have not been described in TET2 KO mouse model (Ko et al., 2011; Li et al., 2011), a behavioral characterization was missing.

Regarding neurophysiology, *in vitro* studies using hippocampal neurons did not show changes in *Tet2* mRNA levels after global synaptic activity increase or decrease, induced by bicuculline or tetrodotoxin, respectively. However, the association of this enzyme with basal synaptic transmission has been observed since hippocampal neurons with decreased *Tet2* expression exhibited increased mEPSC, similarly to what was observed in *Tet1* KD (Yu et al., 2015).

Additionally, a role for TET2 in neurogenesis was firstly proposed by Hahn and collaborators, as the double knockdown of *Tet2* and *Tet3* in the mouse embryonic cortex led to defects in the differentiation of the cells migrating from the subventricular zone to the cortical plate (Hahn et al., 2013). More recently, another work using a TET2 KO mouse model showed that depletion of TET2 leads to increased adult neural stem cell proliferation, but reduced differentiation capacity *in vitro* and *in vivo* (Li et al., 2017). Mechanistically, the authors show that Tet2 physically interacts with forkhead box O3 (Foxoa3) and regulates expression of genes related to neural stem cell proliferation. Foxoa3 is a mammalian forkhead family member, well known to regulate gene expression and help preserve an intact pool of neural stem cells, at least in part by negatively regulating neuronal differentiation (Rafalski and Brunet, 2011). To overcome the limitations of a constitutive full knockout model, a more recent work used a conditional model ablating Tet2 in adult Neural Precursor Cells (NPCs) and demonstrated that the specific deletion of this enzyme in adult NPCs is sufficient to impair the neurogenic process, translated by a significant decrease in the number of Doublecortin (Dcx)-positive newly born neurons, Bromodeoxyuridne (BrdU)-positive cells and BrdU/NeuN-positive mature differentiated neurons (Gontier et al., 2018). The authors also observed that decreased levels of *Tet2* expression, achieved by shRNA injection in the hippocampal neurogenic niche, resulted in a significant decrease in the number of NPCs and newly born neurons, as observed by conditional deletion in NPCs.

Additionally, for the first time, a behavioral evaluation was performed, showing that reducing *Tet2* levels in the hippocampus impairs cognitive function, namely hippocampal-dependent learning and memory which were assessed using radial arm water maze (RAWM) and contextual fear-conditioning (CFC) paradigms (Gontier et al., 2018). Both the animals presenting a global abrogation of TET2 in the Dentate Gyrus (known as the adult hippocampal neurogenic niche) and mice carrying a conditional deletion of TET2 in adult NPCs showed worse performance in finding the platform location during both short-term and long-term learning and memory probes. When measuring the freezing time after fear conditioning training, both TET2 ablation models showed decreased freezing time during contextual but not cued, memory testing. Thus, TET2 decreased levels in the adult neurogenic niche, or specifically in adult NPCs resulted in impaired long-term hippocampal-dependent spatial learning and memory and associative fear memory acquisition. Interestingly, the authors also observed that restoration of TET2 levels in the aged brain was sufficient to rescue age-related regenerative decline as observed by the increased number of NPCs and newly-born neurons, the similar learning capacity in RAWM performance and an increased freezing time during contextual memory test when comparing animals under this rescue with the control

group (Gontier et al., 2018). These findings suggest an important role for TET2 in the regulation of neurogenesis and cognitive functions, and a key molecular mediator of neurogenic rejuvenation.

1.3.3. TET3

The most highly expressed TET enzyme member in the brain, TET3, was also described as an essential enzyme in neuronal differentiation, including maintenance of NPCs *in vitro (Li et al., 2015a)*. More recently, this enzyme was also associated with NSCs maintenance *in vivo*. Its ablation causes large reduction in the NPCs pool in the SVZ niche (Montalban-Loro et al., 2019). Also, neuroespheres isolated from $Tet3^{flox\ flox}$-Gfap-Cre adult mice, yielded fewer primary and secondary neurospheres when compared to control. Yet, contrary to the observed effect of TET3 deficiency in neural progenitors derived from ESCs, which presented increased apoptosis and decreased survival rates (Li et al., 2015a), *Tet3* deficiency in adult NSCs does not modify apoptosis or survival rates (Montalban-Loro et al., 2019). However, *Tet3* deletion triggered premature differentiation of NSCs into astrocytes, justified by the involvement of TET3 in the direct binding to the paternal transcribed allele of the imprinted gene Small nuclear ribonucleoprotein-associated polypeptide N (*Snrpn*). Importantly, it was demonstrated that TET3 binds to *Snrpn* promoter independently of its catalytic function (Montalban-Loro et al., 2019).

The possible impact of TET3 deletion in adult NSCs was not addressed in mouse behavior depending on neurogenesis. However, *Snrpn* belongs to the Prader-Willi imprinted gene cluster and patients with Prader-Willi syndrome lack expression of *Snrpn* and exhibit neurological problems including learning difficulties (Buiting, 2010; Butler, 2011). Montalbán-Loro and colleagues suggested that *Snrpn* overexpression impacts the NSC pool in adults, opening perspectives to the etiology of this disorder (Montalbán-Loro et al., 2019).

Regarding neurophysiology, TET3 was described as a synaptic activity sensor, since TET3 levels are sensible to neuronal activity, and this enzyme reacts to it, mediating homeostatic synaptic transmission (Yu et al., 2015). Synaptic activity bi-directionally regulates neuronal Tet3 expression, and consequently, Tet3 controls glutamatergic synaptic transmission through regulation of target genes, namely GluR1 levels (Yu et al., 2015). Neurons with *Tet3* knockdown exhibited substantially larger miniature glutamatergic excitatory postsynaptic current (mEPSC) amplitudes whereas *Tet3* overexpression decreased this parameter. It should be noted that although both *Tet1* and *Tet2* knockdowns also increase mEPSC amplitudes, the effects are less pronounced. Furthermore, when DNA demethylation was inhibited through the blocking of the two major components of the BER pathway, the poly (ADP-ribose) polymerase

or the apurinic/apyrimidinic endonuclease, the mEPSC amplitudes were also increased, resembling the *Tet3* KD (Yu et al., 2015). These results suggest that excitatory synaptic transmission in neurons is regulated through DNA oxidation via TET and, subsequently, BER.

Additionally, it was shown that Tet3 is required for homeostatic synaptic plasticity. Both Tet3 KD and BER inhibition elevated mEPSC amplitudes linearly across the spectrum under basal conditions, which was comparable to the scaling-up effect induced by TTX treatment in normal neurons. Thus, downregulation of Tet3 signaling appears to be sufficient to induce scaling-up. On the other hand, neurons overexpressing Tet3 exhibited reduced mEPSC amplitudes linearly across the spectrum, resembling bicuculline-induced scaling-down in normal neurons. Hence, the authors suggested that global synaptic activity modulates Tet3 expression and DNA demethylation activity, which in turn mediate homeostatic synaptic scaling-up or scaling-down (Yu et al., 2015).

A key cellular mechanism regulating both basal glutamatergic synaptic transmission and homeostatic scaling is the control of surface levels of glutamate receptors. Yu and colleagues have shown that Tet3 regulates basal excitatory synaptic transmission via regulating surface glutamate receptor 1 (GluR1) levels (Yu et al., 2015). Also, *Tet3* knockdown was sufficient to elevate surface GluR1 levels and prevented further changes induced by TTX or bicuculline treatments. Regulation of Arc levels appears to explain changes in surface GluR1 levels following Tet3 KD. Together, these results suggest that Tet3 and active DNA demethylation signaling respond to changes in global synaptic activity to re-establish a responsive cellular state. Moreover, transcriptome analysis of *Tet3*-KD neurons revealed differential expression of genes involved in the synapse and synaptic transmission, suggesting an essential role of Tet3 in regulating gene expression in response to changes in global synaptic activity. *Bdnf*, already described as undergoing active demethylation in depolarized neurons (Ma et al., 2009a) and implicated in synaptic transmission and synaptic scaling (Rutherford et al., 1998), was hypermethylated at the promoter IV region in *Tet3* KD neurons, with a consequent decrease in its expression. Interestingly, whereas Tet1-deficient neurons exhibited hypermethylation at Arc and Npas4 promoters (Rudenko et al., 2013), Tet3-KD neurons did not. No changes in methylation were observed at the *Arc* or *Npas4* promoter regions, suggesting that activity-induced expression of immediate early genes Arc and Npas4 is mediated by the oxidative function of Tet1, but not of Tet3. A physical interaction between TET3 and *Bdnf IV* promoter region was described by the authors in neurons, using chromatin immunoprecipitation (ChIP)-PCR analysis (Yu et al., 2015).

A recent paper used CRISPR-Cas9 technology, termed 2-cell embryo-CRISPR-Cas9 injection (2CC), to induce *in vivo Tet3* loss-of-function and recorded AMPAR-mediated miniature excitatory postsynaptic currents (mEPSCs) from layer 2/3 pyramidal neurons of the primary somatosensory cortex of P14

chimeric mice and from hippocampal CA1 neurons (Wang et al., 2017). The authors observed that *Tet3*-mutant neurons had a significantly higher mEPSC frequency and a similar mEPSC amplitude in layer 2/3 neurons whereas in the hippocampus both the frequency and amplitudes were significantly increased, suggesting an important role of endogenous Tet3 in negatively regulating excitatory synaptic transmission in young mice. These findings corroborated Yu and colleagues *in vitro* studies reporting the role of TET3 in the downregulation of excitatory synaptic transmission. Bisulfite sequencing analyses revealed slightly increased CpG methylation at the *Bdnf* IV, IX and *Wfdc2* promoter regions, consistent with Yu and colleagues, but not on the Npas4 promoter-exon 1 junction or the Fgf1G and Ndst1 promoter regions. Additionally, loss of TET3 function significantly reduced both the frequency and amplitude of $GABA_AR$-mediated inhibitory synaptic transmission, as measured by miniature inhibitory post-synaptic currents (mIPSCs) in the cortical layers 2/3 pyramidal neurons and hippocampal CA1 region, suggesting a promoting role of endogenous *Tet3* in regulating inhibitory synaptic transmission as well (Wang et al., 2017).

In vivo behavioral studies correlated *Tet3* mRNA expression levels in the hippocampus with neuronal activity after Contextual Fear Conditioning (CFC) behavioral test. The authors observed that *Tet3* mRNA transcripts, but not *Tet1* and *Tet2*, were upregulated after 30 min and 3h, but returned to baseline after 24h (Kremer et al., 2018). Importantly, Tet3 expression was not modified by cold swim stress suggesting that the changes were specific to memory formation in CFC and were not related to the stress response elicited by fear conditioning. When the NMDA (N-methyl-D-aspartate) receptors were activated in primary hippocampal neurons, *Tet3* mRNA levels were upregulated, suggesting that NMDA receptor signaling increases Tet3 transcription. Expression levels of *mir-29b* were also altered, being downregulated, after NMDA receptors stimulation indicating another target of this glutamate receptor. Transcriptional analysis in hippocampus 30 minutes after training showed that synaptic plasticity and genes related with memory, such as *Notch1*, *Creb1*, *Crebbp* and *Gadd45b* are sensitive to TET3 upregulation (Kremer et al., 2018).

Li and collaborators described upregulation of *Tet3* transcript levels, but not *Tet1* as reported by others (Guo et al., 2011b; Zhang et al., 2013), in primary cortical neurons after 7h and 10h of KCl-induced depolarization (Li et al., 2014). Consistently, Tet3 was also upregulated in the infralimbic prefrontal cortex (ILPFC) after fear extinction training. Moreover, *Tet3* knockdown in the ILPFC resulted in normal fear memory acquisition but impairment in fear extinction memory (Li et al., 2014). Genome-wide analyses revealed that 16% of genes with 5hmC gain after fear extinction training were associated with synaptic signaling. One example was *Gephyrin* gene, which anchors GABA receptors to the postsynaptic membrane and is directly involved in fear extinction, showing a gain of 5hmC accompanied by a 5mC

decrease within an intron, 24h post-extinction training. An increase in *Gephyrin* mRNA transcripts was also observed transiently 2 hours after extinction training, together with an increase in TET3 occupancy surrounding the *Gephyrin* gene, suggesting that DNA methylation can be dynamically regulated after learning. The effect of extinction learning on Tet3 occupancy at the gephyrin locus, as well as the dynamic changes in the accumulation of 5hmC and 5mC, gephyrin mRNA and associated effects on the chromatin landscape were completely blocked in the presence of Tet3 shRNA (Li et al., 2014). Together, these results suggest that Tet3 activity within the ILPFC is necessary for the learning-dependent accumulation of 5hmC and related chromatin modifications, which underpins rapid behavioral adaptation.

Overall, these studies suggest that *Tet3* has an important role in fear extinction memory, probably through modulation of synaptic genes. However, it is still unclear if TET3 influences other cognitive behaviors, such as memory and learning, and what are the mechanisms underlying the neuronal activity, mediated by this enzyme.

Table 1 Phenotypes of full or conditional knockout (cKO) and knockdown (KD) of TET enzymes in neuronal plasticity and behavior (Antunes et al., 2019).

TET	Type of deletion	Region/Cell type	Behavioral and Neurophysiologic Phenotype	Molecular alterations	References
TET1	KO (*in vivo*)	Constitutive	Impairment in memory extinction; enhanced LTD	Decreased expression of Arc, Npas4, c-Fos; hypermethylation of Npas4 in the hippocampus and cortex	(Rudenko et al., 2013)
	KO (*in vivo*)	Constitutive	Impairment in spatial learning and short- term memory	Decreased expression and hypermethylation of Gal, Cspg4 and Ngb in TET1 KO NPCs	(Zhang et al., 2013)
	KO (*in vivo*)	Constitutive	Enhancement in memory consolidation and long-term storage	Decreased expression of Arc, Egr1, Npas4 and c-Fos; increased expression of Creb1, Bdnf, Calcineurin, Cdk5, Nr4a2 in the hippocampal CA1 region	(Kumar et al., 2015)
	KD (in vivo)	Dorsal Hippocampus	Enhancement of spatial memory for object location	No analyzes were performed	(Kumar et al., 2015)
	KD (*in vitro*)	Neurons	Increased mEPSC amplitudes	No analyzes were performed	(Yu et al., 2015)
TET2	cKO (*in vivo*)	Adult neural progenitor cells	Impairment of short and long-term learning and memory	No analyzes were performed	(Gontier et al., 2018)
	KD (*in vitro*)	Neurons	Increased mEPSC amplitudes	No analyzes were performed	(Yu et al., 2015)
TET3	KD (*in vivo*)	ILPF cortex	Impairment in fear extinction memory	Inhibition of the increase of expression and 5hmC gain of Gephyrin locus in the ILPFC	(Li et al., 2014)
	cKO(*in vivo*)	Adult neural stem cells	No analyses were performed	Increased expression of Snrpn and BMP2	(Montalban-Loro et al., 2019)
	KO (*in vivo; CRISPR-mediated*)	Constitutive (Tet3-mutant chimeras)	Increased mEPSC frequency in CA1 and cortex layer 2/3 neurons	Slight hypermethylation (and decrease in expression) of Bdnf IV, IX and Wfdc2	(Wang et al., 2017)
	KD (*in vitro*)	Neurons	Increased mEPSC amplitudes and decreased mIPSC frequency and amplitudes	Increased expression of Glur1 and decreased expression and hypermethylation of Bdnf IV	(Yu et al., 2015)

Context and Aims

5-Hydroxymethylcytosine (5hmC), converted from 5-methylcytocine (5mC) by TET enzymes, is enriched in embryonic stem cells (ESCs) and in the brain. Additionally, neural differentiation is under strict epigenetic regulation. Thus, the role of TET enzymes in neural precursor cells maintenance and differentiation is a central topic of research. Simultaneously, DNA demethylation is a dynamic process regulating gene expression in an experience-dependent manner and, consequently, a reasonable mediator of neuronal plasticity and behavior. TET3 is the most expressed isoform in the brain, remaing to elucidate its specific role. Thus, the foremost goal of this thesis is to unravel the role of TET3 enzyme in brain function; and the main hypothesis is that TET3 is able to regulate the expression of genes involved in neural precursor cells differentiation and neuronal function. For that, two distinct cell types were targeted, *in vitro* and *in vivo* respectively, Neural Precursor Cells (NPCs) and post-mitotic neurons.

In this context two major aims were established:

1. To characterize the expression levels of TET enzymes and the impact of *Tet3* KD in neural precursor cells (NPCs). Concretely, to analyse the expression of both, pluripotency and neural markers, in *Tet3* KD cells and the respective control. Additionally, to perform an analyze of genome-wide DNA methylation in both experimental groups.

2. To accomplish a comprehensive characterization using a mouse model to induce conditional and inducible deletion of *Tet3* enzyme. To characterize the behavior of males and females mice, at emotional and cognitive level, and the molecular impact of *Tet3* deletion performing RNA sequencing and/or qPCR analysis.

Chapter II

TET3 regulates cellular identity and DNA methylation in neural progenitor cells

Mafalda Santiago, Claudia Antunes, Marta Guedes, Michelina Iacovino, Michael Kyba, Wolf Reik, Nuno Sousa, Luísa Pinto, Miguel R. Branco, C. Joana Marques

Manuscript accepted for publication in October of 2019 in Cellular and Molecular Life Sciences (CMLS)

TET3 regulates cellular identity and DNA methylation in neural progenitor cells

Mafalda Santiago[1,2,8], Claudia Antunes[1,2,8], Marta Guedes[1,2], Michelina Iacovino[3], Michael Kyba[3,4], Wolf Reik[5,6], Nuno Sousa[1,2], Luísa Pinto[1,2], Miguel R. Branco[7*], C. Joana Marques[1,2,9*]

[1]Life and Health Sciences Research Institute (ICVS), School of Medicine, University of Minho, Braga, 4710-057, Portugal.

[2]ICVS/3B's - PT Government Associate Laboratory, Braga/ Guimarães, 4710-057, Portugal.

[3]Lillehei Heart Institute, University of Minnesota, Minneapolis, MN, 55455, USA.

[4] Department of Pediatrics, University of Minnesota, Minneapolis, MN, 55455, USA.

[5]Epigenetics Programme, The Babraham Institute, Cambridge CB22 3AT UK;

[6]The Wellcome Trust Sanger Institute, Cambridge CB10 1SA, UK.

[7]Blizard Institute, Barts and The London School of Medicine and Dentistry, Queen Mary University of London, London, E1 2AT, UK.

[8]Co-first authors

[9]Present address: Genetics, Department of Pathology, Faculty of Medicine, University of Porto, Porto, 4200-319, Portugal; i3S – Instituto de Investigação e Inovação em Saúde, Universidade do Porto, Porto 4200-135, Portugal

*Corresponding author:

Joana Marques - cmarques@med.up.pt or Miguel Branco - m.branco@qmul.ac.uk

Address: Genetics, Department of Pathology

Faculty of Medicine, University of Porto

Porto, 4200-319, Portugal

2.1. Abstract

TET enzymes oxidize 5-methylcytosine (5mC) into 5-hydroxymethylcytosine (5hmC), a process thought to be intermediary in an active DNA demethylation mechanism. Notably, 5hmC is highly abundant in the brain and in neuronal cells. Here we interrogated the function of *Tet3* in neural precursor cells (NPCs), using a stable and inducible knockdown system and an *in vitro* neural differentiation protocol. We show that *Tet3* is upregulated during neural differentiation, whereas *Tet1* is downregulated. Surprisingly, *Tet3* knockdown led to a de-repression of pluripotency-associated genes such as *Oct4*, *Nanog* or *Tcl1*, with concomitant hypomethylation. Moreover, in *Tet3* knockdown NPCs we observed the appearance of OCT4-positive cells forming cellular aggregates, suggesting de-differentiation of the cells. Notably, *Tet3* KD led to a genome-scale loss of DNA methylation and hypermethylation of a smaller number of CpGs that are located at neurogenesis-related genes and at imprinting control regions (ICRs) of *Peg10*, *Zrsr1* and *Mcts2* imprinted genes. Overall, our results suggest that TET3 is necessary to maintain silencing of pluripotency genes and consequently neural stem cell identity, possibly through regulation of DNA methylation levels in neural precursor cells.

2.2. Introduction

DNA methylation, or 5-methylcytosine (5mC), is an epigenetic modification that consists of a methyl group added to the fifth position of cytosines, occurring more frequently in the context of CpG dinucleotides (Bird, 2002). Albeit deemed as a very stable chemical modification, waves of global loss of DNA methylation occur during critical periods of development such as in the zygote and in primordial germ cells (Seisenberger et al., 2013). Additionally, loss of DNA methylation has been observed in post-mitotic cells, with activity-dependent demethylation occurring in mature neurons upon depolarization (Guo et al., 2011a; Ma et al., 2009b). This mechanism of active DNA demethylation remained elusive for a long time, but the finding that TET enzymes can convert 5mC into 5-hydroxymethylcytosine (5hmC), and subsequently into 5-formylcytosine (5fC) and 5-carboxylcytosine (5caC) (Ito et al., 2011; Kriaucionis and Heintz, 2009; Pfaffeneder et al., 2011; Tahiliani et al., 2009b), shed light into this mechanism. Importantly, 5hmC was shown to accumulate in the paternal pronucleus and in PGCs concomitantly with methylation loss (Hackett et al., 2013; Iqbal et al., 2011; Wossidlo et al., 2011) and to appear in an antagonistic way to 5mC in the genome of dentate granule neurons (Guo et al., 2014b). Three members

- TET1, TET2 and TET3 - compose the family of TET enzymes, which are Fe^{2+} and 2-oxoglutarate-dependent dioxygenases. TET1 and TET3 contain a CXXC zinc finger domain at their amino-terminus that is known to bind CpG sequences, whereas TET2 partners with IDAX, an independent CXXC-containing protein (Ko et al., 2013a; Kohli and Zhang, 2013). 5hmC was first described in mouse embryonic stem (ES) cells and in Purkinje neurons (Kriaucionis and Heintz, 2009; Tahiliani et al., 2009b) and was later shown to be most abundant in the brain, namely at the cerebellum, cortex and hippocampus brain regions (Szwagierczak et al., 2010). Moreover, TET enzymes were shown to be expressed in these brain regions, with *Tet3* showing highest expression (Szwagierczak et al., 2010). Additionally, in the embryonic mouse brain, 5hmC levels were shown to increase during neuronal differentiation, as the cells migrate from the ventricular zone to the cortical plate (Hahn et al., 2013). In neurons, 5hmC was associated with gene bodies of activated neuronal function-related genes and gain of 5hmC was concomitant with loss of the repressive histone mark H3K27me3 (Hahn et al., 2013). Notably, TET enzymes have also been implicated in brain processes and functions such as neurogenesis, cognition and memory (Gontier et al., 2018; Kaas et al., 2013; Li et al., 2014; Rudenko et al., 2013; Zhang et al., 2013).

Here we addressed the functional role of TET enzymes in neural precursor cells (NPCs) by using an *in vitro* differentiation system where highly proliferative ES cells are differentiated into a homogeneous population of NPCs that are PAX6-positive radial glial cells (Bibel et al., 2004b) and a stable and inducible RNAi knockdown system (Iacovino et al., 2011a). We observed that knockdown (KD) of *Tet3* in NPCs resulted in upregulation of pluripotency genes and genome-wide loss of DNA methylation. Nevertheless, gain of methylation was also observed, particularly in genes involved in neural differentiation. Our data suggests that TET3 plays a role in maintaining both cellular identity and DNA methylation levels in neural precursor cells.

2.3. Results

Neural differentiation leads to *Tet3* upregulation

To investigate the effects of the knockdown of TET enzymes in NPCs, we established a stable and inducible knockdown system in mouse ES cells containing shRNAs targeting *Tet3* (Fig. S1a) (Ficz et al., 2011; Iacovino et al., 2011a) and a neural differentiation system that results in a homogeneous population of PAX6-positive radial glial-like neural precursor cells (**Fig. 1a, S1b, c**) (Bibel et al., 2007). In this differentiation protocol, ES cells are maintained in a highly proliferative state and then cultured in non-adherent conditions forming cellular aggregates; addition of Retinoic Acid (RA) four days after cellular

aggregates are formed results in upregulation of neural markers such as *Pax6*, *Nestin*, *Tubb3* (B3-tubulin) and *TrkB* (*Nrtk2*) (**Fig. 1b**), with between 92-96% of the differentiated cells staining positively for PAX6 (Fig. S1b, c). This indicates homogeneous differentiation of ES cells into NPCs as described in the original protocol (Bibel et al., 2004b). Positive staining of Beta 3-tubulin, which is one of the earliest markers of neuronal differentiation (Menezes and Luskin, 1994), was also observed (**Fig. S1b**). On the other hand, SOX2, which is a marker for neural stem cells that becomes inactivated in NPCs (Chew et al., 2005; Diaz de Leon-Guerrero et al., 2011), was nearly undetected (**Fig. S1b**). During differentiation, there was also a marked decrease in the expression of pluripotency genes such as *Oct4* and *Nanog*, as expected (**Fig. 1b**). Regarding epigenetic modifiers, we observed increased levels of *Tet3* and *Dnmt3a* during differentiation, whilst levels of *Tet1* decreased (**Fig. 1b**). Upregulation of *Tet3* during neuronal differentiation has been previously observed (Li et al., 2015b; Tan et al., 2013) and suggests a prominent role for *Tet3* in the neuronal lineage. We also confirmed the presence of TET3 protein in NPCs by immunostaining, showing a predominantly cytoplasmic distribution (**Fig. 1c**); this is consistent with a putative role for TET3 in oxidizing 5mC to 5hmC in RNA molecules (Fu et al., 2014).

Knockdown of *Tet3* in NPCs results in de-repression of pluripotency genes

We performed stable and inducible knockdown of *Tet3* in NPCs, using two independent shRNAs (**Fig. 2a and b**); *Tet3* knockdown was detected at both the mRNA and protein levels (**Fig. 2b and S2a**). Interestingly, we observed a significant upregulation of pluripotency genes, namely *Oct4, Nanog, Tcl1* and *Esrrb*, after *Tet3* KD (**Fig. 2b**), using two independent shRNAs. To further elucidate the observed upregulation of pluripotency genes, we performed immunostaining for OCT4 and observed the presence of OCT4-positive cells that appeared as cellular aggregates (**Fig. 2c**), representing around 14% of the total number of cells. Of note, OCT4-positive cells were not observed in NPCs treated with the Scrambled shRNA (**Fig. S3**); this suggests that Tet3 KD NPCs might have undergone a de-differentiation event due to downregulation of *Tet3* expression. This is in line with a recent report showing that *Tet3* can promote a rapid and efficient conversion of fibroblasts into neurons, showing that *Tet3* plays an important role in inducing and maintaining neural cell identity (Zhang et al., 2016a). In order to better understand the nature of these ES-cell like NPCs, we performed flow cytometry using Propidium iodide staining in KD NPCs and observed that *Tet3* KD NPCs still resemble control NPCs (Scrambled shRNA) more than ES cells, which show an extended S-phase comparing to NPCs (**Fig. S2b**). Additionally, we observed a significant increase in *Dnmt1* and decrease in *Dnmt3a* expression after *Tet3* KD (**Fig. 2b**), pointing to a co-regulation between TET enzymes and DNA methyltransferases.

These results suggest that functional perturbation of *Tet3* in NPCs leads to de-repression of pluripotency genes which might affect maintenance of the neural precursor cell identity.

Tet3 knockdown results in genome-scale loss of DNA methylation

As the above-mentioned results pointed to a critical role for *Tet3* in neural differentiation, we performed oxRRBS (oxidative Reduced Representation Bisulfite Sequencing) to analyse genome-wide changes in distribution of 5mC and 5hmC after *Tet3* knockdown. RRBS is a bisulfite-based protocol that enriches for CpG-rich parts of the genome, thereby reducing the amount of sequencing required, since it only covers 1% of the genome while capturing the majority of promoters and CpG islands (Gu et al., 2011a). In order to distinguish 5hmC from 5mC and since conventional sodium bisulphite treatment does not discriminate between the two modifications (Huang et al., 2010), we first added potassium perruthenate ($KRuO_4$) that triggers selective chemical oxidation of 5hmC to 5-formylcytosine (5fC), before bisulphite treatment. 5fC is then further converted to uracil after bisulphite treatment and subtraction of oxidative bisulphite readout from the bisulphite-only one allows determining the amount of 5hmC at a particular nucleotide, in a single-base resolution and quantitative manner (Booth et al., 2012; Booth et al., 2013). As the bisulphite signal is always expected to be larger than that of oxidative bisulphite, negative values are artefacts used to estimate the false discovery rate (FDR; see Methods). Notably, we could only detect 2,191 hydroxymethylated CpGs (out of ~0.5M) at a high FDR of 45% (**Fig. S4a**), which is in contrast with the low FDR (~3%) that we previously obtained in ES cells (Booth et al., 2012). This is likely due to the fact that 5hmC levels are low in NPCs comparing to mouse ES cells and hippocampus brain region (**Fig. S4b**, c) (Tan et al., 2013) and mostly present in intragenic regions (Hahn et al., 2013), whereas oxRRBS mainly captures promoters and CpG islands (Gu et al., 2011a).

Notwithstanding, we observed an unexpected global loss of 5mC after *Tet3* KD (Fig. 3a, b). Loci showing loss of methylation covered the whole range of methylation levels but particularly regions that had more than 40% of 5mC in control NPCs (**Fig. 3b**). We performed detection of differentially methylated positions (DMPs; q-value<0.01; >10% difference), which yielded a total of 88,437 hypomethylated CpGs that were enriched at genic regions when compared to the distribution of CpGs captured by RRBS (**Fig. 3c**). In contrast, very few hypo-DMPs were located in promoters and CpG islands, which can be explained by the fact that these are already frequently devoid of methylation (Bird, 2002; Meissner et al., 2008). On the other hand, we detected only 588 hypermethylated CpGs, which were mainly located at CpG islands and genic regions (**Fig. 3c**).

To investigate whether the hypomethylation pattern seen in *Tet3* knockdown NPCs resembles ES cells, we compared our NPC dataset to a previously published oxRRBS dataset on ES cells (Booth et al., 2012). We first noted that many CpG islands in control NPCs displayed higher 5mC levels when compared to ES cells, whilst a group of CpG islands was highly methylated (>70%) in both cell types (**Fig. 3d**). Upon *Tet3* KD, 5mC levels did become closer to those seen in ES cells, but only for lowly methylated CpG islands. Importantly, *Tet3* KD led to demethylation of highly methylated CpG islands, which does not match the ES cell profile (**Fig. 3d**). Were an ES cell subpopulation to be responsible for 5mC loss in *Tet3* KD NPC population, this would have led to maintenance of 5mC levels at highly methylated CpG islands. This prediction was confirmed by simulating 5mC patterns for cell mixtures of ES cells and NPCs, where increasing the proportion of ES cells only decreases the methylation at low-methylation CpG islands, whereas high-methylation CpG islands remain largely unchanged (**Fig. S4e**). These results suggest that the DNA hypomethylation observed in *Tet3* knockdown NPCs might reflect an epigenetic reprogramming event specific to the depletion of *Tet3* in NPCs.

Tet3 knockdown alters DNA methylation at developmentally relevant gene promoters

To expand on these observations, we performed gene ontology analysis of genes associated with promoters harbouring groups of hypomethylated CpGs. For this purpose, differentially methylated regions (DMRs) were defined has regions showing at least 3DMPs with differences in the same direction. Promoters were defined -1kb to +0.5kb from mRNA TSSs. Promoters associated with hypomethylated DMRs (Supplemental file "Hyper_Hypo_promoters.xlsx") were enriched for terms such as development, differentiation and neurogenesis (**Fig. 4a**), suggesting that the observed hypomethylation is a regulated process coupled to the differentiation process between ES cells and NPCs. Of the genes involved in neurogenesis, *Slit1*, *Bdnf*, *Nr2e1* (*Tlx*), *Fgfr1*, *Runx1* and *Wnt3* are striking examples of genes that have been described to be involved in the proliferation of neural precursor cells (Borrell et al., 2012; David et al., 2010; Lee et al., 2002; Ohkubo et al., 2004; Shi et al., 2004; Theriault et al., 2005). Expression analysis of *Slit1* showed a tendency for increased mRNA transcription (**Fig. S5**), consistent with its hypomethylated state.

Moreover, loss of methylation was also observed at *Esrrb* and *Tcl1* early-pluripotency genes (**Fig. 4b**), which is in line with the observed upregulation of gene expression. Loss of methylation at *Tcl1* was confirmed by standard bisulfite sequencing (**Fig. 4c**).

For DNA hypermethylation, we only detected 6 genes with three or more hypermethylated CpGs at their promoters (Supplemental file "Hyper_Hypo_promoters.xlsx"). Notably, three of these genes are imprinted

genes - *Peg10*, *Zrsr1* and *Mcts2*. Interestingly, it has been shown previously that loss of function of *Tet1* also leads to hypermethylation of imprinted genes, namely *Peg10* (Yamaguchi et al., 2013). Expression analysis of these imprinted genes showed decreased expression in *Tet3* KD NPCs (**Fig. 4d**). More recently, it was also shown that *Tet3* regulates NSCs maintenance through repression of *Snrpn* imprinted gene (Montalban-Loro et al., 2019). In accordance with this study, expression analysis of *Snrpn* in Tet3 KD NPCs showed increased transcription in one of the shRNAs (**Fig. S5**). To enable gene ontology analysis of hypermethylated sites, we changed our criteria to include promoters with a minimum of one hypermethylated CpG, yielding a total of 116 genes. Despite this low stringency, gene ontology analysis revealed significant associations with brain development, particularly with neuron differentiation and neurogenesis (**Fig. 4e**). Amongst these genes, *Wnt3a*, *Dlx2*, *Otx2* and *Rac3* are examples of genes described to promote neuronal differentiation (de Melo et al., 2005; Di Giovannantonio et al., 2013; Munji et al., 2011; Vaghi et al., 2014), suggesting that TET3 plays a role in neurogenesis by maintaining hypomethylation of neuronal genes.

2.4. Discussion

Several studies have previously addressed the role of TET1 in the brain, showing that it regulates processes such as memory and cognition, as well as expression of neuronal activity-regulated genes and hippocampal neurogenesis (Kaas et al., 2013; Rudenko et al., 2013; Zhang et al., 2013). However, the role of TET3 in the nervous system remains largely unexplored. Here we investigated the role of *Tet3* in NPCs, using a stable and inducible RNAi knockdown system and an *in vitro* neural differentiation protocol. Surprisingly, we observed that the knockdown of *Tet3* leads to de-repression of pluripotency genes and appearance of OCT4-positive aggregates of cells, suggesting that a reprogramming event is taking place in these cells. Indeed, when we analysed 5mC changes, we observed a dramatic genome-wide loss of methylation in *Tet3* KD NPCs. Hypomethylated CpGs were localized in genes involved in development, differentiation and neurogenesis. Loss of methylation was also observed in *Tcl1* and *Esrrb* pluripotency-associated genes suggesting a connection between loss of methylation, de-repression of pluripotency genes and de-differentiation of NPCs. A recent report on genome-wide DNA methylation in NPCs has shown an extensive demethylation from E18.5 NPCs relative to E11.5 NPCs, whereas only 1.5% of the identified DMRs gained methylation, suggesting that the acquisition of multipotency in E18.5 NPCs is associated with a wide loss of DNA methylation (Sanosaka et al., 2017). Furthermore, in mouse ES cells, it has been shown that *Tet2* knockdown results in both loss of 5hmC and 5mC at DMRs and promoters

while only few DMRs show the expected loss of 5hmC and gain of 5mC (Huang et al., 2014). More recently, another study from the Rao lab reported that TET deficiency in diverse cell types resulted in localized increases in DNA methylation in active euchromatic regions, concurrently with unexpected losses of DNA methylation and reactivation of repeat elements (Lopez-Moyado et al., 2019).

Interestingly, we observed hypermethylation at three imprinted genes after *Tet3* knockdown. It had previously been shown that *Tet1* is necessary to induce 5mC oxidation at imprinting control regions (ICRs) of *H19/IGF2*, *PEG3* and *SNRPN/SNURF* imprinted genes, in a cell-fusion-mediated pluripotency reprogramming model (Piccolo et al., 2013). Another study has shown that heterozygous offspring of *Tet1*/ *Tet2* double knockout (DKO) mice show increased methylation levels across 94 ICRs, including *Peg10*, *Zrsr1* and *Mcts2* (Dawlaty et al., 2013a).

A critical role for *Tet3* in neural progenitor cell maintenance and terminal differentiation of neurons has been reported before (Li et al., 2015b). As in our study, the authors observed an upregulation of *Tet3* upon neural differentiation and that *Tet3* KO in NPCs did not change expression of neural markers, such as *Pax6* and *Nestin*. Here we also observed that neural markers are not altered but pluripotency markers are de-repressed in *Tet3* KD NPCs, which suggests that the cells undergo de-differentiation upon downregulation of *Tet3* expression. We also observed that *Tet3* KD NPCs undergo a genome-scale loss of methylation, which is in contrast to what would be expected considering this enzyme as a demethylating agent. Indeed, we also observed hypermethylation but in a more restricted number of sites, which are preferentially located in neuronal-related genes. The observed loss of methylation could potentially be caused by the concomitant decrease in *Dnmt3a* expression, which is a *de novo* methyltransferase playing a pivotal role in the nervous system (Feng et al., 2005; Wu et al., 2012). In fact, a functional interplay between TET1 and DNMT3A was shown in mouse embryonic stem cells (Gu et al., 2018). Another interesting and perhaps more plausible explanation for the observed global demethylation might resides in the fact that TET enzymes might actually function as guides for *de novo* DNA methylation (Amouroux et al., 2016; Hill et al., 2018). In this context, it was reported that, in zygotes, *Tet3* might have a function in targeting *de novo* methylation activities whereby *Tet3*-driven hydroxylation is predominantly implicated in the protection of the newly acquired hypomethylated state from accumulating new DNA methylation (Amouroux et al., 2016).

Intriguingly, Hahn and collaborators reported that functional perturbation of *Tet2* and *Tet3* in the embryonic cortex led to defects in neuronal differentiation with abnormal accumulation of cell clusters along the radial axis in the intermediate and ventricular zones (Hahn et al., 2013). Clustered cells did not express neuronal marker *B3-Tubulin* and some of the cells showed expression of *Nestin* in their

processes, suggesting a defect in the progression of differentiation. This is in line with our observation that *Tet3* KD NPCs form clusters of cells that resemble ES-colonies and are OCT4-positive. Additionally, TET3 has been implicated in regulation of synaptic transmission (Wang et al., 2017; Yu et al., 2015) and fear-extinction memory (Li et al., 2014), which suggests a pivotal role in the nervous system.

In conclusion, our findings suggest that TET3 acts as a regulator of neural cell identity by maintaining DNA methylation levels in neural precursor cells.

2.5. Methods

Embryonic stem cell culture and neural differentiation

A2lox.cre mouse embryonic stem cells (Iacovino et al., 2011a), were expanded on feeder cells (SNL767 feeder cell line, kindly provided by the Wellcome Trust Sanger Institute, UK) in complete ES medium – DMEM (4500 mg/L glucose; Gibco) supplemented with 110 mg/L sodium pyruvate (Gibco), 2 mM L-Glutamine (Gibco), 15% fetal bovine serum (Gibco, ES-cell tested), 1x penicillin/streptomycin (Gibco), 0.1 mM MEM non-essential amino acids (Gibco) and 10^3 U/ml LIF (ESGRO Millipore).

Neural differentiation of embryonic stem cells was performed as previously described (Bibel et al., 2007). Briefly, A2lox.cre ES cells (passage 17) containing shRNAs for *Tet1* and *Tet3* were cultured on feeders for 3 passages and on 0.2% gelatine (Sigma) for another 3 passages. Subsequently, $4x10^6$ cells were plated onto bacterial non-adherent dishes (Greiner) for formation of non-adherent cellular aggregates (CA) in CA medium (DMEM 4500 mg/L glucose supplemented with 110 mg/L sodium pyruvate, 2 mM L-Glutamine, 10% fetal bovine serum, 1x penicillin/streptomycin and 0.1mM MEM non-essential amino acids). CA medium was changed every other day and 5 μM of retinoic acid (RA; Sigma) was added from day 4 to day 8. CAs were then dissociated with freshly prepared Trypsin 0.05% (Sigma, powder) in 0.05% EDTA/PBS and plated onto Poly-DL-Ornithine and laminin-coated plates in N2 medium [DMEM/F12/Glutamax medium supplemented with 1x Penicillin-Streptomycin, 1x N2 supplement (Gibco) and 50 μg/ mL BSA (Sigma)]. After two days, the medium was changed to a complete medium (N2B27: Neurobasal medium (Gibco), supplemented with 1x GlutaMAX (Gibco), 1x Penicillin-Streptomycin, 1x N2 supplement, 1x N2B27 supplement (Gibco)).

Stable and inducible knockdown system

We used a stable and inducible knockdown system previously described by Iacovino and collaborators (Iacovino et al., 2011a). Briefly, shRNA-mir cassettes for *Tet3* gene (sequences on **supplementary Table**

S1) were amplified from pSM2 retroviral vectors containing the shRNAmir sequences (Open Biosystems) and cloned into the p2Lox vector using HindII and NotI restriction sites. The p2Lox derivatives were transfected into the A2lox.cre ES cells (derived from the E14 male cell line strain 129P2/OlaHsd) expressing Cre after addition of doxycycline (0.5 μg/ml) to the medium one day before transfection. ES cells were transfected using Lipofectamine 2000 (Invitrogen) at a concentration of $5x10^5$ cells/ml. One day after transfection, selection medium containing geneticin (G418, Melford - 300 μg/ml active concentration) was added to the cells during 10 days. After selection, ES cell clones containing the shRNAmir were expanded in ES complete medium and neural differentiation was performed as described above. For shRNA expression, doxycycline (2 μg/ml) was added to the medium during 5 days. An ES clone containing eGFP was used to control for positive induction after doxycycline addition. After these 5 days, the cells were trypsinized and the pellet was stored at -80°C until DNA/RNA/Protein extraction.

Quantitative reverse transcription PCR

RNA was extracted using the AllPrep DNA/RNA mini kit (Qiagen) and cDNA was synthesized from 200 ng of RNA using the qScript cDNA Supermix (Quanta Biosciences). cDNA was diluted 1:10 and used as template for quantitative real-time PCR reactions using the 5x HOT FIREPol EvaGreen qPCR supermix (Solis Biodyne) and primers designed to specifically amplify each gene of interest (Supplementary Table S2). Cycling reactions were performed in duplicate and cycle threshold (Ct) fluorescence data recorded on Applied Biosystems 7500 Fast Real-time PCR System. The relative abundance of each gene of interest was calculated on the basis of the Delta Delta Ct method (Livak and Schmittgen, 2001), where results were normalised to two housekeeping genes (*Atp5b* and *Hsp90ab1*). Statistical analysis was performed by multiple t-tests using GraphPad Prism version 6.0 for Mac (GraphPad Software, La Jolla California USA).

Immunofluorescence microscopy and image analysis

Antibody staining of DNA methylation and hydroxymethylation was performed as previously described (Ficz et al., 2011), with few modifications. Briefly, neural precursor cells were plated on glass coverslips and fixed with 2% paraformaldehyde for 30 minutes at room temperature (RT). Cells were permeabilised with phosphate buffered saline (PBS) 0.5% Triton X-100 and treated with 2N HCl for 30 minutes at RT. The coverslips were washed in PBS 0.05% Tween-20 (PBST) and blocked overnight in PBST with 1% bovine serum albumin (BSA) (BS). Cells were incubated with both primary antibodies rabbit anti-5hmC (1:500, Active Motif, 39792) and mouse anti-5mC (1:250, Eurogentec, BS-Mecy-0100) for 1h at RT. For antibody staining of pluripotency and neuronal markers, cells were incubated with blocking buffer (BS)

for 1h at RT before incubation with primary antibodies overnight at 4 °C. Primary antibodies were: rabbit anti-PAX6 (1:250, Millipore, AB2237), mouse anti-NESTIN (1:200, Millipore MAB353), rabbit anti-OCT4 (1:750, Abcam, ab18976), rabbit anti-SOX2 (1:1000, Abcam, ab97959), mouse anti-beta III tubulin (1:100, Millipore, MAB1637) and rabbit anti-TET3 (1:100, Abcam, 139805). After washing with BS for 1h at RT, primary antibody staining was revealed with appropriate Alexa-Fluor-conjugated secondary antibodies (1:500, Molecular Probes). For both procedures, the nuclei were counterstained with DAPI. After washing with PBST, cells were mounted with Immu-mount (Thermo Scientific). Images were acquired on an Olympus BX61 or Olympus FV1000 (Japan) confocal microscope and analysed using ImageJ software®.

Western blot for detection of TET3

Protein was extracted using the AllPrep DNA/RNA mini kit (Qiagen) and resuspended in 5% SDS. The protein concentration of the supernatants was determined using BCA kit (Pierce). Total lysates of 14 µg of protein were denatured in NuPage LDS sample buffer and NuPage reducing reagent by heating for 10 min at 95 °C. Proteins were separated on NuPage 4-12% Bis-Tris gels using MOPS running buffer (Thermofisher). Wet transfer onto a nitrocelulose membrane (Amersham Biosciences) was performed using MOPS running buffer with 20% methanol. Membranes were blocked with 10% milk/1% BSA in Tris-buffered saline (TBS)/0,1%Tween (TBS-T) overnight at 4 °C. Primary antibodies mouse anti-TET3 (1:1000, Abcam, ab174862) and mouse anti-α-Tubulin (1:5000, Sigma-Aldrich, T6074) diluted in blocking buffer and incubated 2h at RT. Membranes were washed in TBS/T and incubated with the secondary antibody coupled to horseradish peroxidase (BioRad) 1h at RT. The bound antibodies were visualized by chemiluminescence using ImageQuant LAS4000 mini (GE Healthcare). Bands were analyzed using ChemiDoc (Bio-Rad) and quantification was performed with ImageLab software (Bio-Rad). α-Tubulin was used as loading control.

Dotblot and ELISA analysis of 5hmC

DNA was extracted using the AllPrep DNA/RNA mini kit (Qiagen). Genomic DNA (100 ng) was denatured at 99 °C for 5 min and spotted on nitrocellulose blotting membranes (Amersham Hybond-N+). The membrane was UV-crosslinked for 2 min and then blocked in 10% milk/1% BSA in PBST overnight at 4 °C. The membranes were then incubated with rabbit anti-5hmC (1:500, Active Motif, 39769) for 1 hour at RT. After washes with PBST (PBS 0,1% Tween-20), membranes were incubated with 1:10000 dilution of HRP-conjugated anti-rabbit, washed with PBST and then treated with Amersham ECL (GE Healthcare).

Dot blot intensities were analysed using ChemiDoc (Bio-Rad) and quantification was performed with ImageLab software (Bio-Rad).

The global level of 5-hmC was also assessed using Quest 5-hmC DNA ELISA Kit (Zymo Research). The procedure was followed according to the manufacturer's instructions, loading 100 ng of DNA per well.

Cell cycle analysis using flow cytometry for propidium iodide staining

For cell cycle analysis, NPCs were dissociated with Accutase (Sigma-Aldrich) for 10 minutes and re-suspended in 70% ethanol and kept at -20 °C for 24 hours for fixation. After fixation, cells were washed in 1x PBS and incubated with PI staining solution - Propidium Iodide 20 μg/ml (eBioscience) in PBS/ 0.1% Triton-X 100 and RNase 0.25 mg/ml (Invitrogen) - for 1 hour at room temperature in the dark. Cell staining was then analysed by flow cytometry in a BD LSRII flow cytometer (BD Biosciences; 20.000 events). Analysis of the cell cycle was performed with ModFit LT (Verity Software House).

Genome-wide analysis of DNA methylation and hydroxymethylation by oxRRBS

Genomic DNA was isolated using the Qiagen AllPrep DNA/RNA Mini kit (Qiagen) following manufacturers' instructions. Oxidative Reduced Representation Bisulfite Sequencing (oxRRBS) was used for genome-wide analysis of DNA methylation and hydroxymethylation. This method relies on oxidation of DNA prior to bisulfite treatment in order to convert 5-hydroxymethylcytosine (5hmC) into 5-formylcytosine (5fC) which in turn will be converted to uracil (thymine after PCR amplification) (Fig. 4). 5-methylcytosine (5mC) remains unchanged after oxidation and bisulfite treatment and unmethylated cytosines will be converted to uracil (thymine after PCR amplification). By subtracting the two libraries, it is then possible to infer 5mC and 5hmC levels at a single-base resolution and in a quantitative manner (Booth et al., 2012).

Briefly, 100 ng of DNA were digested with MspI restriction enzyme and the reaction was cleaned up with AMPure XP beads (Agencourt). A library was then prepared with the NEBNext Ultra DNA library Prep for Illumina (NEB) for End repair, A-tailing and ligation of methylated adaptors (NEBNext, E7535), according to manufacturer's' instructions. Oxidation of the DNA was then carried out starting by purifying DNA in a Micro Bio-Spin column (BioRad), denaturing DNA with NaOH and adding 2 μL of Potassium Perruthenate ($KRuO_4$, Alfa Aeser) solution (15 mM in 0.05 M NaOH). The reaction was held on ice for 1 hour, purified with Micro Bio-Spin column (BioRad) and subjected to bisulfite treatment using the Qiagen Epitect kit, according to the manufacturer's instructions for FFPE samples, except that the thermal cycle was run twice over. Final library amplification (18 cycles) was performed using Pfu Turbo Cx (Agilent) and adaptor-specific primers (barcoded TruSeq primers, Illumina), after which the libraries were purified using AMPure XP beads (Agencourt). To check for oxidation success, a spike-in control was added before oxidation step

and amplified and digested with TaqI restriction enzyme at the end of library amplification.

Sequencing and data processing

Sequencing (single-end, 75 bp reads) was performed on the Illumina NextSeq platform, high-throughput mode. Quality control of sequencing reads was performed with FASTQC (Babraham Bioinformatics). Trimming of the reads to remove adaptors and low-quality bases was performed using Trim-Galore with --rrbs option (Babraham Bioinformatics). The alignment was performed using Bismark with bowtie2 and methylation extraction with the options -s –comprehensive (Krueger and Andrews, 2011). SeqMonk (Babraham Bioinformatics) and the R-package Methylkit (Akalin et al., 2012) were used for downstream analysis.

DMPs were detected using the Methylkit (Akalin et al., 2012). We overlapped DMPs with genomic features. Promoters were defined -1kb to +0.5kb from mRNA TSSs (and deduplicated if >50% overlapped), CpG islands are from Illingworth et al. (Illingworth et al., 2010) and enhancers are from ChIA-PET data (Zhang et al., 2012). Gene ontology analyses were performed using the topGO R package, focusing on biological process terms.

All sequencing data are available under Gene Expression Omnibus (GEO) accession number GSE123110.

Gene-specific methylation levels by standard bisulfite sequencing

Genomic DNA was isolated using the AllPrep DNA/RNA Minikit (Qiagen) following manufacturers' instructions. Five hundred nanograms of DNA were subjected to bisulfite treatment using the Epitect Bisulfite Kit (Qiagen). A CpG island on intron 1 of *Tcl1* gene (chromosome position 12:106,460,347-106,460,634, NCBI37 (mm9) mouse reference genome) was amplified using primers described in supplementary table S2 and HostStar MasterMix (Qiagen) with the following cycling conditions: 95°C for 15 min followed by 35 cycles of 95°C for 1 min, 58°C for 1 min and 72°C for 1 min, with a final extension of 72°C for 20 minutes. PCR products were then cloned using the TOPO TA Cloning kit for sequencing (Invitrogen) and NZYalpha competent cells (NZYtech). Ten clones for each sample were picked and plasmid DNA amplified using M13 primers. PCR products for each clone were sequenced using the BigDye Terminator v3.1 cycle sequencing kit (Applied Biosystems) in an ABI 3500 Genetic Analyzer (Applied Biosystems). Only clones with more than 95% non-CpG cytosines converted were considered for the analysis, using BiQ Analyzer Software (Bock et al., 2005).

2.6. Author contributions

M.S, C.A. and M.G performed the experiments and analysed the data; M.I. and M.K. contributed with the A2lox.cre ES cell line; W.R. contributed with the stable and inducible shRNA ES cell clones; M.R.B. performed oxRRBS and bioinformatics analysis and wrote the manuscript; N.S., L.P. and C.J.M. designed the study, analysed the data and wrote the manuscript; All authors revised and approved the final manuscript.

2.7. Acknowledgments

We thank Yves-Alain Barde (Biozentrum, Switzerland) for help with the neural differentiation protocol, Patrícia Patrício and Belém Marques (ICVS-UM) for help with propidium iodide flow cytometry and ModFit analysis and Patrícia Monteiro (ICVS-UM) for critical reading of the manuscript.

This work was supported by the Portuguese Foundation for Science and Technology (FCT) with a project grant (PTDC/BIA-BCM/121276/2010) to C.J.M. and funded by EpiGeneSys with a Small Collaborative project to M.R.B and L.P. CJ Marques and L Pinto are the recipients of an FCT salary contracts (IF/00047/2012 and CEECIND/00371/2017 to C.J.M. and IF/01079/2014 to L.P.). C Antunes is the recipient of a PhD fellowship from the Doctoral Program PhDOC from FCT (PD/BD/106049/2015). M.R.B. is a Sir Henry Dale Fellow (101225/Z/13/Z), jointly funded by the Wellcome Trust and the Royal Society. This work has also been funded by Northern Portugal Regional Operational Programme (NORTE 2020), under the Portugal 2020 Partnership Agreement, through the European Regional Development Fund (FEDER; NORTE-01-0145-FEDER-000013); FEDER funds, through the Competitiveness Factors Operational Programme (COMPETE), and National Funds, through the FCT (POCI-01-0145-FEDER-007038).

2.9. References

Akalin, A., Kormaksson, M., Li, S., Garrett-Bakelman, F.E., Figueroa, M.E., Melnick, A., and Mason, C.E. (2012). methylKit: a comprehensive R package for the analysis of genome-wide DNA methylation profiles. Genome biology *13*, R87.

Amouroux, R., Nashun, B., Shirane, K., Nakagawa, S., Hill, P.W., D'Souza, Z., Nakayama, M., Matsuda, M., Turp, A., Ndjetehe, E.*, et al.* (2016). De novo DNA methylation drives 5hmC accumulation in mouse zygotes. Nature Cell Biology *18*, 225-233.

Bibel, M., Richter, J., Lacroix, E., and Barde, Y.-A. (2007). Generation of a defined and uniform population of CNS progenitors and neurons from mouse embryonic stem cells. Nature Protocols *2*, 1034-1043.

Bibel, M., Richter, J., Schrenk, K., Tucker, K.L., Staiger, V., Korte, M., Goetz, M., and Barde, Y.A. (2004). Differentiation of mouse embryonic stem cells into a defined neuronal lineage. Nature neuroscience *7*, 1003-1009.

Bird, A. (2002). DNA methylation patterns and epigenetic memory. Genes & development *16*, 6-21.

Bock, C., Reither, S., Mikeska, T., Paulsen, M., Walter, J., and Lengauer, T. (2005). BiQ Analyzer: visualization and quality control for DNA methylation data from bisulfite sequencing. Bioinformatics *21*, 4067-4068.

Booth, M.J., Branco, M.R., Ficz, G., Oxley, D., Krueger, F., Reik, W., and Balasubramanian, S. (2012). Quantitative sequencing of 5-methylcytosine and 5-hydroxymethylcytosine at single-base resolution. Science *336*, 934-937.

Booth, M.J., Ost, T.W., Beraldi, D., Bell, N.M., Branco, M.R., Reik, W., and Balasubramanian, S. (2013). Oxidative bisulfite sequencing of 5-methylcytosine and 5-hydroxymethylcytosine. Nature protocols *8*, 1841-1851.

Borrell, V., Cardenas, A., Ciceri, G., Galceran, J., Flames, N., Pla, R., Nobrega-Pereira, S., Garcia-Frigola, C., Peregrin, S., Zhao, Z.*, et al.* (2012). Slit/Robo signaling modulates the proliferation of central nervous system progenitors. Neuron *76*, 338-352.

Chew, J.L., Loh, Y.H., Zhang, W., Chen, X., Tam, W.L., Yeap, L.S., Li, P., Ang, Y.S., Lim, B., Robson, P.*, et al.* (2005). Reciprocal transcriptional regulation of Pou5f1 and Sox2 via the Oct4/Sox2 complex in embryonic stem cells. Molecula Cell Biology *25*, 6031-6046.

David, M.D., Canti, C., and Herreros, J. (2010). Wnt-3a and Wnt-3 differently stimulate proliferation and neurogenesis of spinal neural precursors and promote neurite outgrowth by canonical signaling. Journal of neuroscience research *88*, 3011-3023.

Dawlaty, M.M., Breiling, A., Le, T., Raddatz, G., Barrasa, M.I., Cheng, A.W., Gao, Q., Powell, B.E., Li, Z., Xu, M.*, et al.* (2013). Combined Deficiency of Tet1 and Tet2 Causes Epigenetic Abnormalities but Is Compatible with Postnatal Development. Developmental Cell, 1-14.

de Melo, J., Du, G., Fonseca, M., Gillespie, L.A., Turk, W.J., Rubenstein, J.L., and Eisenstat, D.D. (2005). Dlx1 and Dlx2 function is necessary for terminal differentiation and survival of late-born retinal ganglion cells in the developing mouse retina. Development *132*, 311-322.

Di Giovannantonio, L.G., Di Salvio, M., Acampora, D., Prakash, N., Wurst, W., and Simeone, A. (2013). Otx2 selectively controls the neurogenesis of specific neuronal subtypes of the ventral tegmental area and compensates En1-dependent neuronal loss and MPTP vulnerability. Development Biology *373*, 176-183.

Diaz de Leon-Guerrero, S., Pedraza-Alva, G., and Perez-Martinez, L. (2011). In sickness and in health: the role of methyl-CpG binding protein 2 in the central nervous system. European Journal of Neuroscience *33*, 1563-1574.

Feng, J., Chang, H., Li, E., and Fan, G. (2005). Dynamic expression of de novo DNA methyltransferases Dnmt3a and Dnmt3b in the central nervous system. Journal of neuroscience research *79*, 734-746.

Ficz, G., Branco, M.R., Seisenberger, S., Santos, F., Krueger, F., Hore, T.A., Marques, C.J., Andrews, S., and Reik, W. (2011). Dynamic regulation of 5-hydroxymethylcytosine in mouse ES cells and during differentiation. Nature *473*, 398-402.

Fu, L., Guerrero, C.R., Zhong, N., Amato, N.J., Liu, Y., Liu, S., Cai, Q., Ji, D., Jin, S.G., Niedernhofer, L.J.*, et al.* (2014). Tet-mediated formation of 5-hydroxymethylcytosine in RNA. Journal of the American Chemical Society *136*, 11582-11585.

Gontier, G., Iyer, M., Shea, J.M., Bieri, G., Wheatley, E.G., Ramalho-Santos, M., and Villeda, S.A. (2018). Tet2 Rescues Age-Related Regenerative Decline and Enhances Cognitive Function in the Adult Mouse Brain. Cell reports *22*, 1974-1981.

Gu, H., Smith, Z.D., Bock, C., Boyle, P., Gnirke, A., and Meissner, A. (2011). Preparation of reduced representation bisulfite sequencing libraries for genome-scale DNA methylation profiling. Nature Protocols *6*, 468-481.

Gu, T., Lin, X., Cullen, S.M., Luo, M., Jeong, M., Estecio, M., Shen, J., Hardikar, S., Sun, D., Su, J.*, et al.* (2018). DNMT3A and TET1 cooperate to regulate promoter epigenetic landscapes in mouse embryonic stem cells. Genome biology *19*, 88.

Guo, J.U., Ma, D.K., Mo, H., Ball, M.P., Jang, M.H., Bonaguidi, M.A., Balazer, J.A., Eaves, H.L., Xie, B., Ford, E.*, et al.* (2011). Neuronal activity modifies the DNA methylation landscape in the adult brain. Nature neuroscience *14*, 1345-1351.

Guo, J.U., Szulwach, K.E., Su, Y., Li, Y., Yao, B., Xu, Z., Shin, J.H., Xie, B., Gao, Y., Ming, G.L.*, et al.* (2014). Genome-wide antagonism between 5-hydroxymethylcytosine and DNA methylation in the adult mouse brain. Frontiers in Biology (Beijing) *9*, 66-74.

Hackett, J.A., Sengupta, R., Zylicz, J.J., Murakami, K., Lee, C., Down, T.A., and Surani, M.A. (2013). Germline DNA demethylation dynamics and imprint erasure through 5-hydroxymethylcytosine. Science *339*, 448-452.

Hahn, M.A., Qiu, R., Wu, X., Li, A.X., Zhang, H., Wang, J., Jui, J., Jin, S.G., Jiang, Y., Pfeifer, G.P.*, et al.* (2013). Dynamics of 5-hydroxymethylcytosine and chromatin marks in Mammalian neurogenesis. Cell reports *3*, 291-300.

Hill, P.W.S., Leitch, H.G., Requena, C.E., Sun, Z., Amouroux, R., Roman-Trufero, M., Borkowska, M., Terragni, J., Vaisvila, R., Linnett, S.*, et al.* (2018). Epigenetic reprogramming enables the transition from primordial germ cell to gonocyte. Nature *555*, 392-396.

Huang, Y., Chavez, L., Chang, X., Wang, X., Pastor, W.A., Kang, J., Zepeda-Martinez, J.A., Pape, U.J., Jacobsen, S.E., Peters, B.*, et al.* (2014). Distinct roles of the methylcytosine oxidases Tet1 and Tet2 in mouse embryonic stem cells. Proceedings National Academy Sciences U S A *111*, 1361-1366.

Huang, Y., Pastor, W.A., Shen, Y., Tahiliani, M., Liu, D.R., and Rao, A. (2010). The behaviour of 5-hydroxymethylcytosine in bisulfite sequencing. PLoS One *5*, e8888.

Iacovino, M., Bosnakovski, D., Fey, H., Rux, D., Bajwa, G., Mahen, E., Mitanoska, A., Xu, Z., and Kyba, M. (2011). Inducible cassette exchange: a rapid and efficient system enabling conditional gene expression in embryonic stem and primary cells. Stem cells (Dayton, Ohio) *29*, 1580-1588.

Illingworth, R.S., Gruenewald-Schneider, U., Webb, S., Kerr, A.R., James, K.D., Turner, D.J., Smith, C., Harrison, D.J., Andrews, R., and Bird, A.P. (2010). Orphan CpG islands identify numerous conserved promoters in the mammalian genome. PLoS Genet *6*, e1001134.

Iqbal, K., Jin, S.G., Pfeifer, G.P., and Szabo, P.E. (2011). Reprogramming of the paternal genome upon fertilization involves genome-wide oxidation of 5-methylcytosine. Proceedings National Academy Sciences of the U S A *108*, 3642-3647.

Ito, S., Shen, L., Dai, Q., Wu, S.C., Collins, L.B., Swenberg, J.A., He, C., and Zhang, Y. (2011). Tet proteins can convert 5-methylcytosine to 5-formylcytosine and 5-carboxylcytosine. Science *333*, 1300-1303.

Kaas, G.A., Zhong, C., Eason, D.E., Ross, D.L., Vachhani, R.V., Ming, G.L., King, J.R., Song, H., and Sweatt, J.D. (2013). TET1 controls CNS 5-methylcytosine hydroxylation, active DNA demethylation, gene transcription, and memory formation. Neuron *79*, 1086-1093.

Ko, M., An, J., Bandukwala, H.S., Chavez, L., Aijo, T., Pastor, W.A., Segal, M.F., Li, H., Koh, K.P., Lahdesmaki, H.*, et al.* (2013). Modulation of TET2 expression and 5-methylcytosine oxidation by the CXXC domain protein IDAX. Nature *497*, 122-126.

Kohli, R.M., and Zhang, Y. (2013). TET enzymes, TDG and the dynamics of DNA demethylation. Nature *502*, 472-479.

Kriaucionis, S., and Heintz, N. (2009). The nuclear DNA base 5-hydroxymethylcytosine is present in Purkinje neurons and the brain. Science *324*, 929-930.

Krueger, F., and Andrews, S.R. (2011). Bismark: a flexible aligner and methylation caller for Bisulfite-Seq applications. Bioinformatics *27*, 1571-1572.

Lee, J., Duan, W., and Mattson, M.P. (2002). Evidence that brain-derived neurotrophic factor is required for basal neurogenesis and mediates, in part, the enhancement of neurogenesis by dietary restriction in the hippocampus of adult mice. Jounal Neurochemistry *82*, 1367-1375.

Li, T., Yang, D., Li, J., Tang, Y., Yang, J., and Le, W. (2015). Critical role of Tet3 in neural progenitor cell maintenance and terminal differentiation. Molecular Neurobiology *51*, 142-154.

Li, X., Wei, W., Zhao, Q.Y., Widagdo, J., Baker-Andresen, D., Flavell, C.R., D'Alessio, A., Zhang, Y., and Bredy, T.W. (2014). Neocortical Tet3-mediated accumulation of 5-hydroxymethylcytosine promotes rapid behavioral adaptation. Proceedings National Academy Sciences U S A *111*, 7120-7125.

Livak, K.J., and Schmittgen, T.D. (2001). Analysis of relative gene expression data using real-time quantitative PCR and the 2(-Delta Delta C(T)) Method. Methods (San Diego, Calif) *25*, 402-408.

Lopez-Moyado, I.F., Tsagaratou, A., Yuita, H., Seo, H., Delatte, B., Heinz, S., Benner, C., and Rao, A. (2019). Paradoxical association of TET loss of function with genome-wide DNA hypomethylation. Proceedings National Academy Sciences USA.

Ma, D.K., Jang, M.H., Guo, J.U., Kitabatake, Y., Chang, M.L., Pow-Anpongkul, N., Flavell, R.A., Lu, B., Ming, G.L., and Song, H. (2009). Neuronal activity-induced Gadd45b promotes epigenetic DNA demethylation and adult neurogenesis. Science *323*, 1074-1077.

Meissner, A., Mikkelsen, T.S., Gu, H., Wernig, M., Hanna, J., Sivachenko, A., Zhang, X., Bernstein, B.E., Nusbaum, C., Jaffe, D.B.*, et al.* (2008). Genome-scale DNA methylation maps of pluripotent and differentiated cells. Nature *454*, 766-770.

Menezes, J.R., and Luskin, M.B. (1994). Expression of neuron-specific tubulin defines a novel population in the proliferative layers of the developing telencephalon. The Journal of neuroscience : the official journal of the Society for Neuroscience *14*, 5399-5416.

Montalban-Loro, R., Lozano-Urena, A., Ito, M., Krueger, C., Reik, W., Ferguson-Smith, A.C., and Ferron, S.R. (2019). TET3 prevents terminal differentiation of adult NSCs by a non-catalytic action at Snrpn. Nature communications *10*, 1726.

Munji, R.N., Choe, Y., Li, G., Siegenthaler, J.A., and Pleasure, S.J. (2011). Wnt signaling regulates neuronal differentiation of cortical intermediate progenitors. The Journal of neuroscience : the official journal of the Society for Neuroscience *31*, 1676-1687.

Ohkubo, Y., Uchida, A.O., Shin, D., Partanen, J., and Vaccarino, F.M. (2004). Fibroblast growth factor receptor 1 is required for the proliferation of hippocampal progenitor cells and for hippocampal growth in mouse. The Journal of neuroscience : the official journal of the Society for Neuroscience *24*, 6057-6069.

Pfaffeneder, T., Hackner, B., Truss, M., Munzel, M., Muller, M., Deiml, C.A., Hagemeier, C., and Carell, T. (2011). The discovery of 5-formylcytosine in embryonic stem cell DNA. Angewandte Chemie *50*, 7008-7012.

Piccolo, F.M., Bagci, H., Brown, K.E., Landeira, D., Soza-Ried, J., Feytout, A., Mooijman, D., Hajkova, P., Leitch, H.G., Tada, T.*, et al.* (2013). Different roles for Tet1 and Tet2 proteins in reprogramming-mediated erasure of imprints induced by EGC fusion. Molecular cell *49*, 1023-1033.

Rudenko, A., Dawlaty, M.M., Seo, J., Cheng, A.W., Meng, J., Le, T., Faull, K.F., Jaenisch, R., and Tsai, L.H. (2013). Tet1 is critical for neuronal activity-regulated gene expression and memory extinction. Neuron *79*, 1109-1122.

Sanosaka, T., Imamura, T., Hamazaki, N., Chai, M., Igarashi, K., Ideta-Otsuka, M., Miura, F., Ito, T., Fujii, N., Ikeo, K.*, et al.* (2017). DNA Methylome Analysis Identifies Transcription Factor-Based Epigenomic Signatures of Multilineage Competence in Neural Stem/Progenitor Cells. Cell Reports *20*, 2992-3003.

Seisenberger, S., Peat, J.R., Hore, T.A., Santos, F., Dean, W., and Reik, W. (2013). Reprogramming DNA methylation in the mammalian life cycle: building and breaking epigenetic barriers. Philosophical transactions of the Royal Society of London Series B, Biological sciences *368*, 20110330.

Shi, Y., Chichung Lie, D., Taupin, P., Nakashima, K., Ray, J., Yu, R.T., Gage, F.H., and Evans, R.M. (2004). Expression and function of orphan nuclear receptor TLX in adult neural stem cells. Nature *427*, 78-83.

Szwagierczak, A., Bultmann, S., Schmidt, C.S., Spada, F., and Leonhardt, H. (2010). Sensitive enzymatic quantification of 5-hydroxymethylcytosine in genomic DNA. Nucleic acids research *38*, e181.

Tahiliani, M., Koh, K.P., Shen, Y., Pastor, W.A., Bandukwala, H., Brudno, Y., Agarwal, S., Iyer, L.M., Liu, D.R., Aravind, L.*, et al.* (2009). Conversion of 5-methylcytosine to 5-hydroxymethylcytosine in mammalian DNA by MLL partner TET1. Science *324*, 930-935.

Tan, L., Xiong, L., Xu, W., Wu, F., Huang, N., Xu, Y., Kong, L., Zheng, L., Schwartz, L., Shi, Y.*, et al.* (2013). Genome-wide comparison of DNA hydroxymethylation in mouse embryonic stem cells and neural progenitor cells by a new comparative hMeDIP-seq method. Nucleic acids research *41*, e84.

Theriault, F.M., Nuthall, H.N., Dong, Z., Lo, R., Barnabe-Heider, F., Miller, F.D., and Stifani, S. (2005). Role for Runx1 in the proliferation and neuronal differentiation of selected progenitor cells in the mammalian nervous system. The Journal of neuroscience : the official journal of the Society for Neuroscience *25*, 2050-2061.

Vaghi, V., Pennucci, R., Talpo, F., Corbetta, S., Montinaro, V., Barone, C., Croci, L., Spaiardi, P., Consalez, G.G., Biella, G.*, et al.* (2014). Rac1 and rac3 GTPases control synergistically the development of cortical and hippocampal GABAergic interneurons. Cerebral Cortex *24*, 1247-1258.

Wang, L., Li, M.Y., Qu, C., Miao, W.Y., Yin, Q., Liao, J., Cao, H.T., Huang, M., Wang, K., Zuo, E.*, et al.* (2017). CRISPR-Cas9-mediated genome editing in one blastomere of two-cell embryos reveals a novel Tet3 function in regulating neocortical development. Cell research *27*, 815-829.

Wossidlo, M., Nakamura, T., Lepikhov, K., Marques, C.J., Zakhartchenko, V., Boiani, M., Arand, J., Nakano, T., Reik, W., and Walter, J. (2011). 5-Hydroxymethylcytosine in the mammalian zygote is linked with epigenetic reprogramming. Nature communications *2*, 241.

Wu, Z., Huang, K., Yu, J., Le, T., Namihira, M., Liu, Y., Zhang, J., Xue, Z., Cheng, L., and Fan, G. (2012). Dnmt3a regulates both proliferation and differentiation of mouse neural stem cells. Journal of neuroscience research *90*, 1883-1891.

Yamaguchi, S., Shen, L., Liu, Y., Sendler, D., and Zhang, Y. (2013). Role of Tet1 in erasure of genomic imprinting. Nature *504*, 460-464.

Yu, H., Su, Y., Shin, J., Zhong, C., Guo, J.U., Weng, Y.L., Gao, F., Geschwind, D.H., Coppola, G., Ming, G.L.*, et al.* (2015). Tet3 regulates synaptic transmission and homeostatic plasticity via DNA oxidation and repair. Nature neuroscience *18*, 836-843.

Zhang, J., Chen, S., Zhang, D., Shi, Z., Li, H., Zhao, T., Hu, B., Zhou, Q., and Jiao, J. (2016). Tet3-Mediated DNA Demethylation Contributes to the Direct Conversion of Fibroblast to Functional Neuron. Cell Reports *17*, 2326-2339.

Zhang, J., Poh, H.M., Peh, S.Q., Sia, Y.Y., Li, G., Mulawadi, F.H., Goh, Y., Fullwood, M.J., Sung, W.K., Ruan, X.*, et al.* (2012). ChIA-PET analysis of transcriptional chromatin interactions. Methods *58*, 289-299.

Zhang, R.R., Cui, Q.Y., Murai, K., Lim, Y.C., Smith, Z.D., Jin, S., Ye, P., Rosa, L., Lee, Y.K., Wu, H.P.*, et al.* (2013). Tet1 regulates adult hippocampal neurogenesis and cognition. Cell stem cell *13*, 237-245.

2.10. Figures

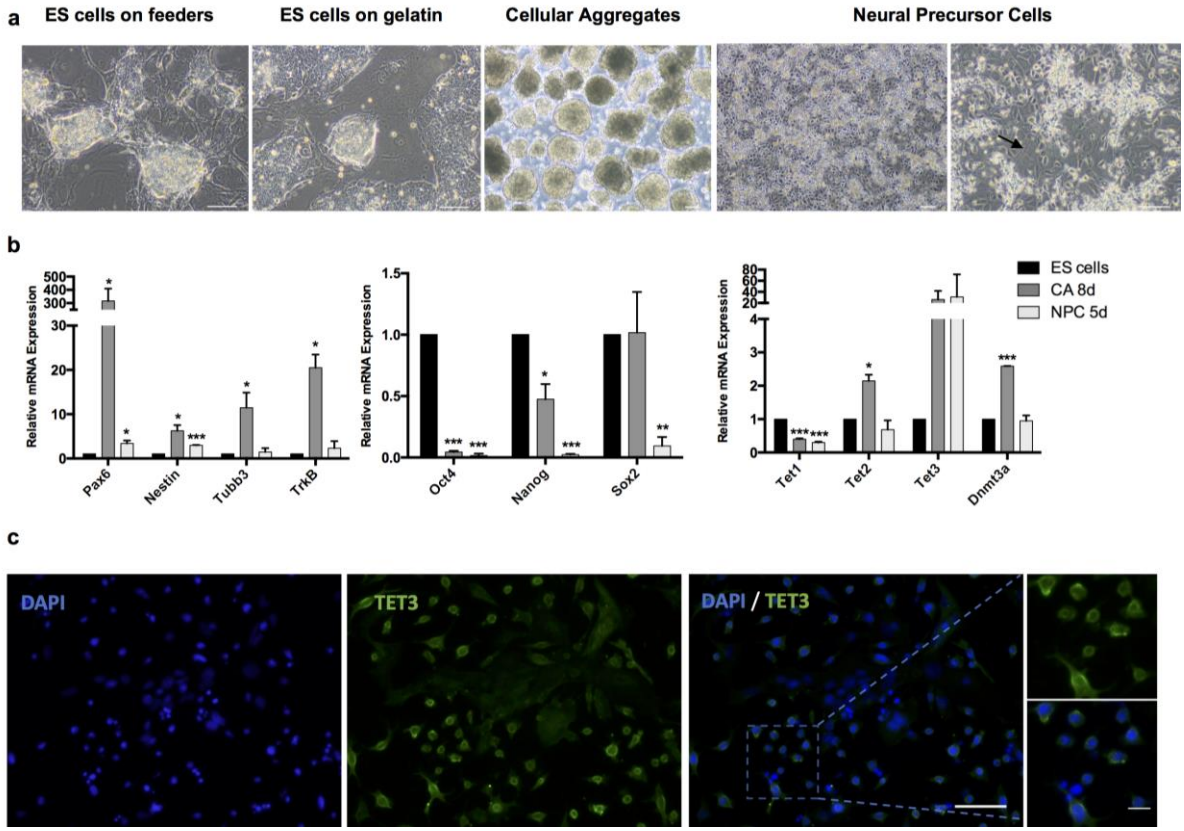

Figure 1 - *Tet3* is upregulated during neural differentiation.

(a) Neural differentiation protocol with representative images of key transition points - embryonic stem (ES) cells on feeders, ES cells on gelatin, cellular aggregates (CAs) and neural precursor cells (NPCs). Arrows show neurites forming between the cells; Scale bars – 100 µm.

(b) Relative expression of neural markers (*Pax6*, *Nestin*, *Tubb3* and *TrkB*), pluripotency markers (*Oct4*, *Nanog* and *Sox2*) and epigenetic regulators (*Tet1*, *Tet2*, *Tet3* and *Dnmt3a*) in several stages of the neural differentiation process - ES cells on gelatin (ES cells), CA after addition of Retinoic Acid (CA 8d), NPC after 5 days in culture (NPC 5d); n=2 independent experiments; *p<0.05; **p<0.01; ***p<0.001; t-test.

(c) Immunostaining of TET3 in differentiated NPCs. Scale bars – 100 µm and 25 µm.

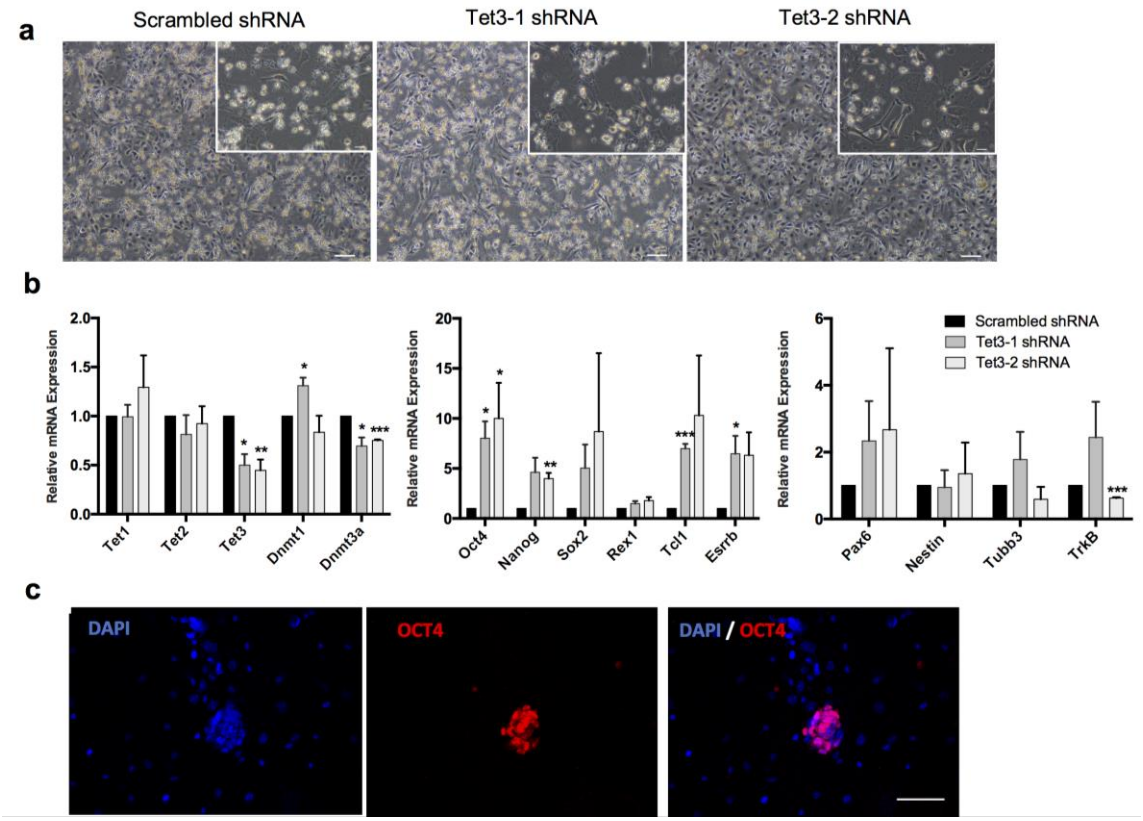

Figure 2 - Knockdown of *Tet3* in NPCs results in de-repression of pluripotency genes.

(a) Phase-contrast images of NPCs after Tet3 knockdown during 5 days in culture. Scrambled shRNA - control; Tet3-1 and Tet3-2 shRNAs - shRNA against *Tet3*. Scale bars - 100 µm and 50 µm in the insets.

(b) mRNA transcript levels of epigenetic regulators (*Tet* and *Dnmt* enzymes), pluripotency genes (*Oct4*, *Nanog*, *Sox2*, *Rex1* and *Tcl1*) and neural markers ((stem cell markers - *Pax6* and *Nestin*; mature differentiation markers - B3-tubulin (*Tubb3*) and Neurotrophic tyrosine kinase, receptor, type 2 (*TrkB* or *Ntrk2*)) after *Tet3* knockdown. (*p<0.05, **p<0.01, ***p<0.001; t-test). Error bars represent SEM for three (Tet3-1 shRNA) and two (Tet3-2 shRNA) independent experiments.

(c) Immunostaining of OCT4 in NPCs after *Tet3* KD, using Tet3-2 shRNA, shows OCT4-positive cells forming aggregates that resemble ES cell colonies. Scale bar – 50 µm.

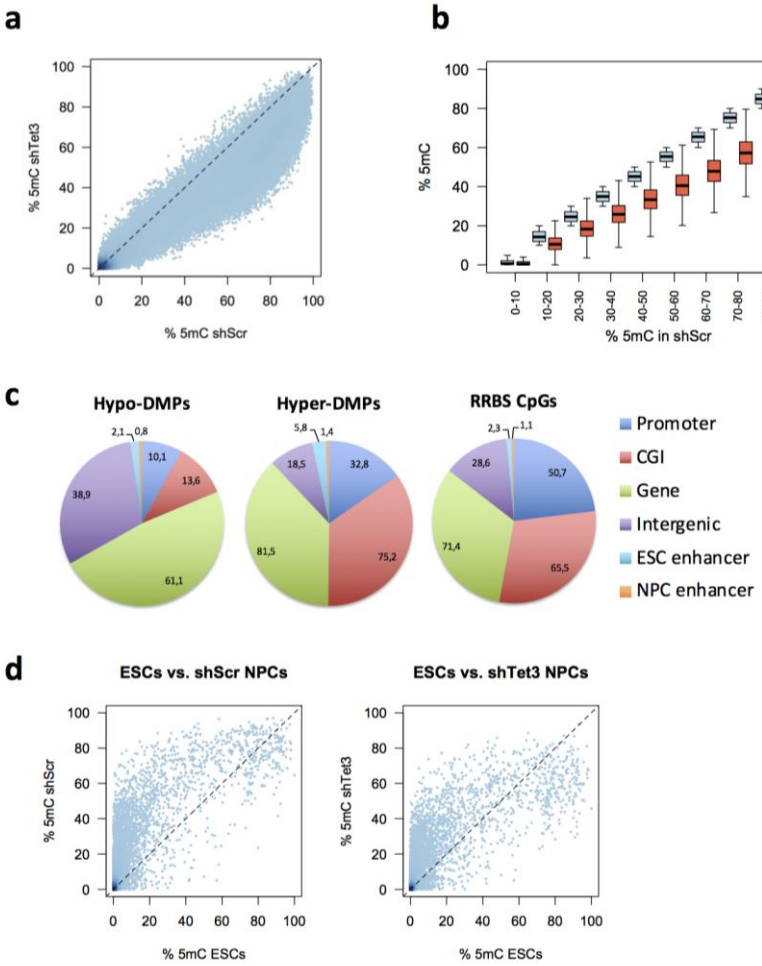

Figure 3 - *Tet3* knockdown results in genome-scale loss of DNA methylation.

(a) Scatter plot of 5mC levels at individual CpGs, showing a bulk shift in methylation after *Tet3* KD, using Tet3-2 shRNA.

(b) To better visualize differences in 5mC levels, CpGs were grouped based on their % 5mC in control NPCs. The plot displays the distributions of 5mC levels for control (blue) and *Tet3* KD (red) within each group. Loss of methylation is observed across the whole range of methylation levels.

(c) Genomic features associated with differentially methylated positions (DMPs) after *Tet3* KD, showing that hypo-DMPs are enriched at genic regions and depleted at promoters and CpG islands.

(d) Comparison of our oxRRBS datasets with a published dataset for ES cells [35], displaying average 5mC levels per CpG island.

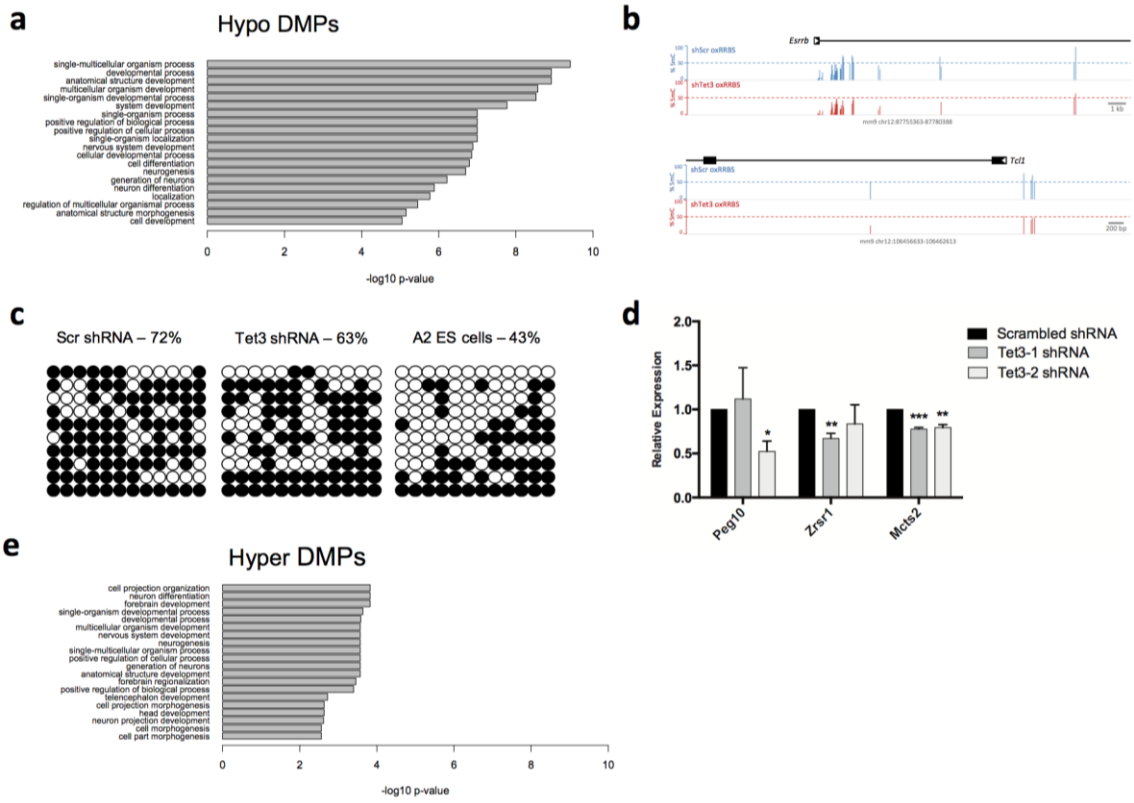

Figure 4 - *Tet3* knockdown alters DNA methylation of developmentally relevant gene promoters.

(a) Gene Ontology analysis of genes that loose methylation (Hypo DMPs) shows an association with development, differentiation and neurogenesis.

(b) Genome browser snapshots of oxRRBS data at *Esrrb* and *Tcl1* pluripotency genes, showing a reduction in 5mC levels after *Tet3* KD.

(c) *Tcl1* bisulfite cloning analysis; black circles - methylated CpGs; white circles - unmethylated CpGs.

(d) Expression analysis of imprinted genes showing hypermethylation after Tet3 KD (*p<0.05; ***p<0.001; t-test); n=2 independent experiments.

(e) Gene Ontology analysis of genes that gain methylation (Hyper DMPs) shows an association with neural differentiation processes.

2.11. Supplementary material

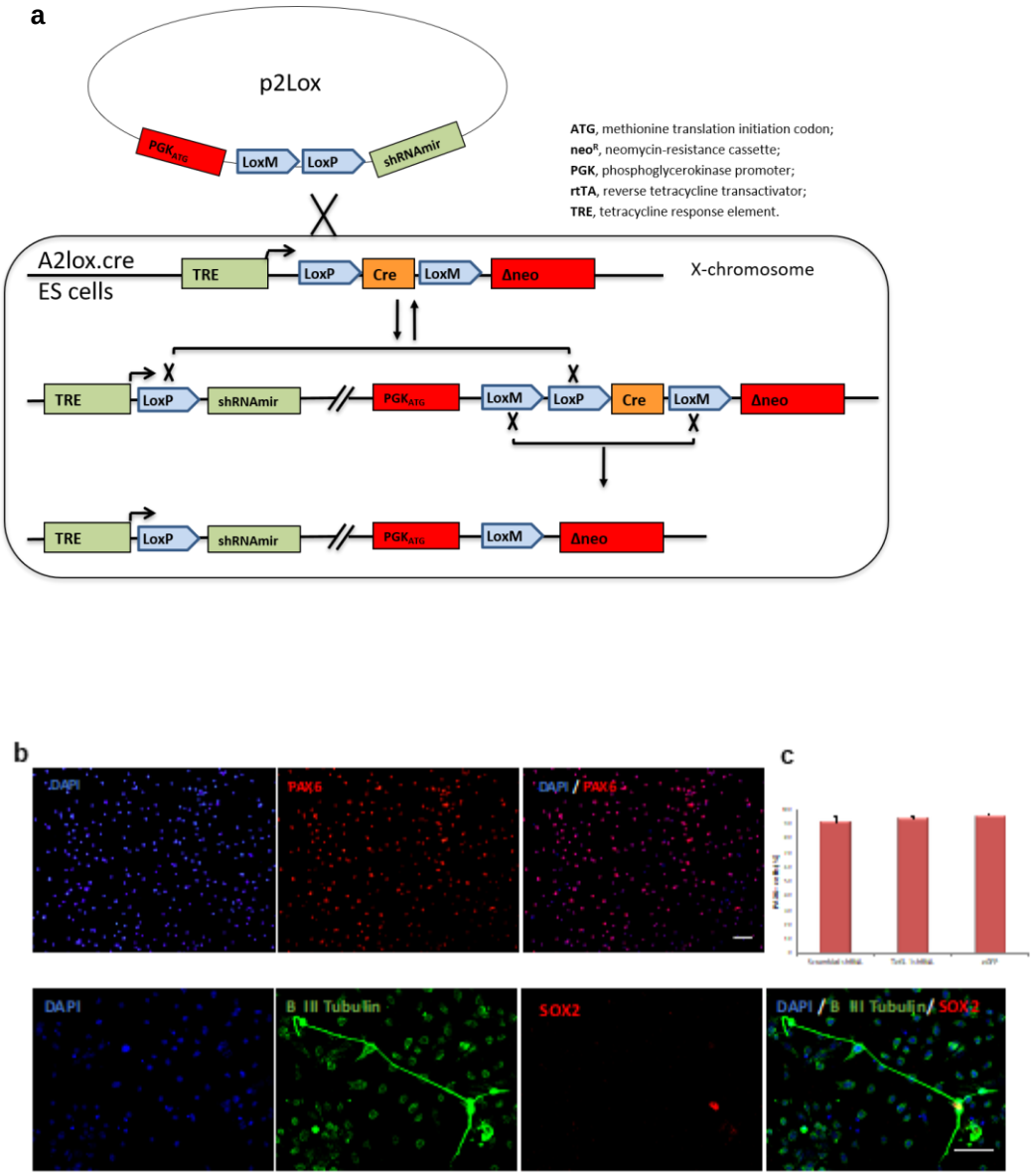

Figure S1 - Stable and inducible systems for *Tet1* and *Tet3* knockdown in NPCs (related to Figure 1).
(a) Schematic representation of the stable and inducible knockdown system using p2Lox as a vector containing the shRNAmir cassette that is transfected in A2lox.cre ES cells containing a tetracycline inducible element and pLox sites for site-specific recombination.
(b) Immunostaining for PAX6, B3-tubulin and SOX2, in NPCs after 1 day in culture in N2 medium (scale bars – 50 μm).
(c) Percentage of PAX6-positive NPCs in clones containing shRNAs and eGFP as control.

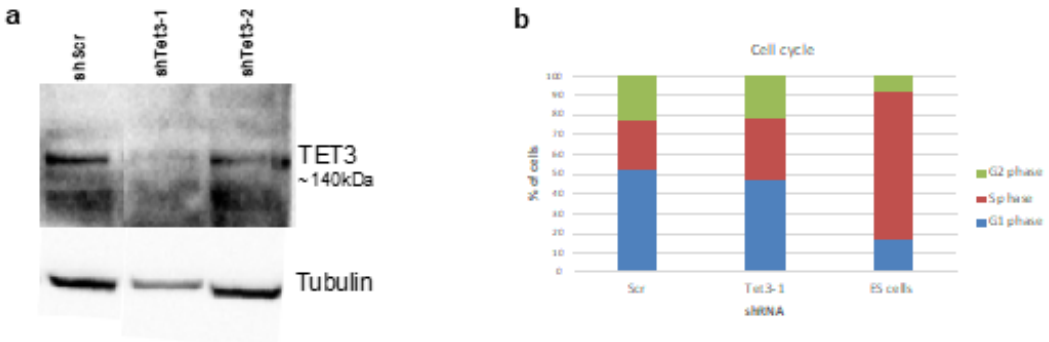

NPCs	Ratio TET3/Tubulin	Normalized
shScr	0,2264	1,00
shTet3-1	0,1995	0,88
shTet3-2	0,1599	0,71

Figure S2 - Knockdown of *Tet3* in Neural Progenitor Cells (related to Figure 2).
(a) Western blot analysis of TET3 in KD in NPCs and quantification.
(b) Cell cycle analysis by flow cytometry, using propidium iodide (PI) staining, of NPCs after knockdown of Tet1 and Tet3 shows a lower S-phase in all NPCs comparing to ES cells.
Control NPCs - Scrambled shRNA (shScr); NPCs containing shRNAs against +against Tet3 (shTet3-1 and shTet3-2).

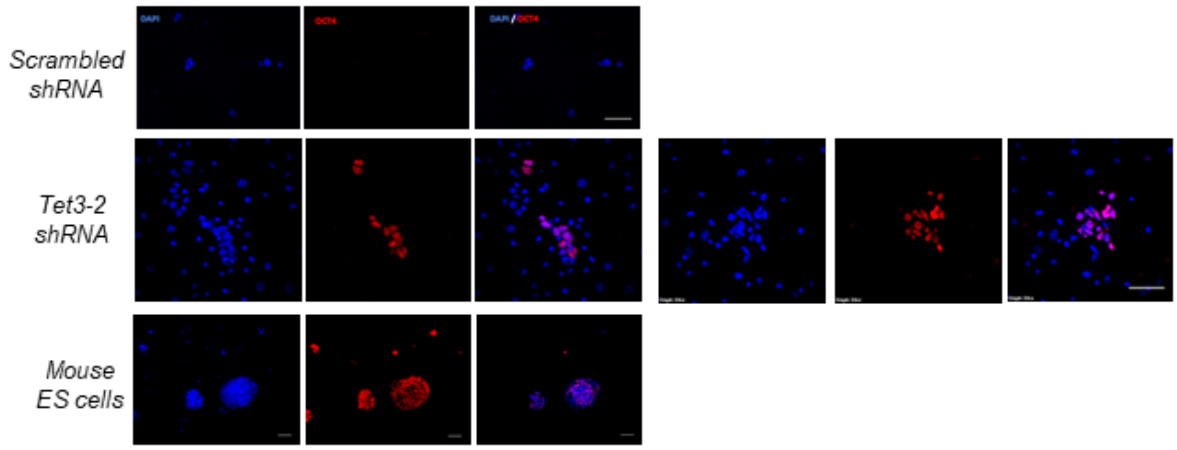

Figure S3 – OCT4 detection in Neural Precursor Cells (related to Figure 2)
Immunostaining of OCT4 in NPCs showing OCT4-positive cells aggregating to form ES cell-like colonies after *Tet3* KD. shScr - Scrambled control shRNA; shTet3-2 - shRNA against Tet3; mES cells - mouse embryonic stem cells. Scale bars - 50 µm

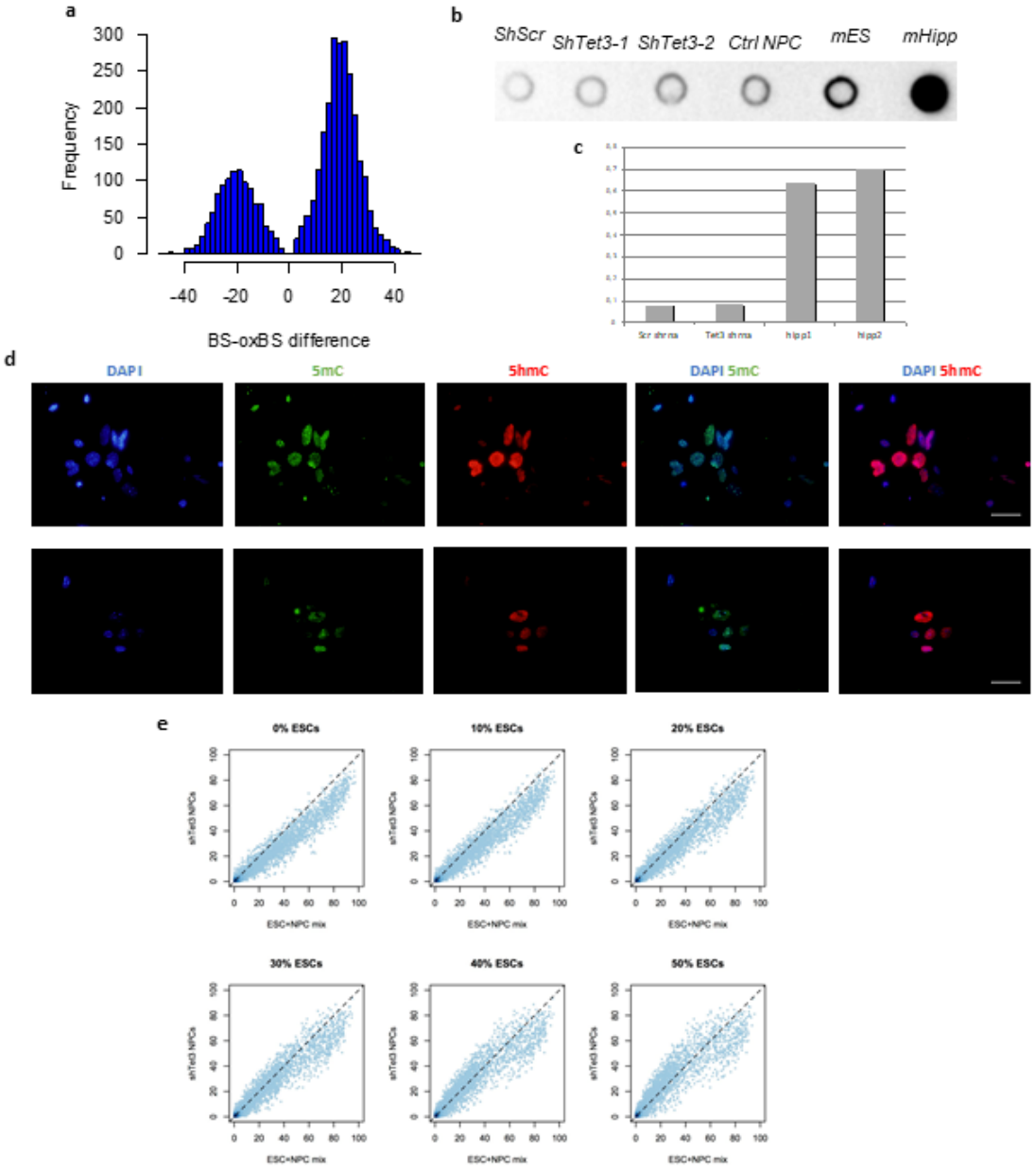

Figure S4 - 5hmC and 5mC analysis in NPCs after *Tet3* KD (related to Figure 3).

(a) oxRRBS data shows very little to no 5hmC signal in all the samples analysed

(b) Dot blot analysis of 5hmC in NPCs after *Tet3* KD. shScr - Scrambled control shRNA; shTet3-1 and shTet3-2 - shRNAs against *Tet3*. DNA from mouse ES cells (mES) and mouse hippocampal brain region (mHipp) were used as controls. 100 ng of DNA were loaded for all the samples.

(c) 5hmC detection by ELISA. DNA from mouse hippocampus (hipp1 and hipp2) was used as a positive control.

(d) Imunofluorescent detection of 5mC and 5hmC in NPCs shows that cells stain positively for both epigenetic marks. Scale bars – 50 µm.

(e) Comparison of oxRRBS methylation data between *Tet3* KD NPCs and different proportions of ES+NPC mixes.

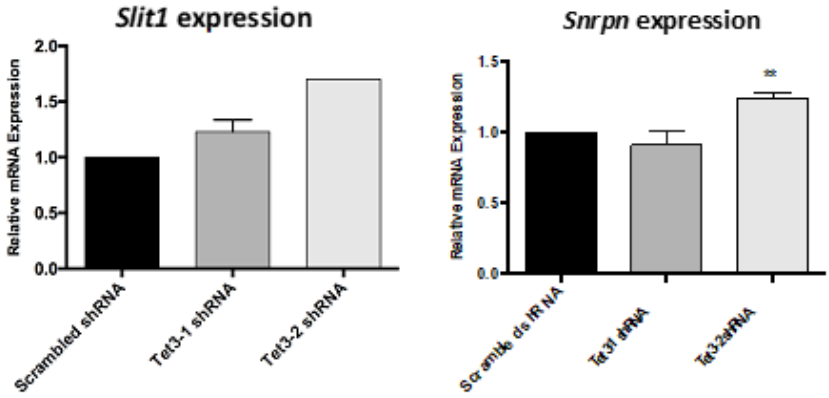

Figure S5 – Expression analysis of a hypomethylated gene (*Slit1*) and an imprinted gene (*Snrpn*).
(**p<0.01; t-test). Error bars represent SEM of three independent experiments for *Snrpn* and two independent experiments for *Slit1* (except Tet3-2 shRNA in which n=1 independent experiment).

Supplementary Table S1. shRNAs sequences

shRNA sequences	
Scrambled (Scr)	tgctgttgacagtgagcgggtatattggaagcagaccttgtagtgaagccacagatgtacaaggtctgcttccaatatacctgcctactgcctcgga
Tet3-1	tgctgttgacagtgagcgcgcccttgagctccaacgagaatagtgaagccacagatgtattctcgttggagctcaagggcatgcctactgcctcgga
Tet3-2	tgctgttgacagtgagcgcgcagtgtgtattcctaccatttagtgaagccacagatgtaaatggtaggaatacacactgcttgcctactgcctcgga
Color codes: mir-30 context; sense; loop; anti-sense.	

Supplementary Table S2. Primer list and sequences

			Product size (bp)	Reference
Bisulfite				
Tcl1 (12:106,460,347-106,460,634)	Fwd	AAATAGGAGGGTTAGGGAGATT	288	
	Rev	AAACACCAACATTAAAACCCA		
RT-qPCR				
Atp5b		GGCCAAGATGTCCTGCTGTT GCTGGTAGCCTACAGCAGAAGG	106	Ficz *et al.*, 2011
Hsp90ab1		GCTGGCTGAGGACAAGGAGA CGTCGGTTAGTGGAATCTTCATG	93	Ficz *et al.*, 2011
Tet1		CCATTCTCACAAGGACATTCACA GCAGGACGTGGAGTTGTTCA	116	Ficz *et al.*, 2011
Tet2		GCCATTCTCAGGAGTCACTGC ACTTCTCGATTGTCTTCTCTATTGAGG	120	Ficz *et al.*, 2011
Tet3		GGTCACAGCCTGCATGGACT AGCGATTGTCTTCCTTGGTCAG	104	
Dnmt1		TGTTCTGTCGTCTGCAACCT CCCTCACACACTCCTTTTCTG	155	
Dnmt3a		CCTGCAATGACCTCTCCATT CAGGAGGCGGTAGAACTCAA	89	
Oct4		GAAGCCGACAACAATGAGAACC CTCCAGACTCCACCTCACACG	111	
Nanog		CAGTGGTTGAAGACTAGCAATGGT AGGCTTCCAGATGCGTTCAC	113	
Sox2		GAGTGGAAACTTTTGTCCGAGA GAAGCGTGTACTTATCCTTCTTCAT	151	
Rex1 (Zfp42)		CGATGCTGGAGTGTCCTCAAG GCCACACTCTGCACACACGT	113	Ficz *et al.*, 2011
Tcl1		CTCCATGTATTGGCAGATCCTGTA CTCCGAGTCTATCAGTTCAAGCAA	79	Ficz *et al.*, 2011
Esrrb		AGTACAAGCGACGGCTGGAT CCTAGTAGATTCGAGACGATCTTAGTCA	103	Ficz *et al.*, 2011
Pax6		CAGATGCAAAAGTCCAGGTG TCTGTCTCGGATTTCCCAAG	209	Bibel *et al.*, 2007
Nestin		TCGCTCAGATCCTGGAAGGTGG GCTTCAGCTTGGGGTCAGGAAAG	165	
Tubb3		GTGAAGTCAGCATGAGGGAGA TGGGCACATACTTGTGAGAGGA	195	
TrkB		CTGGGGCTTATGCCTGCTG AGGCTCAGTACACCAAATCCTA	100	Bibel *et al.*, 2007
Gfap		CGAAGAAAACCGCATCACCATTCC TTGGCCTTCCCCTTCTTTGGTG	88	
Peg10		AGAGCAGCCAACCGAGAAGGT AACCCGCCTGTTCCACACGA	164	
Zrsr1		ATGGTACGCAGGACGACAGC AGTCCAAGCCGGAGGAGACAT	193	
Mcts2		ACCCGTTTATCCTGCCACACC TGACTCCGACACACAGGGCAT	180	
Slit1		CAGGCTTTGGTGGCCCTGAATG TGTGGAGACCTGAAGAGTGATGTT	125	
Snrpn		TGAGTTCAGGAAGATCAAGCCAAAG GCCCTCCACAGTCATTGAAAC	115	

Chapter III

Tet3 deletion in adult brain neurons increases anxiety-like behavior and impairs spatial orientation in male mice

Cláudia Antunes, Jorge D. Silva, Sónia Guerra-Gomes, Nuno D. Alves, Fábio Ferreira, Eduardo Loureiro-Campos, Wolf Reik, Nuno Sousa, Luisa Pinto and C. Joana Marques

Manuscript submitted

Tet3 deletion in adult brain neurons increases anxiety-like behavior and impairs spatial orientation in male mice

Cláudia Antunes[1,2], Jorge D. Da Silva[1,2], Sónia Guerra-Gomes[1,2], Nuno D. Alves[1,2], Fábio Ferreira[1,2], Eduardo Loureiro-Campos[1,2], Nuno Sousa[1,2], Wolf Reik[3,4], Luísa Pinto[1,2,7*] and C. Joana Marques[5,6,7*]

[1]Life and Health Sciences Research Institute (ICVS), School of Medicine, University of Minho, Braga, 4710-057, Portugal.

[2]ICVS/3B's - PT Government Associate Laboratory, Braga/ Guimarães, 4710-057, Portugal.

[3]Epigenetics Programme, The Babraham Institute, Cambridge CB22 3AT UK.

[4]The Wellcome Trust Sanger Institute, Cambridge CB10 1SA, UK.

[5]Genetics, Department of Pathology, Faculty of Medicine, University of Porto, 4200-319, Portugal.

[6]i3S – Instituto de Investigação e Inovação em Saúde, Universidade do Porto, Porto 4200-135, Portugal.

[7] Co-last authors

*Correspondence to: Joana Marques - cmarques@med.up.pt or Luísa Pinto- luisapinto@med.uminho.pt

Address: Life and Health Sciences Research Institute (ICVS)

School of Medicine, University of Minho

Campus Gualtar

4710-57 Braga, Portugal

3.1. Abstract

TET3 is a member of the Ten-eleven translocation (TET) family of enzymes which convert 5-methylcytosine (5mC) into 5-hydroxymethylcytosine (5hmC). *Tet3* is highly expressed in the brain, where 5hmC levels are most abundant. In adult mice, we observed that TET3 is present in mature neurons and oligodendrocytes but is absent in astrocytes. To investigate the function of TET3 in adult post-mitotic neurons, we used a *Tet3* conditional knockout (cKO) mouse model crossed with a Cre-expressing line, *Camk2a-CreERT2*. Ablation of *Tet3* in adult mature neurons resulted in increased anxiety-like behavior with concomitant increased corticosterone basal levels, and impaired hippocampal-dependent spatial orientation. Transcriptome and gene-specific expression analysis of the hippocampus showed dysregulation of genes involved in glucocorticoid signaling pathway (HPA axis) in the ventral hippocampus, whereas upregulation of immediate early genes (IEGs) was observed in both dorsal and ventral hippocampal areas. Additionally, Tet3 cKO mice exhibit increased dendritic spine maturation in the ventral CA1 hippocampal subregion. Based on these observations, we suggest that TET3 is involved in molecular alterations, that govern hippocampal-dependent functions. These results reveal a critical role for epigenetic modifications in modulating brain functions, opening new insights into the molecular basis of neurological disorders.

3.2. Introduction

Neurons are long-lived cells, governed by a strict molecular regulation to maintain genomic stability, but also possess a remarkable plasticity to respond to external stimuli. The dynamic nature of neuronal function is strictly regulated by epigenetic changes (Feng, Fouse et al. 2007). At the DNA level, 5-methylcytosine is one of the most well studied epigenetic marks and the conversion of 5-methylcytosine (5mC) to 5-hydroxymethylcytosine (5hmC), catalyzed by Ten- Eleven Translocation (TET) family of dioxygenases (Tahiliani, Koh et al. 2009), has gained the interest of the field.

High 5hmC content is positively correlated with gene transcription and is a feature of post-mitotic neurons, since very low levels were detected in immature neurons and non-neuronal cell types (Szulwach, Li et al. 2011, Cadena-del-Castillo, Valdes-Quezada et al. 2014). *Tet* genes have also been shown to be highly transcribed in the brain, with *Tet3* being the most abundant enzyme. *Tet3* levels are similar across different forebrain regions, such as cortex, hippocampus and cerebellum (Szwagierczak, Bultmann et al. 2010). A putative link between neuronal TET protein function and cognitive processes gained more relevance following the discovery that (de)methylation of DNA in the brain appears to be relevant for learning and memory (Miller and Sweatt 2007, Miller, Campbell et al. 2008). Indeed, TET1 and TET2

were later implicated in learning and memory processes in adult mice (Kaas, Zhong et al. 2013, Rudenko, Dawlaty et al. 2013, Zhang, Cui et al. 2013, Kumar, Aggarwal et al. 2015, Gontier, Iyer et al. 2018). TET3 deletion in mice leads to neonatal lethality, remaining yet to clarify whether this is related with neurodevelopemental deficits (Gu, Guo et al. 2011). Nonetheless, TET3 has been linked with brain function. Specifically, fear extinction leads to TET3-mediated accumulation of 5hmC, and the knockdown of this enzyme in the infralimbic prefrontal cortex (ILPFC) leads to a significant impairment in fear extinction memory (Li, Wei et al. 2014). Kremer and colleagues further showed that T*et3* expression, but not *Tet1* or *Tet2*, is regulated in an activity-dependent manner after contextual fear conditioning; moreover, expression of genes related with memory, such as *Notch1*, *Creb1*, *Crebbp* and *Gadd45b* are sensitive to *Tet3* upregulation (Kremer, Gaur et al. 2018). Importantly, *Tet3* was described as a synaptic sensor, able to regulate neuronal activity, since *Tet3* knockdown in hippocampal neuronal cultures increased glutamatergic synaptic transmission, whereas overexpressing *Tet3* decreased it (Yu, Su et al. 2015). Concordantly*, Tet3* deletion in young mice increases excitatory synaptic transmission (Wang, Li et al. 2017). Moreover, RNA seq analyses revealed a key role for TET3 in regulating gene expression in response to synaptic activity (Yu, Su et al. 2015). Here, we addressed the role of TET3 in adult behavior. We specifically induced *Tet3* deletion in mature forebrain neurons, at an adult stage, by crossing a *Tet3* conditional knock-out mouse line with calcium/calmodulin-dependent protein kinase II alpha-(*Camk2a)-CreERT2*-expressing transgenic line. Then, we performed behavioral analysis to assess anxiety- and depressive-like behaviors, as well as cognitive function.

Studies have disclosed that emotion and cognition are not independent behavioral dimensions. In fact most of neural regions related with modulation of emotional behavior, are also involved in cognitive processes, such as the hippocampus and the prefrontal cortex (Liu, Fu et al. 2009). We mainly focused our study in hippocampal-dependent behaviors, since this structure presents a complex connectivity with numerous cortical and subcortical structures, integrating the neural circuitry of cognitive and emotional functions (Strange, Witter et al. 2014). Indeed, the dorsal hippocampus is essential for spatial memory and navigation tasks. The ventral hippocampus establishes connections with structures such as, prefrontal cortex (PFC), amygdala and bed nucleus of stria terminalis (BNST), responsible for emotions like anxiety and fear (Fanselow and Dong 2010). Accordingly, the division in dorsal and ventral counterparts is reflected not only anatomically, but also functionally.

Results showed that TET3 ablation in post-mitotic neurons leads to increased anxiety and impaired spatial orientation; these behavioral changes were paralleled by increased corticosterone levels, and transcriptomic analysis unveiled a deregulation of genes involved in glucocorticoid signaling pathway,

controlled by the hypothalamic-pituitary-adrenal (HPA) axis, specifically in the ventral hippocampus. Additionally, quantification of gene-specific transcript levels demonstrated that immediate-early genes (IEGs) were upregulated in both dorsal and ventral hippocampus. Furthermore, Tet3 cKO mice showed increased synaptic maturation at the ventral CA1 hippocampal region. Thus, our study points to a role for TET3 as a regulator of HPA axis and neuronal activity-regulated genes, possibly associated with anxiety-like behavior and spatial orientation alterations in adult mice.

3.3.Results

TET3 protein is present in mature neurons and oligodendrocytes, but not in astrocytes, in adult mouse cortex and hippocampus brain regions.

In order to understand whether forebrain regions presented a distinct pattern of expression of *Tet3*, we decide to measure *Tet3* levels in the PFC, hippocampus, amygdala and BNST. The results showed that *Tet3* transcript levels are relatively similar in these brain regions (**Supplemental figure 1a**).

To elucidate in which cell types TET3 is present in the adult brain cortex and hippocampus, we performed double immunofluorescence staining for TET3 and typical markers for post-mitotic neurons (NeuN, Neuronal nuclear protein), astrocytes (GFAP, Glial fibrillary acidic protein) or oligodendrocytes (CNPase, 2',3'-Cyclic-nucleotide 3'-phosphodiesterase). We observed a strong co-localization of TET3 and NeuN in the cortical and hippocampal brain regions, pointing out neurons as the main source of TET3 protein (**Figure 1a**). We did not observe GFAP and TET3-double positive cells, and only a few number of cells co-expressed CNPase and TET3, suggesting that TET3 is absent in astrocytes and slightly expressed in oligodendrocytes (**Figure 1a**).

Adult *Tet3* conditional knockout mice show significant reduction of *Tet3* levels in forebrain regions

In order to determine the function of TET3 in mature neurons at an adult stage, we used a previously generated *Tet3* conditional knockout mouse model, in which the exon 7 (corresponding to the exon 5 in the coding sequence) of *Tet3* gene, is flanked by LoxP sites for Cre-induced site-specific recombination (Santos, Peat et al. 2013, Peat, Dean et al. 2014) and a *Camk2a-CreERT2* inducible line to specifically delete *Tet3* in mature forebrain neurons, after tamoxifen administration. *Tet3* was disrupted by deletion of the targeted exon resulting in a truncated protein lacking the catalytic domain. *Tet3* deletion was

confirmed at the DNA and mRNA levels, by PCR and RT-PCR, respectively (**Supplementary figure 2a-b**). Tet3 cKO mice showed a significant reduction of *Tet3* mRNA levels in several forebrain regions - PFC, amygdala, dorsal and ventral hippocampus (**Figure 1b-e**) (*t*-test, $p<0.05$). However, no reduction of Tet3 transcripts was found in the BNST region (**Figure 1f**). Of note, decreased levels of *Tet3* did not interfere with transcript levels of *Tet1* or *Tet2* (**Figure 1b-e**). To better determine the effectiveness of the conditional knockout strategy in neuronal cells, we quantified the number of post-mitotic neurons (NeuN-positive cells) showing TET3 staining in the hippocampus of control and Tet3 cKO mice, and observed a significant reduction in TET3/NeuN-positive cells (Adjusted t-test, $p<0.05$, $\omega^2_p = 0.841$; **Figure 1g-h**). We further assessed whether the conditional deletion of *Tet3* affected global 5hmC levels in forebrain regions using an ELISA-based assay, and observed no changes in the prefrontal cortex, hippocampus and amygdala of Tet3 cKO mice when comparing to the control group (**Supplementary Figure 1b**).

Tet3 deletion in neurons results in increased anxiety-like behavior and basal corticosterone levels, and impaired spatial orientation

In order to ascertain if *Tet3* ablation in adult post-mitotic neurons could have an effect in the behavioral performance of mice, we performed a battery of behavioral tests assessing various paradigms related to emotional and cognitive domains. We used two behavioral tests to detect anxiety-like behavior, namely the open-field (OF) test and the elevated plus maze (EPM), and the forced swimming test (FST) and tail suspension test (TST) to assess antidepressant-like behavior. Analysis of the total distance traveled in the open arena and EPM arms revealed no differences between genotypes, as they presented similar locomotor activity (**Supplementary figure 3b and 3d**). Additionally, no differences were found in the average velocity and vertical counts in the OF test (**Supplementary figure 3a and 3c**). Regarding the anxiety-like behavioral dimension, Tet3 cKO mice spent less time in the center of the OF (**Figure 2b**). No *p*-value differences were found in the time spent in the open arms of the EPM when compared to the control group (**Figure 2d**), but the magnitude effect, represent by Cohen's d, is medium-large (*t*-test, OF, $p<0.05$, $d=0.810$; EPM, $p= 0.114$, $d=0.684$). Moreover, in the EPM test, we found that Tet3 cKO mice showed significantly lower frequency of head hips in the open arms (**Figure 2d,** $p<0.01$, $d=1.400$) and higher latency to enter for the first time in the open arms when compared with control animals (**Figure 2e,** $p<0.05$, $d=0.881$). Additionally, we discovered a significant positive correlation between the performance in the OF and EPM behavioral tests ($r=0.652$; $p<0.01$) (**Figure 2f**). Altogether, these

parameters are indicative of increased anxiety-like behavior in Tet3 cKO animals.

In contrast, we did not observe differences in immobility times between the two groups in the FST and TST (*t*-test, FST, p=0.316, d=0.353; TST, p=0.270, d=0.511) (**Figure 2g-h**). Considering the involvement of the HPA axis in the modulation of behavior, we further determined the serum basal levels of corticosterone in control and Tet3 cKO mice. Both in nadir and zenith time points, Tet3 cKO mice presented an overactivation of the HPA axis, as suggested by the increased levels of corticosterone (Adjusted t-test, $p<0.01$, $\omega^2_p = 0.417$; **Figure 2i**).

Next, we assessed the possible effect of *Tet3* neuronal ablation in different cognitive domains, such as learning and memory. We tested Tet3 cKO mice in the Morris water maze (MWM) test to assess reference memory, a task that relies on hippocampal activity. Both, Tet3 cKO and control mice were able to successfully learn the spatial reference memory task, as confirmed by the decreasing latencies during the trials (**Figure 3a;** mixed ANOVA, genotype, p=0.274, $\omega^2_p = 0.015$) and by their performance in the probe trial, assessed by the same preference (percentage of time swum) for the goal quadrant where the platform was located during the acquisition phase (*t*-test, p=0.417, d = 0.417) (**Figure 3b**). However, analysis of the strategies adopted by the mice to achieve the escape platform in the MWM task, divided in random searching/scanning (non-hippocampal strategies) or directed strategies (hippocampal strategies) (Graziano, Petrosini et al. 2003), revealed that Tet3 cKO mice adopted significantly less hippocampal-dependent strategies when compared with control mice (Chi-square test, $p<0.05$, $\varphi = 0.466$), indicating a poor spatial orientation (**Figure 3c**).

To evaluate recognition memory, we performed the novel object recognition test. In this task, Tet3 cKO and control mice showed similar time exploring the object displaced after a short period of time (1 h) (**Figure 3d;** *t*-test, p=0.553, d=0.379) indicating normal object location memory. Tet3 cKO and control mice dedicated similar percentages of time exploring the novel object displayed 24 h after habituation to familiar objects, indicating no deficits in long-term object recognition memory (**Figure 3e;** *t*-test, p=0.462, d=0.267). Moreover, when short-term memory was evaluated, Tet3 cKO displayed identical discrimination index, indicating no deficits of short-term memory as well (**Figure 3f;** *t*-test, p=0.504, d=0.235).

Transcriptomic analysis revealed that *Tet3* deletion affects gene expression mainly in the ventral hippocampus

To determine which genes were affected by the loss of *Tet3* and considering the impairment of hippocampal-dependent function described above, we performed a transcriptomic analysis, using QuantSeq RNA (Pamela Moll 2014), in RNA extracted from dorsal and ventral hippocampus of Tet3 cKO and control mice. Notably, only 20 transcripts were found to be differentially expressed in the dorsal hippocampus of Tet3 cKO mice, with only 7 being protein coding and with no particular relevance for this study (**Fig. 4a-b and Supplemental table S2**); however, in ventral hippocampus, the number of differentially expressed genes was higher - 143 (**Figures 4a and 4c and Supplemental table S3**), with 90 being downregulated and 53 upregulated. This reveals a greater sensitivity of the ventral hippocampus to conditional deletion of neuronal *Tet3.*

Gene ontology analysis of differentially expressed transcripts in the ventral hippocampus, using the Panther® classification system (Mi, Muruganujan et al. 2013), revealed that the most common molecular function was binding activity, and the most represented protein classes were transporters, hydrolases and enzyme modulators (**Figures 4d, e**). Moreover, we performed a level 4 and 5 gene ontology classification using the Consensus Pathway Database (Kamburov, Stelzl et al. 2013); while none of the top 10 categories were specifically related with neuronal activity (**Figures 4f**), pathway enrichment analysis revealed an impact in the glucocorticoid signaling pathway (HPA axis) and FOXA1 transcription factor network, amongst others. (**Figure 4g**). Regarding HPA axis, we confirmed by qRT-PCR the downregulation of *corticotropin releasing hormone receptor type 2 (Crhr2)*, involved in stress-related disorders, such as anxiety and depression (Reul and Holsboer 2002) (**Figure 4h**). For FOXA1 transcription factor related genes, we confirmed the downregulation of *Poua2af1, Col8a1* and *Lmx1a* (**Figure 4h**). Additionally, we obtained information from the Ingenuity Pathway Analysis software (Kramer, Green et al. 2014), namely in canonical pathways (where glucocorticoid receptor signaling was newly identified), upstream regulators (where Dopamine Receptor D2 (DRD2) appears) or diseases and disorders (being the most enriched category cancer) (**Supplemental figures 4a-c**).

Tet3 cKO mice displayed increased expression of neuronal activity-regulated genes in the hippocampus

A plethora of neuronal genes is involved in neural plasticity related to learning and memory processes and transcriptional activity of these genes is crucial to control these cognitive processes. The QuantSeq RNA results allowed to identify *c-fos*, as an upregulated gene in Tet3 cKO animals (**Supplemental Table 3**). Hence, we explored whether *Tet3* deletion in neurons leads to dysregulation of other activity-induced genes involved in synaptic plasticity in the hippocampus (**Fig. 4i-j**) and observed an increase in transcript levels of some of these genes. The Immediate Early Genes (IEGs) *Npas4* and *c-fos* were the most

significantly up-regulated. In the dorsal hippocampus of Tet3 cKO mice both IEGs were upregulated (**Figure 4i;** adjusted t-test, c-fos $p<0.05$, $d=1.534$; Npas4 $p<0.01$, $d=2.321$). Nevertheless, in the ventral part only Npas4 was significantly increased (**Figure 4i;** adjusted t-test: Npas4, $p<0.05$, $d=0.520$; c-fos, $p=0.248$, $d = 0.523$). These results suggest that TET3 regulates these IEG's levels.

Tet3 cKO mice harbor increased dendritic spine maturation in ventral hippocampal pyramidal neurons

To further correlate the observed behavioral and neuronal activity-regulated gene expression changes in Tet3 cKO mice with putative alterations in neural plasticity mechanisms, we analyzed neuronal and spines morphology of pyramidal neurons in the adult dorsal and ventral hippocampus CA1. We did not observe alterations in dendritic length and complexity of their arborization in the dorsal and ventral regions of Tet3 cKO (**Figure 5 a-b; e-f**). However, and although Tet3 deletion in neurons did not impact on spines density **(Figure 5c and 5g)**, Tet3 cKO mice displayed a decrease in the proportion of immature thin spines and an increase in the mature mushroom type of spines in the ventral region of the hippocampus (**Figure 5h;** Factorial ANOVA, genotype, $p<0{,}001$, $\omega^2_p < 0$), suggesting that TET3 regulates spine maturation in the ventral CA1 region.

3.4. Discussion

Despite recent advances, the role of TET enzymes in the brain, particularly of TET3 which is highly transcribed, is largely unknown. Here, we show that, in forebrain regions of the adult brain, TET3 is present in neurons but and sparsely expressed or absent in oligodendrocytes and in astrocytes respectively. We thus confirmed that neurons heavily express TET3, as previously observed by others (Li, Wei et al. 2014, Montalbán-Loro, Lozano-Ureña et al. 2019).

As TET3 is highly expressed in mature neurons in forebrain regions of the adult brain, we used a conditional and inducible knockout mouse model to ablate *Tet3* in *Camk2a*-positive mature neurons allowing to study the function of TET3 in these cells at an adult stage. Importantly, Tet3 deletion did not affect *Tet1* and *Tet2* expression; in fact, this deletion did not influence the global genomic levels of 5hmC, and this might reflect compensatory activities of *Tet1* and *Tet2*, which influence the demethylation activity independently of levels of these.

Our results show that neuronal *Tet3* deletion increases anxiety-like behavior and impairs hippocampal spatial orientation. Regarding TET enzymes and their possible implications in anxiety-like behavior control,

only the role of one TET enzyme, *Tet1,* was previously addressed. Although TET1 KO mice showed normal anxiety and depression-related behaviors (Rudenko, Dawlaty et al. 2013), Feng and colleagues showed that neuronal *Tet1* deletion in neurons of Nucleus Accumbens (NAc) produced antidepressant-like effects in several behavioral assays (Feng, Pena et al. 2017). In contrast, in our model in which we deleted *Tet3* in mature forebrain neurons, we observed an anxiety-like phenotype. Nevertheless, the deletion of *Tet1* and *Tet3* in these two studies was performed in distinct brain regions, possibly influencing the observed results. On the other hand, the distinct behavioral phenotype triggered by deletion of *Tet1* and *Tet3* might suggest a different regulatory activity for these enzymes in the anxiety regulation of the adult brain.

We further showed that *Tet3* cKO mice displayed a specific impairment of hippocampal-dependent spatial orientation; other hippocampal-dependent tasks, such as object location and long- and short-term recognition memories, remained unaffected. Importantly, *Tet1* and *Tet2* were shown to be relevant to control spatial learning (Zhang, Cui et al. 2013, Gontier, Iyer et al. 2018), but *Tet3* seems to be only critical to control spatial orientation, since the spatial learning remained unaltered in our model. This observation, linked to the finding of role of the ventral hippocampus in spatial navigation (McDonald, Balog et al. 2018), supports the impact of *Tet3* in the function of ventral hippocampus. Additionally, the impairment in the use of directed strategies reflects alteration of the goal-directed behavior, and can be correlated with the anxiety-like behavior, since the ability to demonstrate goal-directed behavior requires a suppression of emotional states, namely anxiety (Jimenez, Su et al. 2018, Yoshida, Drew et al. 2019).

The molecular mechanisms through which TET3 controls anxiety and spatial orientation remained to be explained. Hence, we studied whether *Tet3* deletion could impact the expression of gene networks known to be involved in the dysregulation of behavioral domains. We performed a transcriptomic analysis of the hippocampus of Tet3 cKO mice that showed few dysregulated genes in the dorsal region, but several networks were altered in the ventral region. The ventral hippocampus has been shown to be involved in the modulation of emotional behavior, namely anxiety (Fanselow and Dong 2010). Strikingly, an impact of neuronal *Tet3* deletion in key networks involved in the regulation of anxiety-like behaviour was observed in the ventral hippocampal region.

Enrichment pathway analysis of differentially expressed targets identified the glucocorticoid signaling pathway (HPA axis), specifically in this hippocampal subregion. In fact, dysfunction of the HPA axis has been implicated in the pathogenesis of psychiatric disorders, including anxiety disorders (Faravelli, Lo Sauro et al. 2012). The persistent activation of the HPA system results in a sustained increase of cortisol (humans) or corticosterone (rodents) levels, and is one of the most consistent findings in psychiatry diseases, namely anxiety and depression (Faravelli, Lo Sauro et al. 2012). Importantly, Tet3 cKO animals

presented increased levels of corticosterone in the blood serum suggesting an overactivation of the HPA axis, which can be correlated with the increased anxiety-like behavior. Remarkably, we also found *Crhr2* to be downregulated in the ventral hippocampus of Tet3 cKO mice; and CRHR2-deficient mice display increased anxiety-like behavior (Bale, Contarino et al. 2000, Kishimoto, Radulovic et al. 2000), suggesting that the observed decrease of *Crhr2* levels in the ventral hippocampus of Tet3 cKO mice can be linked to the development of this altered emotional behavior. However, Kishimoto and colleagues suggest that *Crhr2* predominantly mediates a central anxiolytic effect independent of the HPA axis activity, since they did not observe hypercortisolism in *Crhr2* +/+ and -/- mice at basal levels. Nevertheless, hypercortisolism was observed in *Crhr2*-/- mice upon acute stress in Kishimoto et al. work (Kishimoto, Radulovic et al. 2000), and in various other studies (Coste, Kesterson et al. 2000, Preil, Müller et al. 2001). Yet, the direct or indirect causeal relationship between *Crhr2* decrease, corticosterone increases, and stress has not been established. Importantly, it is relevant to consider that Kishimoto et al. used a full KO mouse model, which can display compensatory development effects, hiding alterations in the basal corticosterone levels.

Neuronal activity-regulated genes are known to play important roles in diverse cellular processes such as neurotransmission, neuronal plasticity, learning and memory (Loebrich and Nedivi 2009, Coutellier, Beraki et al. 2012). Notably, and contrary to TET3 function in our model, TET1 was shown to be a positive regulator of IEGs expression (Kaas, Zhong et al. 2013, Rudenko, Dawlaty et al. 2013, Kumar, Aggarwal et al. 2015). Amongst all the IEGs analysed in Tet3 cKO, we showed that the key upstream regulatory gene *Npas4* displayed the highest magnitude of change amongst all the IEGs analysed in Tet3 cKO. *Npas4* controls a transcriptional program involving neural activity-regulated genes and is essential for cognitive function (Ramamoorthi, Fropf et al. 2011, Coutellier, Beraki et al. 2012). Moreover, this gene is involved in neural circuitry plasticity, maintaining circuit homeostasis (Ploski, Monsey et al. 2011, Ramamoorthi, Fropf et al. 2011). Thus, we speculate that the aberrant increase in *Npas4* and *c-fos* transcript levels in the dorsal hippocampus of Tet3 cKO mice, might lead to a dysregulation of neuronal activity and possibly explain the spatial orientation impairment observed. Despite the vast amount of data supporting changes in IEGs expression in cognitive processes, in psychiatric conditions, only few studies have evaluated the direct implication of IEGs. However, it was already shown that *Npas4*KO mice are less anxiety when compared to control animals (Jaehne, Klaric et al. 2015). Accordingly, Tet3 cKO mice showed increased anxiety-like behavior and increased expression of *Npas4* mRNA transcript in the ventral hippocampus. Based on our results, we hypothesize that upregulation of *Npas4* can lead to an increase in the expression of its targets, namely *c-fos*, promoting increased hippocampal neuronal activity. This

dysfunctional hippocampal neuronal activity may alter the capacity of neurons to correctly respond to stimulus and culminate in behavioral dysfunction. Our hypothesis is in agreement with findings that TET3 is a negative regulator of synaptic activity (Yu, Su et al. 2015, Wang, Li et al. 2017). In accordance, we herein observed that *Tet3* deletion triggered a shift of thin immature spines to the mushroom mature type in the ventral CA1 hippocampus. This increased synaptic complexity (Berry and Nedivi 2017) fits with the observations of increased glutamatergic transmission in *Tet3* deficient animals (Wang, Li et al. 2017) and with the role of glutamate in spine maturation (McKinney 2010, Mattison, Popovkina et al. 2014). Although potentially expected, our data are describing that dendritic spine morphology is modified by Tet3 deletion specifically in mature neurons, for the first time. This overactivation of the ventral hippocampus is suggestive of an anxiogenic phenotype in these animals and may reveal to be an interesting therapeutic target.

In summary, we here suggest that *Tet3* plays an important role in modulation of anxiety-like behavior, as well as in spatial orientation tasks. The epigenetic control of behavior and neurophysiology is a topical subject currently and very relevant to various neurological and psychiatric conditions (Antunes, Sousa et al. 2019). However, TET3 has been poorly studied in the context of psychiatric disorders, and to our knowledge, there is only one report showing no alterations in *Tet3* levels in the parietal cortex of psychotic patients (Dong, Gavin et al. 2012). Future research on TET3 function, as well as on other members of TET family, may critically contribute to our understanding of epigenetic regulation impact on behavioral performance. Particularly TET3, can represent a potential therapeutic target in pathologies related with anxiety spectrum.

3.5. Methods

Animals and treatment

Tet3$^{fl/fl}$ mice on a C57BL/6N background (Santos, Peat et al. 2013, Peat, Dean et al. 2014) were crossed with B6;129S6 mice ((Madisen, Zwingman et al. 2010) JAX stock #012362 – *Camk2a-CreERT2*) expressing a tamoxifen-inducible Cre recombinase under the control of the mouse *Camk2a* promoter region to generate mice heterozygous for the floxed *Tet3* allele (Santos, Peat et al. 2013, Peat, Dean et al. 2014) and Cre- recombinase. These mice were interbred with C57BL/6N mice homozygous for the floxed *Tet3* allele to generate mice heterozygous for Cre-recombinase and homozygous for the floxed *Tet3* allele, designated as Tet3 cKO mice. Mice homozygous for the *Tet3* floxed allele, but not carrying Cre-recombinase, were designated as control mice. Animals were genotyped by PCR analysis using genomic DNA and primers specific to Cre-recombinase and the floxed *Tet3* allele. Detection of flox transgene was

done using a primer specific to the fragment, which allowed to detect the deleted or floxed allele (**Supplemental table 1**).

To induce Tet3 deletion, male mice were administrated with tamoxifen (Sigma, St. Louis, MO; T-5648) dissolved in corn oil (Sigma; C-8267) at 20 mg/ml. Six-week-old mice were injected intraperitoneally with 50 mg/kg of tamoxifen twice a day for 5 consecutive days, with 7 days break followed by injections for 5 additional consecutive days (**Fig. 2a**). One month after tamoxifen treatment, blood samples were collected from the animals and corticosterone levels were measured using the commercial kit (Enzo Life Sciences, New York, USA). All procedures were carried out in accordance with EU Directive 2010/63/EU and NIH guidelines on animal care and experimentation and were approved by the Portuguese Government/Direção Geral de Alimentação e Veterinária (DGAV) with the project reference 0421/000/000/2017.

Behavioral analyses

We used standard tests that evaluate motor and locomotor activity (OF), emotional behavior (anxiety (OF, EPM) and antidepressant-like states (FST, TST)), and cognition (NOR, MWM).

Animals were submitted to behavioral testing 1 month after tamoxifen treatment. Mice were studied during the light phase and habituated to testing rooms for at least 30 min before each test. Behavioral assessment was performed following this order: Open Field (OF), Elevated Plus Maze (EPM), Forced-swim Test (FST), Tail suspension Test (TST), Novel Object Recognition (NOR) and Morris Water Maze (MWM). The tests details are described bellow.

Open Field

In the open field (OF) test, each animal was placed in the center of the arena (square arena [43.2 cm × 43.2 cm]) surrounded by tall perspex walls (Med Associates Inc., St. Albans City, VT) and allowed to freely explore it for 5 min. Infrared beams and manufacturer's software were used to automatically register animals' movements. Data was analyzed using the activity monitor software (Med Associates, Inc.).

Elevated Plus Maze

The elevated plus maze (EPM) apparatus (ENV-560; Med Associates Inc., St.Albans, VT,USA) consisted of two opposite open arms (50.8cm × 10.2 cm) and two closed arms (50.8cm × 10.2 cm × 40.6 cm). Briefly, each animal was freely let to explore the maze for 5 min. The time spent in the open arms and the time to enter in the open arms (latency to enter an open arm timed from the start of the test), were

analyzed using EthoVision XT 11.5 software (Noldus, The Netherlands). The frequency number of head hips (number of times that the animal look at the floor when is in the open arms) was manually analyzed by a single researcher.

Forced-swim Test

Learned-helplessness was assessed through the forced-swim test (FST). Briefly, assays were conducted by placing each animal, individually, in transparent cylinders filled with water (25^{O}C; depth 30 cm) for 6 min. The trials were videotaped, and the immobility time measured during the last 4 min, using the EthoVision XT 11.5 software (Noldus, The Netherlands). Immobility was considered when the animal was only floating. Learned-helplessness behavior was defined as an increase in time of immobility.

Tail suspension Test

In the tail suspension test (TST) mice were suspended 50 cm above the floor by adhesive tape placed approximately 1 cm from the tip of the tail. Tail climbing behaviors were prevented by passing mouse tails through a small plastic cylinder prior to suspension. For each mouse, immobility time was assessed during a 6 min period. The trials were videotaped, and the immobility time measured during the trial, using the EthoVision XT 11.5 software (Noldus, The Netherlands). Immobility was considered when the animal was not moving the limbs or the entire body.

Novel object recognition

The test was conducted under dim white-light illumination in a lusterless white box (30 x 30 x 30 cm). Briefly, animals were habituated to an open arena for 3 consecutive days for 20 min. In the fourth day, two similar objects (glass bottles) were symmetrically placed on the center of the box and animals could freely explore both objects for 10 min. After an interval of 1 h in their home cages, the novel object was displaced to the opposite side of the box and mice were allowed to explore this new configuration. This trial allowed the assessment of the spatial recognition memory of the subjects. In order to evaluate long-term recognition memory, one of the familiar objects was replaced by a novel one (Lego® brick) 24 h afterwards, and mice were placed in the arena and allowed to explore both for 10 min. In the last day, two new objects were placed in the boxes and mice were place in the arena and allowed to explore both for 10 min. 1 h after one object was replaced by a novel, and the animals placed again to explore these, in order to evaluate short-term memory.

Boxes were cleaned between trials and subjects, with 10% ethanol. Animals were considered to be exploring whenever the nose was facing the object. Exploration time of the novel objects over the total exploration time was used as measure of object preference. Behavior was video-recorded and analyzed using EthoVision XT 11.5 software (Noldus, The Netherlands).

Morris water maze

Mice were tested in a circular pool (106 cm diameter) filled with water (23 ± 1 °C) and placed in a dim light room. In order to increase the contrast to detect the mice, water was made opaque with the addition of nontoxic titanium dioxide (Sigma-Aldrich; 250 mg/L). Spatial cues were placed in the walls around the pool (square, stripes, triangle and a cross). The pool was divided into four imaginary quadrants and a hidden transparent platform (a circular escape platform (10 cm diameter, 22 cm height)) was placed in one of the quadrants. Trials were video-captured by a video-tracking system (Viewpoint, Champagne-au-Mont-d'Or, France). The 4 days of protocol consisted in a hippocampal-dependent task whose goal was to assess the ability of mice to learn the position of the hidden platform kept always in the same position. Each day, mice performed four consecutive trials (maximum of 60 s, with a 30 s intertrial interval) being placed in the pool facing the maze wall and oriented to each of the extrinsic cues in random order. Whenever mice failed to reach the platform, animals were guided to the platform and allowed to stay in it for 30 s. On the fifth day, the platform was removed and a single trial of 60 s was performed (probe trial). For strategy analysis, we defined two blocks of strategies: "non-hippocampal dependent strategies" (Thigmotaxis, Random Swim and Scanning) and "hippocampal dependent strategies" (Directed Search, Focal Search and Direct Swim) as previously described by (Graziano et al. 2003).

Serum corticosterone levels

Two independent collections were made in two different time points, 8 a.m. and 8 p.m., with an interval of 24 h in between. The blood was rapidly collected after a small incision in the tail of the animals. The collected blood was centrifuged at 13,000 rpm for 10 min and the supernatant removed and stored at −80 °C until use. Corticosteroid levels in serum were measured by radioimmunoassay using a commercial kit (Enzo Life Sciences, New York, USA), according to manufacturer's instructions.

DNA/RNA Extraction

After behavior assessment, the animals were first anesthetized with a mixture of ketamine (75 mg/kg, i.p.; Imalgene 1000, Merial, EUA) and medetomidine (1 mg/kg, i.p.; Dorbene Vet, Pfizer, EUA), and

transcardially perfused with 0.9% saline. Brains were carefully removed and macrodissected, and tissue samples were stored at -80 ^{O}C. The tissues were prepared by homogenization using Trizol® reagent (Invitrogen), and extracted according to the manufacturer's instructions. The RNA was treated with DNase I (Thermo Scientific) and a total 500 ng RNA was used for cDNA synthesis using the qScriptTM cDNA SuperMix (Quanta Biosciences, USA).

PCR analysis

Detection of flox and deleted transgenes was performed using specific primers to the fragment, which allowed to detect the deleted or floxed allele (deleted: 237bp; floxed: 400bp). The detection of the Cre allele was done using a specific pair of primers (fragment of 184bp). The final concentrations in the PCR reactions were: 30 ng of extracted DNA, 0.2 U/µL NZYTaq II 2x Green Master Mix (Nzytech), 0.2 µM of forward primer and 0.1 µM of each reverse primer for Tet3 allelles and 1µM of each forward and reverse Cre allele. The primers' sequences are indicated in **Supplemental table 1**. Amplification was performed on the Veriti® Thermal Cycler (Life Technologies). Bands were visualized on the BioRad Gel Doc™ EZ System (BioRad).

qRT-PCR

Sense and antisense sequences can be found in **Supplemental table2**. Each qPCR reaction was run in duplicate for each sample in 20µl reactions using 5x HOT FIREPol ® EvaGreen ® qPCR Mix Plus ROX (Solis Biodyne, Estonia). The reaction was then performed on a Fast Real-Time PCR System (Applied Biosystems, USA). The relative abundance of each gene of interest was calculated on the basis of the ΔΔCt method, with results being normalized to the average Ct of *Atp5b*.

RNA Sequencing Analysis

RNA integrity was evaluated through chip-based capillary electrophoresis (Fragment Analyzer, Agilent®), with all samples having a RQN > 8.0. A total of 500 ng RNA was used for library construction, using the 3'mRNA-Seq Library Prep Kit (Lexogen). The resulting library was then sequenced on Illumina NextSeq500. RNA-seq analysis was carried out on two independent technical replicates. Quality control was carried out on raw datasets using FastQC, with no adapters being found. Differential expression analysis was performed using edgeR (Robinson, McCarthy et al. 2010) and genes were considered differentially expressed between conditions if attaining an FDR < 5% and an absolute fold change > 2.

Gene ontology classification of obtained hits was carried out using Panther® and Ingenuity Pathway Analysis (IPA, Qiagen, Redwood City, CA, USA) software.

Quantification of 5hmC

The global level of 5hmC was assessed using a Quest 5hmC DNA ELISA Kit (Zymo research, California, USA). The procedure was followed according to the manufacturer's instructions, having loaded 100 ng of genomic DNA of each brain region per well.

Immunofluorescence analysis

Brains were transcardially perfused with phosphate-buffered saline (PBS) and fixed overnight in 4% PFA. Coronal cryosections (20 µm) were incubated O/N at 4 ^{O}C, with primary antibodies, sequentially. Used antibodies were: NeuN (Cell signaling, rabbit, D4640, 1:100), Tet3 (Abcam, rabbit, ab153724, 1:100), GFAP (mouse, Thermo scientific, MA5-12023, 1:100) and CNPase (mouse, Millipore, MAB326, 1:200). The subclass-specific antibodies - Alexa Fluor 488 and Alexa Fluor 594 (Molecular Probes) - were used for detection, and incubation was performed for 2h at RT. Nuclei were counterstained using DAPI during 10 minutes at RT. Fluorescence images were acquired with the Olympus Fluoview FV1000 confocal microscope (Olympus, Hamburg, Germany) and the number of double-positive cells calculated using FIJI software (3 sections for each animal; n = 3 animals per group).

3D-reconstruction of neurons

To assess the 3D dendritic morphology of hippocampal pyramidal neurons, we used the Golgi-Cox impregnation technique. Dendritic arborization and spine numbers/density/types were analyzed in the dorsal and ventral CA1 of Control and Tet3 cKO mice, as described previously (Bessa, Ferreira et al. 2008, Mateus-Pinheiro, Alves et al. 2016). Briefly, brains were immersed in Golgi-Cox solution for 21 days and then transferred to a 30% sucrose solution and cut on a vibratome. Coronal sections (200 µm thickness) were collected in 6% sucrose and blotted dry onto gelatin-coated microscope slides. They were subsequently alkalinized in 18,7% ammonia, developed in Dektol (Kodak, Rochester, NY, USA), fixed in Kodak Rapid Fix, dehydrated, xylene cleared, mounted and coverslipped. All incubation steps were done in a dark room. The 3D-reconstruction of Golgi-impregnated neurons from the dorsal and ventral CA1 (dCA1 and vCA1) were achieved following the mouse brain atlas. CA1 neurons were identified by their typical triangular soma-shape, apical dendrites extending toward the striatum radiatum. For each experimental group, four animals were studied and, for each one, five neurons per area were

reconstructed and evaluated (a total of 20 neurons per area). Neurons were selected for reconstruction following these criteria: (i) identification of soma within the pyramidal layer of CA1 (ii) full impregnation along the entire length of the dendritic tree; (iii) no morphological changes attributable to incomplete dendritic impregnation of Golgi-Cox staining or truncated branches. The dendritic reconstruction was performed at 100x (oil) magnification using a motorized microscope (BX51, Olympus) and Neurolucida software (Microbrightfield). The analyzed dendritic features were: total length, number of endings and nodes, and Sholl analysis (number of dendrite intersections at radial intervals of 20 mm). Dendritic spine density (calculated as number of spines/dendritic length), was evaluated in proximal and distal segments of dendrites. To identify changes in spine morphology, spines in the selected segments were classified into thin, mushroom, thick or ramified and the proportion of spines in each category was calculated for each neuron. *(n* = 4-6 neurons for each animal; *n* = 3-4 per group).

Statistical analysis

A confidence interval of 95% was assumed for hypothesis testing. Assumptions for all variables were validated prior to statistical testing. For the comparison of two means, the two-tailed unpaired Student's t-test was carried out, followed by the Benjamini, Krieger and Yekuteli correction when multiple hypotheses were tested. Analysis of variance (ANOVA) was used when 2 or more factors were tested, followed by Sidak's *post hoc* test. Comparison of proportions was carried out using a two-tailed Chi-square statistic. Appropriate effect size measures were reported for all statistical tests. All statistical analyses were carried out using SPSS 22.0® or GraphPad Prism 8.0®. Test details are described in figure captions,and **Supplemental Table S4**.

3.6. Author contributions

C.A designed the study, performed the experiments, analysed the data and wrote the manuscript; J.D.S. performed gene ontology analysis of QuantSeq results, statistical analysis and wrote the manuscript. S.G.G. and N.D.A. helped with the behavioural tests and respective analysis. E.L.C. helped with the behavioural tests. F. F. helped with neuronal morphology analysis. N.S. organized and wrote the manuscript; W.R. contributed with the *Tet3* conditional mouse strain; L.P. and C.J.M. designed the study, organized and wrote the manuscript. All authors revised and approved the final manuscript.

3.7. Acknowledgments

This work was supported by National Funds through Foundation for Science and Technology (FCT) fellowships (PD/BD/106049/2015 to CA, PD/BD/128074/2016 to J.D.S, IF/01079/2014 to LP, SFRH/BD/ 101298/2014 to S. GG, SFRH/BD/131278/2017 to E.LC and IF/00047/2012 and CEECIND/00371/2017 to C.J.M); FCT project grant (PTDC/BIA-BCM/121276/2010) to C.J.M; EpiGeneSys Small Collaborative project to LP; BIAL Foundation Grant 427/14 to LP; Northern Portugal Regional Operational Programme (NORTE 2020), under the Portugal 2020 Partnership Agreement, through the European Regional Development Fund (FEDER; NORTE-01-0145-FEDER-000013); FEDER funds, through the Competitiveness Factors Operational Programme (COMPETE), and National Funds, through the FCT (POCI-01-0145-FEDER-007038). The authors declare that they have no conflict of interest.

3.9. References

Antunes, C., N. Sousa, L. Pinto and C. J. Marques (2019). TET enzymes in neurophysiology and brain function.Neuroscience & Biobehavioral Reviews. *102*, 337-344.

Bale, T. L., A. Contarino, G. W. Smith, R. Chan, L. H. Gold, P. E. Sawchenko, G. F. Koob, W. W. Vale and K. F. Lee (2000). Mice deficient for corticotropin-releasing hormone receptor-2 display anxiety-like behaviour and are hypersensitive to stress. Nature Genetics 24(4): 410-414.

Berry, K. P. and E. Nedivi (2017). Spine Dynamics: Are They All the Same? Neuron 96(1): 43-55.

Bessa, J. M., D. Ferreira, I. Melo, F. Marques, J. J. Cerqueira, J. A. Palha, O. F. X. Almeida and N. Sousa (2008). The mood-improving actions of antidepressants do not depend on neurogenesis but are associated with neuronal remodeling. Molecular Psychiatry 14: 764.

Cadena-del-Castillo, C., C. Valdes-Quezada, F. Carmona-Aldana, C. Arias, F. Bermudez-Rattoni and F. Recillas-Targa (2014). Age-dependent increment of hydroxymethylation in the brain cortex in the triple-transgenic mouse model of Alzheimer's disease.Journal of Alzheimer's Disease 41(3): 845-854.

Coste, S. C., R. A. Kesterson, K. A. Heldwein, S. L. Stevens, A. D. Heard, J. H. Hollis, S. E. Murray, J. K. Hill, G. A. Pantely, A. R. Hohimer, D. C. Hatton, T. J. Phillips, D. A. Finn, M. J. Low, M. B. Rittenberg, P. Stenzel and M. P. Stenzel-Poore (2000). Abnormal adaptations to stress and impaired cardiovascular function in mice lacking corticotropin-releasing hormone receptor-2. Nature Genetics 24(4): 403-409.

Coutellier, L., S. Beraki, P. M. Ardestani, N. L. Saw and M. Shamloo (2012). Npas4: a neuronal transcription factor with a key role in social and cognitive functions relevant to developmental disorders. PLoS One 7(9): e46604.

Dong, E., D. P. Gavin, Y. Chen and J. Davis (2012). Upregulation of TET1 and downregulation of APOBEC3A and APOBEC3C in the parietal cortex of psychotic patients. Translational psychiatry 2(9): e159-e159.

Fanselow, M. S. and H.-W. Dong (2010). Are the dorsal and ventral hippocampus functionally distinct structures? Neuron 65(1): 7-19.

Faravelli, C., C. Lo Sauro, L. Lelli, F. Pietrini, L. Lazzeretti, L. Godini, L. Benni, G. Fioravanti, G. A. Talamba, G. Castellini and V. Ricca (2012). The role of life events and HPA axis in anxiety disorders: a review. Current Pharmaceutical Design 18(35): 5663-5674.

Feng, J., S. Fouse and G. Fan (2007). Epigenetic regulation of neural gene expression and neuronal function. Pediatric Research 61(5 Pt 2): 58r-63r.

Feng, J., C. J. Pena, I. Purushothaman, O. Engmann, D. Walker, A. N. Brown, O. Issler, M. Doyle, E. Harrigan, E. Mouzon, V. Vialou, L. Shen, M. M. Dawlaty, R. Jaenisch and E. J. Nestler (2017). Tet1 in Nucleus Accumbens Opposes Depression- and Anxiety-Like Behaviors. Neuropsychopharmacology 42(8): 1657-1669.

Gontier, G., M. Iyer, J. M. Shea, G. Bieri, E. G. Wheatley, M. Ramalho-Santos and S. A. Villeda (2018). Tet2 Rescues Age-Related Regenerative Decline and Enhances Cognitive Function in the Adult Mouse Brain. Cell Reports 22(8): 1974-1981.

Graziano, A., L. Petrosini and A. Bartoletti (2003). Automatic recognition of explorative strategies in the Morris water maze. Jounal of Neuroscience Methods 130(1): 33-44.

Gu, T. P., F. Guo, H. Yang, H. P. Wu, G. F. Xu, W. Liu, Z. G. Xie, L. Shi, X. He, S. G. Jin, K. Iqbal, Y. G. Shi, Z. Deng, P. E. Szabo, G. P. Pfeifer, J. Li and G. L. Xu (2011). The role of Tet3 DNA dioxygenase in epigenetic reprogramming by oocytes. Nature 477(7366): 606-610.

Huff, N. C., M. Frank, K. Wright-Hardesty, D. Sprunger, P. Matus-Amat, E. Higgins and J. W. Rudy (2006). Amygdala regulation of immediate-early gene expression in the hippocampus induced by contextual fear conditioning. Jounal of Neuroscience 26(5): 1616-1623.

Jaehne, E. J., T. S. Klaric, S. A. Koblar, B. T. Baune and M. D. Lewis (2015). Effects of Npas4 deficiency on anxiety, depression-like, cognition and sociability behaviour. Behavioural Brain Research 281: 276-282.

Jimenez, J. C., K. Su, A. R. Goldberg, V. M. Luna, J. S. Biane, G. Ordek, P. Zhou, S. K. Ong, M. A. Wright, L. Zweifel, L. Paninski, R. Hen and M. A. Kheirbek (2018). Anxiety Cells in a Hippocampal-Hypothalamic Circuit. Neuron 97(3): 670-683.e676.

Kaas, G. A., C. Zhong, D. E. Eason, D. L. Ross, R. V. Vachhani, G. L. Ming, J. R. King, H. Song and J. D. Sweatt (2013). TET1 controls CNS 5-methylcytosine hydroxylation, active DNA demethylation, gene transcription, and memory formation. Neuron 79(6): 1086-1093.

Kamburov, A., U. Stelzl, H. Lehrach and R. Herwig (2013). The ConsensusPathDB interaction database: 2013 update. Nucleic acids research 41(Database issue): D793-D800.

Kishimoto, T., J. Radulovic, M. Radulovic, C. R. Lin, C. Schrick, F. Hooshmand, O. Hermanson, M. G. Rosenfeld and J. Spiess (2000). Deletion of crhr2 reveals an anxiolytic role for corticotropin-releasing hormone receptor-2. Nature Genetics 24(4): 415-419.

Kramer, A., J. Green, J. Pollard, Jr. and S. Tugendreich (2014). Causal analysis approaches in Ingenuity Pathway Analysis. Bioinformatics 30(4): 523-530.

Kremer, E. A., N. Gaur, M. A. Lee, O. Engmann, J. Bohacek and I. M. Mansuy (2018). Interplay between TETs and microRNAs in the adult brain for memory formation. Science Reports 8(1): 1678.

Kumar, D., M. Aggarwal, G. A. Kaas, J. Lewis, J. Wang, D. L. Ross, C. Zhong, A. Kennedy, H. Song and J. D. Sweatt (2015). Tet1 Oxidase Regulates Neuronal Gene Transcription, Active DNA Hydroxy-methylation, Object Location Memory, and Threat Recognition Memory. Neuroepigenetics 4: 12-27.

Li, X., W. Wei, Q. Y. Zhao, J. Widagdo, D. Baker-Andresen, C. R. Flavell, A. D'Alessio, Y. Zhang and T. W. Bredy (2014). Neocortical Tet3-mediated accumulation of 5-hydroxymethylcytosine promotes rapid behavioral adaptation.Proceedings National Academy Sciences U S A 111(19): 7120-7125.

Liu, Y., Q. Fu and X. Fu (2009). The interaction between cognition and emotion. Chinese Science Bulletin 54(22): 4102.

Loebrich, S. and E. Nedivi (2009). The function of activity-regulated genes in the nervous system. Physiological Reviews 89(4): 1079-1103.

Madisen, L., T. A. Zwingman, S. M. Sunkin, S. W. Oh, H. A. Zariwala, H. Gu, L. L. Ng, R. D. Palmiter, M. J. Hawrylycz, A. R. Jones, E. S. Lein and H. Zeng (2010). A robust and high-throughput Cre reporting and characterization system for the whole mouse brain. Nature Neurosciences 13(1): 133-140.

Mateus-Pinheiro, A., N. D. Alves, P. Patrício, A. R. Machado-Santos, E. Loureiro-Campos, J. M. Silva, V. M. Sardinha, J. Reis, H. Schorle, J. F. Oliveira, J. Ninkovic, N. Sousa and L. Pinto (2016). AP2γ controls adult hippocampal neurogenesis and modulates cognitive, but not anxiety or depressive-like behavior. Molecular Psychiatry 22: 1725.

Mattison, H. A., D. Popovkina, J. P. Y. Kao and S. M. Thompson (2014). The role of glutamate in the morphological and physiological development of dendritic spines. The European journal of neuroscience 39(11): 1761-1770.

McDonald, R. J., R. J. Balog, J. Q. Lee, E. E. Stuart, B. B. Carrels and N. S. Hong (2018). Rats with ventral hippocampal damage are impaired at various forms of learning including conditioned inhibition, spatial navigation, and discriminative fear conditioning to similar contexts. Behavioural Brain Research 351: 138-151.

McKinney, R. A. (2010). Excitatory amino acid involvement in dendritic spine formation, maintenance and remodelling. The Journal of physiology 588(Pt 1): 107-116.

Mi, H., A. Muruganujan and P. D. Thomas (2013). PANTHER in 2013: modeling the evolution of gene function, and other gene attributes, in the context of phylogenetic trees. Nucleic Acids Research 41(Database issue): D377-386.

Miller, C. A., S. L. Campbell and J. D. Sweatt (2008). DNA methylation and histone acetylation work in concert to regulate memory formation and synaptic plasticity. Neurobiology of Learning and Memory 89(4): 599-603.

Miller, C. A. and J. D. Sweatt (2007). Covalent modification of DNA regulates memory formation. Neuron 53(6): 857-869.

Montalbán-Loro, R., A. Lozano-Ureña, M. Ito, C. Krueger, W. Reik, A. C. Ferguson-Smith and S. R. Ferrón (2019). TET3 prevents terminal differentiation of adult NSCs by a non-catalytic action at Snrpn. Nature Communications 10(1): 1726.

Pamela Moll, M. A., Alexander Seitz & Torsten Reda (2014). QuantSeq 3' mRNA sequencing for RNA quantification. NATURE METHODS: i-iii.

Peat, J. R., W. Dean, S. J. Clark, F. Krueger, S. A. Smallwood, G. Ficz, J. K. Kim, J. C. Marioni, T. A. Hore and W. Reik (2014). Genome-wide bisulfite sequencing in zygotes identifies demethylation targets and maps the contribution of TET3 oxidation. Cell Reports 9(6): 1990-2000.

Ploski, J. E., M. S. Monsey, T. Nguyen, R. J. DiLeone and G. E. Schafe (2011). The Neuronal PAS Domain Protein 4 (Npas4) Is Required for New and Reactivated Fear Memories. PLOS ONE 6(8): e23760.

Preil, J., M. B. Müller, A. Gesing, J. M. H. M. Reul, I. Sillaber, M. M. van Gaalen, J. Landgrebe, F. Holsboer, M. Stenzel-Poore and W. Wurst (2001). Regulation of the Hypothalamic-Pituitary-Adrenocortical System in Mice Deficient for CRH Receptors 1 and 2. Endocrinology 142(11): 4946-4955.

Ramamoorthi, K., R. Fropf, G. M. Belfort, H. L. Fitzmaurice, R. M. McKinney, R. L. Neve, T. Otto and Y. Lin (2011). Npas4 regulates a transcriptional program in CA3 required for contextual memory formation. Science 334(6063): 1669-1675.

Reul, J. M. H. M. and F. Holsboer (2002). On the role of corticotropin-releasing hormone receptors in anxiety and depression. Dialogues in clinical neuroscience 4(1): 31-46.

Robinson, M. D., D. J. McCarthy and G. K. Smyth (2010). edgeR: a Bioconductor package for differential expression analysis of digital gene expression data. Bioinformatics 26(1): 139-140.

Rudenko, A., M. M. Dawlaty, J. Seo, A. W. Cheng, J. Meng, T. Le, K. F. Faull, R. Jaenisch and L. H. Tsai (2013). Tet1 is critical for neuronal activity-regulated gene expression and memory extinction. Neuron 79(6): 1109-1122.

Santos, F., J. Peat, H. Burgess, C. Rada, W. Reik and W. Dean (2013). Active demethylation in mouse zygotes involves cytosine deamination and base excision repair. Epigenetics Chromatin 6(1): 39.

Strange, B. A., M. P. Witter, E. S. Lein and E. I. Moser (2014). Functional organization of the hippocampal longitudinal axis. Nature Reviews in Neuroscience 15(10): 655-669.

Szulwach, K. E., X. Li, Y. Li, C. X. Song, H. Wu, Q. Dai, H. Irier, A. K. Upadhyay, M. Gearing, A. I. Levey, A. Vasanthakumar, L. A. Godley, Q. Chang, X. Cheng, C. He and P. Jin (2011). 5-hmC-mediated epigenetic dynamics during postnatal neurodevelopment and aging. Nature Neuroscience 14(12): 1607-1616.

Szwagierczak, A., S. Bultmann, C. S. Schmidt, F. Spada and H. Leonhardt (2010). Sensitive enzymatic quantification of 5-hydroxymethylcytosine in genomic DNA. Nucleic Acids Research 38(19): e181.

Tahiliani, M., K. P. Koh, Y. Shen, W. A. Pastor, H. Bandukwala, Y. Brudno, S. Agarwal, L. M. Iyer, D. R. Liu, L. Aravind and A. Rao (2009). Conversion of 5-Methylcytosine to 5-Hydroxymethylcytosine in Mammalian DNA by MLL Partner TET1. Science (New York, N.Y.) 324(5929): 930-935.

Wang, L., M. Y. Li, C. Qu, W. Y. Miao, Q. Yin, J. Liao, H. T. Cao, M. Huang, K. Wang, E. Zuo, G. Peng, S. X. Zhang, G. Chen, Q. Li, K. Tang, Q. Yu, Z. Li, C. C. Wong, G. Xu, N. Jing, X. Yu and J. Li (2017). CRISPR-Cas9-mediated genome editing in one blastomere of two-cell embryos reveals a novel Tet3 function in regulating neocortical development. Cell Research 27(6): 815-829.

Yoshida, K., M. R. Drew, M. Mimura and K. F. Tanaka (2019). Serotonin-mediated inhibition of ventral hippocampus is required for sustained goal-directed behavior. Nature Neuroscience 22(5): 770-777.

Yu, H., Y. Su, J. Shin, C. Zhong, J. U. Guo, Y. L. Weng, F. Gao, D. H. Geschwind, G. Coppola, G. L. Ming and H. Song (2015). Tet3 regulates synaptic transmission and homeostatic plasticity via DNA oxidation and repair. Nature Neuroscience 18(6): 836-843.

Zhang, R. R., Q. Y. Cui, K. Murai, Y. C. Lim, Z. D. Smith, S. Jin, P. Ye, L. Rosa, Y. K. Lee, H. P. Wu, W. Liu, Z. M. Xu, L. Yang, Y. Q. Ding, F. Tang, A. Meissner, C. Ding, Y. Shi and G. L. Xu (2013). Tet1 regulates adult hippocampal neurogenesis and cognition. Cell Stem Cell 13(2): 237-245.

3.10. Figures

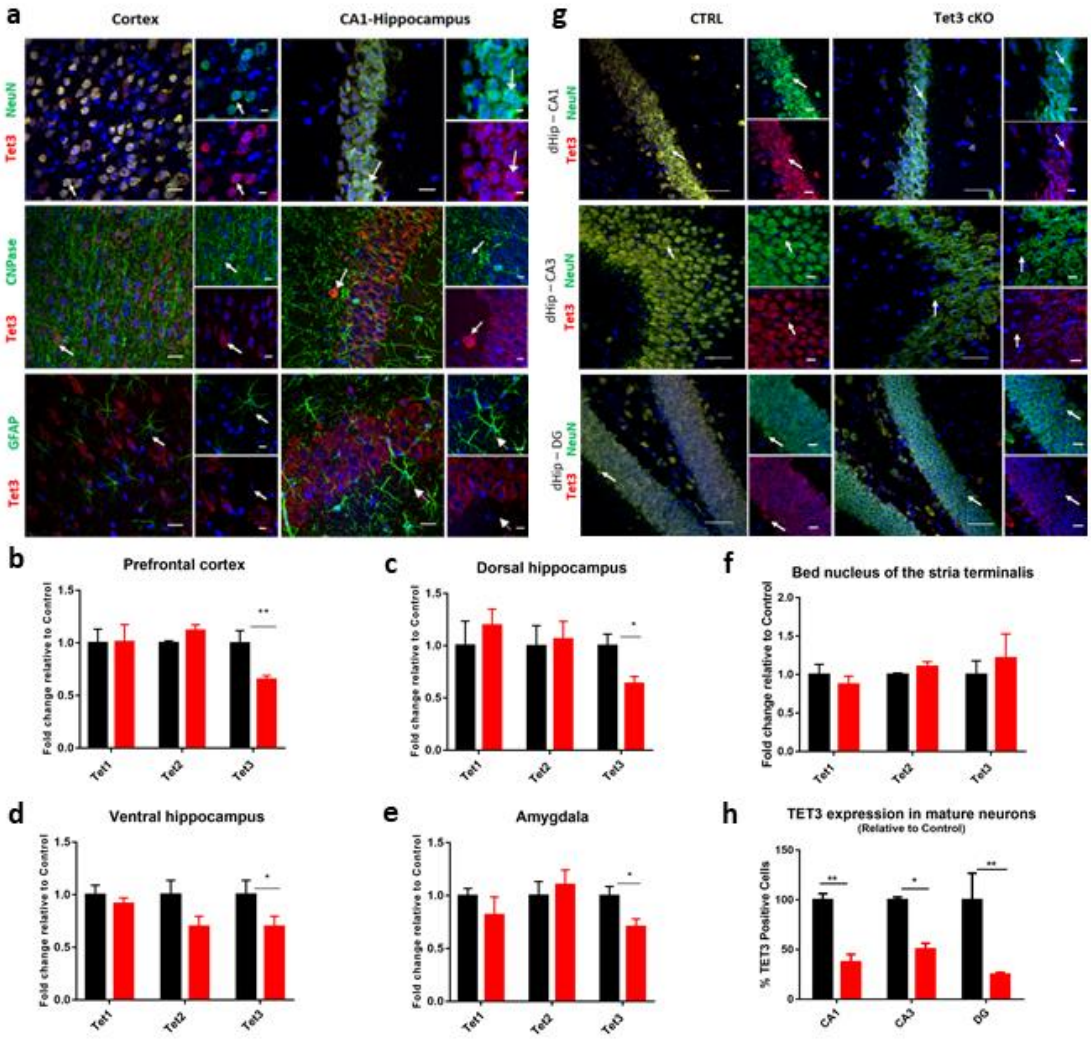

Figure 1. TET3 is present in mature neurons and diminished in the brain of Tet3 cKO mice.

(**a**) Representative double immunostaining for NeuN and Tet3 proteins, showing strong expression of Tet3 in post-mitotic neurons in the cortex and dorsal CA1 brain regions. Tet3 expression was detected in some oligodendrocytes stained with CNPase marker. Astrocytes do not express Tet3, no Tet3 staining was found in GFAP positive cells. Scale bars, 50 and 25 μm.

(**b-f**) Reduction in Tet3 mRNA levels and maintenance of Tet1 and Tet2 levels was observed in Tet3 cKO animals. mRNA expression in forebrain regions was measured by qRT-PCR in control and Tet3 cKO animals in **(b)** prefrontal cortex; **(c)** dorsal hippocampus; **(d)** ventral hippocampus; **(e)** amygdala and (**f**) BNST (n=3-5 per group).

(**f**) Representative double immunostaining for NeuN and Tet3 proteins in the CA1, CA3 and DG hippocampal regions, showing reduction in Tet3 expression in the Tet3 cKO animals. Scale bars, 50 and 25 μm.

(**g-h**) The percentage of TET3 positive cells in NeuN positive cells (post-mitotic neurons) was quantified in Tet3 cKO animals, relative to controls (n=3 per group).

Quantifications are presented as the mean ± SEM. **(b-f)** Two-tailed Student's t-test; *p < 0.05, **p<0.01; **(g)** Adjusted two-tailed Student's t-test; *p < 0.05, ** p< 0.01

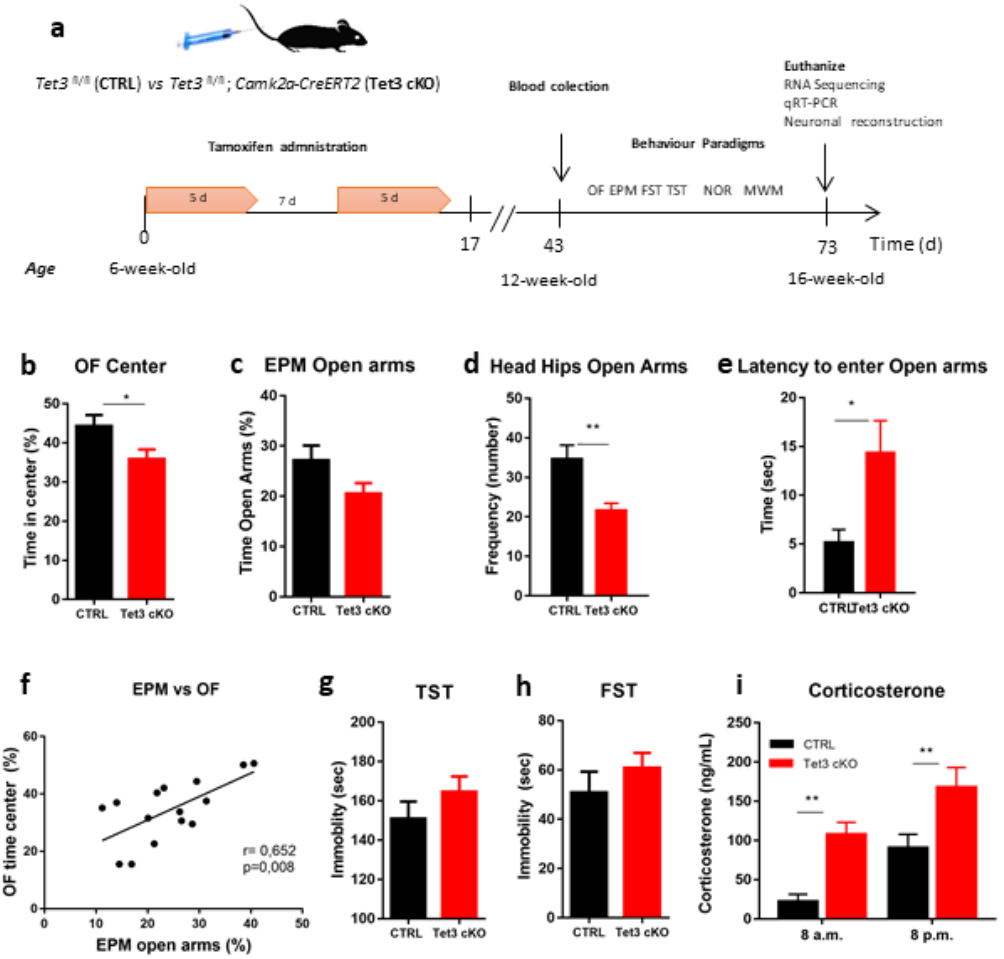

Figure 2. Tet3 cKO mice showed increased anxiety-like behavior and corticosterone levels.

(a) Scheme illustrating the protocol used to induce Tet3 deletion and the behavior paradigm timeline. Six-week-old mice were injected intraperitoneally with 50 mg/kg of tamoxifen twice a day for 5 consecutive days, with 7 days break, followed by injections for 5 additional consecutive days. Animals were submitted to behavioral testing 1 month after the last tamoxifen injection and euthanized after this assessment.

(b-f) Anxiety-like behavior was tested both in the open-field test (OF) **(b)** and elevated plus maze (EPM) **(c-e)**. **(b)** Time spent in the center of the OF; **(c)** time spent in the open arms of the EPM; **(d)** The frequency number of head hips (EPM); **(e)** Latency to enter open arms (EPM); **(f)** Correlation between OF and EPM performances (*n*=13-18 per group).

(g-h) The presence of depressive-like behavior was assessed in the tail suspension test TST **(g)** and forced swimming test (FST) **(h)** (*n*=13-17 per group).

(i) Basal serum concentration of corticosteroids in control and Tet3 cKO mice, both in the morning and at night, revealed a significant increased production by Tet3 cKO mice (*n*= 8 per group).

Quantifications are presented as the mean ± SEM. **(b-e; g-h)** Two-tailed Student's t-test; *p < 0.05; **(f)** correlation Pearson; p<0.01; **(i)** Adjusted two-tailed Student's t-test; ** p< 0.01

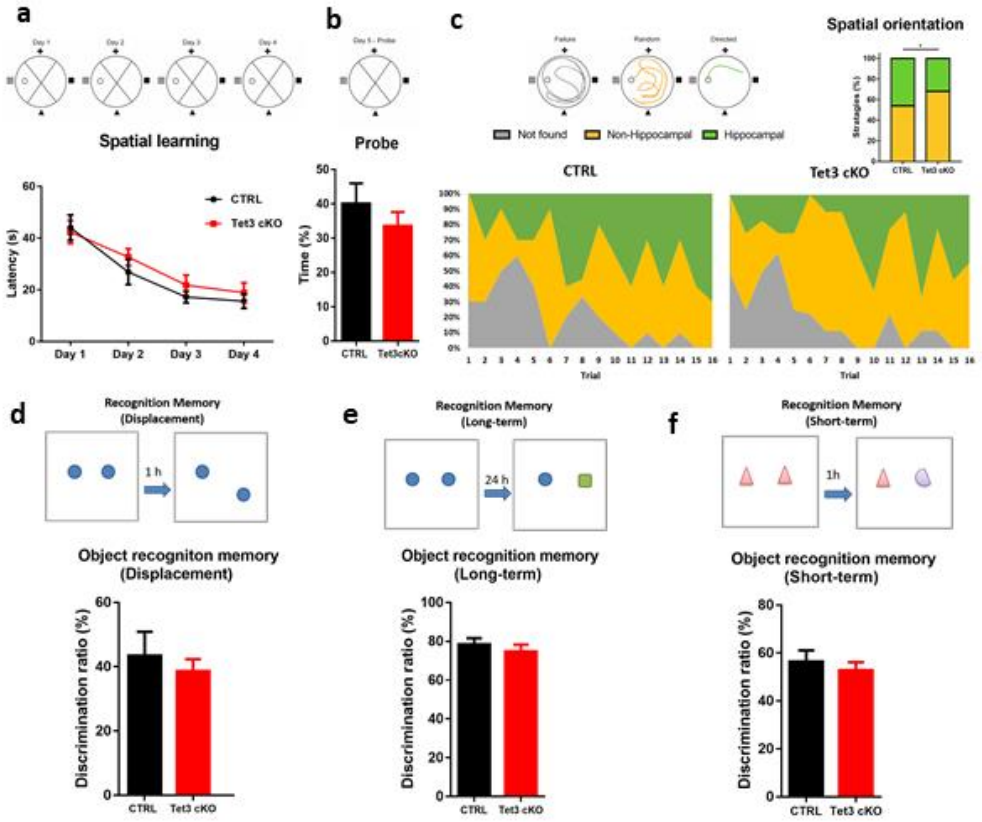

Figure 3. Tet3 cKO mice showed spatial orientation impairment, but normal recognition memory.

(a-c) Morris Water Maze test. (a-c) Spatial acquisition performances were recorded during 4-day training. (**a**) Escape latency. (**b**) Time in the target quadrant. (**c-e**) Cognitive strategies during water maze learning. **(c)** A schematic representation and color code for each group of strategy and the average prevalence by trial number are shown. (**c**) Representation of the percentage of mice using directed strategies (hippocampal dependent strategies) (*n*=8-11 per group).

(d-f) Novel object Recognition test. Animals were allowed to explore two identical objects for 10 min. After an interval of 1 h in their home cages, the novel object was displaced to the opposite side of the box and mice were allowed to explore this new configuration, evaluating spatial recognition memory (displacement) (**d**) After 24 h, mice were returned to the arena, where one of the familiar objects was replaced with a novel one, evaluating long-term memory (**e**) After 24 h, two new objects were placed in the box and mice were allowed to explore them. 1h after, one object was replaced by a novel one, and the animals placed in the arena, evaluating short-term memory (**f**) (*n*=14-18 per group).

Quantifications are presented as mean ± SEM. **(a)** Mixed ANOVA, genotype; **(b)** Two-tailed Student's t-test; **(c)** Chi-square test; * p< 0.05; **(d-f)** two-tailed Student's t-test.

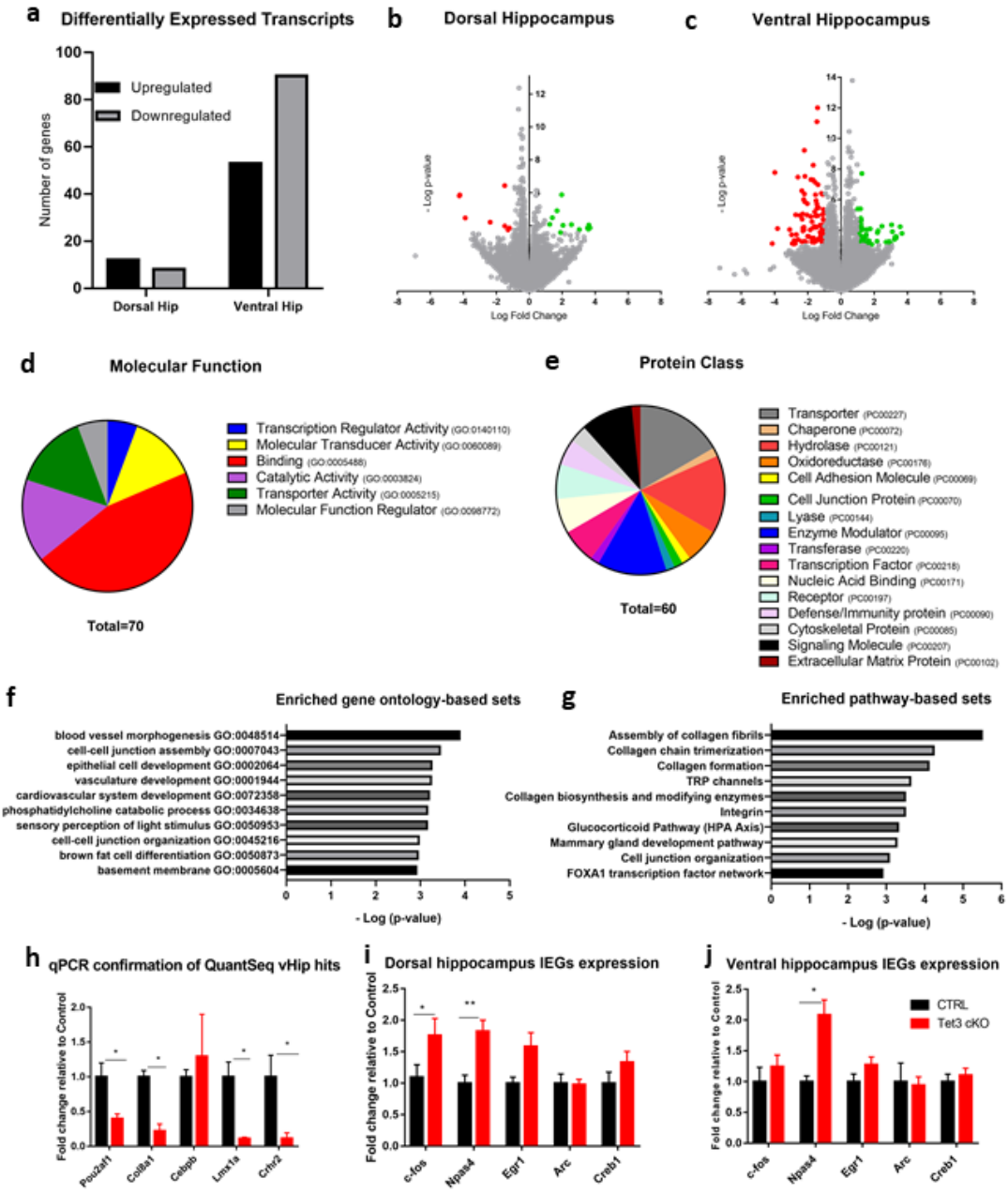

Figure 4- Transcriptome analysis showed a predominant alteration in transcript levels in the ventral hippocampus. Gene expression analysis showed an increase in the expression of neuronal activity-regulated genes in both regions.

(a) Number of differentially expressed genes (up and downregulated) in the dorsal and ventral regions of the hippocampus.

(b-c) Volcano plot of all transcripts identified in the dorsal (29407 targets) and ventral hippocampus (29146 targets). The log fold change represents control versus Tet3 cKO mice.

(d-e) Gene ontology classification of the molecular function and protein class of differentially expressed targets in the ventral hippocampus of Tet3 cKO mice, based on the PANTHER database.

(f-g) Enriched level 4 and 5 gene ontology classes and pathways of differentially expressed targets in the ventral hippocampus of Tet3 cKO mice, based on the Ingenuity Pathway Analysis (IPA).

(h) Expression of selected genes from the IPA analysis was evaluated by qRT-PCR, confirming the QuantSeq results (*n=3* per group).

(i-j) Expression of Immediate early genes (IEGs) in the dorsal and ventral hippocampus (*n*=4-6 per group). Fold change relative to controls was calculated using the $2^{-\Delta\Delta^{CT}}$ relative gene expression analysis.

Quantifications are presented as the mean ± SEM. **(h-j)** Two-tailed Student's t-test; * p< 0.05, ** p< 0.01

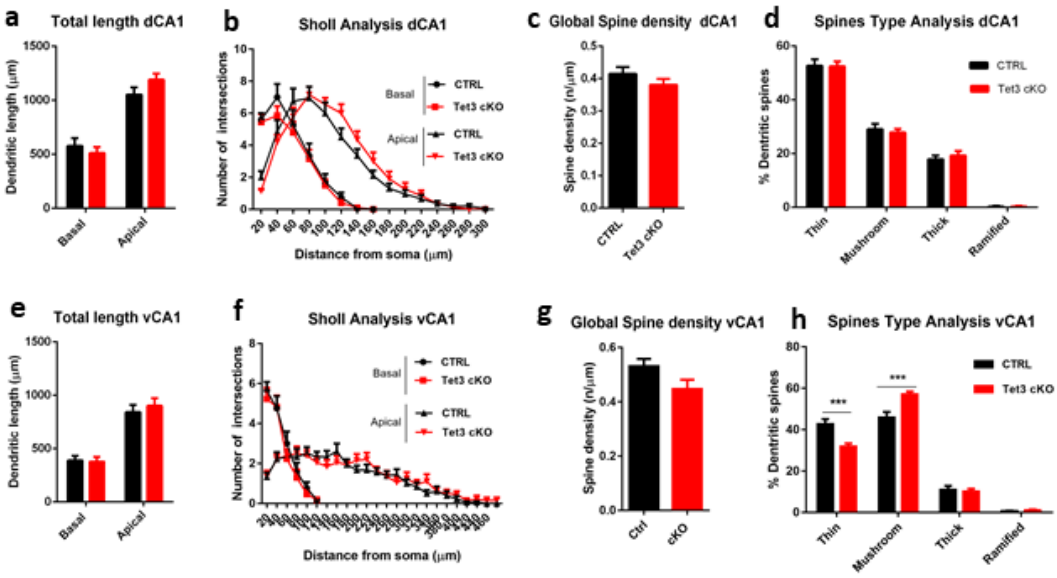

Figure 5. Three-dimensional morphometric analysis of Golgi-impregnated neurons of the CA1 hippocampus reveals an increase in dendritic spine maturation in Tet3 cKO mice.

Tet3 cKO presented no alterations in neuronal morphology, in dorsal and ventral hippocampus, assessed by total length and sholl analysis (**a-b**; **e-f**). Regarding spines analysis, no differences were found at the dorsal part (c-d), but a robust increase in spine differentiation (mushroom type) and a decrease in immature spines (thin type) of the apical dendrites spines was found in the ventral region in Tet3 cKO mice (h), without alterations in spine density (**g**). *n*=13-20 neurons; 3 mice per group.

Quantifications are presented as the mean ± SEM. (**a, b, e, f**) Factorial ANOVA; (**c, g**) Two-tailed Student's t-test; (**d, h**) Factorial ANOVA, genotype; ***p<0.001

3.11. Supplementary Material

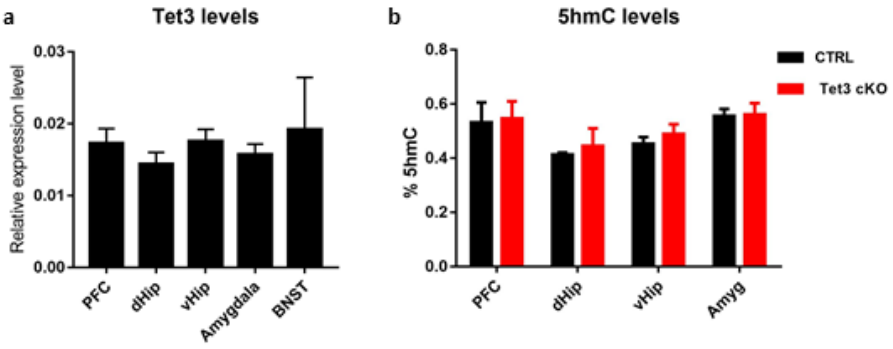

Supplemental S1. Tet3 relative expression and global 5hmC levels in forebrain regions.
(a) Expression of Tet3 transcripts was evaluated by qRT-PCR, and it showed comparable relative *Tet3* levels in forebrain regions (PFC, dorsal and ventral hippocampus, amygdala and BNST) (n=4-6 per group). Normalized expression to Atp5b. **(b)** No alterations were found in the global 5hmC levels in forebrain regions evaluated by ELISA (n=3 per group). Quantifications are presented as the mean ± SEM

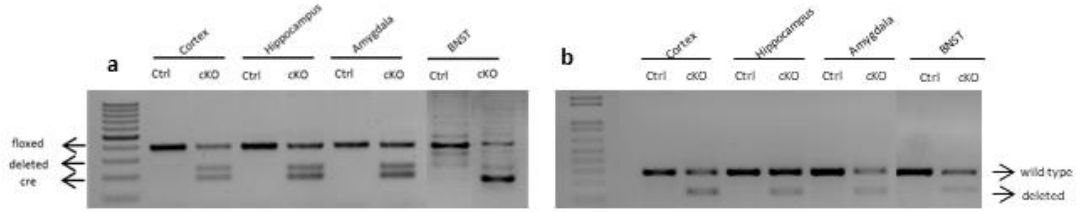

Supplemental S2. Generation of TET3 conditional deletion.
(a) PCR genotyping of forebrain regions 26 days after induction of deletion. In the Tet3 cKO animals are observed three bands with 184, 237 and 400 base pairs corresponding to the cre, deleted and floxed alleles respectively. Control animals do not show the bands corresponding to cre and deleted bands (100 bp Ladder).
(b) Loss of the flanking exon7 at Tet3 RNA level confirmed by RT-PCR assay. In the Tet3 cKO animals two bands are observed with 328 and 178 base pairs corresponding to the wild-type and deleted exon 7, respectively. Control animals do not show the deleted band (100 bp Ladder).

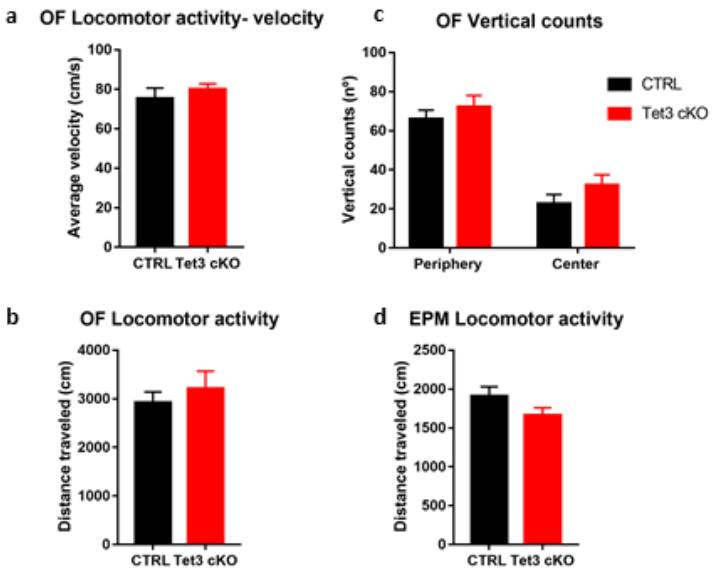

Supplemental S3. Behavior data regarding locomotor activity in the open field (OF) and elevated plus maze (EPM). **(a)** Average velocity (OF); **(b)** distance traveled (OF) and **(c)** vertical counts in the periphery and center in the OF test; **(d)** Distance traveled (EPM). Quantifications are presented as the mean ± SEM (n=13-18 per group)

a

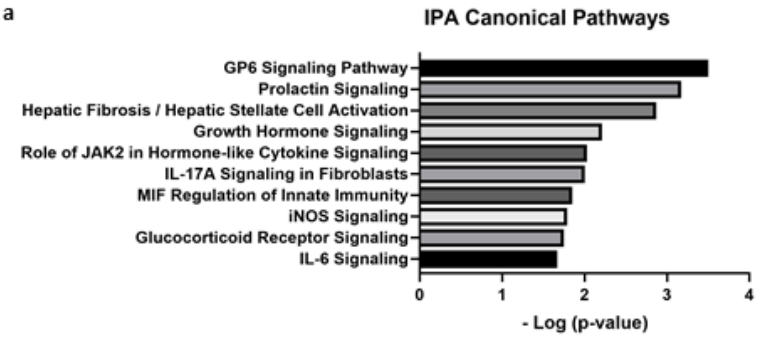

b

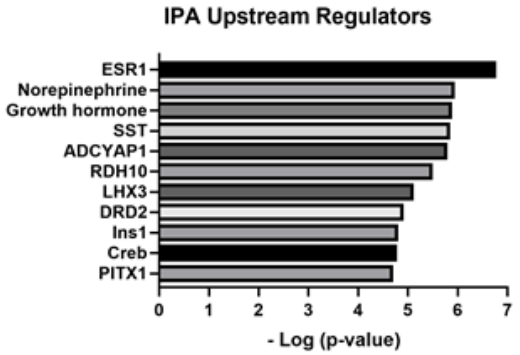

c IPA Diseases and Disorders

Name	p-value range	# Molecules
Cancer	7,08E-03 - 4,87E-06	92
Dermatological Diseases and Conditions	4,40E-03 - 4,87E-06	68
Organismal Injury and Abnormalities	7,08E-03 - 4,87E-06	92
Endocrine System Disorders	6,07E-03 - 6,94E-06	76
Reproductive System Disease	7,08E-03 - 6,94E-06	26

Supplemental S4. Additional analyses of differentially expressed targets in the ventral hippocampus of Tet3 cKO mice, using the Genes2mind and Ingenuity Pathway Analysis software.

(a) Canonical pathways with highest gene enrichment are related with immunological, matrix and hormone signaling.

(b) Upstream regulators with highest enrichment in the evaluated dataset. Most genes are not associated with a transcriptional regulation.

(c) Diseases and conditions mostly associated with the differentially expressed targets, with the most enriched category being cancer.

Supplemental Table S1. List of primers sequence

(a) Primers for genotyping PCR of Tet3 cKO animals.

(b) Primers used for quantitative qRT-PCR analysis

a

Target	Forward Primer (5′- 3′)	Reverse Primer (5′ – 3′)
Cre	AGCTCGTCAATCAAGCTGGT	CAGGTTCTTGCGAACCTCAT
Tet3	TACCTCTGCCTCTGGAGTGCTAA	ATGGCTACTCACAACCCAGTGAC GTCAGGAAAGTCACATGGTTGTTG

b

Target	Forward Primer (5′- 3′)	Reverse Primer (5′ – 3′)
Atp5b	GCCAAGATGTCCTGCTGTT	TCCTTCGGATTGTCTCCCGTG
Tet1	CCATTCTCACAAGGACATTCACA	GCCATTCTCAGGAGTCACTGC
Tet2	GCCATTCTCAGGAGTCACTGC	ACTTCTCGATTGTCTTCTCTATTGAGG
Tet3	GCCTCCTTCTCCTTCGGCTG	TCCTTCGGATTGTCTCCCGTG
Arc	AGCTCGCTGCATGGCCTTTG	GGGGCTTGGCTGAGGTTTCA
c-fos	AGCATCGGCAGAAGGGGCAA	TGATCTGTCTCCGCTTGGAGTGT
Creb1	CACCATTGCCCCTGGAGTTGTT	TCTCTTGCTGCCTCCCTGTTCTT
Egr1	TGAGCACCTGACCACAGAGTCC	GTGATGGGAGGCAACCGAGT
Npas4	TCGGAGAGTGTGAGCGAGCA	AGGCGATCAGCATCCAGAGCA
Col18a1	TCCCTACAGTCCTCCCCTCT	ACCTCCTCAGCAACATTCTCTGG
Pou2af1	AGGCCATACCAGGGTGTTCGAG	TCAAGGCAGGAAGGACCCACA
Crhr2	GGCTTTACCTTGGTGGGTAGGT	AAGTGTCCACAGGGGCTGGT
Lmx1a	AGCGACCCAAACGTCCCAGA	GGCCAGCTTCTTCATCTTGGCT
Cebpb	TGGACACGGGACTGACGCAA	TGCTCGAAACGGAAAAGGTTCTCA

Supplemental Table S2: List of differentially expressed genes in the dorsal hippocampus of Tet3 cKO mice from transcriptomic analysis.

Gene ID	Log Fold Change	- Log p-value
3110070M22Rik	-1,20209	3,84665
4933415A04Rik	-1,29221	3,736981
Cd1d1	-2,37203	4,206204
Cpeb1os1	1,398845	4,477646
Crisp2	-3,88679	4,464898
Echdc3	2,049313	4,010211
Fam209	-4,22367	5,862374
Gm10800	-1,49368	6,427735
Gm1840	-1,49014	3,969004
Gm20696	1,686431	4,900563
Gm24059	3,537662	3,846102
Gm26838	3,588626	3,776476
Gm44967	3,617232	4,028999
Gm47423	1,900197	3,574721
Gm4865	3,685418	3,856333
Gm48872	3,038529	3,75205
Hes3	-4,24508	5,804142
Ifi27l2a	1,96966	5,876405
Pole	2,557432	4,052281

Supplemental Table S3: List of differentially expressed genes in the ventral hippocampus of Tet3 cKO mice, from transcriptomic analysis.

Gene ID	Log Fold Change	- Log p-value
Itpripl1	-1,41549	12,00422
Epn3	-1,44899	11,09568
Gh	-2,20907	9,227526
Krt18	-1,66953	8,253397
Prl	-3,983	7,773058
Sfrp5	-2,1687	7,526324
Rd3	-2,59674	7,473068
Pomc	-1,81588	7,3104
Nek5	-1,68149	7,294199
Slc2a12	-1,56768	7,143234
Mdfic	-1,38898	6,975157
Wdr86	-2,35441	6,579376
Crhr2	-1,18426	6,407602
AC154640.1	-2,21043	6,367751
Gpx8	-1,09072	6,337992
Rdh5	-1,53792	6,316228
Otx2os1	-2,24723	6,008057
Pon3	-1,50077	5,933949
Cldn3	-2,18969	5,870106
Drc7	-2,03195	5,73924
Col8a2	-1,45876	5,714893
Trpm3	-1,35908	5,474352
Col9a3	-1,44759	5,434625
Fam46c	-1,06325	5,352784
Gm34721	-1,57839	5,204102
Cdr2	-1,02408	5,093559
Lmx1a	-2,30293	5,063502
Cgnl1	-1,1099	5,038929
Sult1c2	-2,72724	5,007478
Defb11	-2,04659	4,992894
Gm15222	-2,44072	4,974582
Il17re	-2,46723	4,96714
Bmp6	-1,40105	4,949567
Six3os1	-1,51895	4,93617
Sostdc1	-1,81286	4,891992
Spaca9	-2,33492	4,72121
Mpp7	-1,07161	4,713558
Shroom3	-1,0578	4,66782
Enpp2	-1,74624	4,560972
Ppp1r3b	-1,2431	4,340615
Pla2g5	-1,11001	4,334216
Col18a1	-1,27708	4,283147
Abca4	-1,30082	4,280841
8430408G22Rik	-1,05639	4,249368

Gene ID	Log Fold Change	- Log p-value
Sema3b	-1,59128	4,248659
Lbp	-1,49273	4,186521
Dpep1	-2,23126	4,193625
Trim47	-1,66869	4,190442
Prr32	-1,66523	4,171762
Oca2	-2,29244	4,15247
Defb9	-3,82335	4,107608
Tmc6	-1,12767	4,090068
Ins2	-3,08671	4,042629
Tc2n	-1,85567	4,026224
Gm43323	-2,22903	4,021863
AC166574.1	-2,29452	3,948784
Daw1	-1,03016	3,943906
Sulf1	-1,14863	3,916586
Gm38248	-1,26012	3,879247
Fap	-1,09574	3,763461
Gm28727	-2,6861	3,717493
Tmem184a	-2,97344	3,702916
Ccdc187	-1,21396	3,681407
Lhfpl1	-2,00928	3,600382
Rab20	-1,92909	3,585233
Acox2	-1,65766	3,498352
Cdh3	-1,76138	3,468795
Igfbp2	-1,10301	3,443599
Cnbd2	-1,34984	3,441998
Gpr139	-1,15747	3,410616
Wdr63	-1,3502	3,38732
Pou2af1	-2,58541	3,38358
Gm43775	-1,08539	3,364574
Cpz	-2,81421	3,334454
Gmnc	-1,67578	3,310505
Crb3	-1,49899	3,301001
9530082P21Rik	-1,0536	3,28967
Trpv4	-1,52266	3,287127
Rbm47	-1,69553	3,284469
Rnf26	-1,07504	3,276945
Col8a1	-2,19662	3,27154
Btnl9	-2,3578	3,245468
Gm14275	-2,10706	3,239313
Esm1	-1,75608	3,235532
Prlr	-1,61663	3,212065
Slc13a4	-1,14712	3,206537
Gm11131	-2,76078	3,130294
Gm36745	-2,92999	3,135296
AC140304.2	-4,13677	3,127457

Gene	Log Fold Change	- Log p-value
Gm45358	-2,84999	3,107343
Nkx2-2	1,254524	7,706352
Gm44186	1,170913	5,403127
Gm37788	1,00112	5,394024
Cebpb	1,185702	4,786287
Atn1	1,219084	4,663804
Mir3091	1,071286	4,647169
Abracl	1,097918	4,556304
Tdo2	1,194379	4,434501
Bcl2a1d	3,037757	4,354421
Tspyl4	1,124305	4,281201
Gm11634	1,202588	4,268333
Gm25535	2,461911	4,262398
Neil3	3,55875	4,228767
Mcam	1,265934	4,088752
Gm48678	1,753963	4,08721
Klhl29	1,262373	4,080121
Trpc7	1,352489	4,052122
Gm10801	1,565092	4,045053
Arhgef10l	1,053154	4,004053
A530017D24Rik	1,1915	3,99697
Mterf1b	2,223451	3,963162
Slc35g2	1,070682	3,923304
Gm26739	3,091241	3,908635
Gm47625	2,18761	3,837343
BC048507	3,66137	3,796148
Rpa3	1,511811	3,713448
Numb	1,107318	3,710753
Gm37553	3,31583	3,579997
Gm6467	1,245935	3,575995
Gm10290	3,253034	3,567264
Antxr2	1,482455	3,560297
Rerg	1,330154	3,559579
Golt1a	3,307121	3,485939
Hpgd	1,193296	3,402211
AA986860	1,332444	3,397653
Gm26643	3,210026	3,39844
Ly6g6e	1,156219	3,375154
Gm13463	1,385088	3,365509
Senp3	1,68427	3,315037
Snhg3	2,162247	3,277423
Sox18	2,89969	3,258498
Gdpd3	2,705783	3,224197
Gm9442	1,182333	3,171638
Lamb3	1,616133	3,142604

Gene	Log Fold Change	- Log p-value
Fos	1,344927	3,128513
Abcb10	1,090216	3,132139
Gm36447	1,060925	3,130692
Gabra6	2,989826	3,121653
Tdpx-ps1	1,456465	3,119217
Dclk3	1,047916	3,084715
Asb11	1,857034	3,065455
Mrps28	1,237746	3,044965
Gm11451	1,469336	3,040606

Supplemental Table S4: List of Statistical Reports

Figure number	Statistical Report	Sample Size
Fig. 1b	Tet1: $t(9) = 0.046$, $p = 0.964$, $d = 0.028$ Tet2: $t(9) = 1.880$, $p = 0.092$, $d = 1.183$ Tet3 cKO: $t(9) = 3.013$, $p = 0.014$, $d = 1.742$	5 (CTRL), 6 (cKO)
Fig. 1c	Tet1: $t(9) = 0.985$, $p = 0.353$, $d = 0.624$ Tet2: $t(9) = 0.528$, $p = 0.612$, $d = 0.334$ Tet3 cKO: $t(9) = 2.521$, $p = 0.036$, $d = 1.600$	5 (CTRL), 6 (cKO)
Fig. 1d	Tet1: $t(9) = 0.707$, $p = 0.497$, $d = 0.409$ Tet2: $t(9) = 0.254$, $p = 0.805$, $d = 0.153$ Tet3 cKO: $t(9) = 2.772$, $p = 0.024$, $d = 1.756$	5 (CTRL), 6 (cKO)
Fig. 1e	Tet1: $t(9) = 0.802$, $p = 0.446$, $d = 0.507$ Tet2: $t(9) = 1.831$, $p = 0.104$, $d = 1.159$ Tet3 cKO:$t(9) = 3.434$, $p = 0.014$, $d = 2.771$	5 (CTRL), 6 (cKO)
Fig. 1f	Tet1: $t(8) = 0.750$, $p = 0.475$, $d = 0.474$ Tet2: $t(8) = 1.527$, $p = 0.165$, $d = 0.964$ Tet3: $t(13) = 0.604$, $p = 0.556$, $d = 0.305$	4-7 (CTRL), 6-8 (cKO)
Fig. 1h	Tet3: $F(1,9) = 59.09$, $p < 0.001$, $\omega^2_p = 0.841$	3 (CTRL), 3 (cKO)
Fig. 2b	$t(29) = 2.226$, $p = 0.034$, $d = 0.810$	13 (CTRL), 18 (cKO)
Fig. 2c	$t(28) = 1.606$, $p = 0.114$, $d = 0.684$	14 (CTRL), 16 (cKO)
Fig. 2d	$t(30) = 3.519$, $p = 0.001$, $d = 1.400$	14 (CTRL), 18 (cKO)
Fig. 2e	$t(27) = 2.093$, $p = 0.046$, $d = 0.881$	11 (CTRL), 18 (cKO)
Fig. 2f	$r = 0.652$, $p = 0.008$	16 (cKO)
Fig. 2g	$t(29) = 1.121$, $p = 0.270$, $d = 0.511$	14 (CTRL), 17 (cKO)
Fig. 2d	$t(29) = 1.011$, $p = 0.316$, $d = 0.353$	14 (CTRL), 17 (cKO)
Fig. 2e	Tet3 cKO: $F(1, 28) = 22.490$, $p < 0.001$, $\omega^2_p = 0.417$	8 (CTRL), 8 (cKO)
Fig. 3a	Tet3: $F(1, 16) = 1.282$, $p = 0.274$, $\omega^2_p = 0.015$	8 (CTRL), 11 (cKO)
Fig. 3b	$t(18) = 1.034$, $p = 0.308$, $d = 0.417$	9 (CTRL), 11 (cKO)
Fig. 3c	Tet3 cKO: $\chi^2(1) = 4.119$, $p = 0.042$, $\phi = 0.466$	10 (CTRL), 9 (cKO)
Fig. 3d	$t(9) = 0.605$, $p = 0.553$, $d = 0.379$	4 (CTRL), 7 (cKO)
Fig. 3e	$t(30) = 0.741$, $p = 0.462$, $d = 0.267$	14 (CTRL), 18 (cKO)
Fig. 3f	$t(27) = 0.673$, $p = 0.504$, $d = 0.235$	14 (CTRL), 15 (cKO)
Fig. 4h	Pou2af1: $t(4) = 2.869$, $p = 0.046$, $d = 2.341$	3 (CTRL), 3 (cKO)
	Col8a1: $t(4) = 5.313$, $p = 0.013$, $d = 5.102$	3 (CTRL), 3 (cKO)
	Cebpb: $t(4) = 0.490$, $p = 0.650$, $d = 0.400$	3 (CTRL), 3 (cKO)
	Lmx1a: $t(4) = 3.220$, $p = 0.049$, $d = 3.392$	3 (CTRL), 3 (cKO)
	Crhr2: $t(4) = 3.513$, $p = 0.039$, $d = 2.728$	3 (CTRL), 3 (cKO)

Figure number	Statistical Report	Sample Size
Fig. 4i	c-fos: $t(8) = 2.426$, $p = 0.041$, $d = 1.534$	5 (CTRL), 5 (cKO)
	Npas4: $t(8) = 3.398$, $p = 0.009$, $d = 2.321$	4 (CTRL), 6 (cKO)
	Egr1: $t(8) = 2.091$, $p = 0.070$, $d = 1.473$	4 (CTRL), 6 (cKO)
	Arc: $t(9) = 0.148$, $p = 0.886$, $d = 0.087$	5 (CTRL), 6 (cKO)
	Creb1: $t(9) = 1.353$, $p = 0.209$, $d = 0.822$	5 (CTRL), 6 (cKO)
Fig. 4j	c-fos: $t(7) = 0.827$, $p = 0.248$, $d = 0.523$	5 (CTRL), 4 (cKO)
	Npas4: $t(6) = 0.821$, $p = 0.015$, $d = 0.520$	4 (CTRL), 4 (cKO)
	Egr1: $t(8) = 1.545$, $p = 0.161$, $d = 0.977$	5 (CTRL), 5(cKO)
	Arc: $t(8) = 0.187$, $p = 0.856$, $d = 0.118$	5 (CTRL), 5 (cKO)
	Creb1: $t(8) = 0.624$, $p = 0.550$, $d = 0.395$	5 (CTRL), 5 (cKO)
Fig. 5 a-d	Total Length: Tet3: $F(1, 74) = 0.350$, $p = 0.556$, $\omega^2_p < 0$	20 (CTRL), 20 (cKO)
	Sholl Analysis (Basal): Tet3: $F(1, 304) = 1.409$, $p = 0.236$, $\omega^2_p = 0.001$	20 (CTRL), 20 (cKO)
	Sholl Analysis (Apical): Tet3: $F(1, 570) = 1.120$, $p = 0.290$, $\omega^2_p = 0.001$	
	Global Spine Density: $t(38) = 1.227$, $p = 0.228$, $d = 0.390$	20 (CTRL), 20 (cKO)
	Spine Types: $F(1, 152) = 1.144E\text{-}7$, $p > 0.999$, $\omega^2_p < 0$	20 (CTRL), 20 (cKO)
Fig. 5 e-h	Total Length: Tet3: $F(1, 66) = 0.173$, $p = 0.678$, $\omega^2_p < 0$	19 (CTRL), 17 (cKO)
	Sholl Analysis (Basal): Tet3: $F(1, 192) = 1.258$, $p = 0.264$, $\omega^2_p = 0.001$	17 (CTRL), 17 (cKO)
	Sholl Analysis (Apical): Tet3: $F(1, 864) = 0.540$, $p = 0.463$, $\omega^2_p < 0$	
	Global Spine Density: $t(24) = 1.933$, $p = 0.067$, $d = 0.810$	13 (CTRL), 13 (cKO)
	Spine Types: $F(1, 84) = 2.022E\text{-}8$, $p > 0.999$, $\omega^2_p < 0$	13 (CTRL), 13 (cKO)

Chapter IV

TET3 deletion in adult brain neurons of female mice induces anxiety-like behavior and cognitive impairments

Cláudia Antunes, Jorge D. Silva, Sónia Guerra-Gomes, Nuno D. Alves, Eduardo Loureiro-Campos, Wolf Reik, Nuno Sousa, Luisa Pinto and C. Joana Marques

Manuscript in preparation

Tet3 deletion in adult brain neurons of female mice induces anxiety-like behavior and cognitive impairments

Cláudia Antunes[1,2], Jorge D. Da Silva[1,2], Sónia Guerra-Gomes[1,2], Nuno D. Alves[1,2], Eduardo Loureiro-Campos, MSc[1,2], Nuno Sousa[1,2], Wolf Reik[3,4], Luísa Pinto[1,2,7*] and C. Joana Marques[5,6,7*]

[1]Life and Health Sciences Research Institute (ICVS), School of Medicine, University of Minho, Braga, 4710-057, Portugal.

[2]ICVS/3B's - PT Government Associate Laboratory, Braga/ Guimarães, 4710-057, Portugal.

[3]Epigenetics Programme, The Babraham Institute, Cambridge CB22 3AT UK.

[4]The Wellcome Trust Sanger Institute, Cambridge CB10 1SA, UK.

[5]Genetics, Department of Pathology, Faculty of Medicine, University of Porto, 4200-319, Portugal.

[6]i3S – Instituto de Investigação e Inovação em Saúde, Universidade do Porto, Porto 4200-135, Portugal.

[7] Co-last authors

*Correspondence to: Joana Marques - cmarques@med.up.pt or Luísa Pinto- luisapinto@med.uminho.pt

Address: Department of Genetics, Faculty of Medicine of Porto Alameda Professor Hernâni Monteiro 4200-319

Porto, Portugal Tel: +351 220427615

4.1. Abstract

TET enzymes are a family of three dioxygenases involved in DNA demethylation processes, converting 5-methylcytosine bases (5mC) into 5-hydroxymethylcytosine (5hmC). In line with the observed 5hmC enrichment in the brain, *Tet* genes were also shown to be highly transcribed, with *Tet3* being the most abundant. Previously, in male mice we have shown that Tet3 deletion was associated with anxiety-like behavior and spatial orientation impairment. In this study our goal was to clarify the role of TET3 for brain function in female mice. Using a previous established *in vivo* mouse model *Tet3*$^{fl/fl}$; *Camk2a-CreERT2* (Tet3 cKO), we silenced *Tet3* in post-mitotic neurons in the adult brain, and evaluated its impact on behavioral performance.

Our results show that Tet3 deletion increases anxiety-like behavior and impairs both spatial orientation and short-term memory. At the molecular level, we identified upregulation of immediate-early genes (IEGs) in the hippocampus and prefrontal cortex of Tet3 cKO female mice. This study allowed to improve the understanding of how female mice's behavior is regulated by the Tet3 enzyme.

4.2. Introduction

During the last decades, mouse studies on anxiety and cognition have been focused mostly in males, with its conclusions being inherently biased. There are intrinsic biological variances between males and females, which are important to consider in brain (dys)function. The most evident is hormonal regulation; however, genetic and epigenetic factors are also key variables to consider when unraveling the sex-specific differences in brain function (Ratnu et al., 2017). At the same time, epigenetic regulation represents a crucial set of mechanisms impacting a diversity of behaviors. Histone modifications, non-coding RNAs and DNA (de)methylation are the main classes of epigenetic mechanisms (Snijders et al., 2018). TET enzymes are a family of three dioxygenases involved in the DNA demethylation process, converting 5-methylcytosine bases (5mC) into 5-hydroxymethylcytosine (5hmC), 5-formylcytosine (5fC), and 5-carboxylcytosine (5caC) (Ito et al., 2010; Ito et al., 2011). These bases can result in unmodified cytosines, through the action of thymine DNA glycosylase (TDG) and base excision repair (BER) (Liu et al., 2013). 5hmC is a stable base, highly present in the brain and dynamically regulated by neural activity (Guo et al., 2011; Hahn et al., 2014). In opposition, 5fC and 5caC levels are much lower than 5hmC, probably due to their main intermediate function in the cytosine base reparation pathway.

In adult mice, all TET enzymes have been implicated in learning and memory processes (Gontier et al., 2018; Kaas et al., 2013; Kumar et al., 2015; Li et al., 2014; Rudenko et al., 2013; Zhang et al., 2013).

Interestingly, TET3 is the most expressed member in the brain, but its role is still largely unexplored (Szwagierczak et al., 2010). The main limitation has been the lethal phenotype associated with this full deletion, remaining to clarify whether this is due to neurodevelopment malformations (Gu et al., 2011). So far, it was demonstrated that fear extinction leads to a Tet3-mediated accumulation of 5-hmC, within the infralimbic prefrontal cortex (Li et al., 2014). Regarding neurophysiology, it was shown that synaptic activity bi-directionally regulates neuronal *Tet3* expression and that TET3 regulates synaptic transmission via DNA oxidation and repair pathways in hippocampal neurons (Yu et al., 2015). Transcriptional analysis in the hippocampus 30 minutes after contextual fear conditioning showed that genes related with synaptic plasticity and memory are sensitive to *Tet3* upregulation (Kremer et al., 2018). Our recent work showed that *Tet3* conditional deletion in neurons increases anxiety-like behavior, with a concomitant increase in corticosterone levels, and impairs spatial orientation in male mice (Antunes, et al, unpublished results). Moreover, this deletion modifies the gene expression of genes related with HPA axis and neuronal activity. Here, we evaluated the impact of *Tet3* neuronal deletion in females' mice behavior. In this work we showed that *Tet3* conditional knock out (cKO) females presented an increased anxiety-like behavior, assessed by the EPM and OF tests, and an impairment in spatial orientation, demonstrated by a decrease in the use of hippocampal-dependent strategies in the Morris Water Maze (MWM). Interestingly, we found a solid impact of *Tet3* deletion in short-term memory, which was not previously found in Tet3 cKO males. At the molecular level we observed an upregulation of *Npas4* and *c-fos*, both immediate-early genes, in the hippocampus and pre-frontal cortex of Tet3 cKO females.

Therefore, in the current work we reinforce the role of *Tet3* on anxiety-like behavior and spatial orientation and propose a new function for Tet3 specifically in the acquisition of short-term memory in female mice. This study provided a deeper understanding on how the female brain is susceptible to epigenetic control.

4.3.Results

Adult *Tet3* conditional knockout mice show a significant reduction of Tet3 levels in forebrain regions

To characterize the function of TET3 in mature neurons of adult female mice, we used a previously generated *Tet3* conditional knockout mouse model, in which the exon corresponding to the 5 in the coding sequence of *Tet3* gene is flanked by LoxP sequences for Cre-induced site-specific recombination (Peat et al., 2014; Santos et al., 2013). This mouse line was crossed with a *Camk2a-CreERT2* inducible line to specifically delete *Tet3* in mature forebrain neurons, after tamoxifen administration (see Material and Methods for further details). *Tet3* deletion was confirmed by PCR and RT-PCR (**Supplemental figure 1a-**

b). Tet3 conditional knockout (cKO) mice presented a significant reduction of *Tet3* mRNA levels in all evaluated forebrain regions - prefrontal cortex, amygdala, dorsal and ventral hippocampus (**Figure 1a-d**) (*t*test, $p<0.05$). Importantly, reduced levels of *Tet3* did not affect the transcriptional levels of *Tet1* or *Tet2* in any of the analyzed brain regions (**Figure 1a-d**). Additionally, we evaluated whether the conditional deletion of *Tet3* had impact on global 5hmC levels in forebrain regions using an ELISA-based assay and observed no changes in any of the assessed regions (**Figure 1e)**.

Tet3 deletion in neurons results in increased anxiety-like behavior and impaired spatial orientation and short-term memory

We tested the performance of Tet3 cKO mice in different behavioral paradigms to assess its impact in emotional and cognitive domains (**Fig. 2a**). We used two behavioral tests to assess anxiety-like behavior, the elevated plus maze (EPM) and the open-field (OF) tests; to assess depressive-like behavior we performed the forced swimming test (FST). Tet3 cKO mice spent less time in the open arms of the EPM, when compared to the control group (*t*test, $p=0.02$; **Fig. 2b**). Also, in the OF, Tet3 cKO female mice displayed a decreased percentage of time spent in the center of the arena (*t*test, $p=0.05$; **Fig. 2c**), indicating an anxiety-like behavior. In the FST, Tet3 cKO and control mice displayed similar immobility levels (females: $p=0.824$; **Fig. 2d**), indicating no alterations on learned helplessness in Tet3 cKO female mice. Knowing the involvement of the HPA axis in the modulation of behavior, we further determined the basal corticosterone levels in the serum of control and Tet3 cKO mice. We did not detect any differences in the nadir time point, however in the zenith phase Tet3 cKO mice presented reduced corticosterone levels when comparing to control mice (Adjusted t-test, $p<0.01$; **Figure 2e**).

We further evaluated the impact of Tet3 conditional deletion in cognitive function. We analyzed Tet3 cKO mice in the Morris water maze (MWM) test to assess reference memory, a task-dependent on hippocampal function. Although Tet3 cKO mice needed more time to reach the escape platform in comparison to control mice, both Tet3 cKO and control mice were able to successfully learn the spatial reference memory task, as confirmed by the decreasing latencies during the trials (**Fig. 3a**). In the probe trial, both control and Tet3 cKO mice presented similar performances, shown by the same preference (percentage of time swum) for the goal quadrant where the platform was located during the acquisition phase (*t*test, $p=0.109$) (**Fig. 3b**). However, analysis of the strategies adopted by mice to reach the escape platform in the MWM task, divided in random searching/scanning (non-hippocampal strategies) or directed strategies (hippocampal strategies) (Graziano et al., 2003), revealed that Tet3 cKO female

mice used significantly less hippocampal-dependent strategies than control mice (Chi-square test, p=0.022; **Fig. 3c**), indicating a poor spatial orientation.

To clarify the impact of Tet3 deletion on hippocampal function we performed the novel object recognition test, evaluating recognition memory. In this task, Tet3 cKO and control mice showed similar time exploring the object displaced after a short period (1 h) (t-test, p=0.872; **Fig. 3d**), indicating normal object location memory. Moreover, Tet3 cKO and control mice dedicated similar percentages of time exploring the novel object displayed 24 h after being exposed to two equal objects (familiar), indicating no deficits in long-term object recognition memory (t-test, p=0.708; **Fig. 3e**). After 24 h, two new objects were used and 1 h afterwards replaced with a novel one, evaluating short-term memory. Here, Tet3 cKO females displayed a decreased discrimination percentage, indicating an impairment in short-term memory **(**t-test, p <0.001; **Fig. 3f).**

Importantly, females' estrous cycle was assessed at the end of each behavioral paradigm and all females were in the luteal phase **(Supplemental figure 2)**, suggesting an arrested estrous cycle.

Tet3 cKO mice displayed increased expression of neuronal activity-regulated genes in forebrain regions

Considering our previous work, which showed that Tet3 cKO male mice presented an increase in IEG's expression (Antunes et al., unpublished data), we decided to explore whether *Tet3* deletion in females led to the same effect. We analyzed the PFC, dorsal and ventral hippocampus (dHip/vHip) and amygdala (**Fig. 4a-d**), observing a global increased expression of neuronal activity-regulated genes in Tet3 cKO mice. In the PFC of Tet3 cKO, *Npas4* and *Egr1* expression was significantly increased in Tet3 cKO mice (adjusted t-test, *Npas4*: p=0.047 and *Egr1*: p=0.045; **Fig. 4a**). Regarding the dorsal hippocampus, only *Npas4* was significantly up-regulated in Tet3 cKO animals (adjusted t-test, *Npas4*: p=0.047; **Fig. 4b**). In the ventral hippocampus, Tet3 cKO females presented a significantly increased expression of *c-fos* and *Npas4* (adjusted t-test, *c-fos*: p=0.007 and *Npas4*: p=0.010; **Fig. 4c**). In the amygdala, only Creb1 was significantly increased in Tet3 cKO females (adjusted t-test, p=0.006).

Considering the dendritic and spine remodeling implication in the neuroplastic phenomena known to modulate cognitive performance, we decide to analyze neuronal and spines morphology in the dorsal and ventral CA1 hippocampus subregions. Nevertheless, no differences were found between Tet3 cKO and control mice in the parameters evaluated, namely dendritic length, spine density and categorization (**Supplemental figure 3a-h**).

4.4. Discussion

This study reinforces evidence from our previous reported role for TET3 in post-mitotic neurons as a modulator of complex behavior in the adult mouse brain. Specifically, the absence of *Tet3* in mature neurons leads to an increase in anxiety-like behavior and impairs spatial orientation. Thus, we can conclude that *Tet3* function is gender-independent in some behavioral processes (Antunes, et al., unpublished results). However, a striking difference was the discovery of decreased corticosterone levels at the Zenith period in Tet3 cKO females when compared with control group. In Tet3 cKO males, we reported an increase in corticosterone levels, at both Nadir and Zenith circadian cycle periods (Antunes, et al. unpublished results). This result can be possibly explained by hormonal differences between sexes, since the HPA axis is a neuroendocrine system strongly regulated by the hormone balance (Lucassen et al., 2014).

Emotional behavior was previously analyzed using a TET1 KO mice model, which showed normal anxiety and depression-related behaviors (Rudenko et al., 2013). Feng and colleagues showed that neuronal *Tet1* deletion in Nucleus Accumbens (NAc) neurons produced antidepressant-like effects in several behavioral tests (Feng et al., 2017). In contrast, in our model, in which we deleted *Tet3* in mature forebrain neurons, we observed an anxiety-like phenotype, which was independent of the gender. Regarding object location and long-term recognition memories, Tet3 cKO females do not display any impairment, in agreement with our previous observations in males. However, and contrary to what we observed in males, in short-term recognition memory, Tet3 cKO females showed significant impairment. Importantly, and contrarily to long-term memory, which requires gene expression and new protein synthesis, short-term memory only involves alterations of preexistent proteins (Kandel et al., 2014). Thus, the loss of TET3 demethylation activity and the putative consequent alteration of gene expression cannot explain this impairment by itself. We can speculate that *Tet3* deletion, which starts several weeks before the behavioral assessment, can introduce permanent structural and/or functional neuronal alterations, and consequently affect the short-term memory function. Since short-term memory is dependent on the PFC and hippocampal regions (Preston and Eichenbaum, 2013), we can hypothesize that *Tet3* deletion impairs neuronal structure and/or function in these regions, resulting in short-term memory deficits. It remains elusive how males and females are differentially affected by Tet3 deletion specifically in this type of memory. It is known that males and females present diverse sex-specific differences induced by environmental, hormonal and (epi)genetic factors (Ratnu et al., 2017); studies unraveling epigenetic mechanisms to explain differences in brain function are only now emerging. Particularly relevant for the short-term memory differences could be the variation of the DNA (de)methylation pattern according to the gender. Indeed, it is already known

that the female brain has higher levels of DNA methylation, with more methylated CpG sites than males (Nugent et al., 2015). Moreover, it was suggested the opposite pattern for 5-hydroxylmethylcytosine in the males' prefrontal cortex, since they present higher levels compared to females (Ratnu et al., 2017). Therefore, the activity of TET enzymes, namely TET3, can be different in males and females, explaining the variance in short-term memory performance between sexes.

Throughout behavioral assessment, we observed an arrest in the estrous cycle, which is a probable consequence of tamoxifen administration. Indeed, CreERT2 recombinases are insensitive to endogenous estrogen, but activated by the synthetic estrogens receptor (ER) antagonist 4-hydroxytamoxifen (OHT), which is metabolized from 3,4-dihydroxy tamoxifen (Preston and Eichenbaum, 2013); the OHT has a high affinity to the ERα and ERβ estrogen receptors, interfering with the normal estrogens binding to these receptors and with the estrous cycle regulation (Andersson et al., 2010). Thus, as all females were in the luteal phase of the estrous cycle, it was possible to perform the behavior characterization in a more homogeneous sample. However, it is also important to consider that it led to a loss of diversity of the estrous cycle, which is expected when working with females.

In our study of transcriptional regulation in Tet3 cKO mice, we investigated the expression of a wide variety of known neuronal-activity regulatory genes. These genes are known to play important roles in diverse cellular processes such as neurotransmission, neuronal plasticity, learning and memory (Coutellier et al., 2012; Loebrich and Nedivi, 2009). *Npas4* and *c-fos* have been shown upregulated in the hippocampus of Tet3 cKO male mice (Antunes et al. unpublished results). Notably, and contrary to TET3 function in our model, TET1 was shown to be a positive regulator of IEGs expression (Kumar et al., 2015; Rudenko et al., 2013). Interestingly, in the present study, we found that *Tet3* deletion in forebrain post-mitotic increases the expression of IEGs not only in the hippocampus (in line with the previous report in Tet3 cKO male mice), but also in PFC and amygdala. Given that anxiety in rodents involves strong interaction between brain regions such as PFC, amygdala, and hippocampus (Tovote et al., 2015), we suggest that the anxiety-like behavior can be attributed to the hyperactivation of excitatory neurons in these regions, according to with results showing that endogenous Tet3 regulates negatively excitatory synaptic transmission in young mice (Wang et al., 2017). In one hand, the aberrant increase in *Npas4* and *c-fos* transcript levels in the dorsal hippocampus of Tet3 cKO mice might lead to a dysregulation of neuronal activity and possibly explain the spatial orientation impairment. On another hand, the impairment in the use of directed strategies reflects alteration of the goal-directed behavior, and can be associated with the anxiety-like behavior, since the capacity to demonstrate goal-directed behavior involves suppression of emotional states, namely anxiety (Jimenez et al., 2018; Yoshida et al., 2019).

Importantly, and contrary to males' results, no differences were found in the morphology of CA1 neurons. This is a striking result, pointing out gender-specific differences between sexes. Despite this fact, and considering the impairment in the short-term memory, in the future could be relevant to analyze the neuronal morphology in the PCF. Additionally, another anxiety-related brain region that could be analyzed is the amygdala.

Thus, this work not only complements the previous males' findings, but also extends them by investigating the molecular impact in the PFC and amygdala. As such, these findings add an important piece into the current knowledge on the mechanisms modulating adult mouse behavior, specifically introducing new clues in the females' brain function regulation.

4.5. Methods

Animals

Experiments were performed using mice with inducible Tet3 deletion in forebrain post-mitotic neurons, *Tet3*$^{fl/fl}$; *Camk2a-CreERT2* (Tet3 cKO), and the respective littermate controls *Tet3*$^{fl/fl}$ (Ctrl), obtained as previously described (Antunes et al., unpublished data). Mice homozygous for the Tet3 floxed allele, but not carrying Cre-recombinase, were designated as control mice. Animals were genotyped by PCR analysis using genomic DNA and primers specific to Cre-recombinase and the floxed Tet3 allele. Detection of flox transgene was done using a primer specific to the fragment, which allowed to detect the deleted or floxed allele (**Supplemental table 1**). Experiments started with 6-week old female mice Tet3 cKO and the respective littermate controls, in C57BL/6N&B6;129S6 mixed background.

Mice were housed (five per cage) under standard laboratory conditions (12 h light/12 h night cycles (08 h/20 h), at temperature of 22–24 °C, relative humidity of 55% and with *ad libitum* access to water and food). Cages were enriched with paper rolls and soft paper. All experiments were conducted in accordance with EU Directive 2010/63/EU and NIH guidelines on animal care and experimentation, and were approved by the Portuguese Government/Direção Geral de Alimentação e Veterinária (DGAV) with the project reference 0421/000/000/2017.

Tamoxifen Administration

Mice were injected intraperitoneally twice daily with 50 mg/kg of tamoxifen (Sigma, St. Louis, MO; T-5648), for 5 consecutive days, with 7 days break followed by injections for 5 additional consecutive days.

Behavioral Analysis

The behavior testing was conducted 1 month after the last tamoxifen injection, during the light phase with habituation to testing rooms for 30 min before each test. The behavioral assessment was performed following this order: Elevated Plus Maze (EPM), Open Field (OF), Forced-swimming Test (FST), Novel Object Recognition (NOR) and Morris Water Maze (MWM). All tests were performed as previously reported by Antunes et al., unpublished data. All behavioral data analysis was done with the experimenter blinded to the genotype.

The tests details are described bellow.

Open Field

In the open field (OF) test, each animal was placed in the center of the arena (square arena [43.2 cm × 43.2 cm]) surrounded by tall perspex walls (Med Associates Inc., St. Albans City, VT) and allowed to freely explore it for 5 min. Infrared beams and manufacturer's software were used to automatically register animals' movements. Data was analyzed using the activity monitor software (Med Associates, Inc.).

Elevated Plus Maze

The elevated plus maze (EPM) apparatus (ENV-560; Med Associates Inc., St.Albans, VT,USA) consisted of two opposite open arms (50.8cm × 10.2 cm) and two closed arms (50.8cm × 10.2 cm × 40.6 cm). Briefly, each animal was freely let to explore the maze for 5 min. The time spent in the open arms was analyzed using EthoVision XT 11.5 software (Noldus, The Netherlands).

Forced-swim Test

Learned-helplessness was assessed through the forced-swim test (FST). Briefly, assays were conducted by placing each animal, individually, in transparent cylinders filled with water (25^{O}C; depth 30 cm) for 6 min. The trials were videotaped, and the immobility time measured during the last 4 min, using the EthoVision XT 11.5 software (Noldus, The Netherlands). Immobility was considered when the animal was only floating. Learned-helplessness behavior was defined as an increase in time of immobility.

Novel object recognition

The test was conducted under dim white-light illumination in a lusterless white box (30 x 30 x 30 cm). Briefly, animals were habituated to an open arena for 3 consecutive days for 20 min. In the fourth day, two similar objects (glass bottles) were symmetrically placed on the center of the box and animals could

freely explore both objects for 10 min. After an interval of 1 h in their home cages, the novel object was displaced to the opposite side of the box and mice were allowed to explore this new configuration. This trial allowed the assessment of the spatial recognition memory of the subjects. In order to evaluate long-term recognition memory, one of the familiar objects was replaced by a novel one (Lego® brick) 24 h afterwards, and mice were placed in the arena and allowed to explore both for 10 min. In the last day, two new objects were placed in the boxes and mice were place in the arena and allowed to explore both for 10 min. 1 h after one object was replaced by a novel, and the animals placed again to explore these, in order to evaluate short-term memory.

Boxes were cleaned between trials and subjects, with 10% ethanol. Animals were considered to be exploring whenever the nose was facing the object. Exploration time of the novel objects over the total exploration time was used as a measure of object preference. Behavior was video-recorded and analyzed using EthoVision XT 11.5 software (Noldus, The Netherlands).

Morris water maze

Mice were tested in a circular pool (106 cm diameter) filled with water (23 ± 1 °C) and placed in a dim light room. In order to increase the contrast to detect the mice, water was made opaque with the addition of nontoxic titanium dioxide (Sigma-Aldrich; 250 mg/L). Spatial cues were placed in the walls around the pool (square, stripes, triangle and a cross). The pool was divided into four imaginary quadrants and a hidden transparent platform (a circular escape platform (10 cm diameter, 22 cm height)) was placed in one of the quadrants. Trials were video-captured by a video-tracking system (Viewpoint, Champagne-au-Mont-d'Or, France). The 4 days of protocol consisted in a hippocampal-dependent task whose goal was to assess the ability of mice to learn the position of the hidden platform kept always in the same position. Each day, mice performed four consecutive trials (maximum of 60 s, with a 30 s intertrial interval) being placed in the pool facing the maze wall and oriented to each of the extrinsic cues in random order. Whenever mice failed to reach the platform, animals were guided to the platform and allowed to stay in it for 30 s. On the fifth day, the platform was removed and a single trial of 60 s was performed (probe trial). For strategy analysis, we defined two blocks of strategies: "non-hippocampal dependent strategies" (Thigmotaxis, Random Swim and Scanning) and "hippocampal-dependent strategies" (Directed Search, Focal Search and Direct Swim) as previously described by (Graziano et al. 2003).

Determination of estrous cycle stage

Vaginal smears were collected throughout the behavioral tests, to determine the stage of the estrous cycle. Vaginal smears were performed by inserting a drop of sterile 0.9% saline solution in the vagina with the help of a 1 ml syringe, collecting the cell suspension by inserting a small plastic inoculation loop and performing a smear into a glass slide. Smears were air-dried, fixed in alcohol 96% for 5 min and stained using the Papanicolaou protocol. Briefly, smears were hydrated in tap water, stained with Harris hematoxylin for 1 min, rinsed in running tap water for 2 min, regressively stained by a single dip in alcohol–acid solution, rinsed in tap water for 2 min, dehydrated in alcohol 96% for 1 min, stained with orange G for 1 min, washed in alcohol 96% for 1 min, stained with Eosin Azure 50 for 1 min, dehydrated in a decreasing series of alcohol concentration and cleared with xylene. Slides were analyzed under a light microscope and the proportion of cornified epithelial cells, nucleated epithelial cells and leukocytes were used for the determination of the estrous cycle phases (Byers et al., 2012).

Serum corticosterone levels

Blood samples for basal measurements of corticosterone were collected one week before the behavior assessment. Two independent collections were made at two different time points, 8 a.m. and 8 p.m., with an interval of 24 h in between. The blood was quickly collected after a small incision in the tail of the animals and then centrifuged at 13,000 rpm for 10 min and the supernatant removed and stored at −80 °C until use. Corticosteroid levels in serum were measured by radioimmunoassay using a commercial kit (Enzo Life Sciences, New York, USA), according to the manufacturer's instructions.

DNA/RNA Extraction

Brains were obtained by decapitation after deep anesthesia with a mixture of ketamine (75 mg/kg, i.p.; Imalgene 1000, Merial, EUA) and medetomidine (1 mg/kg, i.p.; Dorbene Vet, Pfizer, EUA), and transcardially perfused with 0.9% saline. Brains were macrodissected, by a single investigator, and tissue samples were stored at -80 ^{O}C. The tissues were prepared by homogenization using Trizol® reagent (Invitrogen). Both nucleic acids were extracted according to the manufacturer's instructions. The RNA was treated with DNase I (Thermo Scientific) and a total 500 ng RNA was used for cDNA synthesis using the qScriptTM cDNA SuperMix (Quanta Biosciences, USA).

qRT-PCR

cDNA was diluted 1:10 and used as template for quantitative real-time PCR reactions using the 5x HOT FIREPol EvaGreen qPCR supermix (Solis Biodyne) and primers designed to specifically amplify each gene of interest (**Supplementary Table S2**). Cycling reactions were performed in duplicate and cycle threshold (Ct) fluorescence data recorded on Applied Biosystems 7500 Fast Real-time PCR System. The relative abundance of each gene of interest was calculated on the basis of the ΔΔCt method (Livak and Schmittgen, 2001) and results were normalised to two replicates of the *Atp5b* housekeeping gene.

Quantification of 5hmC

The global level of 5hmC was measured using a Quest 5hmC DNA ELISA Kit (Zymo research, California, USA). The procedure was performed according to the manufacturer's instructions, with a loaded quantity of 100 ng of genomic DNA per well.

3D-reconstruction of neurons

Neuronal reconstruction was performed as previously described by Antunes et al., unpublished data. Briefly, CA1 neurons were identified by their typical triangular soma-shape, apical dendrites extending toward the striatum radiatum. For each experimental group, four animals were studied and, for each one, five neurons per area were reconstructed and evaluated (a total of 20 neurons per area). Neurons were selected for reconstruction following these criteria: (i) identification of soma within the pyramidal layer of CA1 (ii) full impregnation along the entire length of the dendritic tree; (iii) no morphological changes attributable to incomplete dendritic impregnation of Golgi-Cox staining or truncated branches. The dendritic reconstruction was performed at 100x (oil) magnification using a motorized microscope (BX51, Olympus) and Neurolucida software (Microbrightfield). The analyzed dendritic features were: total length, number of endings and nodes, and Sholl analysis (number of dendrite intersections at radial intervals of 20 mm). Dendritic spine density (calculated as number of spines/dendritic length), was evaluated in proximal and distal segments of dendrites. To identify changes in spine morphology, spines in the selected segments were classified into thin, mushroom, thick or ramified (7) and the proportion of spines in each category was calculated for each neuron.

Statistical analysis

A confidence interval of 95% was assumed for hypothesis testing. Normality was assumed for all continuous variables, after testing with the Shapiro-Wilk test. Homoscedasticity and sphericity were assumed for all respective variables, after testing with Levene's and Mauchly's test respectively. For the

comparison of two means, the two-tailed unpaired Student's t-test was carried out with the two-stage step-up method of Benjamini, Krieger and Yekuteli used for multiple comparisons correction. For the comparison of means with two independent variables, a factorial analysis of variance (ANOVA) was performed; for one independent and one repeated measures variable, a mixed-design ANOVA was used and Post-hoc analysis was performed using the Sidak correction. For the comparison of proportions, the two-sided Chi-square test was carried out. Appropriate effect size measures were reported for all statistical tests. All statistical analyses were carried out using SPSS 22.0® or GraphPad Prism 8.0®.

4.6. Author contributions

C.A designed the study, performed the experiments, analysed the data and wrote the manuscript; J.D.S. performed statistical analysis and wrote the manuscript; S.G.G. and N.D.A. helped with the behavioural tests and respective analysis; E. L.C. helped with the behavioural tests; N.S. organized and wrote the manuscript; W.R. contributed with the *Tet3* conditional mouse strain; L.P. and C.J.M. designed the study, organized and wrote the manuscript. All authors revised and approved the final manuscript.

4.7. Acknowledgments

This work was supported by National Funds through Foundation for Science and Technology (FCT) fellowships (PD/BD/106049/2015 to CA, PD/BD/128074/2016 to J.D.S, SFRH/BD/131278/2017 to E.LC, IF/01079/2014 to LP, SFRH/BD/ 101298/2014 to S. GM; IF/00047/2012 and CEECIND/00371/2017 to C.J.M); FCT project grant (PTDC/BIA-BCM/121276/2010) to C.J.M; EpiGeneSys Small Collaborative project to LP; BIAL Foundation Grant 427/14 to LP; Northern Portugal Regional Operational Programme (NORTE 2020), under the Portugal 2020 Partnership Agreement, through the European Regional Development Fund (FEDER; NORTE-01-0145-FEDER-000013); FEDER funds, through the Competitiveness Factors Operational Programme (COMPETE), and National Funds, through the FCT (POCI-01-0145-FEDER-007038).

4.9. References

Andersson, K.B., Winer, L.H., Mork, H.K., Molkentin, J.D., and Jaisser, F. (2010). Tamoxifen administration routes and dosage for inducible Cre-mediated gene disruption in mouse hearts. Transgenic research *19*, 715-725.

Byers, S.L., Wiles, M.V., Dunn, S.L., and Taft, R.A. (2012). Mouse estrous cycle identification tool and images. PLoS One *7*, e35538.

Coutellier, L., Beraki, S., Ardestani, P.M., Saw, N.L., and Shamloo, M. (2012). Npas4: a neuronal transcription factor with a key role in social and cognitive functions relevant to developmental disorders. PLoS One *7*, e46604.

Feng, J., Pena, C.J., Purushothaman, I., Engmann, O., Walker, D., Brown, A.N., Issler, O., Doyle, M., Harrigan, E., Mouzon, E.*, et al.* (2017). Tet1 in Nucleus Accumbens Opposes Depression- and Anxiety-Like Behaviors. Neuropsychopharmacology *42*, 1657-1669.

Gontier, G., Iyer, M., Shea, J.M., Bieri, G., Wheatley, E.G., Ramalho-Santos, M., and Villeda, S.A. (2018). Tet2 Rescues Age-Related Regenerative Decline and Enhances Cognitive Function in the Adult Mouse Brain. Cell reports *22*, 1974-1981.

Graziano, A., Petrosini, L., and Bartoletti, A. (2003). Automatic recognition of explorative strategies in the Morris water maze. Journal of neuroscience methods *130*, 33-44.

Gu, T.P., Guo, F., Yang, H., Wu, H.P., Xu, G.F., Liu, W., Xie, Z.G., Shi, L., He, X., Jin, S.G.*, et al.* (2011). The role of Tet3 DNA dioxygenase in epigenetic reprogramming by oocytes. Nature *477*, 606-610.

Guo, J.U., Su, Y., Zhong, C., Ming, G.L., and Song, H. (2011). Hydroxylation of 5-methylcytosine by TET1 promotes active DNA demethylation in the adult brain. Cell *145*, 423-434.

Hahn, M.A., Szabó, P.E., and Pfeifer, G.P. (2014). 5-Hydroxymethylcytosine: a stable or transient DNA modification? Genomics *104*, 314-323.

Ito, S., D'Alessio, A.C., Taranova, O.V., Hong, K., Sowers, L.C., and Zhang, Y. (2010). Role of Tet proteins in 5mC to 5hmC conversion, ES-cell self-renewal and inner cell mass specification. Nature *466*, 1129-1133.

Ito, S., Shen, L., Dai, Q., Wu, S.C., Collins, L.B., Swenberg, J.A., He, C., and Zhang, Y. (2011). Tet proteins can convert 5-methylcytosine to 5-formylcytosine and 5-carboxylcytosine. Science *333*, 1300-1303.

Jimenez, J.C., Su, K., Goldberg, A.R., Luna, V.M., Biane, J.S., Ordek, G., Zhou, P., Ong, S.K., Wright, M.A., Zweifel, L.*, et al.* (2018). Anxiety Cells in a Hippocampal-Hypothalamic Circuit. Neuron *97*, 670-683.e676.

Kaas, G.A., Zhong, C., Eason, D.E., Ross, D.L., Vachhani, R.V., Ming, G.L., King, J.R., Song, H., and Sweatt, J.D. (2013). TET1 controls CNS 5-methylcytosine hydroxylation, active DNA demethylation, gene transcription, and memory formation. Neuron *79*, 1086-1093.

Kandel, E.R., Dudai, Y., and Mayford, M.R. (2014). The molecular and systems biology of memory. Cell *157*, 163-186.

Kremer, E.A., Gaur, N., Lee, M.A., Engmann, O., Bohacek, J., and Mansuy, I.M. (2018). Interplay between TETs and microRNAs in the adult brain for memory formation. Scientific reports *8*, 1678.

Kumar, D., Aggarwal, M., Kaas, G.A., Lewis, J., Wang, J., Ross, D.L., Zhong, C., Kennedy, A., Song, H., and Sweatt, J.D. (2015). Tet1 Oxidase Regulates Neuronal Gene Transcription, Active DNA Hydroxymethylation, Object Location Memory, and Threat Recognition Memory. Neuroepigenetics *4*, 12-27.

Li, X., Wei, W., Zhao, Q.Y., Widagdo, J., Baker-Andresen, D., Flavell, C.R., D'Alessio, A., Zhang, Y., and Bredy, T.W. (2014). Neocortical Tet3-mediated accumulation of 5-hydroxymethylcytosine promotes rapid behavioral adaptation. Proceedings National Academy Sciences U S A *111*, 7120-7125.

Liu, S., Wang, J., Su, Y., Guerrero, C., Zeng, Y., Mitra, D., Brooks, P.J., Fisher, D.E., Song, H., and Wang, Y. (2013). Quantitative assessment of Tet-induced oxidation products of 5-methylcytosine in cellular and tissue DNA. Nucleic acids research *41*, 6421-6429.

Livak, K.J., and Schmittgen, T.D. (2001). Analysis of relative gene expression data using real-time quantitative PCR and the 2(-Delta Delta C(T)) Method. Methods (San Diego, Calif) *25*, 402-408.

Loebrich, S., and Nedivi, E. (2009). The function of activity-regulated genes in the nervous system. Physiological Reviews *89*, 1079-1103.

Lucassen, P.J., Pruessner, J., Sousa, N., Almeida, O.F.X., Van Dam, A.M., Rajkowska, G., Swaab, D.F., and Czéh, B. (2014). Neuropathology of stress. Acta Neuropathol *127*, 109-135.

Nugent, B.M., Wright, C.L., Shetty, A.C., Hodes, G.E., Lenz, K.M., Mahurkar, A., Russo, S.J., Devine, S.E., and McCarthy, M.M. (2015). Brain feminization requires active repression of masculinization via DNA methylation. Nature neuroscience *18*, 690-697.

Peat, J.R., Dean, W., Clark, S.J., Krueger, F., Smallwood, S.A., Ficz, G., Kim, J.K., Marioni, J.C., Hore, T.A., and Reik, W. (2014). Genome-wide bisulfite sequencing in zygotes identifies demethylation targets and maps the contribution of TET3 oxidation. Cell reports *9*, 1990-2000.

Preston, A.R., and Eichenbaum, H. (2013). Interplay of hippocampus and prefrontal cortex in memory. Current biology : CB *23*, R764-R773.

Ratnu, V.S., Emami, M.R., and Bredy, T.W. (2017). Genetic and epigenetic factors underlying sex differences in the regulation of gene expression in the brain. Journal of neuroscience research *95*, 301-310.

Rudenko, A., Dawlaty, M.M., Seo, J., Cheng, A.W., Meng, J., Le, T., Faull, K.F., Jaenisch, R., and Tsai, L.H. (2013). Tet1 is critical for neuronal activity-regulated gene expression and memory extinction. Neuron *79*, 1109-1122.

Santos, F., Peat, J., Burgess, H., Rada, C., Reik, W., and Dean, W. (2013). Active demethylation in mouse zygotes involves cytosine deamination and base excision repair. Epigenetics Chromatin *6*, 39.

Snijders, C., Bassil, K.C., and de Nijs, L. (2018). Methodologies of Neuroepigenetic Research: Background, Challenges and Future Perspectives. Progress in molecular biology and translational science *158*, 15-27.

Szwagierczak, A., Bultmann, S., Schmidt, C.S., Spada, F., and Leonhardt, H. (2010). Sensitive enzymatic quantification of 5-hydroxymethylcytosine in genomic DNA. Nucleic acids research *38*, e181.

Tovote, P., Fadok, J.P., and Luthi, A. (2015). Neuronal circuits for fear and anxiety. Nature reviews Neuroscience *16*, 317-331.

Wang, L., Li, M.Y., Qu, C., Miao, W.Y., Yin, Q., Liao, J., Cao, H.T., Huang, M., Wang, K., Zuo, E.*, et al.* (2017). CRISPR-Cas9-mediated genome editing in one blastomere of two-cell embryos reveals a novel Tet3 function in regulating neocortical development. Cell research *27*, 815-829.

Yoshida, K., Drew, M.R., Mimura, M., and Tanaka, K.F. (2019). Serotonin-mediated inhibition of ventral hippocampus is required for sustained goal-directed behavior. Nature neuroscience *22*, 770-777.

Yu, H., Su, Y., Shin, J., Zhong, C., Guo, J.U., Weng, Y.L., Gao, F., Geschwind, D.H., Coppola, G., Ming, G.L.*, et al.* (2015). Tet3 regulates synaptic transmission and homeostatic plasticity via DNA oxidation and repair. Nature neuroscience *18*, 836-843.

Zhang, R.R., Cui, Q.Y., Murai, K., Lim, Y.C., Smith, Z.D., Jin, S., Ye, P., Rosa, L., Lee, Y.K., Wu, H.P.*, et al.* (2013). Tet1 regulates adult hippocampal neurogenesis and cognition. Cell stem cell *13*, 237-245.

4.10. Figures

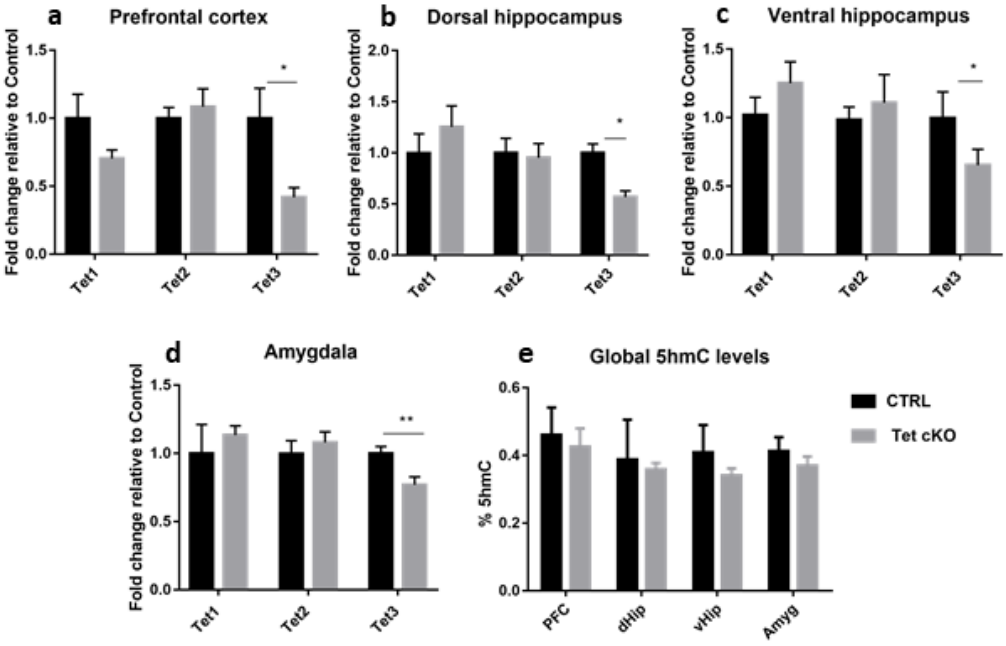

Figure 1. Tet3 deletion in adult brain neurons results in significant reduction of Tet3 levels, with maintenance of Tet1 and Tet2, and no alterations in global 5hmC levels in forebrain regions.

(a-d) Reduction in Tet3 levels and maintenance of Tet1 and Tet2 levels was observed in Tet3 cKO animals. mRNA expression in forebrain regions of control and Tet3 cKO female mice was measured by qPCR in the **(a)** prefrontal cortex, **(b)** dorsal hippocampus, **(c)** ventral hippocampus and **(d)** amygdala (*n*=3-5 per group). **(e)** No alterations were found in the global 5hmC levels in forebrain regions evaluated by ELISA (*n*=3 per group). Quantifications are presented as the mean ± SEM. **(a-d)** Two-tailed Student's t-test; *p < 0.05, **p<0.01

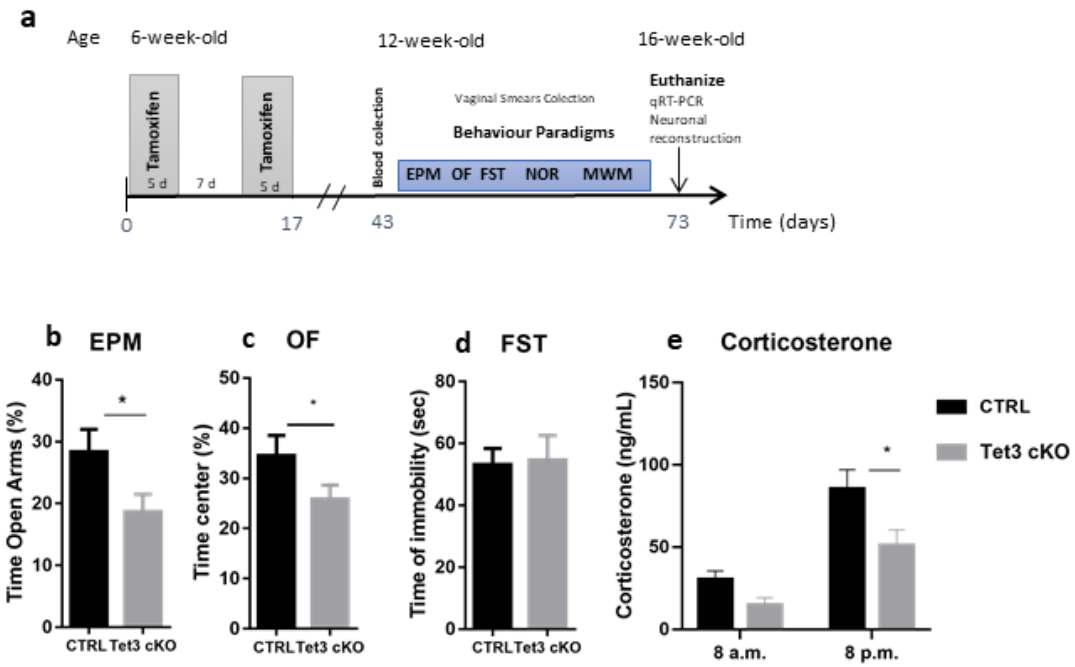

Figure 2. Tet3 cKO female mice showed increased anxiety-like behavior and normal depressive-like behavior.
(a) Scheme illustrating the protocol used to induce Tet3 deletion and the behavior paradigm timeline. Six-week-old mice were injected intraperitoneally with 50 mg/kg of tamoxifen twice a day for 5 consecutive days, with 7 days break, followed by injections for 5 additional consecutive days. Animals were submitted to behavioral testing 1 month after the last tamoxifen injection and euthanized after this assessment. **(b-c)** Anxiety-like behavior was tested both in the elevated plus maze (EPM) (**b**) and in the open-field test (OF) **(c)** showing increased anxiety-like behavior in Tet3 cKO female mice. **(d)** The presence of depressive-like behavior was assessed in the forced swimming test (FST) *(n*=13-17 per group) showing no deficits in Tet3 cKO female mice. **(e)** Basal serum concentration of corticosteroids in control and Tet3 cKo mice, both in the morning and at night, revealed a significant increased production by Tet3 cKO mice *(n*= 8 per group). Quantifications are presented as the mean ± SEM. **(b-d)** Two-tailed Student's t-test; *p < 0.05; **(e)** Adjusted two-tailed Student's t-test; ** p< 0.01.

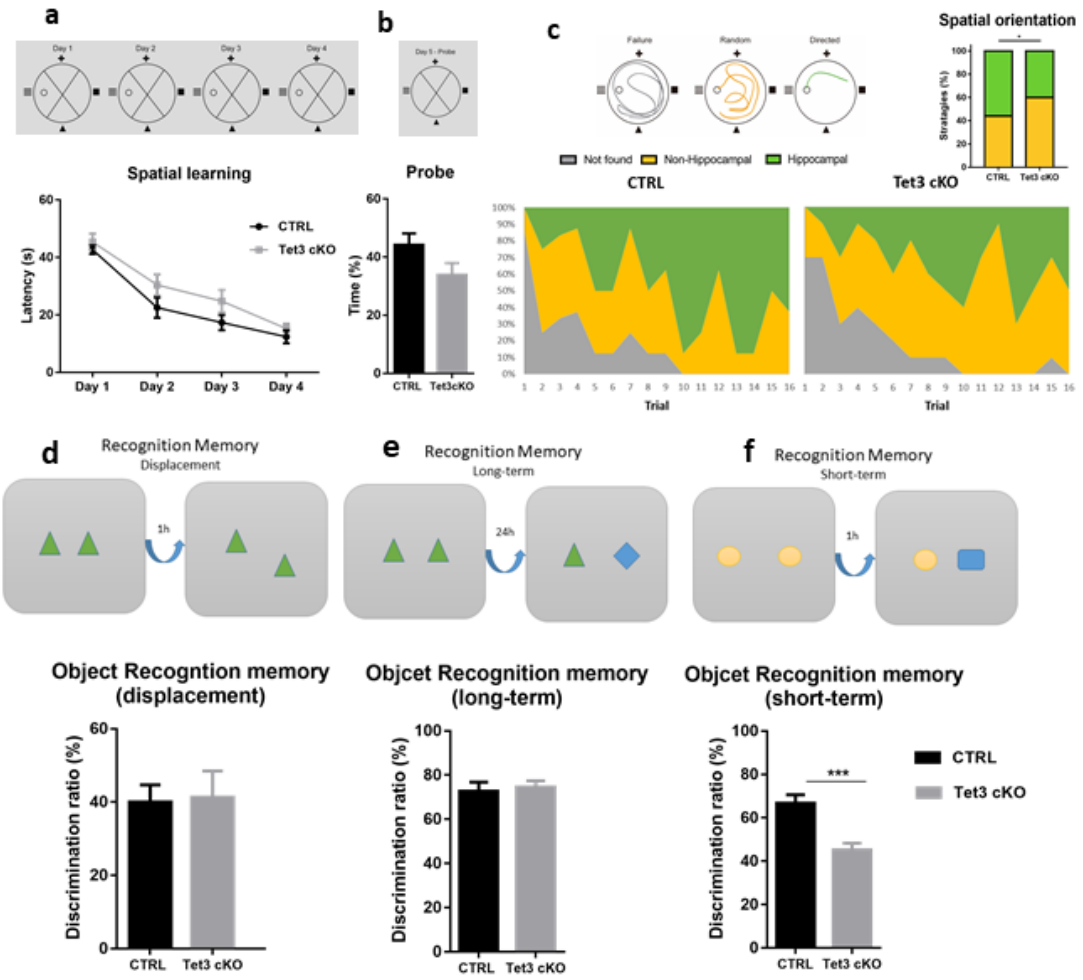

Figure 3. Tet3 cKO female mice show impairment of spatial learning and short-term recognition memory.
(a-c) Morris Water Maze test. Spatial acquisition performances were recorded during 4-day training. (**a**) Escape latency. (**b**) Time in the target quadrant. (**c**) Cognitive strategies to reach the hidden plataform during water maze learning. A schematic representation and color code for each group of strategy and the average prevalence by trial number are shown. Representation of the percentage of mice using directed strategies (hippocampal-dependent strategies) (n=8-11 per group). Results indicate a decrease in hippocampal-dependent strategies in Tet3 cKO female mice. **(d-f)** Novel object recognition test. Animals were allowed to explore two identical objects for 10 min. (**d**) After an interval of 1 h in their home cages, the novel object was displaced to the opposite side of the box and mice were allowed to explore this new configuration, evaluating spatial recognition memory (displacement) (**f**) After 24 h, mice returned to the arena, where one of the familiar objects was replaced by a novel one, evaluating long-term memory (**g**) After 24 h, two new objects were placed in the box and mice were allowed to explore them. 1h after, one object was replaced by a novel one, and the animals placed in the arena, to evaluate short-term memory (**g**) (n=14-18 per group). Results show impairment in short-term memory in Tet3 cKO female mice. Quantifications are presented as mean ± SEM. (**a**) Mixed ANOVA, genotype; **(b)** Two-tailed Student's t-test; **(c)** Chi-square test; * p< 0.05; **(d-f)** two-tailed Student's t-test, *** p< 0.001.

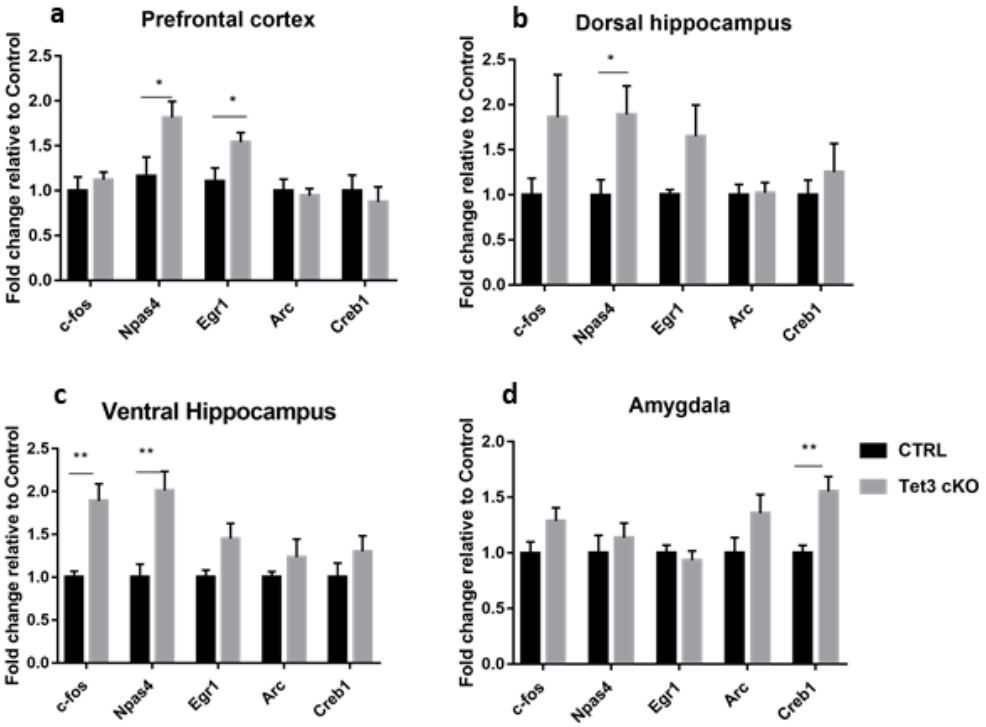

Figure 4- Tet3 cKO female mice showed an increase in the expression of neuronal activity-regulated genes.
(**a-d**) mRNA expression of immediate- early genes (IEGs) in forebrain regions was measured by qPCR in controls and Tet3 cKO animals in the (**a**) prefrontal cortex, (**b**) dorsal hippocampus, (**c**) ventral hippocampus and (**d**) amygdala (*n*=4-6 per group). Quantifications are presented as the mean ± SEM. (**a-d)** Two-tailed Student's t-test; * p< 0.05, ** p< 0.01.

4.11. Supplementary Material

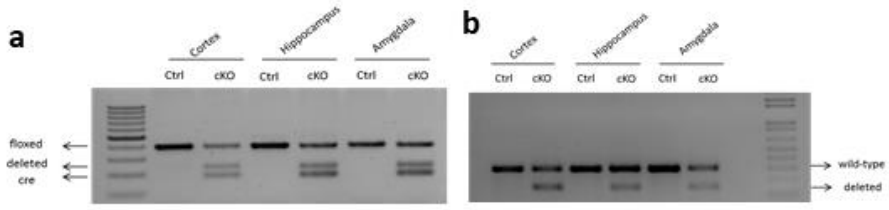

Supplemental S1. Generation of TET3 conditional deletion.
(a) PCR genotyping of forebrain regions 26 days after induction of deletion. In the Tet3 cKO animals are observed three bands with 184, 237 and 400 base pairs corresponding to the cre, deleted and floxed alleles respectively. Control animals do not show the bands corresponding to cre and deleted bands (100 bp Ladder).
(b) Loss of the flanking exon7 at Tet3 RNA level confirmed by RT-PCR assay. In the Tet3 cKO animals two bands are observed with 328 and 178 base pairs corresponding to the wild-type and deleted exon 7, respectively. Control animals do not show the deleted band (100 bp Ladder).

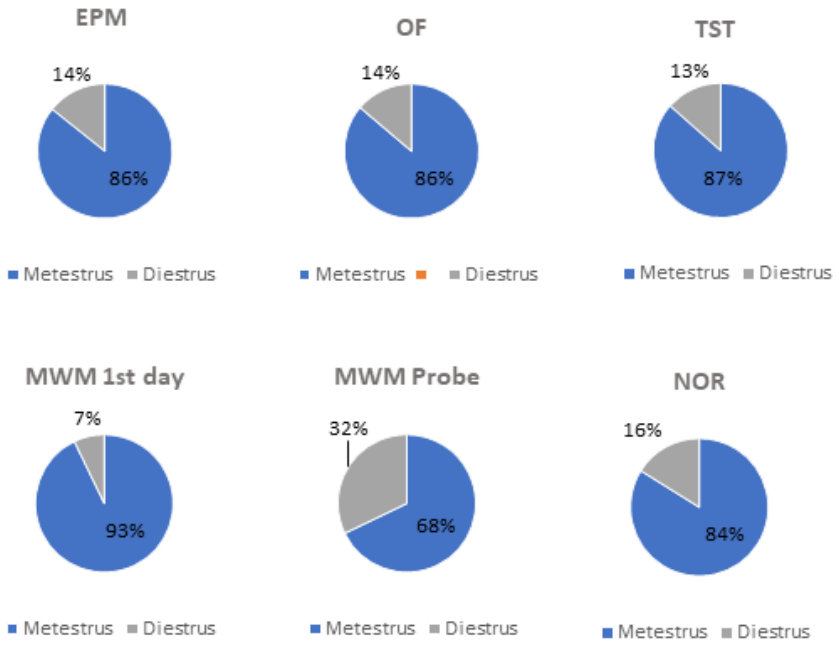

Supplemental S2. All females revealed to be in the luteal phase of the estrous cycle at the end of each behavioral test.
The circular graph represents the percentage of females in the metestrus and diestrus phase, after vaginal cytology analysis (*n*= 14-17 per group).

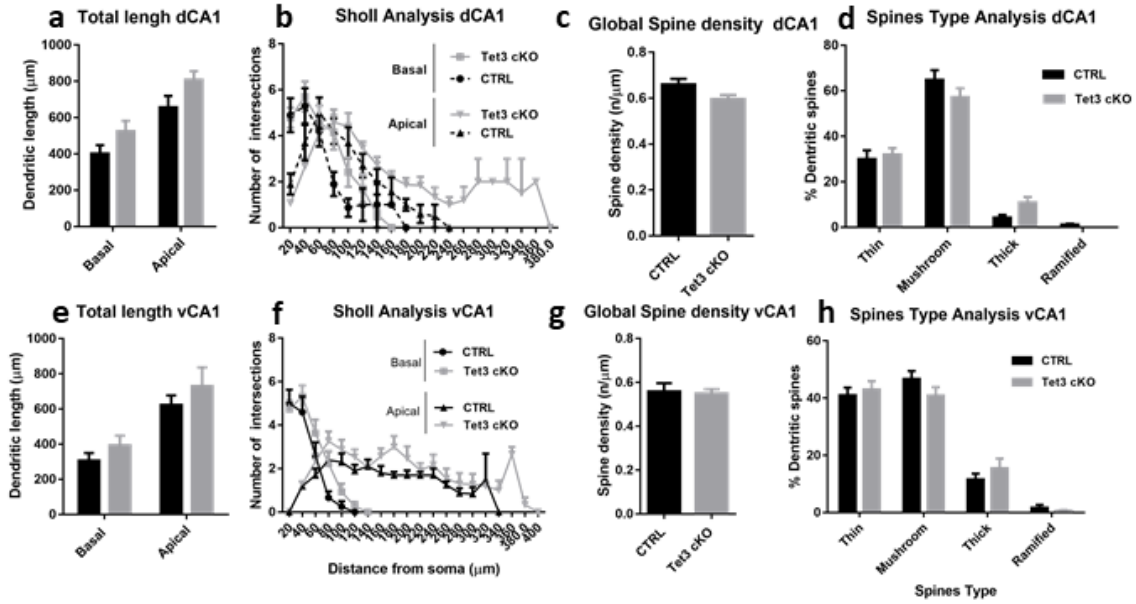

Supplemental S3. Three-dimensional morphometric analysis of Golgi-impregnated neurons of the ventral and dorsal hippocampus sub-regions reveals no major alterations by Tet3 conditional deletion in neuronal morphology and dendritic spine density.

Overall, in Tet3 cKO animals no differences were found in all parameters evaluated **(a,e)** Total length**; (b,f)** Sholl analysis**; (c,g)** Global spine density**; (d,h)** Spynes type analysis**.** *n=9*-15 neurons; 3 mice per group. Quantifications are presented as the mean ± SEM. (**a, b, e, f**) Factorial ANOVA; (**c, g**) Two-tailed Student's t-test; (**d, h**) Factorial ANOVA, genotype.

Supplemental Table S1.Primers list and sequence.

(**a**) Primers for genotyping PCR of Tet3 cKO animals.

(**b**) Primers used for quantitative qRT-PCR analysis

a

Target	Forward Primer (5'- 3')	Reverse Primer (5' – 3')
Cre	AGCTCGTCAATCAAGCTGGT	CAGGTTCTTGCGAACCTCAT
Tet3	TACCTCTGCCTCTGGAGTGCTAA	ATGGCTACTCACAACCCAGTGAC GTCAGGAAAGTCACATGGTTGTTG

b

Target	Forward Primer (5'- 3')	Reverse Primer (5' – 3')
Atp5b	GCCAAGATGTCCTGCTGTT	TCCTTCGGATTGTCTCCCGTG
Tet1	CCATTCTCACAAGGACATTCACA	GCCATTCTCAGGAGTCACTGC
Tet2	GCCATTCTCAGGAGTCACTGC	ACTTCTCGATTGTCTTCTCTATTGAGG
Tet3	GCCTCCTTCTCCTTCGGCTG	TCCTTCGGATTGTCTCCCGTG
Arc	AGCTCGCTGCATGGCCTTTG	GGGGCTTGGCTGAGGTTTCA
c-fos	AGCATCGGCAGAAGGGGCAA	TGATCTGTCTCCGCTTGGAGTGT
Creb1	CACCATTGCCCCTGGAGTTGTT	TCTCTTGCTGCCTCCCTGTTCTT
Egr1	TGAGCACCTGACCACAGAGTCC	GTGATGGGAGGCAACCGAGT
Npas4	TCGGAGAGTGTGAGCGAGCA	AGGCGATCAGCATCCAGAGCA

Supplemental Table S2. List of Statistical Reports

Figure	Statistical Report	Sample Size
Fig. 1a	Tet1: $t(8) = 1.580$, $p = 0.153$, $d = 1.003$ Tet2: $t(8) = 0.564$, $p = 0.588$, $d = 0.356$ Tet3: $t(8) = 2.514$, $p = 0.036$, $d = 1.591$	5 (CTRL), 5(cKO)
Fig. 1b	Tet1: $t(8) = 0.921$, $p = 0.384$, $d = 0.582$ Tet2: $t(8) = 0.240$, $p = 0.816$, $d = 0.152$ Tet3: $t(8) = 3.484$, $p = 0.013$, $d = 2.765$	5 (CTRL), 5(cKO)
Fig. 1c	Tet1: $t(8) = 1.151$, $p = 0.283$, $d = 0.728$ Tet2: $t(8) = 0.561$, $p = 0.590$, $d = 0.354$ Tet3: $t(8) = 2.624$, $p = 0.047$, $d = 1.920$	5 (CTRL), 5(cKO)
Fig. 1d	Tet1: $t(8) = 0.602$, $p = 0.564$, $d = 0.380$ Tet2: $t(8) = 0.662$, $p = 0.527$, $d = 0.418$ Tet3: $t(8) = 4.238$, $p = 0.005$, $d = 3.013$	5 (CTRL), 5(cKO)
Fig. 1e	Tet3: $F(1, 13) = 0.952$, $p = 0.347$, $\omega^2_p < 0$	3 (CTRL), 3 (cKO)
Fig. 2b	$t(29) = 2.394$, $p = 0.020$, $d = 0.762$	15 (CTRL), 16 (cKO)
Fig. 2c	$t(28) = 2.036$, $p = 0.046$, $d = 0.670$	13 (CTRL), 17 (cKO)
Fig. 2d	$t(29) = 0.144$, $p = 0.886$, $d = 0.053$	15 (CTRL), 16 (cKO)
Fig. 3a	$F(1, 17) = 4.723$, $p = 0.044$, $\omega^2_p = 0.164$	10 (CTRL), 9 (cKO)
Fig. 3b	$t(18) = 1.642$, $p = 0.109$, $d = 0.824$	10 (CTRL), 10 (cKO)
Fig. 3c	$\chi^2(1) = 5.128$, $p = 0.024$, $\phi = 0.549$	8 (CTRL), 9 (cKO)
Fig. 3d	$t(8) = 0.164$, $p = 0.872$, $d = 0.096$	5 (CTRL), 5 (cKO)
Fig. 3e	Females: $t(29) = 0.376$, $p = 0.708$, $d = 0.134$	15 (CTRL), 16 (cKO)
Fig. 3f	Females: $t(29) = 1.750$, $p < 0.001$, $d = 1.546$	15 (CTRL), 16 (cKO)

Figure	Statistical Report	Sample Size
Fig. 4a	c-fos: t(6) = 0.703, p = 0.508, d = 0.497	4 (CTRL), 4 (cKO)
	Npas4: t(8) = 2.344, p = 0.047, d = 1.483	5 (CTRL), 5 (cKO)
	Egr1: t(8) = 2.378, p = 0.045, d = 1.503	5 (CTRL), 5 (cKO)
	Arc: t(8) = 0.382, p = 0.713, d = 0.241	5 (CTRL), 5 (cKO)
	Creb1: t(8) = 0.522, p = 0.616, d = 0.330	5 (CTRL), 5 (cKO)
Fig. 4b	c-fos: t(7) = 1.539, p = 0.168, d = 1.089	5 (CTRL), 4 (cKO)
	Npas4: t(6) = 2.492, p = 0.047, d = 1.762	4 (CTRL), 4 (cKO)
	Egr1: t(7) = 1.638, p = 0.146, d = 1.171	5 (CTRL), 4 (cKO)
	Arc: t(8) = 0.135, p = 0.896, d = 0.085	5 (CTRL), 5 (cKO)
	Creb1: t(8) = 0.711, p = 0.497, d = 0.450	5 (CTRL), 5 (cKO)
Fig. 4c	c-fos: t(7) = 3.798, p = 0.007, d = 2.693	5 (CTRL), 4 (cKO)
	Npas4: t(7) = 3.532, p = 0.010, d = 2.444	5 (CTRL), 4 (cKO)
	Egr1: t(7) = 2.109, p = 0.073, d = 1.485	5 (CTRL), 4 (cKO)
	Arc: t(8) = 1.063, p = 0.319, d = 0.672	5 (CTRL), 5 (cKO)
	Creb1: t(8) = 1.219, p = 0.258, d = 0.771	5 (CTRL), 5 (cKO)
Fig. 4d	c-fos: t(8) = 1.876, p = 0.098, d = 1.186	5 (CTRL), 4 (cKO)
	Npas4: t(8) = 0.662, p = 0.527, d = 0.418	4 (CTRL), 4 (cKO)
	Egr1: t(7) = 0.615, p = 0.558, d = 0.410	5 (CTRL), 4 (cKO)
	Arc: t(8) = 1.642, p = 0.139, d = 1.038	5 (CTRL), 5 (cKO)
	Creb1: t(8) = 3.675, p = 0.006, d = 2.323	5 (CTRL), 5 (cKO)

Figure	Statistical Report	Sample Size
Fig. S3 Golgi Dorsal CA1	Total Length: Tet3: $F(1, 46) = 1.506$, $p = 0.226$, $\omega^2_p = 0.010$	10 (CTRL), 15 (cKO)
	Sholl Analysis (Basal): Tet3: $F(1, 87) = 2.312$, $p = 0.132$, $\omega^2_p = 0.015$	10 (CTRL), 15 (cKO)
	Sholl Analysis (Apical): Tet3: $F(1, 92) = 2.760$, $p = 0.100$, $\omega^2_p = 0.018$	
	Global Spine Density: $t(17) = 0.231$, $p = 0.820$, $d = 0.107$	10 (CTRL), 9 (cKO)
	Spine Types: $F(1, 72) = 1.525E\text{-}8$, $p > 0.999$, $\omega^2_p < 0$	10 (CTRL), 10 (cKO)
Fig. S3 Golgi ventral CA1	Total Length: $F(1, 46) = 1.506$, $p = 0.226$, $\omega^2_p = 0.010$	10 (CTRL), 15 (cKO)
	Sholl Analysis (Basal): Tet3: $F(1, 96) = 3.567$, $p = 0.062$, $\omega^2_p = 0.026$	10 (CTRL), 15 (cKO)
	Sholl Analysis (Apical): Tet3: $F(1, 92) = 3.630$, $p = 0.060$, $\omega^2_p = 0.027$	
	Global Spine Density: $t(17) = 0.231$, $p = 0.820$, $d = 0.108$	10 (CTRL), 9 (cKO)
	Spine Types: Tet3: $F(1, 68) = 0.016$, $p = 0.899$, $\omega^2_p < 0$	10 (CTRL), 9 (cKO)

Chapter V

General discussion, conclusions and future perspectives

GENERAL DISCUSSION

Only ten years ago, the discovery of high levels of 5hmC in the DNA of Purkinje neurons and granule cells (Kriaucionis and Heintz, 2009) and that TET1 enzyme, a fusion partner of the MLL gene in acute myeloid leukemia, catalyzed the conversion of 5mC to 5hmC (Tahiliani et al., 2009a) supported the evidence for a putative regulatory function of TET proteins and 5hmC modification in neural and brain function. These discoveries contributed to a new field of research called neuroepigenetics, which has experienced an exponential growth, and for which this work intends to contribute.

Thus, in the present thesis, we have sought for new insights on the role of TET enzymes in the modulation of neural precursors cells (NPCs) fate (chapter II). In this chapter, we were able to implement and characterize an *in vitro* neural differentiation system, from mouse ESCs to NPCs. We observed that *Tet3* is highly upregulated during neuronal differentiation and essential to maintain the silencing of pluripotency-associated genes. In opposition, *Tet1* is downregulated during this process. Moreover, *Tet3* KD leads to a genome-scale loss of DNA methylation and hypermethylation of a smaller number of CpGs that are, notably, located at neurogenesis-related genes and at imprinting control regions (ICRs) of imprinted genes.

In chapter III we described that TET3 is present in mature neurons and oligodendrocytes, but is absent in astrocytes. Additionally, we were able to establish and validate a mouse model for forebrain conditional deletion of *Tet3* enzyme in mature neurons. In chapters III and IV we have shown that *Tet3* deletion in post-mitotic neurons increases anxiety-like behavior and impairs the spatial orientation, in both genders. Specifically, in Tet3 cKO males, we demonstrated increased anxiety-like behavior with concomitant increased corticosterone basal levels, and dysregulation of genes involved in glucocorticoid signaling pathway (HPA axis) in the ventral hippocampus. In both genders, Tet3 deletion increased the expression of immediate-early genes in the dorsal/ventral hippocampus. Specifically, in Tet3 cKO females, we found an impairment in their short-term memory.

In the sections below, we discuss how we addressed methodologically the two main aims of this thesis, and we explore new perspectives that our work has opened.

5.1. Aim 1. To investigate the effects of TET3 enzyme knockdown in NPCs, using an *in vitro* differentiation system from ES cells into NPCs

5.1.1. Technical aspects

To better understand the role of *Tet3* in neuronal differentiation, we studied the impact of *Tet3* KD using an *in vitro* culture system. We took advantage of the high proliferative capacity of mouse ESCs, which are pluripotent and able to generate an unlimited number of any cell type. Additionally, ESCs can be isolated from wild-type or mutant mice, allowing to compare disease contexts implicated in alterations of specific cell types related with CNS disorders. In appropriate conditions, ESCs can be differentiated into neurons, and it is possible to isolate cells at different stages of differentiation, allowing to characterize, for instance, neuronal precursors (Bibel et al., 2004a).

The main limitation in using ESCs to generate neurons is cellular heterogeneity; typically neuronal cultures derived from ESCs contain not only neurons but also non-neural cells, namely glial cells (Rathjen and Rathjen, 2001; Stavridis and Smith, 2003). In the present work, the *in vitro* differentiation system consisted of highly proliferative ES cells (A2lox.cre) (Iacovino et al., 2011a) that were differentiated into a homogeneous population of NPCs which are PAX6-positive radial glial cells. Furthermore, these neuronal precursors can give rise to a homogeneous population of cells that form functional synaptic connections neurons, which are biochemical and functionally characteristic of the cerebral cortex (Bibel et al., 2004a). Our protocol results in more than 90% of the differentiated cells staining positively for PAX6, indicating homogeneous differentiation of ES cells into NPCs, accordingly with the values in the original protocol description (Bibel et al., 2004a).

The knockdown of *Tet* enzymes was facilitated by the use of an inducible cassette exchange (ICE) system, which allows high-efficiency integration of genes of interest into cells bearing a single-copy ICE locus (Iacovino et al., 2011b). This system can be used in any cellular model system; it does not require co-transfection of a Cre-expressing plasmid, and all cells express Cre at the same level prior to recombination. Importantly, the recombination is fast (time frame of days), which is particularly relevant in cells of limited lifespan, or cells in which high passage numbers are undesirable, such as ESCs (Iacovino et al., 2011a). Regarding the knockdown efficiency, at the mRNA level, a decrease of around 50% of *Tet3* transcripts was found for both shRNAs; however at the protein level the deletion was less pronunciated; around 10% and 30% of decrease to Tet3-1 and Tet3-2 shRNAs, respectively. This led us to perform the oxRRBS analysis only with the Tet3-2 shRNA.

5.1.2. Integration of the main results

Previously, all TET enzymes were implicated in adult neurogenesis and NSCs/NPCs pool maintenance (Gontier et al., 2018; Montalban-Loro et al., 2019; Zhang et al., 2013). The *in vivo* relevance of TET1 and

TET2 was similarly addressed in NPCs using the Nestin-Cre promoter. Indeed the single deletion of each TET results in a decrease of around 50% in the NSCs pool from the SGZ. Importantly, this consequently affects the neuronal differentiation process, since the deletion of TET1 or TET2 resulted in a reduction of newborn and mature neurons (Gontier et al., 2018; Zhang et al., 2013). Regarding TET3, the NSCs were targeted using GFAP-Cre promoter and the SVZ region was studied; *Tet3* deletion resulted in a decrease of around 50% in the NSCs pool. Globally, all these works showed that each TET enzyme is crucial to maintain the NSC/NPC pool and to regulate the neurogenic process. Moreover, the functions of TET enzymes do not seem to overlap, since the single deletion of any TET produces significant effects.

Li and colleagues addressed the relevance of *Tet3 in vitro*, revealing upregulation of this dioxygenase upon neural differentiation, and that *Tet3* deletion in NPCs did not result in decreased expression of NPCs markers, such as Pax6 and Nestin (Li et al., 2015a). Our findings are in agreement with both findings. Notably, our work added new perspectives to the molecular mechanisms regulating NPCs maintenance by *Tet3*. Interestingly, *Tet3* knockdown led to a de-repression of pluripotency-associated genes such as *Oct4*, *Nanog* or *Tcl1*, with concomitant hypomethylation. Remarkably, *Tet3* KD led to a genome-scale loss of DNA methylation and hypermethylation of a smaller number of CpGs that are located at neurogenesis-related genes and at imprinting control regions (ICRs). Previously, also *Tet1 and Tet2* were identified as essential enzymes to regulate the expression of many imprinting genes (Dawlaty et al., 2013b; Piccolo et al., 2013).

Importantly, studies have been suggesting that selective regulation of imprinting is a normal mechanism of modulating gene dosage and is related with the control of stem cell potential in the neurogenic niche (Montalbán-Loro et al., 2015). Thus, *Tet3* enzyme can be contributing to the transcriptional regulation of the genes. Interestingly, a recent study showed that TET3 binds directly to the paternal transcribed allele of the imprinted gene *Snrpn*, contributing to transcriptional repression of this gene. When TET3 was ablated in NSCs resulted in increased expression of *Snrpn* (Montalbán-Loro et al., 2019). Notably, we found the same effect in the expression of this imprinted gene in Tet3 KD NPCs.

In conclusion, our findings suggest that TET3 acts as a regulator of neural cell identity by sustaining DNA methylation levels in NPCs. Based on the data that we and others have obtained, we created a model for the loss of DNA methylation and de-repression of pluripotency genes (**Figure 1**). This would involve co-operation between TET3 and DNMT3A, with TET3 marking CpG sites for *de novo* methylation, carried out by DNMT3A. The absence of Tet3 seems to promote hypomethylation of pluripotency genes, such as Tcl1 and Esrrb, and hypermethylation of neuronal genes such as Wnt3a, Dlx2, among others. The final result is a de-repression of pluripotency genes and repression of neuronal genes expression (**Figure 2**).

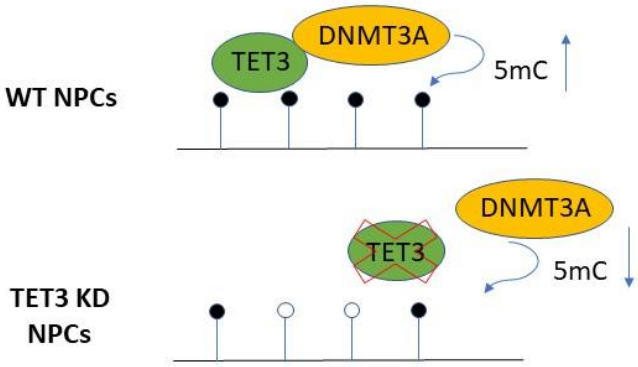

Figure 1 Model for the observed genome-wide loss of methylation, involving co-operation between TET3 and DNMT3A to maintain the methylated state, namely at pluripotency genes.
Black circle – methylated CpG; white circle – unmethylated CpG.

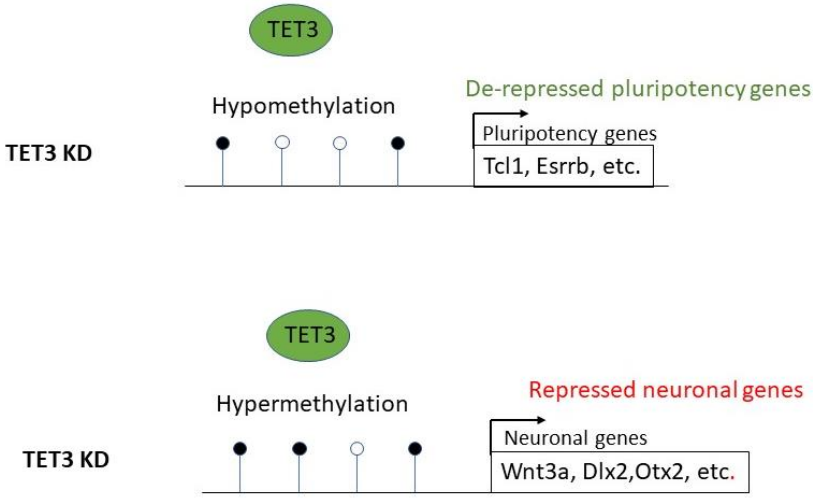

Figure 2 Schematic representation of the putative effect of TET3 deletion in the NPCs.
Black circle – methylated CpG; white circle – unmethylated CpG.

5.2. Aim 2 To establish and characterize the impact of TET3 conditional deletion in post-mitotic neurons, using a conditional knockout mouse model (*Camk2a-CreERT2*)

5.2.1. Technical aspects

The particular enrichment of *Tet3* in the adult brain mice raised the possibility for a putative role of this enzyme in brain function. We and others have seen a strong colocalization of TET3 with post-mitotic neuronal markers (Li et al., 2014), suggesting a relevant function of this enzyme in these cells. Also,

previously, *Tet1* and *Tet2* have been shown as important enzymes regulating brain function (Gontier et al., 2018; Kaas et al., 2013; Kumar et al., 2015; Rudenko et al., 2013; Zhang et al., 2013). Constitutive knockout mouse models for TET1 and TET2 have been used to unravel their functions. Indeed, adult TET1 and TET2 KO mice are viable and fertile, presenting relatively mild behavioral and hematopoietic phenotypes, respectively (Ko et al., 2011; Kumar et al., 2015; Rudenko et al., 2013; Zhang et al., 2013). However, the TET3 KO mice die prematurely at the first stages of postnatal development (Gu et al., 2011b). Therefore, to study TET3 brain function, the use of a conditional approach was mandatory. Taking into account the high neuronal level of *Tet3* expression in forebrain regions, and the consequent assumption of a potential relevant role of this enzyme in brain function, we decided to use a selective deletion in post-mitotic neurons via the *Camk2a* promoter. The strategy was to cross Tet3 floxed mice with *Camk2a-CreERT2* animals, allowing to restrict the observed phenotypic alterations to the effect of *Tet3* ablation in postmitotic neurons in forebrain regions (Achterberg et al., 2014).

Regarding the limitations of this model, the characterization subsequent analyses could be facilitated by the use of a more sophisticated mouse model, in which a reporter gene such as, GFP Tomato or others, could be expressed concomitantly with *Camk2a* to confirm Cre activity. This would allow to identify the recombinant post-mitotic neurons with knockout of the *Tet3* gene. In this context, and to overcome this limitation, we were only able to perform double-staining immunofluorescence analysis for NeuN and TET3, counting the number of NeuN positive cells that underwent deletion of TET3.

In this study, we focused on young adult mice. It is relatively plausible to assume that recombination varies with aging. And indeed, it has been proposed that tamoxifen induces recombination more efficiently in younger mice (Feil et al., 2009). Regarding the magnitude of this deletion, Tet3 cKO animals showed a decrease of *Tet3* mRNA levels lower than 40% in almost all forebrain regions analyzed. This likely reflects that not all post-mitotic neurons were targeted by *Tet3* deletion, as it would be expected, but also that forebrain macrodissections contain non-post mitotic neurons cells expressing *Tet3*. Indeed, TET3 protein quantification by immunofluorescence in the hippocampus of Tet3 cKO animals corroborated this possibility, since the hippocampus presented a deletion of around 60%. Importantly, when comparing the mRNA deletion levels in males and females no differences were found, facilitating drawing conclusions related to sex-specific differences.

Importantly, the inclusion of both sexes constitutes a valuable tool to consider the potential differences between genders. During the last decades, behavioral research has been mainly focused on males, ruling out the possibility of the discovery of important biological differences between males and females.

5.2.2. Integration of the main results

Since 2011, studies have shown the importance of all TET enzymes in neuronal and brain function. Indeed, TET1 was implicated in a wide range of specific behaviors, such as spatial and fear learning, short-term and object location memories (Kaas et al., 2013; Kumar et al., 2015; Zhang et al., 2013). TET2 was shown as a key player in regulating short and long-term spatial learning, as well as memory processes (Gontier et al., 2018). TET3 was identified as a key enzyme to regulate fear extinction memory (Li et al., 2014). However, TET3 role in learning processes and short/long-term memories remained to be determined. Contrarily to TET1 and TET2, which were implicated in the spatial learning of rodents (Gontier et al., 2018; Zhang et al., 2013) our results support that TET3 is not implicated in this process, but seems to be critical to control spatial orientation. Also, neither TET1 or TET2 were implicated in short-term memory, our work being the first to show evidence for TET3 implication in this type of memory. Importantly, our work was the first to address the role of *Tet3* in the modulation of anxiety-like behavior. Apart from our work, only Feng and colleagues reported the role of *Tet1* in this type of behavior (Feng et al., 2017).

Although overall we did not find ample differences in females and males, it is becoming progressively evident that the influence of sex on neuronal function is as significant as the effects of any other important factor. This leads to a need to be careful when a broad view is taken on one sex for the other. There are notorious sex differences in gene expression in the brain of rodents, that are probably required for sex-specific functions, and that may depend on sex-specfic DNA methylation/demethylation (Mosley et al., 2017; Nugent et al., 2015). Moreover, a recent work showed that TET enzymes are differentially expressed in males and females at neonatal period, although no differences were found at the adult stage (Cisternas et al., 2019).

Importantly, our work was the first addressing the role of one TET enzyme in both sexes. Our study, in summary, showed that the main behavior findings were present in both genders, with the exception of a specific impairment of short-term memory in females. The mismatch between Tet3 cKO males and females in this type of memory is striking. However, as discussed in chapter IV, it probably reflects that Tet3 can have a differential role according to the gender, namely in the PFC, since this brain region is particularly important in the control of short-term memory. In the future, it should be interesting to compare the morphology of neurons in the PFC of Tet3 cKO males and females.

At the molecular level, since we did not have the opportunity to perform the RNA-seq analyses in females, this task should be addressed to add more relevant information about the molecular differences between

Tet3 cKO and control females. This should be performed in the hippocampus and also in the PCF, taking in consideration the short-term memory impairment observed specifically in female mice.

In males, we found a clear impact in the ventral hippocampus, specifically an increase in spine maturation and altered expression of mRNA transcripts involved, for instance, in the corticosterone pathway (HPA axis), correlated with the elevated corticosterone levels. Indeed, the ventral hippocampus appears to be involved in anxiety processing, which involves alterations in the HPA axis control (Herman et al., 1995). Given the modifications observed in the ventral hippocampus, it would be relevant to evaluate if the stress response in Tet3 cKO mice is impaired upon stress exposure, submitting the animals to a chronic stress protocol.

The altered expression of some transcripts, relevant for HPA axis function, namely the *Chr2* receptor, which was found downregulated in Tet3 cKO males, arises the possibility of altered methylation patterns at the promoter region of this gene. Thus, it will be interesting to assess their methylation levels, which can be increased by the lack of Tet3 demethylation activity, resulting in decreased expression. In opposition, the IEGs genes were found upregulated which can indicate that these genes could be presenting a decrease of methylation at the promoter gene region.

In conclusion, our findings suggest that TET3 is a key regulator of anxiety-like behavior, spatial orientation and neuronal activity related genes expression in both genders; it is involved in gene regulation of the HPA axis of males and short-term memory of females mice (**Figure 3**).

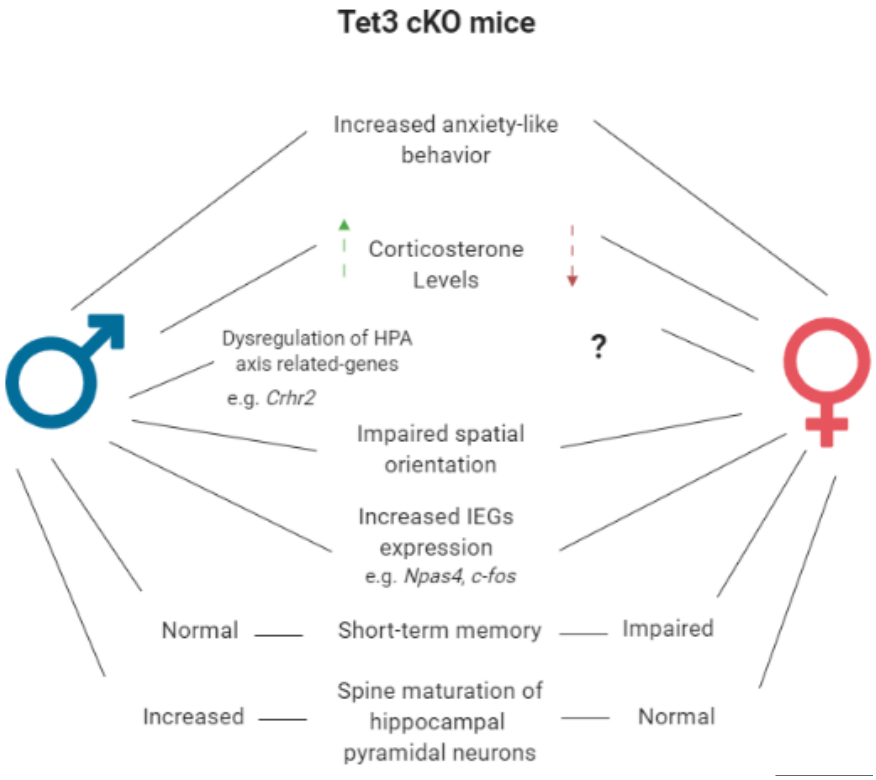

Figure 3 Schematic representation of the effect of Tet3 deletion in males and females mice.

CONCLUSIONS AND FUTURE PERSPECTIVES

Since all three TET enzymes are present in the mammalian brain and share the capacity of oxidizing 5mC into 5hmC, an intermediate in the DNA demethylation process, it was predicted that their functions may be mostly redundant. However, recent publications describing different effects of each TET knockout or knockdown in the brain, have stirred the debate. As we have realized from the present wok, loss of TET3 produced singular findings in both neural precursor cells and post-mitotic neurons, suggesting non-redundant functions for TET3 and its family of enzymes, in the analysed parameters. Globally, this work proposes that TET3 might act as a regulator of neural cell identity by maintaining hypomethylation at neuronal-related genes and by regulating Dnmt3a de novo methylation activities, safeguarding neural precursor cells differentiation programs. Moreover, we concluded that Tet3 is involved in molecular alterations, namely regulation of genes related with corticosterone pathway and neuronal-activity genes, which are putatively regulating hippocampal-dependent functions, namely anxiety-like behavior and spatial orientation. Importantly, we brought new insights for Tet3 function in both sexes, since until now, all studies were only performed in males.

Despite our recent advances, a full understanding of how epigenetic modifications regulate neural differentiation, neuronal physiology and plasticity, as well as cognitive functions, is still a matter of intense investigation. There are still open questions that arise from our data and that warrant further exploration to achieve a better characterization of the influence of TET3 enzyme in both neural and neuronal function:

1. Regarding the role of TET3 during neural differentiation, it is important to address its function *in vivo.* Although this aim was partially addressed before by Montalbán-Loro in the SVZ (Montalbán-Loro et al., 2019); similarly to Zhang et al. and Gontier et al. works, for TET1 and TET2 enzymes respectively (Gontier et al., 2018; Zhang et al., 2013), the targeting of SGZ NPCs through the use of a conditional *Nestin*-CreER^{T2} mouse line crossed with a TET3 floxed mouse should be addressed in the future.

2. Also given the already known role of TET enzymes and 5mC/5hmC modifications in the regulation of adult neurogenesis, the epigenetic manipulation of this process using CRISPR/Cas-based approaches, can be a feasible plan. Indeed, our results suggested that TET3 plays a role in neurogenesis by maintaining hypomethylation of neuronal genes, such as, Wnt3a, Dlx2, Otx2 and Rac3. These genes can constitute a potential target in the use of a precise editing CpG methylation

system, namely dCas9-Tet1 and Dnmt3a for targeted erasure and establishment of DNA methylation, respectively. This technology can be applied in brain disorders associated with neurogenesis impairment, such as depression, addiction and age-related cognitive decline.

3. Regarding the role of TET3 in neuronal function, it will be particularly relevant in the Tet3 cKO model, to evaluate synaptic plasticity through the use of electrophysiological recordings. Since the behavior tests and molecular alterations suggested alterations along the dorsal–ventral axis, and CA1 is a key region in the hippocampal function, long-term potentiation (LTP) and long-term depression (LTD) should be tested in the dorsal and ventral CA1.

4. Additionally, it will be important to address the role of TET3 in disease context, through the knockout or knockdown of TET3 enzyme in the brain of specific models of diseases affecting the CNS. This will allow to investigate the possible contribution of this epigenetic player in disease onset, progression or even possible therapeutics. The biggest challenge will be to modulate brain cognitive processes related to depression, anxiety, among others, in order to accomplish the production of new chemical compounds that could target epigenetic pathways involved in brain dysfunction. Given our work, and the potential role of Tet3 on anxiety-related disorders, a model mimetizing anxiety or depression-like behavior should be an exciting possibility.

References

Achterberg, K.G., Buitendijk, G.H.S., Kool, M.J., Goorden, S.M.I., Post, L., Slump, D.E., Silva, A.J., van Woerden, G.M., Kushner, S.A., and Elgersma, Y. (2014). Temporal and Region-Specific Requirements of αCaMKII in Spatial and Contextual Learning. The Journal of Neuroscience *34*, 11180-11187.

Akalin, A., Kormaksson, M., Li, S., Garrett-Bakelman, F.E., Figueroa, M.E., Melnick, A., and Mason, C.E. (2012). methylKit: a comprehensive R package for the analysis of genome-wide DNA methylation profiles. Genome biology *13*, R87.

Amir, R.E., Van den Veyver, I.B., Wan, M., Tran, C.Q., Francke, U., and Zoghbi, H.Y. (1999). Rett syndrome is caused by mutations in X-linked MECP2, encoding methyl-CpG-binding protein 2. Nature genetics *23*, 185-188.

Amouroux, R., Nashun, B., Shirane, K., Nakagawa, S., Hill, P.W., D'Souza, Z., Nakayama, M., Matsuda, M., Turp, A., Ndjetehe, E.*, et al.* (2016). De novo DNA methylation drives 5hmC accumulation in mouse zygotes. Nature Cell Biology *18*, 225-233.

Antunes, C., Sousa, N., Pinto, L., and Marques, C.J. (2019). TET enzymes in neurophysiology and brain function. Neuroscience and biobehavioral reviews *102*, 337-344.

Bannerman, D.M., Sprengel, R., Sanderson, D.J., McHugh, S.B., Rawlins, J.N., Monyer, H., and Seeburg, P.H. (2014). Hippocampal synaptic plasticity, spatial memory and anxiety. Nature reviews Neuroscience *15*, 181-192.

Becker, N., Wierenga, C.J., Fonseca, R., Bonhoeffer, T., and Nagerl, U.V. (2008). LTD induction causes morphological changes of presynaptic boutons and reduces their contacts with spines. Neuron *60*, 590-597.

Bibel, M., Richter, J., Lacroix, E., and Barde, Y.-A. (2007). Generation of a defined and uniform population of CNS progenitors and neurons from mouse embryonic stem cells. Nature Protocols *2*, 1034-1043.

Bibel, M., Richter, J., Schrenk, K., Tucker, K.L., Staiger, V., Korte, M., Goetz, M., and Barde, Y.-A. (2004a). Differentiation of mouse embryonic stem cells into a defined neuronal lineage. Nature neuroscience *7*, 1003.

Bibel, M., Richter, J., Schrenk, K., Tucker, K.L., Staiger, V., Korte, M., Goetz, M., and Barde, Y.A. (2004b). Differentiation of mouse embryonic stem cells into a defined neuronal lineage. Nature neuroscience *7*, 1003-1009.

Bird, A. (2002). DNA methylation patterns and epigenetic memory. Genes & development *16*, 6-21.

Bird, A. (2007). Perceptions of epigenetics. Nature *447*, 396-398.

Blasco-Serra, A., Gonzalez-Soler, E.M., Cervera-Ferri, A., Teruel-Marti, V., and Valverde-Navarro, A.A. (2017). A standardization of the Novelty-Suppressed Feeding Test protocol in rats. Neuroscience letters *658*, 73-78.

Bliss, T. (2007). The hippocampus book (New York, NY, US: Oxford University Press).

Bock, C., Reither, S., Mikeska, T., Paulsen, M., Walter, J., and Lengauer, T. (2005). BiQ Analyzer: visualization and quality control for DNA methylation data from bisulfite sequencing. Bioinformatics *21*, 4067-4068.

Bond, A.M., Ming, G.L., and Song, H. (2015). Adult Mammalian Neural Stem Cells and Neurogenesis: Five Decades Later. Cell stem cell *17*, 385-395.

Booth, M.J., Branco, M.R., Ficz, G., Oxley, D., Krueger, F., Reik, W., and Balasubramanian, S. (2012). Quantitative sequencing of 5-methylcytosine and 5-hydroxymethylcytosine at single-base resolution. Science *336*, 934-937.

Booth, M.J., Ost, T.W., Beraldi, D., Bell, N.M., Branco, M.R., Reik, W., and Balasubramanian, S. (2013). Oxidative bisulfite sequencing of 5-methylcytosine and 5-hydroxymethylcytosine. Nature protocols *8*, 1841-1851.

Borrell, V., Cardenas, A., Ciceri, G., Galceran, J., Flames, N., Pla, R., Nobrega-Pereira, S., Garcia-Frigola, C., Peregrin, S., Zhao, Z.*, et al.* (2012). Slit/Robo signaling modulates the proliferation of central nervous system progenitors. Neuron *76*, 338-352.

Bourin, M., and Hascoet, M. (2003). The mouse light/dark box test. European journal of pharmacology *463*, 55-65.

Bourin, M., Petit-Demouliere, B., Dhonnchadha, B.N., and Hascoet, M. (2007). Animal models of anxiety in mice. Fundamental & clinical pharmacology *21*, 567-574.

Broadbent, N.J., Squire, L.R., and Clark, R.E. (2004). Spatial memory, recognition memory, and the hippocampus. Proceedings National Acaddemy Sciences U S A *101*, 14515-14520.

Buiting, K. (2010). Prader-Willi syndrome and Angelman syndrome. American journal of medical genetics Part C, Seminars in medical genetics *154c*, 365-376.

Butler, M.G. (2011). Prader-Willi Syndrome: Obesity due to Genomic Imprinting. Current genomics *12*, 204-215.

Can, A., Dao, D.T., Terrillion, C.E., Piantadosi, S.C., Bhat, S., and Gould, T.D. (2012). The tail suspension test. Journal of visualized experiments : JoVE, e3769-e3769.

Chahrour, M., Jung, S.Y., Shaw, C., Zhou, X., Wong, S.T., Qin, J., and Zoghbi, H.Y. (2008). MeCP2, a key contributor to neurological disease, activates and represses transcription. Science *320*, 1224-1229.

Chen, H., Dzitoyeva, S., and Manev, H. (2012). Effect of aging on 5-hydroxymethylcytosine in the mouse hippocampus. Restorative neurology and neuroscience *30*, 237-245.

Chew, J.L., Loh, Y.H., Zhang, W., Chen, X., Tam, W.L., Yeap, L.S., Li, P., Ang, Y.S., Lim, B., Robson, P.*, et al.* (2005). Reciprocal transcriptional regulation of Pou5f1 and Sox2 via the Oct4/Sox2 complex in embryonic stem cells. Molecular Cell Biology *25*, 6031-6046.

Chourbaji, S., Zacher, C., Sanchis-Segura, C., Dormann, C., Vollmayr, B., and Gass, P. (2005). Learned helplessness: validity and reliability of depressive-like states in mice. Brain research Brain research protocols *16*, 70-78.

Ciocchi, S., Passecker, J., Malagon-Vina, H., Mikus, N., and Klausberger, T. (2015). Brain computation. Selective information routing by ventral hippocampal CA1 projection neurons. Science *348*, 560-563.

Cisternas, C.D., Cortes, L.R., Bruggeman, E.C., Yao, B., and Forger, N.G. (2019). Developmental changes and sex differences in DNA methylation and demethylation in hypothalamic regions of the mouse brain. Epigenetics, 1-13.

Clem, R.L., and Huganir, R.L. (2010). Calcium-permeable AMPA receptor dynamics mediate fear memory erasure. Science *330*, 1108-1112.

Cohen, S.J., and Stackman, R.W., Jr. (2015). Assessing rodent hippocampal involvement in the novel object recognition task. A review. Behavioural brain research *285*, 105-117.

Costa, Y., Ding, J., Theunissen, T.W., Faiola, F., Hore, T.A., Shliaha, P.V., Fidalgo, M., Saunders, A., Lawrence, M., Dietmann, S.*, et al.* (2013). NANOG-dependent function of TET1 and TET2 in establishment of pluripotency. Nature *495*, 370-374.

Coutellier, L., Beraki, S., Ardestani, P.M., Saw, N.L., and Shamloo, M. (2012). Npas4: a neuronal transcription factor with a key role in social and cognitive functions relevant to developmental disorders. PLoS One *7*, e46604.

D'Hooge, R., and De Deyn, P.P. (2001). Applications of the Morris water maze in the study of learning and memory. Brain research Brain research reviews *36*, 60-90.

Dalton, G.L., Wang, Y.T., Floresco, S.B., and Phillips, A.G. (2008). Disruption of AMPA receptor endocytosis impairs the extinction, but not acquisition of learned fear. Neuropsychopharmacology : official publication of the American College of Neuropsychopharmacology *33*, 2416-2426.

David, M.D., Canti, C., and Herreros, J. (2010). Wnt-3a and Wnt-3 differently stimulate proliferation and neurogenesis of spinal neural precursors and promote neurite outgrowth by canonical signaling. Journal of neuroscience research *88*, 3011-3023.

Dawlaty, M.M., Breiling, A., Le, T., Raddatz, G., Barrasa, M.I., Cheng, A.W., Gao, Q., Powell, B.E., Li, Z., Xu, M.*, et al.* (2013a). Combined Deficiency of Tet1 and Tet2 Causes Epigenetic Abnormalities but Is Compatible with Postnatal Development. Developmental Cell, 1-14.

Dawlaty, M.M., Breiling, A., Le, T., Raddatz, G., Barrasa, M.I., Cheng, A.W., Gao, Q., Powell, B.E., Li, Z., Xu, M.*, et al.* (2013b). Combined deficiency of Tet1 and Tet2 causes epigenetic abnormalities but is compatible with postnatal development. Developmental cell *24*, 310-323.

Dawlaty, M.M., Ganz, K., Powell, B.E., Hu, Y.C., Markoulaki, S., Cheng, A.W., Gao, Q., Kim, J., Choi, S.W., Page, D.C.*, et al.* (2011). Tet1 is dispensable for maintaining pluripotency and its loss is compatible with embryonic and postnatal development. Cell stem cell *9*, 166-175.

de Melo, J., Du, G., Fonseca, M., Gillespie, L.A., Turk, W.J., Rubenstein, J.L., and Eisenstat, D.D. (2005). Dlx1 and Dlx2 function is necessary for terminal differentiation and survival of late-born retinal ganglion cells in the developing mouse retina. Development *132*, 311-322.

Deaton, A.M., and Bird, A. (2011). CpG islands and the regulation of transcription. Genes & development *25*, 1010-1022.

Deng, W., Aimone, J.B., and Gage, F.H. (2010). New neurons and new memories: how does adult hippocampal neurogenesis affect learning and memory? Nature reviews Neuroscience *11*, 339-350.

Derecki, N.C., Cronk, J.C., Lu, Z., Xu, E., Abbott, S.B.G., Guyenet, P.G., and Kipnis, J. (2012). Wild-type microglia arrest pathology in a mouse model of Rett syndrome. Nature *484*, 105.

Di Giovannantonio, L.G., Di Salvio, M., Acampora, D., Prakash, N., Wurst, W., and Simeone, A. (2013). Otx2 selectively controls the neurogenesis of specific neuronal subtypes of the ventral tegmental area and compensates En1-dependent neuronal loss and MPTP vulnerability. Development Biology *373*, 176-183.

Diaz de Leon-Guerrero, S., Pedraza-Alva, G., and Perez-Martinez, L. (2011). In sickness and in health: the role of methyl-CpG binding protein 2 in the central nervous system. Eurpean Journal of Neuroscience *33*, 1563-1574.

Dupret, D., Revest, J.M., Koehl, M., Ichas, F., De Giorgi, F., Costet, P., Abrous, D.N., and Piazza, P.V. (2008). Spatial relational memory requires hippocampal adult neurogenesis. PLoS One *3*, e1959.

Ehrlich, M., Gama-Sosa, M.A., Huang, L.H., Midgett, R.M., Kuo, K.C., McCune, R.A., and Gehrke, C. (1982). Amount and distribution of 5-methylcytosine in human DNA from different types of tissues of cells. Nucleic acids research *10*, 2709-2721.

Eichenbaum, H. (2004). Hippocampus: cognitive processes and neural representations that underlie declarative memory. Neuron *44*, 109-120.

Fanselow, M.S., and Dong, H.-W. (2010). Are the dorsal and ventral hippocampus functionally distinct structures? Neuron *65*, 7-19.

Feil, S., Valtcheva, N., and Feil, R. (2009). Inducible Cre mice. Methods in molecular biology (Clifton, NJ) *530*, 343-363.

Feng, J., Chang, H., Li, E., and Fan, G. (2005). Dynamic expression of de novo DNA methyltransferases Dnmt3a and Dnmt3b in the central nervous system. Journal of neuroscience research *79*, 734-746.

Feng, J., Pena, C.J., Purushothaman, I., Engmann, O., Walker, D., Brown, A.N., Issler, O., Doyle, M., Harrigan, E., Mouzon, E.*, et al.* (2017). Tet1 in Nucleus Accumbens Opposes Depression- and Anxiety-Like Behaviors. Neuropsychopharmacology : official publication of the American College of Neuropsychopharmacology *42*, 1657-1669.

Feng, J., Zhou, Y., Campbell, S.L., Le, T., Li, E., Sweatt, J.D., Silva, A.J., and Fan, G. (2010). Dnmt1 and Dnmt3a maintain DNA methylation and regulate synaptic function in adult forebrain neurons. Nature neuroscience *13*, 423-430.

Ficz, G., Branco, M.R., Seisenberger, S., Santos, F., Krueger, F., Hore, T.A., Marques, C.J., Andrews, S., and Reik, W. (2011). Dynamic regulation of 5-hydroxymethylcytosine in mouse ES cells and during differentiation. Nature *473*, 398-402.

Frommer, M., McDonald, L.E., Millar, D.S., Collis, C.M., Watt, F., Grigg, G.W., Molloy, P.L., and Paul, C.L. (1992). A genomic sequencing protocol that yields a positive display of 5-methylcytosine residues in individual DNA strands. Proceedings Natinall Academy Sciences U S A *89*, 1827-1831.

Fu, L., Guerrero, C.R., Zhong, N., Amato, N.J., Liu, Y., Liu, S., Cai, Q., Ji, D., Jin, S.G., Niedernhofer, L.J., *et al.* (2014). Tet-mediated formation of 5-hydroxymethylcytosine in RNA. Journal of the American Chemical Society *136*, 11582-11585.

Gage, F.H. (2000). Mammalian neural stem cells. Science *287*, 1433-1438.

Goldberg, A.D., Allis, C.D., and Bernstein, E. (2007). Epigenetics: a landscape takes shape. Cell *128*, 635-638.

Gontier, G., Iyer, M., Shea, J.M., Bieri, G., Wheatley, E.G., Ramalho-Santos, M., and Villeda, S.A. (2018). Tet2 Rescues Age-Related Regenerative Decline and Enhances Cognitive Function in the Adult Mouse Brain. Cell reports *22*, 1974-1981.

Goto, K., Numata, M., Komura, J.I., Ono, T., Bestor, T.H., and Kondo, H. (1994). Expression of DNA methyltransferase gene in mature and immature neurons as well as proliferating cells in mice. Differentiation; research in biological diversity *56*, 39-44.

Gu, H., Smith, Z.D., Bock, C., Boyle, P., Gnirke, A., and Meissner, A. (2011a). Preparation of reduced representation bisulfite sequencing libraries for genome-scale DNA methylation profiling. Nature Protocols *6*, 468-481.

Gu, T., Lin, X., Cullen, S.M., Luo, M., Jeong, M., Estecio, M., Shen, J., Hardikar, S., Sun, D., Su, J., *et al.* (2018). DNMT3A and TET1 cooperate to regulate promoter epigenetic landscapes in mouse embryonic stem cells. Genome biology *19*, 88.

Gu, T.P., Guo, F., Yang, H., Wu, H.P., Xu, G.F., Liu, W., Xie, Z.G., Shi, L., He, X., Jin, S.G., *et al.* (2011b). The role of Tet3 DNA dioxygenase in epigenetic reprogramming by oocytes. Nature *477*, 606-610.

Guo, J.U., Ma, D.K., Mo, H., Ball, M.P., Jang, M.H., Bonaguidi, M.A., Balazer, J.A., Eaves, H.L., Xie, B., Ford, E., *et al.* (2011a). Neuronal activity modifies the DNA methylation landscape in the adult brain. Nature neuroscience *14*, 1345-1351.

Guo, J.U., Su, Y., Shin, J.H., Shin, J., Li, H., Xie, B., Zhong, C., Hu, S., Le, T., Fan, G., *et al.* (2014a). Distribution, recognition and regulation of non-CpG methylation in the adult mammalian brain. Nature neuroscience *17*, 215-222.

Guo, J.U., Su, Y., Zhong, C., Ming, G.L., and Song, H. (2011b). Hydroxylation of 5-methylcytosine by TET1 promotes active DNA demethylation in the adult brain. Cell *145*, 423-434.

Guo, J.U., Szulwach, K.E., Su, Y., Li, Y., Yao, B., Xu, Z., Shin, J.H., Xie, B., Gao, Y., Ming, G.L., *et al.* (2014b). Genome-wide antagonism between 5-hydroxymethylcytosine and DNA methylation in the adult mouse brain. Frontiers in Biology (Beijing) *9*, 66-74.

Guy, J., Cheval, H., Selfridge, J., and Bird, A. (2011). The role of MeCP2 in the brain. Annual review of cell and developmental biology *27*, 631-652.

Hackett, J.A., Sengupta, R., Zylicz, J.J., Murakami, K., Lee, C., Down, T.A., and Surani, M.A. (2013). Germline DNA demethylation dynamics and imprint erasure through 5-hydroxymethylcytosine. Science *339*, 448-452.

Hahn, M.A., Qiu, R., Wu, X., Li, A.X., Zhang, H., Wang, J., Jui, J., Jin, S.G., Jiang, Y., Pfeifer, G.P., *et al.* (2013). Dynamics of 5-hydroxymethylcytosine and chromatin marks in Mammalian neurogenesis. Cell reports *3*, 291-300.

Hajkova, P., Erhardt, S., Lane, N., Haaf, T., El-Maarri, O., Reik, W., Walter, J., and Surani, M.A. (2002). Epigenetic reprogramming in mouse primordial germ cells. Mechanisms of development *117*, 15-23.

Hendrich, B., and Bird, A. (1998). Identification and characterization of a family of mammalian methyl-CpG binding proteins. Molecular and cellular biology *18*, 6538-6547.

Herman, J.P., Adams, D., and Prewitt, C. (1995). Regulatory changes in neuroendocrine stress-integrative circuitry produced by a variable stress paradigm. Neuroendocrinology *61*, 180-190.

Herman, J.P., and Cullinan, W.E. (1997). Neurocircuitry of stress: central control of the hypothalamo-pituitary-adrenocortical axis. Trends in neurosciences *20*, 78-84.

Hill, P.W.S., Leitch, H.G., Requena, C.E., Sun, Z., Amouroux, R., Roman-Trufero, M., Borkowska, M., Terragni, J., Vaisvila, R., Linnett, S., *et al.* (2018). Epigenetic reprogramming enables the transition from primordial germ cell to gonocyte. Nature *555*, 392-396.

Horgusluoglu, E., Nudelman, K., Nho, K., and Saykin, A.J. (2017). Adult neurogenesis and neurodegenerative diseases: A systems biology perspective. American journal of medical genetics Part B, Neuropsychiatric genetics : the official publication of the International Society of Psychiatric Genetics *174*, 93-112.

Huang, Y., Chavez, L., Chang, X., Wang, X., Pastor, W.A., Kang, J., Zepeda-Martinez, J.A., Pape, U.J., Jacobsen, S.E., Peters, B., *et al.* (2014). Distinct roles of the methylcytosine oxidases Tet1 and Tet2 in mouse embryonic stem cells. Proceedings National Academy Sciences U S A *111*, 1361-1366.

Huang, Y., Pastor, W.A., Shen, Y., Tahiliani, M., Liu, D.R., and Rao, A. (2010). The behaviour of 5-hydroxymethylcytosine in bisulfite sequencing. PLoS One *5*, e8888.

Iacovino, M., Bosnakovski, D., Fey, H., Rux, D., Bajwa, G., Mahen, E., Mitanoska, A., Xu, Z., and Kyba, M. (2011a). Inducible cassette exchange: a rapid and efficient system enabling conditional gene expression in embryonic stem and primary cells. Stem cells (Dayton, Ohio) *29*, 1580-1588.

Iacovino, M., Bosnakovski, D., Fey, H., Rux, D., Bajwa, G., Mahen, E., Mitanoska, A., Xu, Z., and Kyba, M. (2011b). Inducible cassette exchange: a rapid and efficient system enabling conditional gene expression in embryonic stem and primary cells. Stem cells (Dayton, Ohio) *29*, 1580-1588.

Illingworth, R.S., Gruenewald-Schneider, U., Webb, S., Kerr, A.R., James, K.D., Turner, D.J., Smith, C., Harrison, D.J., Andrews, R., and Bird, A.P. (2010). Orphan CpG islands identify numerous conserved promoters in the mammalian genome. PLoS Genet *6*, e1001134.

Iqbal, K., Jin, S.G., Pfeifer, G.P., and Szabo, P.E. (2011). Reprogramming of the paternal genome upon fertilization involves genome-wide oxidation of 5-methylcytosine. Proceedings of the National Academy of Sciences of the United States of America *108*, 3642-3647.

Ito, S., D'Alessio, A.C., Taranova, O.V., Hong, K., Sowers, L.C., and Zhang, Y. (2010). Role of Tet proteins in 5mC to 5hmC conversion, ES-cell self-renewal and inner cell mass specification. Nature *466*, 1129-1133.

Ito, S., Shen, L., Dai, Q., Wu, S.C., Collins, L.B., Swenberg, J.A., He, C., and Zhang, Y. (2011). Tet proteins can convert 5-methylcytosine to 5-formylcytosine and 5-carboxylcytosine. Science *333*, 1300-1303.

Jin, S.G., Zhang, Z.M., Dunwell, T.L., Harter, M.R., Wu, X., Johnson, J., Li, Z., Liu, J., Szabo, P.E., Lu, Q.*, et al.* (2016). Tet3 Reads 5-Carboxylcytosine through Its CXXC Domain and Is a Potential Guardian against Neurodegeneration. Cell reports *14*, 493-505.

Jobe, E.M., and Zhao, X. (2017). DNA Methylation and Adult Neurogenesis. Brain plasticity (Amsterdam, Netherlands) *3*, 5-26.

Kaas, G.A., Zhong, C., Eason, D.E., Ross, D.L., Vachhani, R.V., Ming, G.L., King, J.R., Song, H., and Sweatt, J.D. (2013). TET1 controls CNS 5-methylcytosine hydroxylation, active DNA demethylation, gene transcription, and memory formation. Neuron *79*, 1086-1093.

Kandel E, S.J., Jessell T, Siegelbaum S, Hudspeth AJ (2012). Principles of Neural Science, Fifth Edition. McGraw Hill Professional.

Kempermann, G., Song, H., and Gage, F.H. Neurogenesis in the Adult Hippocampus. Cold Spring Harbor perspectives in biology *7*, a018812-a018812.

Khare, T., Pai, S., Koncevicius, K., Pal, M., Kriukiene, E., Liutkeviciute, Z., Irimia, M., Jia, P., Ptak, C., Xia, M.*, et al.* (2012). 5-hmC in the brain is abundant in synaptic genes and shows differences at the exon-intron boundary. Nature structural & molecular biology *19*, 1037-1043.

Kim, J.I., Lee, H.R., Sim, S.E., Baek, J., Yu, N.K., Choi, J.H., Ko, H.G., Lee, Y.S., Park, S.W., Kwak, C.*, et al.* (2011). PI3Kgamma is required for NMDA receptor-dependent long-term depression and behavioral flexibility. Nature neuroscience *14*, 1447-1454.

Ko, M., An, J., Bandukwala, H.S., Chavez, L., Aijo, T., Pastor, W.A., Segal, M.F., Li, H., Koh, K.P., Lahdesmaki, H.*, et al.* (2013a). Modulation of TET2 expression and 5-methylcytosine oxidation by the CXXC domain protein IDAX. Nature *497*, 122-126.

Ko, M., An, J., Bandukwala, H.S., Chavez, L., Äijö, T., Pastor, W.A., Segal, M.F., Li, H., Koh, K.P., Lähdesmäki, H.*, et al.* (2013b). Modulation of TET2 expression and 5-methylcytosine oxidation by the CXXC domain protein IDAX. Nature *497*, 122-126.

Ko, M., Bandukwala, H.S., An, J., Lamperti, E.D., Thompson, E.C., Hastie, R., Tsangaratou, A., Rajewsky, K., Koralov, S.B., and Rao, A. (2011). Ten-Eleven-Translocation 2 (TET2) negatively regulates homeostasis and differentiation of hematopoietic stem cells in mice. Proceedings National Academy Sciences U S A *108*, 14566-14571.

Koch, C.E., Leinweber, B., Drengberg, B.C., Blaum, C., and Oster, H. (2016). Interaction between circadian rhythms and stress. Neurobiology of Stress *6*, 57-67.

Koh, K.P., Yabuuchi, A., Rao, S., Huang, Y., Cunniff, K., Nardone, J., Laiho, A., Tahiliani, M., Sommer, C.A., Mostoslavsky, G.*, et al.* (2011). Tet1 and Tet2 regulate 5-hydroxymethylcytosine production and cell lineage specification in mouse embryonic stem cells. Cell stem cell *8*, 200-213.

Kohli, R.M., and Zhang, Y. (2013). TET enzymes, TDG and the dynamics of DNA demethylation. Nature *502*, 472-479.

Kremer, E.A., Gaur, N., Lee, M.A., Engmann, O., Bohacek, J., and Mansuy, I.M. (2018). Interplay between TETs and microRNAs in the adult brain for memory formation. Scientific reports *8*, 1678.

Kriaucionis, S., and Heintz, N. (2009). The nuclear DNA base 5-hydroxymethylcytosine is present in Purkinje neurons and the brain. Science *324*, 929-930.

Krueger, F., and Andrews, S.R. (2011). Bismark: a flexible aligner and methylation caller for Bisulfite-Seq applications. Bioinformatics *27*, 1571-1572.

Kumar, D., Aggarwal, M., Kaas, G.A., Lewis, J., Wang, J., Ross, D.L., Zhong, C., Kennedy, A., Song, H., and Sweatt, J.D. (2015). Tet1 Oxidase Regulates Neuronal Gene Transcription, Active DNA Hydroxymethylation, Object Location Memory, and Threat Recognition Memory. Neuroepigenetics *4*, 12-27.

Lang, P.J., and McTeague, L.M. (2009). The anxiety disorder spectrum: fear imagery, physiological reactivity, and differential diagnosis. Anxiety, stress, and coping *22*, 5-25.

LaPlant, Q., Vialou, V., Covington, H.E., 3rd, Dumitriu, D., Feng, J., Warren, B.L., Maze, I., Dietz, D.M., Watts, E.L., Iniguez, S.D.*, et al.* (2010). Dnmt3a regulates emotional behavior and spine plasticity in the nucleus accumbens. Nature neuroscience *13*, 1137-1143.

Lee, J., Duan, W., and Mattson, M.P. (2002). Evidence that brain-derived neurotrophic factor is required for basal neurogenesis and mediates, in part, the enhancement of neurogenesis by dietary restriction in the hippocampus of adult mice. Journal of Neurochemistry *82*, 1367-1375.

Li, T., Yang, D., Li, J., Tang, Y., Yang, J., and Le, W. (2015a). Critical Role of Tet3 in Neural Progenitor Cell Maintenance and Terminal Differentiation. Molecular neurobiology *51*, 142-154.

Li, T., Yang, D., Li, J., Tang, Y., Yang, J., and Le, W. (2015b). Critical role of Tet3 in neural progenitor cell maintenance and terminal differentiation. Molecular Neurobiololy *51*, 142-154.

Li, X., Wei, W., Zhao, Q.Y., Widagdo, J., Baker-Andresen, D., Flavell, C.R., D'Alessio, A., Zhang, Y., and Bredy, T.W. (2014). Neocortical Tet3-mediated accumulation of 5-hydroxymethylcytosine promotes rapid behavioral adaptation. Proceedings National Acadedmy Sciences U S A *111*, 7120-7125.

Li, X., Yao, B., Chen, L., Kang, Y., Li, Y., Cheng, Y., Li, L., Lin, L., Wang, Z., Wang, M.*, et al.* (2017). Ten-eleven translocation 2 interacts with forkhead box O3 and regulates adult neurogenesis. Nature communications *8*, 15903.

Li, Z., Cai, X., Cai, C.L., Wang, J., Zhang, W., Petersen, B.E., Yang, F.C., and Xu, M. (2011). Deletion of Tet2 in mice leads to dysregulated hematopoietic stem cells and subsequent development of myeloid malignancies. Blood *118*, 4509-4518.

Lister, R., Mukamel, E.A., Nery, J.R., Urich, M., Puddifoot, C.A., Johnson, N.D., Lucero, J., Huang, Y., Dwork, A.J., Schultz, M.D., *et al.* (2013). Global epigenomic reconfiguration during mammalian brain development. Science *341*, 4.

Liu, M.-Y., Yin, C.-Y., Zhu, L.-J., Zhu, X.-H., Xu, C., Luo, C.-X., Chen, H., Zhu, D.-Y., and Zhou, Q.-G. (2018). Sucrose preference test for measurement of stress-induced anhedonia in mice. Nature protocols *13*, 1686-1698.

Liu, N., Wang, M., Deng, W., Schmidt, C.S., Qin, W., Leonhardt, H., and Spada, F. (2013a). Intrinsic and extrinsic connections of Tet3 dioxygenase with CXXC zinc finger modules. PLoS One *8*, e62755.

Liu, S., Wang, J., Su, Y., Guerrero, C., Zeng, Y., Mitra, D., Brooks, P.J., Fisher, D.E., Song, H., and Wang, Y. (2013b). Quantitative assessment of Tet-induced oxidation products of 5-methylcytosine in cellular and tissue DNA. Nucleic acids research *41*, 6421-6429.

Liu, S.Q., and Cull-Candy, S.G. (2000). Synaptic activity at calcium-permeable AMPA receptors induces a switch in receptor subtype. Nature *405*, 454-458.

Livak, K.J., and Schmittgen, T.D. (2001). Analysis of relative gene expression data using real-time quantitative PCR and the 2(-Delta Delta C(T)) Method. Methods (San Diego, Calif) *25*, 402-408.

Long, H.K., Blackledge, N.P., and Klose, R.J. (2013). ZF-CxxC domain-containing proteins, CpG islands and the chromatin connection. Biochemical Society transactions *41*, 727-740.

Lopez-Moyado, I.F., Tsagaratou, A., Yuita, H., Seo, H., Delatte, B., Heinz, S., Benner, C., and Rao, A. (2019). Paradoxical association of TET loss of function with genome-wide DNA hypomethylation. Proceedings of the National Academy of Sciences of the United States of America.

Lubin, F.D., Roth, T.L., and Sweatt, J.D. (2008). Epigenetic regulation of BDNF gene transcription in the consolidation of fear memory. The Journal of neuroscience : the official journal of the Society for Neuroscience *28*, 10576-10586.

Lucassen, P.J., Pruessner, J., Sousa, N., Almeida, O.F.X., Van Dam, A.M., Rajkowska, G., Swaab, D.F., and Czéh, B. (2014). Neuropathology of stress. Acta Neuropathol *127*, 109-135.

Ma, D.K., Jang, M.-H., Guo, J.U., Kitabatake, Y., Chang, M.-l., Pow-anpongkul, N., Flavell, R.A., Lu, B., Ming, G.-l., and Song, H. (2009a). Neuronal Activity–Induced Gadd45b Promotes Epigenetic DNA Demethylation and Adult Neurogenesis. Science (New York, NY) *323*, 1074-1077.

Ma, D.K., Jang, M.H., Guo, J.U., Kitabatake, Y., Chang, M.L., Pow-Anpongkul, N., Flavell, R.A., Lu, B., Ming, G.L., and Song, H. (2009b). Neuronal activity-induced Gadd45b promotes epigenetic DNA demethylation and adult neurogenesis. Science *323*, 1074-1077.

Mahan, A.L., and Ressler, K.J. (2012). Fear conditioning, synaptic plasticity and the amygdala: implications for posttraumatic stress disorder. Trends in neurosciences *35*, 24-35.

Martinowich, K., Hattori, D., Wu, H., Fouse, S., He, F., Hu, Y., Fan, G., and Sun, Y.E. (2003). DNA methylation-related chromatin remodeling in activity-dependent BDNF gene regulation. Science *302*, 890-893.

Mayer, W., Niveleau, A., Walter, J., Fundele, R., and Haaf, T. (2000). Demethylation of the zygotic paternal genome. Nature *403*, 501.

McEwen, B.S. (1999). STRESS AND HIPPOCAMPAL PLASTICITY. Annual Review of Neuroscience *22*, 105-122.

Meissner, A., Mikkelsen, T.S., Gu, H., Wernig, M., Hanna, J., Sivachenko, A., Zhang, X., Bernstein, B.E., Nusbaum, C., Jaffe, D.B.*, et al.* (2008). Genome-scale DNA methylation maps of pluripotent and differentiated cells. Nature *454*, 766-770.

Mellen, M., Ayata, P., Dewell, S., Kriaucionis, S., and Heintz, N. (2012). MeCP2 binds to 5hmC enriched within active genes and accessible chromatin in the nervous system. Cell *151*, 1417-1430.

Menezes, J.R., and Luskin, M.B. (1994). Expression of neuron-specific tubulin defines a novel population in the proliferative layers of the developing telencephalon. The Journal of neuroscience : the official journal of the Society for Neuroscience *14*, 5399-5416.

Mi, Y., Gao, X., Dai, J., Ma, Y., Xu, L., and Jin, W. (2015). A Novel Function of TET2 in CNS: Sustaining Neuronal Survival. International journal of molecular sciences *16*, 21846-21857.

Miller, C.A., and Sweatt, J.D. (2007). Covalent modification of DNA regulates memory formation. Neuron *53*, 857-869.

Ming, G.L., and Song, H. (2011). Adult neurogenesis in the mammalian brain: significant answers and significant questions. Neuron *70*, 687-702.

Mizuno, K., and Giese, K.P. (2005). Hippocampus-dependent memory formation: do memory type-specific mechanisms exist? Journal of pharmacological sciences *98*, 191-197.

Montalbán-Loro, R., Domingo-Muelas, A., Bizy, A., and Ferrón, S.R. (2015). Epigenetic regulation of stemness maintenance in the neurogenic niches. World Journal of Stem Cells *7*, 700-710.

Montalban-Loro, R., Lozano-Urena, A., Ito, M., Krueger, C., Reik, W., Ferguson-Smith, A.C., and Ferron, S.R. (2019). TET3 prevents terminal differentiation of adult NSCs by a non-catalytic action at Snrpn. Nature communications *10*, 1726.

Montalbán-Loro, R., Lozano-Ureña, A., Ito, M., Krueger, C., Reik, W., Ferguson-Smith, A.C., and Ferrón, S.R. (2019). TET3 prevents terminal differentiation of adult NSCs by a non-catalytic action at Snrpn. Nature communications *10*, 1726.

Morris, R. (1984). Developments of a water-maze procedure for studying spatial learning in the rat. Journal of neuroscience methods *11*, 47-60.

Morris, R.G.M., Garrud, P., Rawlins, J.N.P., and O'Keefe, J. (1982). Place navigation impaired in rats with hippocampal lesions. Nature *297*, 681.

Moser, M.-B., Rowland, D.C., and Moser, E.I. Place cells, grid cells, and memory. Cold Spring Harbor perspectives in biology *7*, a021808-a021808.

Mosley, M., Weathington, J., Cortes, L.R., Bruggeman, E., Castillo-Ruiz, A., Xue, B., and Forger, N.G. (2017). Neonatal Inhibition of DNA Methylation Alters Cell Phenotype in Sexually Dimorphic Regions of the Mouse Brain. Endocrinology *158*, 1838-1848.

Munji, R.N., Choe, Y., Li, G., Siegenthaler, J.A., and Pleasure, S.J. (2011). Wnt signaling regulates neuronal differentiation of cortical intermediate progenitors. The Journal of neuroscience : the official journal of the Society for Neuroscience *31*, 1676-1687.

Munzel, M., Globisch, D., Bruckl, T., Wagner, M., Welzmiller, V., Michalakis, S., Muller, M., Biel, M., and Carell, T. (2010). Quantification of the sixth DNA base hydroxymethylcytosine in the brain. Angewandte Chemie (International ed in English) *49*, 5375-5377.

Nakashiba, T., Cushman, J.D., Pelkey, K.A., Renaudineau, S., Buhl, D.L., McHugh, T.J., Rodriguez Barrera, V., Chittajallu, R., Iwamoto, K.S., McBain, C.J.*, et al.* (2012). Young dentate granule cells mediate pattern separation, whereas old granule cells facilitate pattern completion. Cell *149*, 188-201.

Nelson, J.C., and Charney, D.S. (1981). The symptoms of major depressive illness. The American journal of psychiatry *138*, 1-13.

Neves, G., Cooke, S.F., and Bliss, T.V.P. (2008). Synaptic plasticity, memory and the hippocampus: a neural network approach to causality. Nature Reviews Neuroscience *9*, 65.

Nugent, B.M., Wright, C.L., Shetty, A.C., Hodes, G.E., Lenz, K.M., Mahurkar, A., Russo, S.J., Devine, S.E., and McCarthy, M.M. (2015). Brain feminization requires active repression of masculinization via DNA methylation. Nature neuroscience *18*, 690-697.

Ohkubo, Y., Uchida, A.O., Shin, D., Partanen, J., and Vaccarino, F.M. (2004). Fibroblast growth factor receptor 1 is required for the proliferation of hippocampal progenitor cells and for hippocampal growth in mouse. The Journal of neuroscience : the official journal of the Society for Neuroscience *24*, 6057-6069.

Okano, H., and Temple, S. (2009). Cell types to order: temporal specification of CNS stem cells. Current opinion in neurobiology *19*, 112-119.

Okano, M., Xie, S., and Li, E. (1998). Cloning and characterization of a family of novel mammalian DNA (cytosine-5) methyltransferases. Nature genetics *19*, 219-220.

Oliveira, A.M., Hemstedt, T.J., and Bading, H. (2012). Rescue of aging-associated decline in Dnmt3a2 expression restores cognitive abilities. Nature neuroscience *15*, 1111-1113.

Oswald, J., Engemann, S., Lane, N., Mayer, W., Olek, A., Fundele, R., Dean, W., Reik, W., and Walter, J. (2000). Active demethylation of the paternal genome in the mouse zygote. Current biology : CB *10*, 475-478.

Pastor, W.A., Aravind, L., and Rao, A. (2013). TETonic shift: biological roles of TET proteins in DNA demethylation and transcription. Nature reviews Molecular cell biology *14*, 341-356.

Peter Curzon, N.R.R., and Kaitlin E. Browman. (2009). Methods of Behavior Analysis in Neuroscience, second edition. Buccafusco JJ.

Pfaffeneder, T., Hackner, B., Truss, M., Munzel, M., Muller, M., Deiml, C.A., Hagemeier, C., and Carell, T. (2011). The discovery of 5-formylcytosine in embryonic stem cell DNA. Angewandte Chemie *50*, 7008-7012.

Piccolo, F.M., Bagci, H., Brown, K.E., Landeira, D., Soza-Ried, J., Feytout, A., Mooijman, D., Hajkova, P., Leitch, H.G., Tada, T.*, et al.* (2013). Different roles for Tet1 and Tet2 proteins in reprogramming-mediated erasure of imprints induced by EGC fusion. Molecular cell *49*, 1023-1033.

Porsolt, R.D., Le Pichon, M., and Jalfre, M. (1977). Depression: a new animal model sensitive to antidepressant treatments. Nature *266*, 730-732.

Prokhortchouk, A., Hendrich, B., Jorgensen, H., Ruzov, A., Wilm, M., Georgiev, G., Bird, A., and Prokhortchouk, E. (2001). The p120 catenin partner Kaiso is a DNA methylation-dependent transcriptional repressor. Genes & development *15*, 1613-1618.

Rafalski, V.A., and Brunet, A. (2011). Energy metabolism in adult neural stem cell fate. Progress in Neurobiology *93*, 182-203.

Ramamoorthi, K., Fropf, R., Belfort, G.M., Fitzmaurice, H.L., McKinney, R.M., Neve, R.L., Otto, T., and Lin, Y. (2011). Npas4 regulates a transcriptional program in CA3 required for contextual memory formation. Science (New York, NY) *334*, 1669-1675.

Rathjen, J., and Rathjen, P.D. (2001). Mouse ES cells: experimental exploitation of pluripotent differentiation potential. Current opinion in genetics & development *11*, 587-594.

Raymond, C.R. (2007). LTP forms 1, 2 and 3: different mechanisms for the "long" in long-term potentiation. Trends in neurosciences *30*, 167-175.

Ridder, S., Chourbaji, S., Hellweg, R., Urani, A., Zacher, C., Schmid, W., Zink, M., Hortnagl, H., Flor, H., Henn, F.A.*, et al.* (2005). Mice with genetically altered glucocorticoid receptor expression show altered sensitivity for stress-induced depressive reactions. Journal of Neuroscience *25*, 6243-6250.

Rolando, C., and Taylor, V. (2014). Neural stem cell of the hippocampus: development, physiology regulation, and dysfunction in disease. Current topics in developmental biology *107*, 183-206.

Rudenko, A., Dawlaty, M.M., Seo, J., Cheng, A.W., Meng, J., Le, T., Faull, K.F., Jaenisch, R., and Tsai, L.H. (2013). Tet1 is critical for neuronal activity-regulated gene expression and memory extinction. Neuron *79*, 1109-1122.

Rutherford, L.C., Nelson, S.B., and Turrigiano, G.G. (1998). BDNF has opposite effects on the quantal amplitude of pyramidal neuron and interneuron excitatory synapses. Neuron *21*, 521-530.

Ryu, J., Futai, K., Feliu, M., Weinberg, R., and Sheng, M. (2008). Constitutively active Rap2 transgenic mice display fewer dendritic spines, reduced extracellular signal-regulated kinase signaling, enhanced long-term depression, and impaired spatial learning and fear extinction. The Journal of neuroscience : the official journal of the Society for Neuroscience *28*, 8178-8188.

Sanosaka, T., Imamura, T., Hamazaki, N., Chai, M., Igarashi, K., Ideta-Otsuka, M., Miura, F., Ito, T., Fujii, N., Ikeo, K.*, et al.* (2017). DNA Methylome Analysis Identifies Transcription Factor-Based Epigenomic Signatures of Multilineage Competence in Neural Stem/Progenitor Cells. Cell Reports *20*, 2992-3003.

Santarelli, L., Saxe, M., Gross, C., Surget, A., Battaglia, F., Dulawa, S., Weisstaub, N., Lee, J., Duman, R., Arancio, O.*, et al.* (2003). Requirement of hippocampal neurogenesis for the behavioral effects of antidepressants. Science *301*, 805-809.

Santiago, M., Antunes, C., Guedes, M., Sousa, N., and Marques, C.J. (2014). TET enzymes and DNA hydroxymethylation in neural development and function - how critical are they? Genomics *104*, 334-340.

Seisenberger, S., Peat, J.R., Hore, T.A., Santos, F., Dean, W., and Reik, W. (2013). Reprogramming DNA methylation in the mammalian life cycle: building and breaking epigenetic barriers. Philosophical transactions of the Royal Society of London Series B, Biological sciences *368*, 20110330.

Seri, B., Garcia-Verdugo, J.M., Collado-Morente, L., McEwen, B.S., and Alvarez-Buylla, A. (2004). Cell types, lineage, and architecture of the germinal zone in the adult dentate gyrus. The Journal of comparative neurology *478*, 359-378.

Shi, Y., Chichung Lie, D., Taupin, P., Nakashima, K., Ray, J., Yu, R.T., Gage, F.H., and Evans, R.M. (2004). Expression and function of orphan nuclear receptor TLX in adult neural stem cells. Nature *427*, 78-83.

Shin, J., Ming, G.-l., and Song, H. (2014). DNA modifications in the mammalian brain. Philosophical Transactions of the Royal Society B: Biological Sciences *369*, 20130512.

Smith, Z.D., and Meissner, A. (2013). DNA methylation: roles in mammalian development. Nature reviews Genetics *14*, 204-220.

Snijders, C., Bassil, K.C., and de Nijs, L. (2018). Methodologies of Neuroepigenetic Research: Background, Challenges and Future Perspectives. Progress in molecular biology and translational science *158*, 15-27.

Snyder, J.S., Hong, N.S., McDonald, R.J., and Wojtowicz, J.M. (2005). A role for adult neurogenesis in spatial long-term memory. Neuroscience *130*, 843-852.

Snyder, J.S., Soumier, A., Brewer, M., Pickel, J., and Cameron, H.A. (2011). Adult hippocampal neurogenesis buffers stress responses and depressive behaviour. Nature *476*, 458-461.

Song, C.X., Szulwach, K.E., Fu, Y., Dai, Q., Yi, C., Li, X., Li, Y., Chen, C.H., Zhang, W., Jian, X.*, et al.* (2011). Selective chemical labeling reveals the genome-wide distribution of 5-hydroxymethylcytosine. Nature biotechnology *29*, 68-72.

Spruijt, C.G., Gnerlich, F., Smits, A.H., Pfaffeneder, T., Jansen, P.W., Bauer, C., Munzel, M., Wagner, M., Muller, M., Khan, F.*, et al.* (2013). Dynamic readers for 5-(hydroxy)methylcytosine and its oxidized derivatives. Cell *152*, 1146-1159.

Stavridis, M.P., and Smith, A.G. (2003). Neural differentiation of mouse embryonic stem cells. Biochemical Society transactions *31*, 45-49.

Strange, B.A., Witter, M.P., Lein, E.S., and Moser, E.I. (2014). Functional organization of the hippocampal longitudinal axis. Nature reviews Neuroscience *15*, 655-669.

Szulwach, K.E., Li, X., Li, Y., Song, C.-X., Wu, H., Dai, Q., Irier, H., Upadhyay, A.K., Gearing, M., Levey, A.I., *et al.* (2011). 5-hmC-mediated epigenetic dynamics during postnatal neurodevelopment and aging. Nature neuroscience *14*, 1607-1616.

Szwagierczak, A., Bultmann, S., Schmidt, C.S., Spada, F., and Leonhardt, H. (2010). Sensitive enzymatic quantification of 5-hydroxymethylcytosine in genomic DNA. Nucleic acids research *38*, e181.

Tahiliani, M., Koh, K.P., Shen, Y., Pastor, W.A., Bandukwala, H., Brudno, Y., Agarwal, S., Iyer, L.M., Liu, D.R., Aravind, L., *et al.* (2009a). Conversion of 5-Methylcytosine to 5-Hydroxymethylcytosine in Mammalian DNA by MLL Partner TET1. Science (New York, NY) *324*, 930-935.

Tahiliani, M., Koh, K.P., Shen, Y., Pastor, W.A., Bandukwala, H., Brudno, Y., Agarwal, S., Iyer, L.M., Liu, D.R., Aravind, L., *et al.* (2009b). Conversion of 5-methylcytosine to 5-hydroxymethylcytosine in mammalian DNA by MLL partner TET1. Science *324*, 930-935.

Tan, L., Xiong, L., Xu, W., Wu, F., Huang, N., Xu, Y., Kong, L., Zheng, L., Schwartz, L., Shi, Y., *et al.* (2013). Genome-wide comparison of DNA hydroxymethylation in mouse embryonic stem cells and neural progenitor cells by a new comparative hMeDIP-seq method. Nucleic acids research *41*, e84.

Tatton-Brown, K., Seal, S., Ruark, E., Harmer, J., Ramsay, E., Del Vecchio Duarte, S., Zachariou, A., Hanks, S., O'Brien, E., Aksglaede, L., *et al.* (2014). Mutations in the DNA methyltransferase gene DNMT3A cause an overgrowth syndrome with intellectual disability. Nature genetics *46*, 385-388.

Terry, A.V., Jr. (2009). Frontiers in Neuroscience

Spatial Navigation (Water Maze) Tasks. In Methods of Behavior Analysis in Neuroscience, nd, and J.J. Buccafusco, eds. (Boca Raton (FL): CRC Press/Taylor & FrancisTaylor & Francis Group, LLC.).

Theriault, F.M., Nuthall, H.N., Dong, Z., Lo, R., Barnabe-Heider, F., Miller, F.D., and Stifani, S. (2005). Role for Runx1 in the proliferation and neuronal differentiation of selected progenitor cells in the mammalian nervous system. The Journal of neuroscience : the official journal of the Society for Neuroscience *25*, 2050-2061.

Thomson, J.P., and Meehan, R.R. (2017). The application of genome-wide 5-hydroxymethylcytosine studies in cancer research. Epigenomics *9*, 77-91.

Tsetsenis, T., Younts, T.J., Chiu, C.Q., Kaeser, P.S., Castillo, P.E., and Sudhof, T.C. (2011). Rab3B protein is required for long-term depression of hippocampal inhibitory synapses and for normal reversal learning. Proceedings National Academy Sciences U S A *108*, 14300-14305.

Vaghi, V., Pennucci, R., Talpo, F., Corbetta, S., Montinaro, V., Barone, C., Croci, L., Spaiardi, P., Consalez, G.G., Biella, G., *et al.* (2014). Rac1 and rac3 GTPases control synergistically the development of cortical and hippocampal GABAergic interneurons. Cerebral Cortex *24*, 1247-1258.

Walf, A.A., and Frye, C.A. (2007). The use of the elevated plus maze as an assay of anxiety-related behavior in rodents. Nature protocols *2*, 322-328.

Wang, L., Li, M.Y., Qu, C., Miao, W.Y., Yin, Q., Liao, J., Cao, H.T., Huang, M., Wang, K., Zuo, E., *et al.* (2017). CRISPR-Cas9-mediated genome editing in one blastomere of two-cell embryos reveals a novel Tet3 function in regulating neocortical development. Cell research *27*, 815-829.

Wei, Q., Lu, X.Y., Liu, L., Schafer, G., Shieh, K.R., Burke, S., Robinson, T.E., Watson, S.J., Seasholtz, A.F., and Akil, H. (2004). Glucocorticoid receptor overexpression in forebrain: a mouse model of increased emotional lability. Proceedings National Academy Sciences U S A *101*, 11851-11856.

Wen, L., Li, X., Yan, L., Tan, Y., Li, R., Zhao, Y., Wang, Y., Xie, J., Zhang, Y., Song, C.*, et al.* (2014). Whole-genome analysis of 5-hydroxymethylcytosine and 5-methylcytosine at base resolution in the human brain. Genome biology *15*, R49.

Wossidlo, M., Nakamura, T., Lepikhov, K., Marques, C.J., Zakhartchenko, V., Boiani, M., Arand, J., Nakano, T., Reik, W., and Walter, J. (2011). 5-Hydroxymethylcytosine in the mammalian zygote is linked with epigenetic reprogramming. Nature communications *2*, 241.

Wu, H., D'Alessio, A.C., Ito, S., Wang, Z., Cui, K., Zhao, K., Sun, Y.E., and Zhang, Y. (2011a). Genome-wide analysis of 5-hydroxymethylcytosine distribution reveals its dual function in transcriptional regulation in mouse embryonic stem cells. Genes & development *25*, 679-684.

Wu, H., D'Alessio, A.C., Ito, S., Xia, K., Wang, Z., Cui, K., Zhao, K., Sun, Y.E., and Zhang, Y. (2011b). Dual functions of Tet1 in transcriptional regulation in mouse embryonic stem cells. Nature *473*, 389-393.

Wu, X., and Zhang, Y. (2017). TET-mediated active DNA demethylation: mechanism, function and beyond. Nature reviews Genetics *18*, 517-534.

Wu, Z., Huang, K., Yu, J., Le, T., Namihira, M., Liu, Y., Zhang, J., Xue, Z., Cheng, L., and Fan, G. (2012). Dnmt3a regulates both proliferation and differentiation of mouse neural stem cells. Journal of neuroscience research *90*, 1883-1891.

Yamaguchi, S., Shen, L., Liu, Y., Sendler, D., and Zhang, Y. (2013). Role of Tet1 in erasure of genomic imprinting. Nature *504*, 460-464.

Yamazaki, Y., Mann, M.R.W., Lee, S.S., Marh, J., McCarrey, J.R., Yanagimachi, R., and Bartolomei, M.S. (2003). Reprogramming of primordial germ cells begins before migration into the genital ridge, making these cells inadequate donors for reproductive cloning. Proceedings of the National Academy of Sciences of the United States of America *100*, 12207-12212.

Yang, M., Weber, M.D., and Crawley, J.N. (2008). Light phase testing of social behaviors: not a problem. Front Neurosci *2*, 186-191.

Yong, W.-S., Hsu, F.-M., and Chen, P.-Y. (2016). Profiling genome-wide DNA methylation. Epigenetics & chromatin *9*, 26-26.

Yu, H., Su, Y., Shin, J., Zhong, C., Guo, J.U., Weng, Y.L., Gao, F., Geschwind, D.H., Coppola, G., Ming, G.L.*, et al.* (2015). Tet3 regulates synaptic transmission and homeostatic plasticity via DNA oxidation and repair. Nature neuroscience *18*, 836-843.

Zhang, J., Chen, S., Zhang, D., Shi, Z., Li, H., Zhao, T., Hu, B., Zhou, Q., and Jiao, J. (2016a). Tet3-Mediated DNA Demethylation Contributes to the Direct Conversion of Fibroblast to Functional Neuron. Cell Rep *17*, 2326-2339.

Zhang, J., Poh, H.M., Peh, S.Q., Sia, Y.Y., Li, G., Mulawadi, F.H., Goh, Y., Fullwood, M.J., Sung, W.K., Ruan, X.*, et al.* (2012). ChIA-PET analysis of transcriptional chromatin interactions. Methods *58*, 289-299.

Zhang, R.R., Cui, Q.Y., Murai, K., Lim, Y.C., Smith, Z.D., Jin, S., Ye, P., Rosa, L., Lee, Y.K., Wu, H.P.*, et al.* (2013). Tet1 regulates adult hippocampal neurogenesis and cognition. Cell stem cell *13*, 237-245.

Zhang, W., Xia, W., Wang, Q., Towers, A.J., Chen, J., Gao, R., Zhang, Y., Yen, C.A., Lee, A.Y., Li, Y.*, et al.* (2016b). Isoform Switch of TET1 Regulates DNA Demethylation and Mouse Development. Molecular cell *64*, 1062-1073.

Zhao, X., Dai, J., Ma, Y., Mi, Y., Cui, D., Ju, G., Macklin, W.B., and Jin, W. (2014). Dynamics of ten-eleven translocation hydroxylase family proteins and 5-hydroxymethylcytosine in oligodendrocyte differentiation. Glia *62*, 914-926.

ANNEXES

Cellular and Molecular Life Sciences
https://doi.org/10.1007/s00018-019-03335-7

ORIGINAL ARTICLE

Tet3 regulates cellular identity and DNA methylation in neural progenitor cells

Mafalda Santiago[1,2] · Claudia Antunes[1,2] · Marta Guedes[1,2] · Michelina Iacovino[3,9] · Michael Kyba[3] · Wolf Reik[4,5] · Nuno Sousa[1,2] · Luísa Pinto[1,2] · Miguel R. Branco[6] · C. Joana Marques[1,2,7,8]

Received: 30 May 2019 / Revised: 26 September 2019 / Accepted: 3 October 2019
© Springer Nature Switzerland AG 2019

Author Proof

Abstract

TET enzymes oxidize 5-methylcytosine (5mC) into 5-hydroxymethylcytosine (5hmC), a process thought to be intermediary in an active DNA demethylation mechanism. Notably, 5hmC is highly abundant in the brain and in neuronal cells. Here, we interrogated the function of *Tet3* in neural precursor cells (NPCs), using a stable and inducible knockdown system and an in vitro neural differentiation protocol. We show that *Tet3* is upregulated during neural differentiation, whereas *Tet1* is downregulated. Surprisingly, *Tet3* knockdown led to a de-repression of pluripotency-associated genes such as *Oct4*, *Nanog* or *Tcl1*, with concomitant hypomethylation. Moreover, in *Tet3* knockdown NPCs, we observed the appearance of OCT4-positive cells forming cellular aggregates, suggesting de-differentiation of the cells. Notably, *Tet3* KD led to a genome-scale loss of DNA methylation and hypermethylation of a smaller number of CpGs that are located at neurogenesis-related genes and at imprinting control regions (ICRs) of *Peg10*, *Zrsr1* and *Mcts2* imprinted genes. Overall, our results suggest that TET3 is necessary to maintain silencing of pluripotency genes and consequently neural stem cell identity, possibly through regulation of DNA methylation levels in neural precursor cells.

Keywords TET enzymes · 5-hydroxymethylcytosine · Imprinted genes · Neural stem cells · Pluripotency · Neurogenesis

Introduction

DNA methylation, or 5-methylcytosine (5mC), is an epigenetic modification that consists of a methyl group added to the fifth position of cytosines, occurring more frequently in the context of CpG dinucleotides [1]. Albeit deemed as a very stable chemical modification, waves of global loss of DNA methylation occur during critical periods of development such as in

UNCORRECTED PROOF

Electronic supplementary material The online version of this article (https://doi.org/10.1007/s00018-019-03335-7) contains supplementary material, which is available to authorized users.

Mafalda Santiago and Claudia Antunes contributed equally.

✉ Miguel R. Branco
m.branco@qmul.ac.uk

✉ C. Joana Marques
cmarques@med.up.pt

[1] Life and Health Sciences Research Institute (ICVS), School of Health Sciences, University of Minho, 4710-057 Braga, Portugal

[2] ICVS/3B's—PT Government Associate Laboratory, 4710-057 Braga/Guimarães, Portugal

[3] Lillehei Heart Institute and Department of Pediatrics, University of Minnesota, Minneapolis, MN 55455, USA

[4] Epigenetics Programme, The Babraham Institute, Cambridge CB22 3AT, UK

[5] The Wellcome Trust Sanger Institute, Cambridge CB10 1SA, UK

[6] Blizard Institute, Barts and The London School of Medicine and Dentistry, Queen Mary University of London, London E1 2AT, UK

[7] Genetics Unit, Department of Pathology, Faculty of Medicine, University of Porto, 4200-319 Porto, Portugal

[8] i3S—Instituto de Investigação e Inovação em Saúde, Universidade do Porto, 4200-135 Porto, Portugal

[9] Present Address: Division of Medical Genetics, Department of Pediatrics, Harbor UCLA Medical Center, Los Angeles Biomedical Research Institute, Torrance, CA 90502, USA

Journal : Large 18 | Article No : 3335 | Pages : 13 | MS Code : 3335 | Dispatch : 17-10-2019

Author Proof

the zygote and in primordial germ cells [2]. Additionally, loss of DNA methylation has been observed in post-mitotic cells, with activity-dependent demethylation occurring in mature neurons upon depolarization [3, 4]. This mechanism of active DNA demethylation remained elusive for a long time, but the AQ2 finding that TET enzymes can convert 5mC into 5-hydroxymethylcytosine (5hmC), and subsequently into 5-formylcytosine (5fC) and 5-carboxylcytosine (5caC) [5–8], shed light into this mechanism. Importantly, 5hmC was shown to accumulate in the paternal pronucleus and in PGCs concomitantly with methylation loss [9–11] and to appear in an antagonistic way to 5mC in the genome of dentate granule neurons [12]. Three members—TET1, TET2 and TET3—compose the family of TET enzymes, which are Fe^{2+} and 2-oxoglutarate-dependent dioxygenases. TET1 and TET3 contain a CXXC zinc finger domain at their amino-terminus that is known to bind CpG sequences, whereas TET2 partners with IDAX, an independent CXXC-containing protein [13, 14]. 5hmC was first described in mouse embryonic stem (ES) cells and in Purkinje neurons [7, 8] and was later shown to be most abundant in the brain, namely at the cerebellum, cortex and hippocampus brain regions [15]. Moreover, TET enzymes were shown to be expressed in these brain regions, with *Tet3* showing highest expression [15]. Additionally, in the embryonic mouse brain, 5hmC levels were shown to increase during neuronal differentiation, as the cells migrate from the ventricular zone to the cortical plate [16]. In neurons, 5hmC was associated with gene bodies of activated neuronal function-related genes and gain of 5hmC was concomitant with loss of the repressive histone mark H3K27me3 [16]. Notably, TET enzymes have also been implicated in brain processes and functions such as neurogenesis, cognition and memory [17–21].

Here, we addressed the functional role of TET3 enzyme in neural precursor cells (NPCs) using an in vitro differentiation system, where highly proliferative ES cells are differentiated into a homogeneous population of NPCs that are PAX6-positive radial glial cells [22] and a stable and inducible RNAi knockdown system [23]. We observed that knockdown (KD) of *Tet3* in NPCs resulted in upregulation of pluripotency genes and genome-wide loss of DNA methylation. Nevertheless, gain of methylation was also observed, particularly in genes involved in neural differentiation. Our data suggest that TET3 plays a role in maintaining both cellular identity and DNA methylation levels in neural precursor cells.

Results

Neural differentiation leads to *Tet3* upregulation

To investigate the effects of the knockdown of TET3 enzyme in NPCs, we established a stable and inducible knockdown system in mouse ES cells containing shRNAs targeting *Tet3* (Fig. S1a) [23, 24] and a neural differentiation system that results in a homogeneous population of PAX6-positive radial glial-like neural precursor cells (Fig. 1a, S1b, c) [25]. In this differentiation protocol, ES cells are maintained in a highly proliferative state and then cultured in non-adherent conditions forming cellular aggregates; addition of retinoic acid (RA) 4 days after cellular aggregates are formed results in upregulation of neural markers, such as *Pax6*, *Nestin*, *Tubb3* (B3-tubulin) and *TrkB* (*Nrtk2*) (Fig. 1b), with between 92 and 96% of the differentiated cell staining positively for PAX6 (Fig. S1b, c). This indicates homogeneous differentiation of ES cells into NPCs as described in the original protocol [22]. Positive staining of Beta 3-tubulin, which is one of the earliest markers of neuronal differentiation [26], was also observed (Fig. S1b). On the other hand, SOX2, which is a marker for neural stem cells that becomes inactivated in NPCs [27, 28], was nearly undetected (Fig. S1b). During differentiation, there was also a marked decrease in the expression of pluripotency genes such as *Oct4* and *Nanog*, as expected (Fig. 1b). Regarding epigenetic modifiers, we observed increased levels of *Tet3* and *Dnmt3a* during differentiation, whilst levels of *Tet1* decreased (Fig. 1b). Upregulation of *Tet3* during neuronal differentiation has been previously observed [29, 30] and suggests a prominent role for *Tet3* in the neuronal lineage. We also confirmed the presence of TET3 protein in NPCs by immunostaining, showing a predominantly cytoplasmic distribution (Fig. 1c); this is consistent with a putative role for TET3 in oxidizing 5mC to 5hmC in RNA molecules [31].

Knockdown of *Tet3* in NPCs results in de-repression of pluripotency genes

We performed stable and inducible knockdown of *Tet3* in NPCs, using two independent shRNAs (Fig. 2a, b); *Tet3* knockdown was detected at both the mRNA and protein levels (Fig. 2b and S2a). Interestingly, we observed a significant upregulation of pluripotency genes, namely *Oct4, Nanog, Tcl1* and *Esrrb*, after *Tet3* KD (Fig. 2b), using two independent shRNAs. To further elucidate the observed upregulation of pluripotency genes, we performed immunostaining for OCT4 and observed the presence of OCT4-positive cells that appeared as cellular aggregates (Fig. 2c), representing around 14% of the total number of cells. Of note, OCT4-positive cells were not observed in NPCs treated with the Scrambled shRNA (Fig. S3); this suggests that Tet3 KD NPCs might have undergone a de-differentiation event due to downregulation of *Tet3* expression. This is in line with a recent report showing that *Tet3* can promote a rapid and efficient conversion of fibroblasts into neurons, showing that *Tet3* plays an important role in inducing and maintaining neural cell identity [32]. To better understand the nature of these ES cells like NPCs, we

UNCORRECTED PROOF

Journal : Large 18 | Article No : 3335 | Pages : 13 | MS Code : 3335 | Dispatch : 17-10-2019

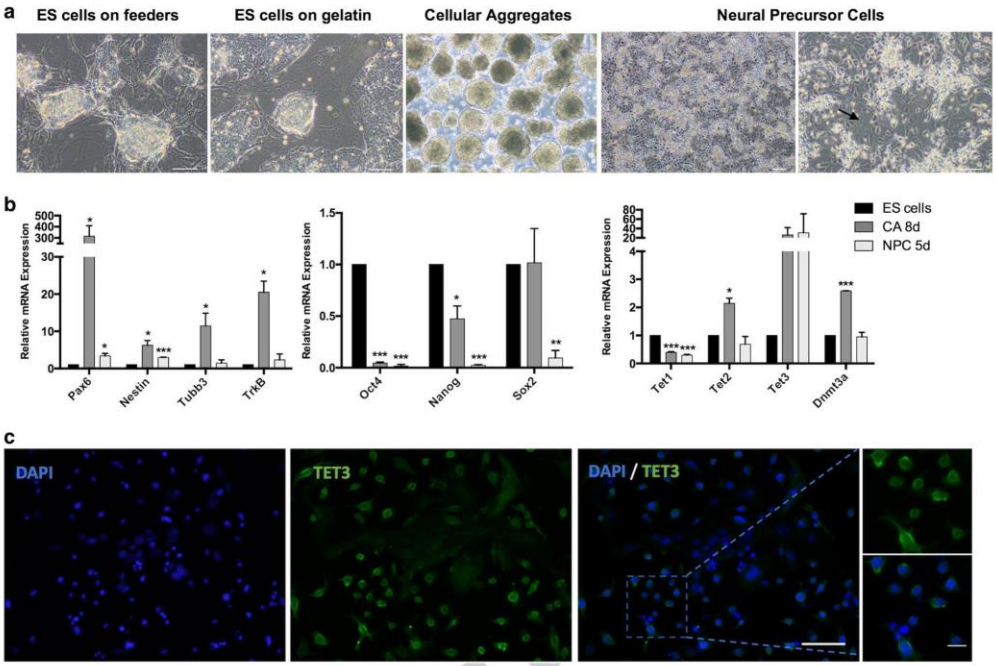

Fig. 1 *Tet3* is upregulated during neural differentiation. **a** Neural differentiation protocol with representative images of key transition points—embryonic stem (ES) cells on feeders, ES cells on gelatin, cellular aggregates (CAs) and neural precursor cells (NPCs). Arrows show neurites forming between the cells; Scale bars—100 µm. **b** Relative expression of neural markers (*Pax6*, *Nestin*, *Tubb3* and *TrkB*), pluripotency markers (*Oct4*, *Nanog* and *Sox2*) and epigenetic regulators (*Tet1*, *Tet2*, *Tet3* and *Dnmt3a*) in several stages of the neural differentiatioTET3. n process—ES cells on gelatin (ES cells), CA after addition of Retinoic Acid (CA 8d), NPC after 5 days in culture (NPC 5d); $n=2$ independent experiments; $*p<0.05$; $**p<0.01$; $***p<0.001$; *t* tests. **c** Immunostaining of TET3 in differentiated NPCs. Scale bars—100 µm and 25 µm

performed flow cytometry using Propidium iodide staining in KD NPCs and observed that *Tet3* KD NPCs still resemble control NPCs (Scrambled shRNA) more than ES cells, which show an extended S-phase comparing to NPCs (Fig. S2b). Additionally, we observed a significant increase in *Dnmt1* and decrease in *Dnmt3a* expression after *Tet3* KD (Fig. 2b), pointing to a co-regulation between TET enzymes and DNA methyltransferases.

These results suggest that functional perturbation of *Tet3* in NPCs leads to de-repression of pluripotency genes which might affect maintenance of the neural precursor cell identity.

Tet3 knockdown results in genome-scale loss of DNA methylation

As the above-mentioned results pointed to a critical role for *Tet3* in neural differentiation, we performed oxRRBS (oxidative Reduced Representation Bisulfite Sequencing) to analyse genome-wide changes in distribution of 5mC and 5hmC after *Tet3* knockdown. RRBS is a bisulfite-based protocol that enriches for CpG-rich parts of the genome, thereby reducing the amount of sequencing required, since it only covers 1% of the genome while capturing the majority of promoters and CpG islands [33]. To distinguish 5hmC from 5mC and since conventional sodium bisulphite treatment does not discriminate between the two modifications [34], we first added potassium perruthenate ($KRuO_4$) that triggers selective chemical oxidation of 5hmC to 5-formylcytosine (5fC), before bisulphite treatment. 5fC is then further converted to uracil after bisulphite treatment and subtraction of oxidative bisulphite readout from the bisulphite—only one allows determining the amount of 5hmC at a particular nucleotide—in a single-base resolution and quantitative manner [35, 36]. As the bisulphite signal is always expected to be larger than that of oxidative bisulphite, negative values

Journal : Large 18 | Article No : 3335 | Pages : 13 | MS Code : 3335 | Dispatch : 17-10-2019

Author Proof
UNCORRECTED

Author Proof

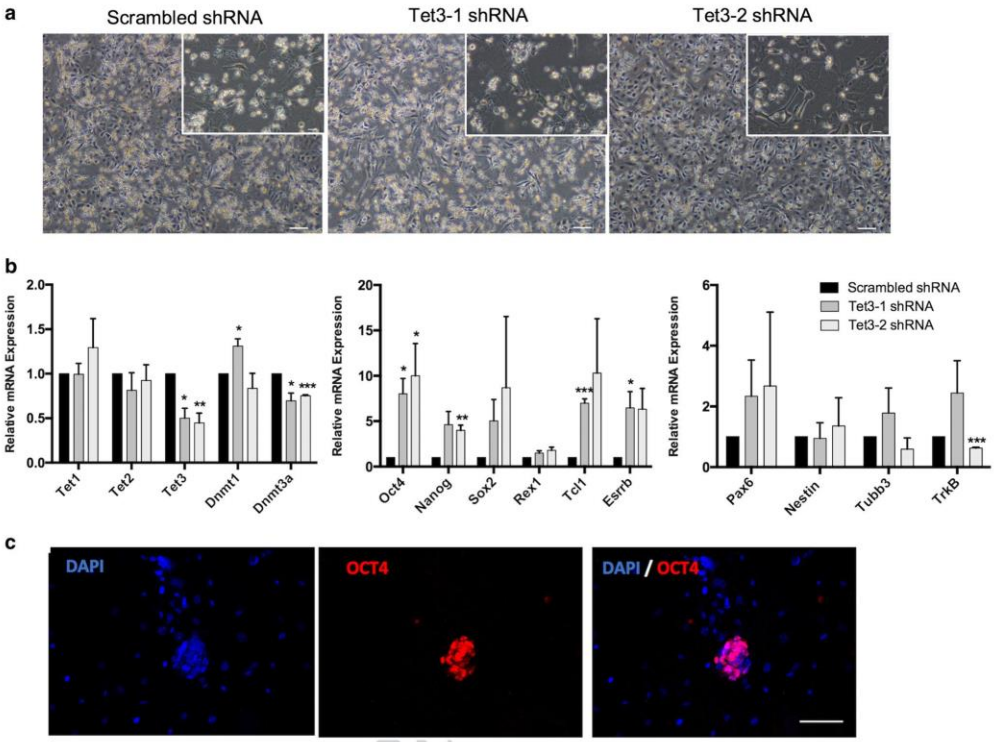

Fig. 2 Knockdown of *Tet3* in NPCs results in de-repression of pluripotency genes. **a** Phase-contrast images of NPCs after Tet3 knockdown during 5 days in culture. Scrambled shRNA—control; Tet3-1 and Tet3-2 shRNAs—shRNA against *Tet3*. Scale bars—100 μm and 50 μm in the insets. **b** mRNA transcript levels of epigenetic regulators (*Tet* and *Dnmt* enzymes), pluripotency genes (*Oct4*, *Nanog*, *Sox2*, *Rex1* and *Tcl1*) and neural markers [(stem cell markers—*Pax6* and *Nestin*; mature differentiation markers—B3-tubulin (*Tubb3*) and Neurotrophic tyrosine kinase, receptor, type 2 (*TrkB* or *Ntrk2*)] after *Tet3* knockdown. (*$p<0.05$, **$p<0.01$, ***$p<0.001$; *t* test). Error bars represent SEM for three (Tet3-1 shRNA) and two (Tet3-2 shRNA) independent experiments. **c** Immunostaining of OCT4 in NPCs after *Tet3* KD, using Tet3-2 shRNA, shows OCT4-positive cells forming aggregates that resemble ES cell colonies. Scale bar—50 μm

UNCORRECTED

are artefacts used to estimate the false discovery rate (FDR; see Methods). Notably, we could only detect 2,191 hydroxymethylated CpGs (out of ~0.5 M) at a high FDR of 45% (Fig. S4a), which is in contrast with the low FDR (~3%) that we previously obtained in ES cells [35]. This is likely due to the fact that 5hmC levels are low in NPCs comparing to mouse ES cells and hippocampus brain region (Fig. S4b, c) [30] and mostly present in intragenic regions [16], whereas oxRRBS mainly captures promoters and CpG islands [33].

Notwithstanding, we observed an unexpected global loss of 5mC after *Tet3* KD (Fig. 3a, b). Loci showing loss of methylation covered the whole range of methylation levels, but particularly regions that had more than 40% of 5mC in control NPCs (Fig. 3b). We performed detection of differentially methylated positions (DMPs; q value <0.01; $>10\%$ difference), which yielded a total of 88,437 hypomethylated CpGs that were enriched at genic regions when compared to the distribution of CpGs captured by RRBS (Fig. 3c). In contrast, very few hypo-DMPs were located in promoters and CpG islands, which can be explained by the fact that these are already frequently devoid of methylation [1, 37]. On the other hand, we detected only 588 hypermethylated CpGs, which were mainly located at CpG islands and genic regions (Fig. 3c).

To investigate whether the hypomethylation pattern seen in *Tet3* knockdown NPCs resembles ES cells, we compared our NPC dataset to a previously published oxRRBS dataset on ES cells [35]. We first noted that many CpG islands in control NPCs displayed higher 5mC levels when compared to ES cells, whilst a group of CpG

Journal : Large 18 | Article No : 3335 | Pages : 13 | MS Code : 3335 | Dispatch : 17-10-2019

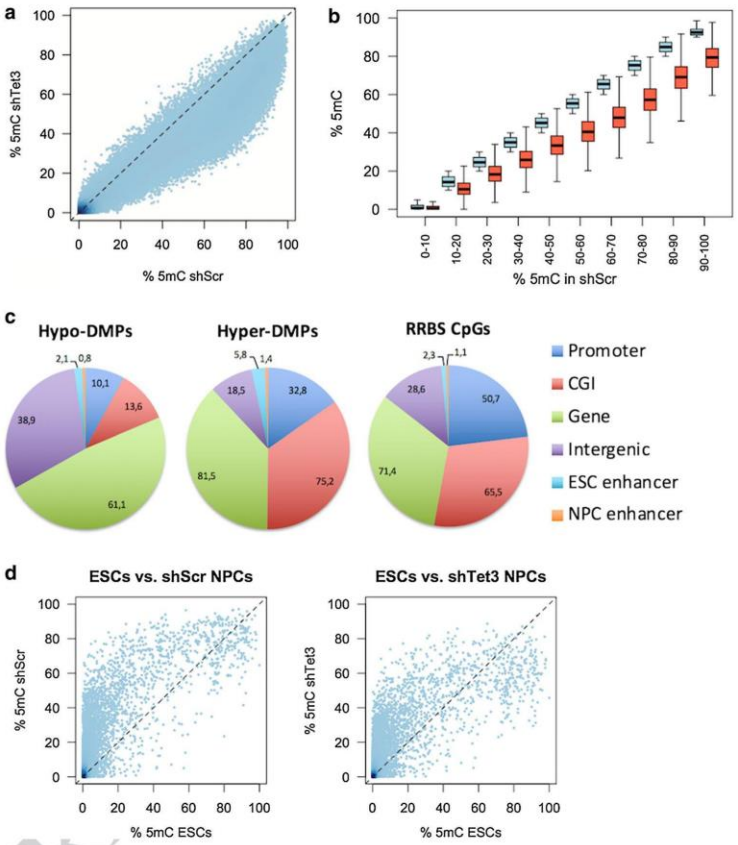

Fig. 3 *Tet3* knockdown results in genome-scale loss of DNA methylation. **a** Scatter plot of 5mC levels at individual CpGs, showing a bulk shift in methylation after *Tet3* KD, using Tet3-2 shRNA. **b** To better visualize differences in 5mC levels, CpGs were grouped based on their % 5mC in control NPCs. The plot displays the distributions of 5mC levels for control (blue) and *Tet3* KD (red) within each group. Loss of methylation is observed across the whole range of methylation levels. **c** Genomic features associated with differentially methylated positions (DMPs) after *Tet3* KD, showing that hypo-DMPs are enriched at genic regions and depleted at promoters and CpG islands. **d** Comparison of our oxRRBS datasets with a published dataset for ES cells [35], displaying average 5mC levels per CpG island

islands was highly methylated (> 70%) in both cell types (Fig. 3d). Upon *Tet3* KD, 5mC levels did become closer to those seen in ES cells, but only for lowly methylated CpG islands. Importantly, *Tet3* KD led to demethylation of highly methylated CpG islands, which does not match the ES cell profile (Fig. 3d). Where an ES cell subpopulation to be responsible for 5mC loss in *Tet3* KD NPC population, this would have led to maintenance of 5mC levels at highly methylated CpG islands. This prediction was confirmed by simulating 5mC patterns for cell mixtures of ES cells and NPCs, where increasing the proportion of ES cells only decreases the methylation at low-methylation CpG islands, whereas high-methylation CpG islands remain largely unchanged (Fig. S4e). These results suggest that the DNA hypomethylation observed in *Tet3* knockdown NPCs might reflect an epigenetic reprogramming event specific to the depletion of *Tet3* in NPCs.

Tet3 knockdown alters DNA methylation at developmentally relevant gene promoters

To expand on these observations, we performed gene ontology analysis of genes associated with promoters harbouring groups of hypomethylated CpGs. For this purpose, differentially methylated regions (DMRs) were defined has regions showing at least 3DMPs with differences in the same direction. Promoters were defined − 1 kb to + 0.5 kb from mRNA TSSs. Promoters associated with hypomethylated DMRs (Supplemental file "Hyper_Hypo_promoters.xlsx") were enriched for terms, such as development, differentiation and neurogenesis (Fig. 4a), suggesting that the observed hypomethylation is a regulated process coupled to the differentiation process between ES cells and NPCs. Of the genes involved in neurogenesis, *Slit1*, *Bdnf*, *Nr2e1* (*Tlx*), *Fgfr1*, *Runx1* and *Wnt3* are striking examples of genes that

Journal : Large 18 | Article No : 3335 | Pages : 13 | MS Code : 3335 | Dispatch : 17-10-2019

Author Proof

Author Proof

have been described to be involved in the proliferation of neural precursor cells [38–43]. Expression analysis of *Slit1* showed a tendency for increased mRNA transcription (Fig. S5), consistent with its hypomethylated state.

Moreover, loss of methylation was also observed at *Esrrb* and *Tcl1* early-pluripotency genes (Fig. 4b), which is in line with the observed upregulation of gene expression. Loss of methylation at *Tcl1* was confirmed by standard bisulfite sequencing (Fig. 4c).

For DNA hypermethylation, we only detected six genes with three or more hypermethylated CpGs at their promoters (Supplemental file "Hyper_Hypo_promoters.xlsx"). Notably, three of these genes are imprinted genes—*Peg10*, *Zrsr1* and *Mcts2*. Interestingly, it has been shown previously that loss of function of *Tet1* also leads to hypermethylation of imprinted genes, namely *Peg10* [44]. Expression analysis of these imprinted genes showed decreased expression in *Tet3* KD NPCs (Fig. 4d). More recently, it was also shown that *Tet3* regulates NSC maintenance through repression of *Snrpn* imprinted gene [45]. In accordance with this study, expression analysis of *Snrpn* in Tet3 KD NPCs showed increased transcription in one of the shRNAs (Fig. S5). To enable gene ontology analysis of hypermethylated sites, we changed our criteria to include promoters with a minimum of one hypermethylated CpG, yielding a total of 116 genes. Despite this low stringency, gene ontology analysis revealed significant associations with brain development, particularly with neuron differentiation and neurogenesis (Fig. 4e). Amongst these genes, *Wnt3a*, *Dlx2*, *Otx2* and *Rac3* are examples of genes described to promote neuronal differentiation [46–49], suggesting that TET3 plays a role in neurogenesis by maintaining hypomethylation of neuronal genes.

PROOF

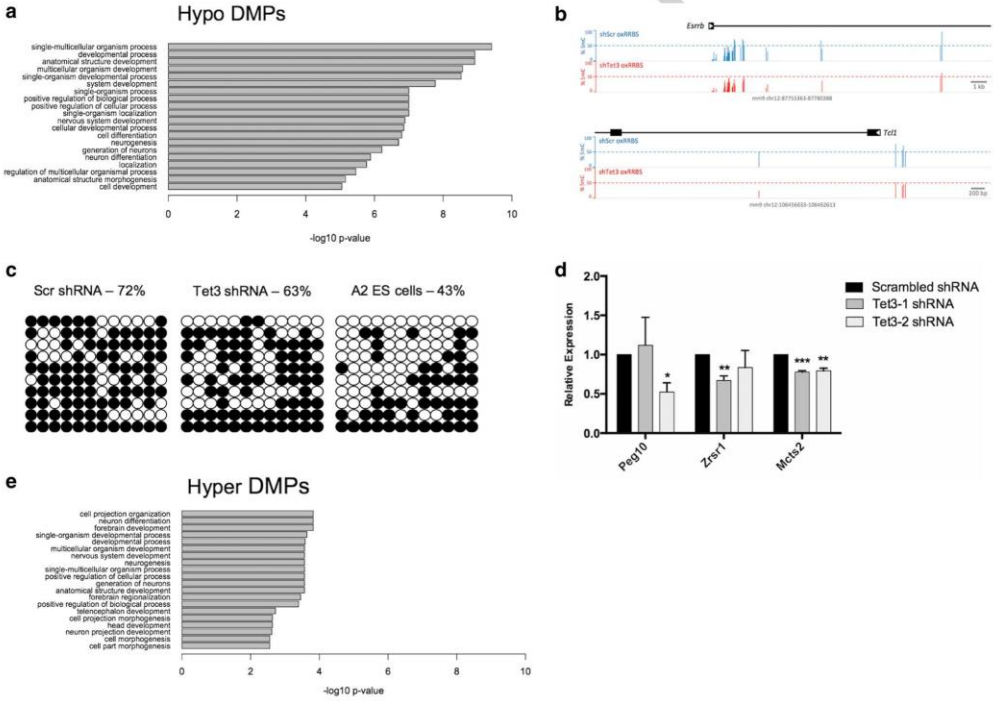

Fig. 4 *Tet3* knockdown alters DNA methylation of developmentally relevant gene promoters. **a** Gene Ontology analysis of genes that loose methylation (Hypo DMPs) shows an association with development, differentiation and neurogenesis. **b** Genome browser snapshots of oxRRBS data at *Esrrb* and *Tcl1* pluripotency genes, showing a reduction in 5mC levels after *Tet3* KD. **c** *Tcl1* bisulfite cloning analysis; black circles—methylated CpGs; white circles—unmethylated CpGs. **d** Expression analysis of imprinted genes showing hypermethylation after Tet3 KD (*$p<0.05$; ***$p<0.001$; *t* test); $n=2$ independent experiments. **e** Gene Ontology analysis of genes that gain methylation (Hyper DMPs) shows an association with neural differentiation processes

Journal : Large 18	Article No : 3335	Pages : 13	MS Code : 3335	Dispatch : 17-10-2019

Author Proof

Discussion

Several studies have previously addressed the role of TET1 in the brain, showing that it regulates processes such as memory and cognition, as well as expression of neuronal activity-regulated genes and hippocampal neurogenesis [17–19]. However, the role of TET3 in the nervous system remains largely unexplored. Here, we investigated the role of *Tet3* in NPCs, using a stable and inducible RNAi knockdown system and an in vitro neural differentiation protocol. Surprisingly, we observed that the knockdown of *Tet3* leads to de-repression of pluripotency genes and appearance of OCT4-positive aggregates of cells, suggesting that a reprogramming event is taking place in these cells. Indeed, when we analysed 5mC changes, we observed a dramatic genome-wide loss of methylation in *Tet3* KD NPCs. Hypomethylated CpGs were localized in genes involved in development, differentiation and neurogenesis. Loss of methylation was also observed in *Tcl1* and *Esrrb* pluripotency-associated genes suggesting a connection between loss of methylation, de-repression of pluripotency genes and de-differentiation of NPCs. A recent report on genome-wide DNA methylation in NPCs has shown an extensive demethylation from E18.5 NPCs relative to E11.5 NPCs, whereas only 1.5% of the identified DMRs gained methylation, suggesting that the acquisition of multipotency in E18.5 NPCs is associated with a wide loss of DNA methylation [50]. Furthermore, in mouse ES cells, it has been shown that *Tet2* knockdown results in both loss of 5hmC and 5mC at DMRs and promoters, while only few DMRs show the expected loss of 5hmC and gain of 5mC [51]. More recently, another study from the Rao lab reported that TET deficiency in diverse cell types resulted in localized increases in DNA methylation in active euchromatic regions, concurrently with unexpected losses of DNA methylation and reactivation of repeat elements [52].

Interestingly, we observed hypermethylation at three imprinted genes after *Tet3* knockdown. It had previously been shown that *Tet1* is necessary to induce 5mC oxidation at imprinting control regions (ICRs) of *H19/IGF2*, *PEG3* and *SNRPN/SNURF* imprinted genes, in a cell-fusion-mediated pluripotency reprogramming model [53]. Another study has shown that heterozygous offspring of *Tet1/Tet2* double knockout (DKO) mice show increased methylation levels across 94 ICRs, including *Peg10*, *Zrsr1* and *Mcts2* [54].

A critical role for *Tet3* in neural progenitor cell maintenance and terminal differentiation of neurons has been reported before [29]. As in our study, the authors observed an upregulation of *Tet3* upon neural differentiation and that *Tet3* KO in NPCs did not change expression of neural markers, such as *Pax6* and *Nestin*. Here, we also observed that neural markers are not altered, but pluripotency markers are de-repressed in *Tet3* KD NPCs, which suggests that the cells undergo de-differentiation upon downregulation of *Tet3* expression. We also observed that *Tet3* KD NPCs undergo a genome-scale loss of methylation, which is in contrast to what would be expected considering this enzyme as a demethylating agent. Indeed, we also observed hypermethylation, but in a more restricted number of sites, which are preferentially located in neuronal-related genes. The observed loss of methylation could potentially be caused by the concomitant decrease in *Dnmt3a* expression, which is a de novo methyltransferase playing a pivotal role in the nervous system [55, 56]. In fact, a functional interplay between TET1 and DNMT3A was shown in mouse embryonic stem cells [57]. Another interesting and perhaps more plausible explanation for the observed global demethylation might resides in the fact that TET enzymes might actually function as guides for de novo DNA methylation [58, 59]. In this context, it was reported that, in zygotes, *Tet3* might have a function in targeting de novo methylation activities, whereby *Tet3*-driven hydroxylation is predominantly implicated in the protection of the newly acquired hypomethylated state from accumulating new DNA methylation [58].

Intriguingly, Hahn and collaborators reported that functional perturbation of *Tet2* and *Tet3* in the embryonic cortex led to defects in neuronal differentiation with abnormal accumulation of cell clusters along the radial axis in the intermediate and ventricular zones [16]. Clustered cells did not express neuronal marker *B3-Tubulin* and some of the cells showed expression of *Nestin* in their processes, suggesting a defect in the progression of differentiation. This is in line with our observation that *Tet3* KD NPCs form clusters of cells that resemble ES-colonies and are OCT4-positive. Additionally, TET3 has been implicated in regulation of synaptic transmission [60, 61] and fear-extinction memory [21], which suggests a pivotal role in the nervous system.

In conclusion, our findings suggest that TET3 acts as a regulator of neural cell identity by maintaining DNA methylation levels in neural precursor cells.

Experimental procedures

Embryonic stem cell culture and neural differentiation

A2lox.cre mouse embryonic stem cells [23], were expanded on feeder cells (SNL767 feeder cell line, kindly provided by the Wellcome Trust Sanger Institute, UK) in complete ES medium–DMEM (4500 mg/L glucose; Gibco) supplemented with 110 mg/L sodium pyruvate (Gibco), 2 mM L-Glutamine

UNCORRECTED PROOF

Journal : Large 18	Article No : 3335	Pages : 13	MS Code : 3335	Dispatch : 17-10-2019

Author Proof

(Gibco), 15% fetal bovine serum (Gibco, ES-cell tested), 1 × penicillin/streptomycin (Gibco), 0.1 mM MEM non-essential amino acids (Gibco) and 10^3 U/ml LIF (ESGRO Millipore).

Neural differentiation of embryonic stem cells was performed as previously described [25]. Briefly, A2lox.cre ES cells (passage 17) containing shRNAs for *Tet3* were cultured on feeders for three passages and on 0.2% gelatine (Sigma) for another three passages. Subsequently, 4×10^6 cells were plated onto bacterial non-adherent dishes (Greiner) for formation of non-adherent cellular aggregates (CA) in CA medium (DMEM 4500 mg/L glucose supplemented with 110 mg/L sodium pyruvate, 2 mM L-Glutamine, 10% fetal bovine serum, 1× penicillin/streptomycin and 0.1 mM MEM non-essential amino acids). CA medium was changed every other day and 5 µM of retinoic acid (RA; Sigma) was added from day 4 to day 8. CAs were then dissociated with freshly prepared Trypsin 0.05% (Sigma, powder) in 0.05% EDTA/PBS and plated onto Poly-DL-Ornithine and laminin-coated plates in N2 medium [DMEM/F12/Glutamax medium supplemented with 1x Penicillin–Streptomycin, 1× N2 supplement (Gibco) and 50 µg/mL BSA (Sigma)]. After 2 days, the medium was changed to a complete medium (N2B27: Neurobasal medium (Gibco), supplemented with 1× GlutaMAX (Gibco), 1x Penicillin–Streptomycin, 1× N2 supplement, 1x N2B27 supplement (Gibco)).

Stable and inducible knockdown system

We used a stable and inducible knockdown system previously described by Iacovino and collaborators [23]. Briefly, shRNA-mir cassettes for *Tet3* gene (sequences on supplementary Table S1) were amplified from pSM2 retroviral vectors containing the shRNAmir sequences (Open Biosystems) and cloned into the p2Lox vector using HindII and NotI restriction sites. The p2Lox derivatives were transfected into the A2lox.cre ES cells (derived from the E14 male cell line strain 129P2/OlaHsd) expressing Cre after addition of doxycycline (0.5 µg/ml) to the medium 1 day before transfection. ES cells were transfected using Lipofectamine 2000 (Invitrogen) at a concentration of 5×10^5 cells/ml. One day after transfection, selection medium containing geneticin (G418, Melford—300 µg/ml active concentration) was added to the cells during 10 days. After selection, ES cell clones containing the shRNAmir were expanded in ES complete medium and neural differentiation was performed as described above. For shRNA expression, doxycycline (2 µg/ml) was added to the medium during 5 days. An ES clone containing eGFP was used to control for positive induction after doxycycline addition. After these 5 days, the cells were trypsinized and the pellet was stored at − 80 °C until DNA/RNA/Protein extraction.

Quantitative reverse transcription PCR

RNA was extracted using the AllPrep DNA/RNA mini kit (Qiagen) and cDNA was synthesized from 200 ng of RNA using the qScript cDNA Supermix (Quanta Biosciences). cDNA was diluted 1:10 and used as template for quantitative real-time PCR reactions using the 5x HOT FIREPol EvaGreen qPCR supermix (Solis Biodyne) and primers designed to specifically amplify each gene of interest (Supplementary Table S2). Cycling reactions were performed in duplicate and cycle threshold (Ct) fluorescence data recorded on Applied Biosystems 7500 Fast Real-time PCR System. The relative abundance of each gene of interest was calculated on the basis of the Delta Delta Ct method [62], where results were normalized to two housekeeping genes (*Atp5b* and *Hsp90ab1*). Statistical analysis was performed by multiple t tests using GraphPad Prism version 6.0 for Mac (GraphPad Software, La Jolla, CA, USA).

Immunofluorescence microscopy and image analysis

Antibody staining of DNA methylation and hydroxymethylation was performed as previously described [24], with few modifications. Briefly, neural precursor cells were plated on glass coverslips and fixed with 2% paraformaldehyde for 30 min at room temperature (RT). Cells were permeabilised with phosphate-buffered saline (PBS) 0.5% Triton X-100 and treated with 2 N HCl for 30 min at RT. The coverslips were washed in PBS 0.05% Tween-20 (PBST) and blocked overnight in PBST with 1% bovine serum albumin (BSA) (BS). Cells were incubated with both primary antibodies rabbit anti-5hmC (1:500, Active Motif, 39792) and mouse anti-5mC (1:250, Eurogentec, BS-Mecy-0100) for 1 h at RT. For antibody staining of pluripotency and neuronal markers, cells were incubated with blocking buffer (BS) for 1 h at RT before incubation with primary antibodies overnight at 4 °C. Primary antibodies were rabbit anti-PAX6 (1:250, Millipore, AB2237), mouse anti-NESTIN (1:200, Millipore MAB353), rabbit anti-OCT4 (1:750, Abcam, ab18976), rabbit anti-SOX2 (1:1000, Abcam, ab97959), mouse anti-beta III tubulin (1:100, Millipore, MAB1637) and rabbit anti-TET3 (1:100, Abcam, 139805). After washing with BS for 1 h at RT, primary antibody staining was revealed with appropriate Alexa-Fluor-conjugated secondary antibodies (1:500, Molecular Probes). For both procedures, the nuclei were counterstained with DAPI. After washing with PBST, cells were mounted with Immu-mount (Thermo Scientific). Images were acquired on an Olympus BX61 or Olympus FV1000 (Japan) confocal microscope and analysed using ImageJ software®.

UNCORRECTED PROOF

Journal : Large 18 | Article No : 3335 | Pages : 13 | MS Code : 3335 | Dispatch : 17-10-2019

Author Proof

Western blot for detection of TET3

Protein was extracted using the AllPrep DNA/RNA mini kit (Qiagen) and resuspended in 5% SDS. The protein concentration of the supernatants was determined using BCA kit (Pierce). Total lysates of 14 µg of protein were denatured in NuPage LDS sample buffer and NuPage reducing reagent by heating for 10 min at 95 °C. Proteins were separated on NuPage 4–12% Bis–Tris gels using MOPS running buffer (Thermofisher). Wet transfer onto a nitrocelulose membrane (Amersham Biosciences) was performed using MOPS running buffer with 20% methanol. Membranes were blocked with 10% milk/1% BSA in Tris-buffered saline (TBS)/0.1%Tween (TBS-T) overnight at 4 °C. Primary antibodies mouse anti-TET3 (1:1000, Abcam, ab174862) and mouse anti-α-Tubulin (1:5000, Sigma-Aldrich, T6074) diluted in blocking buffer and incubated 2 h at RT. Membranes were washed in TBS/T and incubated with the secondary antibody coupled to horseradish peroxidase (BioRad) 1 h at RT. The bound antibodies were visualized by chemiluminescence using ImageQuant LAS4000 mini (GE Healthcare). Bands were analysed using ChemiDoc (Bio-Rad) and quantification was performed with ImageLab software (Bio-Rad). α-Tubulin was used as loading control.

Dotblot and ELISA analysis of 5hmC

DNA was extracted using the AllPrep DNA/RNA mini kit (Qiagen). Genomic DNA (100 ng) was denatured at 99 °C for 5 min and spotted on nitrocellulose blotting membranes (Amersham Hybond-N+). The membrane was UV-crosslinked for 2 min and then blocked in 10% milk/1% BSA in PBST overnight at 4 °C. The membranes were then incubated with rabbit anti-5hmC (1:500, Active Motif, 39769) for 1 h at RT. After washes with PBST (PBS 0.1% Tween-20), membranes were incubated with 1:10,000 dilution of HRP-conjugated anti-rabbit, washed with PBST and then treated with Amersham ECL (GE Healthcare). Dot blot intensities were analysed using ChemiDoc (Bio-Rad) and quantification was performed with ImageLab software (Bio-Rad).

The global level of 5-hmC was also assessed using Quest 5-hmC DNA ELISA Kit (Zymo Research). The procedure was followed according to the manufacturer's instructions, loading 100 ng of DNA per well.

Cell cycle analysis using flow cytometry for propidium iodide staining

For cell cycle analysis, NPCs were dissociated with Accutase (Sigma-Aldrich) for 10 min and re-suspended in 70% ethanol and kept at − 20 °C for 24 h for fixation. After fixation, cells were washed in 1× PBS and incubated with PI staining solution—Propidium Iodide 20 µg/ml (eBioscience) in PBS/0.1% Triton-X 100 and RNase 0.25 mg/ml (Invitrogen)—for 1 h at room temperature in the dark. Cell staining was then analysed by flow cytometry in a BD LSRII flow cytometer (BD Biosciences; 20,000 events). Analysis of the cell cycle was performed with ModFit LT (Verity Software House).

Genome-wide analysis of DNA methylation and hydroxymethylation by oxRRBS

Genomic DNA was isolated using the Qiagen AllPrep DNA/RNA Mini kit (Qiagen) following manufacturers' instructions. Oxidative Reduced Representation Bisulfite Sequencing (oxRRBS) was used for genome-wide analysis of DNA methylation and hydroxymethylation. This method relies on oxidation of DNA prior to bisulfite treatment to convert 5-hydroxymethylcytosine (5hmC) into 5-formylcytosine (5fC) which in turn will be converted to uracil (thymine after PCR amplification) (Fig. 4). 5-methylcytosine (5mC) remains unchanged after oxidation and bisulfite treatment and unmethylated cytosines will be converted to uracil (thymine after PCR amplification). By subtracting the two libraries, it is then possible to infer 5mC and 5hmC levels at a single-base resolution and in a quantitative manner [35].

Briefly, 100 ng of DNA were digested with MspI restriction enzyme and the reaction was cleaned up with AMPure XP beads (Agencourt). A library was then prepared with the NEBNext Ultra DNA library Prep for Illumina (NEB) for End repair, A-tailing and ligation of methylated adaptors (NEBNext, E7535), according to manufacturer's' instructions. Oxidation of the DNA was then carried out starting by purifying DNA in a Micro Bio-Spin column (BioRad), denaturing DNA with NaOH and adding 2 µL of Potassium Perruthenate (KRuO4, Alfa Aeser) solution (15 mM in 0.05 M NaOH). The reaction was held on ice for 1 h, purified with Micro Bio-Spin column (BioRad) and subjected to bisulfite treatment using the Qiagen Epitect kit, according to the manufacturer's instructions for FFPE samples, except that the thermal cycle was run twice over. Final library amplification (18 cycles) was performed using Pfu Turbo Cx (Agilent) and adaptor-specific primers (barcoded TruSeq primers, Illumina), after which the libraries were purified using AMPure XP beads (Agencourt). To check for oxidation success, a spike-in control was added before oxidation step and amplified and digested with TaqI restriction enzyme at the end of library amplification.

Sequencing and data processing

Sequencing (single-end, 75 bp reads) was performed on the Illumina NextSeq platform, high-throughput mode. Quality control of sequencing reads was performed with FASTQC

UNCORRECTED PROOF

(Babraham Bioinformatics). Trimming of the reads to remove adaptors and low-quality bases was performed using Trim-Galore with –rrbs option (Babraham Bioinformatics). The alignment was performed using Bismark with bowtie2 and methylation extraction with the options -s –comprehensive [63]. SeqMonk (Babraham Bioinformatics) and the R-package Methylkit [64] were used for downstream analysis.

DMPs were detected using the Methylkit [64]. We overlapped DMPs with genomic features. Promoters were defined − 1 kb to + 0.5 kb from mRNA TSSs (and deduplicated if > 50% overlapped), CpG islands are from Illingworth et al. [65] and enhancers are from ChIA-PET data [66]. Gene ontology analyses were performed using the topGO R package, focusing on biological process terms.

All sequencing data are available under Gene Expression Omnibus (GEO) accession number GSE123110.

Gene-specific methylation levels by standard bisulfite sequencing

Genomic DNA was isolated using the AllPrep DNA/RNA Minikit (Qiagen) following manufacturers' instructions. Five hundred nanograms of DNA were subjected to bisulfite treatment using the Epitect Bisulfite Kit (Qiagen). A CpG island on intron 1 of *Tcl1* gene (chromosome position 12:106,460,347–106,460,634, NCBI37 (mm9) mouse reference genome) was amplified using primers described in supplementary table S2 and HostStar MasterMix (Qiagen) with the following cycling conditions: 95 °C for 15 min followed by 35 cycles of 95 °C for 1 min, 58 °C for 1 min and 72 °C for 1 min, with a final extension of 72 °C for 20 min. PCR products were then cloned using the TOPO TA Cloning kit for sequencing (Invitrogen) and NZYalpha competent cells (NZYtech). Ten clones for each sample were picked and plasmid DNA amplified using M13 primers. PCR products for each clone were sequenced using the BigDye Terminator v3.1 cycle sequencing kit (Applied Biosystems) in an ABI 3500 Genetic Analyzer (Applied Biosystems). Only clones with more than 95% non-CpG cytosines converted were considered for the analysis, using BiQ Analyzer Software [67].

Acknowledgments We thank Yves-Alain Barde (Biozentrum, Switzerland) for helping with the neural differentiation protocol, Patrícia Patrício and Belém Marques (ICVS-UM) for helping with propidium iodide flow cytometry and ModFit analysis and Patrícia Monteiro (ICVS-UM) for critical reading of the manuscript.

Author contributions MS, CA and MG performed the experiments and analysed the data; MI and MK contributed with the A2lox.cre ES cell line; WR contributed with the stable and inducible shRNA ES cell clones; MRB performed oxRRBS and bioinformatics analysis and wrote the manuscript; NS, LP, CJM designed the study, analysed the data and wrote the manuscript; all authors revised and approved the final manuscript.

Funding This work was supported by the Portuguese Foundation for Science and Technology (FCT) with a project grant (PTDC/BIA-BCM/121276/2010) to C.J.M. and funded by EpiGeneSys with a Small Collaborative project to M.R.B and L.P. CJ Marques and L Pinto are the recipients of an FCT salary contracts (IF/00047/2012 and CEEC-IND/00371/2017 to C.J.M. and IF/01079/2014 to L.P.). C Antunes is the recipient of a PhD fellowship from the Doctoral Program PhDOC from FCT (PD/BD/106049/2015). M.R.B. is a Sir Henry Dale Fellow (101225/Z/13/Z), jointly funded by the Wellcome Trust and the Royal Society. This work has also been funded by Northern Portugal Regional Operational Programme (NORTE 2020), under the Portugal 2020 Partnership Agreement, through the European Regional Development Fund (FEDER; NORTE-01-0145-FEDER-000013); FEDER funds, through the Competitiveness Factors Operational Programme (COMPETE), and National Funds, through the FCT (POCI-01-0145-FEDER-007038).

References

1. Bird A (2002) DNA methylation patterns and epigenetic memory. Genes Dev 16(1):6–21. https://doi.org/10.1101/gad.947102
2. Seisenberger S, Peat JR, Hore TA, Santos F, Dean W, Reik W (2013) Reprogramming DNA methylation in the mammalian life cycle: building and breaking epigenetic barriers. Philos Trans R Soc Lond B Biol Sci 368(1609):20110330. https://doi.org/10.1098/rstb.2011.0330
3. Guo JU, Ma DK, Mo H, Ball MP, Jang MH, Bonaguidi MA, Balazer JA, Eaves HL, Xie B, Ford E, Zhang K, Ming GL, Gao Y, Song H (2011) Neuronal activity modifies the DNA methylation landscape in the adult brain. Nat Neurosci 14(10):1345–1351. https://doi.org/10.1038/nn.2900
4. Ma DK, Jang MH, Guo JU, Kitabatake Y, Chang ML, Pow-Anpongkul N, Flavell RA, Lu B, Ming GL, Song H (2009) Neuronal activity-induced Gadd45b promotes epigenetic DNA demethylation and adult neurogenesis. Science 323(5917):1074–1077. https://doi.org/10.1126/science.1166859
5. Ito S, Shen L, Dai Q, Wu SC, Collins LB, Swenberg JA, He C, Zhang Y (2011) Tet proteins can convert 5-methylcytosine to 5-formylcytosine and 5-carboxylcytosine. Science 333(6047):1300–1303. https://doi.org/10.1126/science.1210597
6. Pfaffeneder T, Hackner B, Truss M, Munzel M, Muller M, Deiml CA, Hagemeier C, Carell T (2011) The discovery of 5-formylcytosine in embryonic stem cell DNA. Angew Chem 50(31):7008–7012. https://doi.org/10.1002/anie.201103899
7. Kriaucionis S, Heintz N (2009) The nuclear DNA base 5-hydroxymethylcytosine is present in Purkinje neurons and the brain. Science 324(5929):929–930. https://doi.org/10.1126/science.1169786
8. Tahiliani M, Koh KP, Shen Y, Pastor WA, Bandukwala H, Brudno Y, Agarwal S, Iyer LM, Liu DR, Aravind L, Rao A (2009) Conversion of 5-methylcytosine to 5-hydroxymethylcytosine in mammalian DNA by MLL partner TET1. Science 324(5929):930–935. https://doi.org/10.1126/science.1170116
9. Hackett JA, Sengupta R, Zylicz JJ, Murakami K, Lee C, Down TA, Surani MA (2013) Germline DNA demethylation dynamics and imprint erasure through 5-hydroxymethylcytosine. Science 339(6118):448–452. https://doi.org/10.1126/science.1229277
10. Iqbal K, Jin SG, Pfeifer GP, Szabo PE (2011) Reprogramming of the paternal genome upon fertilization involves genome-wide oxidation of 5-methylcytosine. Proc Natl Acad Sci USA 108(9):3642–3647. https://doi.org/10.1073/pnas.1014033108
11. Wossidlo M, Nakamura T, Lepikhov K, Marques CJ, Zakhartchenko V, Boiani M, Arand J, Nakano T, Reik W, Walter J (2011) 5-Hydroxymethylcytosine in the mammalian zygote is linked

Author Proof
UNCORRECTED PROOF

Author Proof

with epigenetic reprogramming. Nat Commun 2:241. https://doi.org/10.1038/ncomms1240

12. Guo JU, Szulwach KE, Su Y, Li Y, Yao B, Xu Z, Shin JH, Xie B, Gao Y, Ming GL, Jin P, Song H (2014) Genome-wide antagonism between 5-hydroxymethylcytosine and DNA methylation in the adult mouse brain. Front Biol (Beijing) 9(1):66–74. https://doi.org/10.1007/s11515-014-1295-1
13. Kohli RM, Zhang Y (2013) TET enzymes, TDG and the dynamics of DNA demethylation. Nature 502(7472):472–479. https://doi.org/10.1038/nature12750
14. Ko M, An J, Bandukwala HS, Chavez L, Aijo T, Pastor WA, Segal MF, Li H, Koh KP, Lahdesmaki H, Hogan PG, Aravind L, Rao A (2013) Modulation of TET2 expression and 5-methylcytosine oxidation by the CXXC domain protein IDAX. Nature 497(7447):122–126. https://doi.org/10.1038/nature12052
15. Szwagierczak A, Bultmann S, Schmidt CS, Spada F, Leonhardt H (2010) Sensitive enzymatic quantification of 5-hydroxymethylcytosine in genomic DNA. Nucleic Acids Res 38(19):e181. https://doi.org/10.1093/nar/gkq684
16. Hahn MA, Qiu R, Wu X, Li AX, Zhang H, Wang J, Jui J, Jin SG, Jiang Y, Pfeifer GP, Lu Q (2013) Dynamics of 5-hydroxymethylcytosine and chromatin marks in Mammalian neurogenesis. Cell Rep 3(2):291–300. https://doi.org/10.1016/j.celrep.2013.01.011
17. Kaas GA, Zhong C, Eason DE, Ross DL, Vachhani RV, Ming GL, King JR, Song H, Sweatt JD (2013) TET1 controls CNS 5-methylcytosine hydroxylation, active DNA demethylation, gene transcription, and memory formation. Neuron 79(6):1086–1093. https://doi.org/10.1016/j.neuron.2013.08.032
18. Rudenko A, Dawlaty MM, Seo J, Cheng AW, Meng J, Le T, Faull KF, Jaenisch R, Tsai LH (2013) Tet1 is critical for neuronal activity-regulated gene expression and memory extinction. Neuron 79(6):1109–1122. https://doi.org/10.1016/j.neuron.2013.08.003
19. Zhang RR, Cui QY, Murai K, Lim YC, Smith ZD, Jin S, Ye P, Rosa L, Lee YK, Wu HP, Liu W, Xu ZM, Yang L, Ding YQ, Tang F, Meissner A, Ding C, Shi Y, Xu GL (2013) Tet1 regulates adult hippocampal neurogenesis and cognition. Cell Stem Cell 13(2):237–245. https://doi.org/10.1016/j.stem.2013.05.006
20. Gontier G, Iyer M, Shea JM, Bieri G, Wheatley EG, Ramalho-Santos M, Villeda SA (2018) Tet2 rescues age-related regenerative decline and enhances cognitive function in the adult mouse brain. Cell Rep 22(8):1974–1981. https://doi.org/10.1016/j.celrep.2018.02.001
21. Li X, Wei W, Zhao QY, Widagdo J, Baker-Andresen D, Flavell CR, D'Alessio A, Zhang Y, Bredy TW (2014) Neocortical Tet3-mediated accumulation of 5-hydroxymethylcytosine promotes rapid behavioral adaptation. Proc Natl Acad Sci USA 111(19):7120–7125. https://doi.org/10.1073/pnas.1318906111
22. Bibel M, Richter J, Schrenk K, Tucker KL, Staiger V, Korte M, Goetz M, Barde YA (2004) Differentiation of mouse embryonic stem cells into a defined neuronal lineage. Nat Neurosci 7(9):1003–1009. https://doi.org/10.1038/nn1301
23. Iacovino M, Bosnakovski D, Fey H, Rux D, Bajwa G, Mahen E, Mitanoska A, Xu Z, Kyba M (2011) Inducible cassette exchange: a rapid and efficient system enabling conditional gene expression in embryonic stem and primary cells. Stem Cells 29(10):1580–1588
24. Ficz G, Branco MR, Seisenberger S, Santos F, Krueger F, Hore TA, Marques CJ, Andrews S, Reik W (2011) Dynamic regulation of 5-hydroxymethylcytosine in mouse ES cells and during differentiation. Nature 473(7347):398–402. https://doi.org/10.1038/nature10008
25. Bibel M, Richter J, Lacroix E, Barde Y-A (2007) Generation of a defined and uniform population of CNS progenitors and neurons from mouse embryonic stem cells. Nat Protoc 2(5):1034–1043. https://doi.org/10.1038/nprot.2007.147
26. Menezes JR, Luskin MB (1994) Expression of neuron-specific tubulin defines a novel population in the proliferative layers of the developing telencephalon. J Neurosci 14(9):5399–5416
27. Chew JL, Loh YH, Zhang W, Chen X, Tam WL, Yeap LS, Li P, Ang YS, Lim B, Robson P, Ng HH (2005) Reciprocal transcriptional regulation of Pou5f1 and Sox2 via the Oct4/Sox2 complex in embryonic stem cells. Mol Cell Biol 25(14):6031–6046. https://doi.org/10.1128/MCB.25.14.6031-6046.2005
28. Diaz de Leon-Guerrero S, Pedraza-Alva G, Perez-Martinez L (2011) In sickness and in health: the role of methyl-CpG binding protein 2 in the central nervous system. Eur J Neurosci 33(9):1563–1574. https://doi.org/10.1111/j.1460-9568.2011.07658.x
29. Li T, Yang D, Li J, Tang Y, Yang J, Le W (2015) Critical role of Tet3 in neural progenitor cell maintenance and terminal differentiation. Mol Neurobiol 51(1):142–154. https://doi.org/10.1007/s12035-014-8734-5
30. Tan L, Xiong L, Xu W, Wu F, Huang N, Xu Y, Kong L, Zheng L, Schwartz L, Shi Y, Shi YG (2013) Genome-wide comparison of DNA hydroxymethylation in mouse embryonic stem cells and neural progenitor cells by a new comparative hMeDIP-seq method. Nucleic Acids Res 41(7):e84. https://doi.org/10.1093/nar/gkt091
31. Fu L, Guerrero CR, Zhong N, Amato NJ, Liu Y, Liu S, Cai Q, Ji D, Jin SG, Niedernhofer LJ, Pfeifer GP, Xu GL, Wang Y (2014) Tet-mediated formation of 5-hydroxymethylcytosine in RNA. J Am Chem Soc 136(33):11582–11585. https://doi.org/10.1021/ja505305z
32. Zhang J, Chen S, Zhang D, Shi Z, Li H, Zhao T, Hu B, Zhou Q, Jiao J (2016) Tet3-mediated DNA demethylation contributes to the direct conversion of fibroblast to functional neuron. Cell Rep 17(9):2326–2339. https://doi.org/10.1016/j.celrep.2016.10.081
33. Gu H, Smith ZD, Bock C, Boyle P, Gnirke A, Meissner A (2011) Preparation of reduced representation bisulfite sequencing libraries for genome-scale DNA methylation profiling. Nat Protoc 6(4):468–481. https://doi.org/10.1038/nprot.2010.190
34. Huang Y, Pastor WA, Shen Y, Tahiliani M, Liu DR, Rao A (2010) The behaviour of 5-hydroxymethylcytosine in bisulfite sequencing. PLoS One 5(1):e8888. https://doi.org/10.1371/journal.pone.0008888
35. Booth MJ, Branco MR, Ficz G, Oxley D, Krueger F, Reik W, Balasubramanian S (2012) Quantitative sequencing of 5-methylcytosine and 5-hydroxymethylcytosine at single-base resolution. Science 336(6083):934–937. https://doi.org/10.1126/science.1220671
36. Booth MJ, Ost TW, Beraldi D, Bell NM, Branco MR, Reik W, Balasubramanian S (2013) Oxidative bisulfite sequencing of 5-methylcytosine and 5-hydroxymethylcytosine. Nat Protoc 8(10):1841–1851. https://doi.org/10.1038/nprot.2013.115
37. Meissner A, Mikkelsen TS, Gu H, Wernig M, Hanna J, Sivachenko A, Zhang X, Bernstein BE, Nusbaum C, Jaffe DB, Gnirke A, Jaenisch R, Lander ES (2008) Genome-scale DNA methylation maps of pluripotent and differentiated cells. Nature 454(7205):766–770. https://doi.org/10.1038/nature07107
38. David MD, Canti C, Herreros J (2010) Wnt-3a and Wnt-3 differently stimulate proliferation and neurogenesis of spinal neural precursors and promote neurite outgrowth by canonical signaling. J Neurosci Res 88(14):3011–3023. https://doi.org/10.1002/jnr.22464
39. Lee J, Duan W, Mattson MP (2002) Evidence that brain-derived neurotrophic factor is required for basal neurogenesis and mediates, in part, the enhancement of neurogenesis by dietary restriction in the hippocampus of adult mice. J Neurochem 82(6):1367–1375
40. Ohkubo Y, Uchida AO, Shin D, Partanen J, Vaccarino FM (2004) Fibroblast growth factor receptor 1 is required for the

UNCORRECTED PROOF

proliferation of hippocampal progenitor cells and for hippocampal growth in mouse. J Neurosci 24(27):6057–6069. https://doi.org/10.1523/JNEUROSCI.1140-04.2004
41. Shi Y, Chichung Lie D, Taupin P, Nakashima K, Ray J, Yu RT, Gage FH, Evans RM (2004) Expression and function of orphan nuclear receptor TLX in adult neural stem cells. Nature 427(6969):78–83. https://doi.org/10.1038/nature02211
42. Theriault FM, Nuthall HN, Dong Z, Lo R, Barnabe-Heider F, Miller FD, Stifani S (2005) Role for Runx1 in the proliferation and neuronal differentiation of selected progenitor cells in the mammalian nervous system. J Neurosci 25(8):2050–2061. https://doi.org/10.1523/JNEUROSCI.5108-04.2005
43. Borrell V, Cardenas A, Ciceri G, Galceran J, Flames N, Pla R, Nobrega-Pereira S, Garcia-Frigola C, Peregrin S, Zhao Z, Ma L, Tessier-Lavigne M, Marin O (2012) Slit/Robo signaling modulates the proliferation of central nervous system progenitors. Neuron 76(2):338–352. https://doi.org/10.1016/j.neuron.2012.08.003
44. Yamaguchi S, Shen L, Liu Y, Sendler D, Zhang Y (2013) Role of Tet1 in erasure of genomic imprinting. Nature 504(7480):460–464. https://doi.org/10.1038/nature12805
45. Montalban-Loro R, Lozano-Urena A, Ito M, Krueger C, Reik W, Ferguson-Smith AC, Ferron SR (2019) TET3 prevents terminal differentiation of adult NSCs by a non-catalytic action at Snrpn. Nat Commun 10(1):1726. https://doi.org/10.1038/s41467-019-09665-1
46. de Melo J, Du G, Fonseca M, Gillespie LA, Turk WJ, Rubenstein JL, Eisenstat DD (2005) Dlx1 and Dlx2 function is necessary for terminal differentiation and survival of late-born retinal ganglion cells in the developing mouse retina. Development 132(2):311–322. https://doi.org/10.1242/dev.01560
47. Di Giovannantonio LG, Di Salvio M, Acampora D, Prakash N, Wurst W, Simeone A (2013) Otx2 selectively controls the neurogenesis of specific neuronal subtypes of the ventral tegmental area and compensates En1-dependent neuronal loss and MPTP vulnerability. Dev Biol 373(1):176–183. https://doi.org/10.1016/j.ydbio.2012.10.022
48. Munji RN, Choe Y, Li G, Siegenthaler JA, Pleasure SJ (2011) Wnt signaling regulates neuronal differentiation of cortical intermediate progenitors. J Neurosci 31(5):1676–1687. https://doi.org/10.1523/JNEUROSCI.5404-10.2011
49. Vaghi V, Pennucci R, Talpo F, Corbetta S, Montinaro V, Barone C, Croci L, Spaiardi P, Consalez GG, Biella G, de Curtis I (2014) Rac1 and rac3 GTPases control synergistically the development of cortical and hippocampal GABAergic interneurons. Cereb Cortex 24(5):1247–1258. https://doi.org/10.1093/cercor/bhs402
50. Sanosaka T, Imamura T, Hamazaki N, Chai M, Igarashi K, Ideta-Otsuka M, Miura F, Ito T, Fujii N, Ikeo K, Nakashima K (2017) DNA methylome analysis identifies transcription factor-based epigenomic signatures of multilineage competence in neural stem/progenitor cells. Cell Rep 20(12):2992–3003. https://doi.org/10.1016/j.celrep.2017.08.086
51. Huang Y, Chavez L, Chang X, Wang X, Pastor WA, Kang J, Zepeda-Martinez JA, Pape UJ, Jacobsen SE, Peters B, Rao A (2014) Distinct roles of the methylcytosine oxidases Tet1 and Tet2 in mouse embryonic stem cells. Proc Natl Acad Sci USA 111(4):1361–1366. https://doi.org/10.1073/pnas.1322921111
52. Lopez-Moyado IF, Tsagaratou A, Yuita H, Seo H, Delatte B, Heinz S, Benner C, Rao A (2019) Paradoxical association of TET loss of function with genome-wide DNA hypomethylation. Proc Natl Acad Sci USA. https://doi.org/10.1073/pnas.1903059116
53. Piccolo FM, Bagci H, Brown KE, Landeira D, Soza-Ried J, Feytout A, Mooijman D, Hajkova P, Leitch HG, Tada T, Kriaucionis S, Dawlaty MM, Jaenisch R, Merkenschlager M, Fisher AG (2013) Different roles for Tet1 and Tet2 proteins in reprogramming-mediated erasure of imprints induced by EGC fusion. Mol Cell 49(6):1023–1033. https://doi.org/10.1016/j.molcel.2013.01.032
54. Dawlaty MM, Breiling A, Le T, Raddatz G, Barrasa MI, Cheng AW, Gao Q, Powell BE, Li Z, Xu M, Faull KF, Lyko F, Jaenisch R (2013) Combined deficiency of Tet1 and Tet2 causes epigenetic abnormalities but is compatible with postnatal development. Dev Cell. https://doi.org/10.1016/j.devcel.2012.12.015
55. Feng J, Chang H, Li E, Fan G (2005) Dynamic expression of de novo DNA methyltransferases Dnmt3a and Dnmt3b in the central nervous system. J Neurosci Res 79(6):734–746. https://doi.org/10.1002/jnr.20404
56. Wu Z, Huang K, Yu J, Le T, Namihira M, Liu Y, Zhang J, Xue Z, Cheng L, Fan G (2012) Dnmt3a regulates both proliferation and differentiation of mouse neural stem cells. J Neurosci Res 90(10):1883–1891. https://doi.org/10.1002/jnr.23077
57. Gu T, Lin X, Cullen SM, Luo M, Jeong M, Estecio M, Shen J, Hardikar S, Sun D, Su J, Rux D, Guzman A, Lee M, Qi LS, Chen JJ, Kyba M, Huang Y, Chen T, Li W, Goodell MA (2018) DNMT3A and TET1 cooperate to regulate promoter epigenetic landscapes in mouse embryonic stem cells. Genome Biol 19(1):88. https://doi.org/10.1186/s13059-018-1464-7
58. Amouroux R, Nashun B, Shirane K, Nakagawa S, Hill PW, D'Souza Z, Nakayama M, Matsuda M, Turp A, Ndjetehe E, Encheva V, Kudo NR, Koseki H, Sasaki H, Hajkova P (2016) De novo DNA methylation drives 5hmC accumulation in mouse zygotes. Nat Cell Biol 18(2):225–233. https://doi.org/10.1038/ncb3296
59. Hill PWS, Leitch HG, Requena CE, Sun Z, Amouroux R, Roman-Trufero M, Borkowska M, Terragni J, Vaisvila R, Linnett S, Bagci H, Dharmalingham G, Haberle V, Lenhard B, Zheng Y, Pradhan S, Hajkova P (2018) Epigenetic reprogramming enables the transition from primordial germ cell to gonocyte. Nature 555(7696):392–396. https://doi.org/10.1038/nature25964
60. Wang L, Li MY, Qu C, Miao WY, Yin Q, Liao J, Cao HT, Huang M, Wang K, Zuo E, Peng G, Zhang SX, Chen G, Li Q, Tang K, Yu Q, Li Z, Wong CC, Xu G, Jing N, Yu X, Li J (2017) CRISPR-Cas9-mediated genome editing in one blastomere of two-cell embryos reveals a novel Tet3 function in regulating neocortical development. Cell Res 27(6):815–829. https://doi.org/10.1038/cr.2017.58
61. Yu H, Su Y, Shin J, Zhong C, Guo JU, Weng YL, Gao F, Geschwind DH, Coppola G, Ming GL, Song H (2015) Tet3 regulates synaptic transmission and homeostatic plasticity via DNA oxidation and repair. Nat Neurosci 18(6):836–843. https://doi.org/10.1038/nn.4008
62. Livak KJ, Schmittgen TD (2001) Analysis of relative gene expression data using real-time quantitative PCR and the 2(-Delta Delta C(T)) Method. Methods 25(4):402–408. https://doi.org/10.1006/meth.2001.1262
63. Krueger F, Andrews SR (2011) Bismark: a flexible aligner and methylation caller for Bisulfite-Seq applications. Bioinformatics 27(11):1571–1572. https://doi.org/10.1093/bioinformatics/btr167
64. Akalin A, Kormaksson M, Li S, Garrett-Bakelman FE, Figueroa ME, Melnick A, Mason CE (2012) methylKit: a comprehensive R package for the analysis of genome-wide DNA methylation profiles. Genome Biol 13(10):R87. https://doi.org/10.1186/gb-2012-13-10-r87
65. Illingworth RS, Gruenewald-Schneider U, Webb S, Kerr AR, James KD, Turner DJ, Smith C, Harrison DJ, Andrews R, Bird AP (2010) Orphan CpG islands identify numerous conserved promoters in the mammalian genome. PLoS Genet 6(9):e1001134. https://doi.org/10.1371/journal.pgen.1001134

Author Proof
UNCORRECTED PROOF

Neuroscience and Biobehavioral Reviews 102 (2019) 337–344

Contents lists available at ScienceDirect

Neuroscience and Biobehavioral Reviews

journal homepage: www.elsevier.com/locate/neubiorev

TET enzymes in neurophysiology and brain function

Cláudia Antunes[a,b], Nuno Sousa[a,b], Luisa Pinto[a,b,*], C. Joana Marques[c,d,*]

[a] Life and Health Sciences Research Institute (ICVS), School of Medicine, University of Minho, Campus Gualtar, Braga 4710-057, Portugal
[b] ICVS/3B's-PT Government Associate Laboratory, Braga/Guimarães, Portugal
[c] Department of Genetics, Faculty of Medicine, University of Porto, 4200-319 Porto, Portugal
[d] i3S-Instituto de Investigação e Inovação em Saúde, Universidade do Porto, 4200-135 Porto, Portugal

ARTICLE INFO

Keywords:
Neuronal plasticity
Behavior
Epigenetics
TET enzymes
5hmC

ABSTRACT

The dynamic nature of epigenetic DNA modifications is crucial for regulating gene expression in an experience-dependent manner and, thus, a potential mediator of neuronal plasticity and behavior. The discovery of the involvement of 5-hydroxymethylcytosine (5hmC) and Ten Eleven Translocation (TET) family of enzymes in the demethylation pathway uncovered a potential link between neuronal TET protein function and cognitive processes. In this review, we provide an overview on how profile of 5hmC and TET enzymes are powerful mechanisms to explain neuronal plasticity and long-term behaviors, such as cognition. More specifically, we discuss how the current knowledge integrates the function of each TET enzyme in neurophysiology and brain function.

1. Introduction

Given the post-mitotic nature of mature differentiated neurons, which are long-lived cells, there is a constant challenge to maintain genomic stability within a context of high plasticity that permits adaptation to diverse stimuli. Long-lasting changes in synaptic plasticity are dynamic processes which regulate higher functions, such as learning and memory, that require a tight regulation of gene expression. Epigenetic marks, consisting of chemical modifications on the DNA and histone tails, regulate the binding of transcription factors by modulating their accessibility to genomic regulatory regions. At the DNA level, site-specific modifications catalyzed by DNA methyltransferases (DNMTs) and TET enzymes subsequently affect the assembly of proteins that recognize methylated/demethylated bases (Pastor et al., 2013). Hence, epigenetic mechanisms and the neuronal epigenome constitute a valuable tool for marking past, current and future actions.

One of the most well studied epigenetic modifications is DNA methylation, which occur at the 5-carbon position of cytosine (C) residues and is located mainly at CpG dinucleotides. CpG sites are usually methylated but when occurring in CG-dense regions, termed CpG islands and associated with gene promoters, are largely resistant to DNA methylation (Smith and Meissner, 2013); nevertheless, methylation at these regions is usually associated with gene repression, acting to lock in the silent state (Deaton and Bird, 2011). DNA Methylation is also observed, albeit less frequently, in non-CpG contexts, known as CpH dinucleotides (H = A/T/C), and the function of non-CpG methylation is suggested to be repressive as well (Guo et al., 2014). Importantly, neurons (and embryonic stem cells) have a high amount of non-CpG methylation compared with other tissues, but the specific meaning of this fact remains to be clarified (Shin et al., 2014). However, Guo and colleagues showed that non-CpG methylation supports nearby CpG methylation by the recruitment of methyl-binding proteins and consequent suppressing of transcriptional activities *in vivo* (Guo et al., 2014).

DNA methylation is distributed throughout the mammalian genome and plays a crucial role in various biological functions, such as transposon silencing, genomic imprinting and X-chromosome inactivation, amongst others (Bird, 2002). Although DNA methylation is regarded as a stable feature, 5-methylcytosine (5mC) can be converted to 5-hydroxymethylcytosine (5hmC) by the Ten-Eleven Translocation (TET) family of enzymes, a process thought to be involved in the DNA demethylation process (Branco et al., 2011). Importantly, DNA methylation and hydroxymethylation have been implicated in neurophysiological processes, but also in neuropathology (Day and Sweatt, 2011; Sweatt, 2013). While 5mC levels are similar in the brain and other organs, the 5hmC modification is singularly enriched in the CNS, being up to ten times more abundant in the CNS than in peripheral tissues (Globisch et al., 2010; Kriaucionis and Heintz, 2009; Munzel et al., 2010; Szwagierczak et al., 2010). Mature neurons seem to be the major

* Corresponding authors at: Department of Genetics, Faculty of Medicine of Porto, Alameda Professor Hernâni Monteiro, 4200-319 Porto, Portugal and Life and Health Sciences Research Institute (ICVS), School of Medicine, University of Minho, Campus Gualtar, Braga 4710-057, Portugal.
E-mail addresses: luisapinto@med.uminho.pt (L. Pinto), cmarques@med.up.pt (C.J. Marques).

https://doi.org/10.1016/j.neubiorev.2019.05.006
Received 5 November 2018; Received in revised form 8 May 2019; Accepted 8 May 2019
Available online 09 May 2019
0149-7634/ © 2019 Elsevier Ltd. All rights reserved.

contributors for 5hmC brain levels, since 5hmC levels are higher in neuronal than in non-neuronal cell types (Cadena-del-Castillo et al., 2014; Szulwach et al., 2011). Consistently, 5hmC levels in the brain greatly increase after birth, a time when synaptogenesis and neuronal maturation occurs, with no concomitant 5mC decrease (Song et al., 2011; Szulwach et al., 2011). 5hmC enrichment at promoters and gene bodies is positively correlated with gene expression levels, being particularly relevant during the postnatal period in the brain (Hahn et al., 2013; Song et al., 2011; Szulwach et al., 2011). Furthermore, 5hmC was shown to increase during development and with aging, in the mouse cerebellum and hippocampus brain regions (Szulwach et al., 2011). In parallel, several brain regions also show elevated levels of *Tet* transcripts (Szwagierczak et al., 2010). Proper synaptic function requires tight regulation of many genes involved in synaptic formation and plasticity (Azpurua and Eaton, 2015). Manipulation of TET enzymes have been shown to interfere with expression and methylation levels of some of these genes, suggesting they can influence synaptic activity through their catalytic demethylating action (Campbell and Wood, 2019). Thus, the abundance and dynamic profile of 5hmC and TET enzymes have been suggested as a powerful mechanism to explain neuronal plasticity and long-term behaviors.

2. TET enzymes in brain function

The TET family of enzymes consists of TET1, TET2 and TET3, all dependent on α-ketoglutarate (α-KG, also called 2-oxoglutarate) and Fe (II) and sharing the ability to convert 5mC to 5hmC (Ito et al., 2010; Pastor et al., 2013). TETs also mediate the oxidation of 5hmC to 5-formylcytosine (5fC) and subsequently to 5-carboxylcytosine (5caC) (Ito et al., 2011), adding another layer of complexity in the efforts to uncover the specific function of these enzymes in the brain. 5fC and 5caC bases are suggested to be intermediates in the DNA demethylation process, since these bases can be subjected to deamination by the glycosylase-dependent excision, mediated by thymine DNA glycosylase (TDG) and consequent repair by base excision repair (BER), resulting in unmodified cytosines (Branco et al., 2011). Also, 5mC and 5hmC bases can be converted to thymine and 5-hydroxymethyluracil (5hmU) respectively, by the action of activation-induced cytidine deaminase/apolipoprotein B mRNA editing enzyme, catalytic polypeptide (AID/APOBEC) cytosine deaminases. TET-induced oxidation is not limited to 5mC but thymine is also a substrate that gives 5hmU at least in mouse embryonic stem cells (Pfaffeneder et al., 2014). Thymine and 5hmU can be further the substrate for DNA glycosylases, such as TDG, strand-selective monofunctional uracil-DNA glycosylase 1 (SMUG), and methyl-CpG- binding domain protein 4 (MBD4) and ultimately, repaired by base excision repair (BER), resulting in unmodified cytosines (Fig. 1). 5hmU base has been reported to affect protein-binding to DNA and may also be an important intermediate in the generation of site-specific mutations (Kawasaki et al., 2017). In the brain, the 5hmC derivatives 5caC and 5fC have also been detected, although at much lower levels than 5hmC (a ratio of ~10,000:11:1 in human brain and ~4700:12:1 in mouse brain, for 5hmC, 5fC and 5caC respectively, was reported) (Liu et al., 2013), their relevance still being largely unknown. Structurally, the three TET enzymes share a conserved C-terminal catalytic domain that contains the metal-binding residues indispensable for the oxidation reaction and a less conserved N-terminal region (Kohli and Zhang, 2013). TET1 and TET3 also contain a N-terminal zinc finger cysteine-X-X-cysteine (CXXC) domain, that binds to methylated and unmethylated CpGs (Xu et al., 2011, 2012; Zhang et al., 2010), and recruits chromatin-modifying activities to CGI elements (Long et al., 2013). Contrarily, TET2 does not possess a CXXC domain but partners with IDAX, an independent CXXC-containing protein (Ko et al., 2013). In fact, human TET enzymes only share 18–24% sequence identity, raising the possibility of a non-redundant role between the three TETs (UniProt Consortium, 2015; Fasolino et al., 2017). Although all TET enzymes present highly conserved catalytic and Cys-rich domains, the CXXC region exhibits differences between proteins. This might suggest specific roles for each TET enzyme according to the DNA sequence context and genomic regions. Biochemical analyses showed that the CXXC domain of TET1 binds unmodified C or 5mC- or 5hmC-modified CpG-rich DNA, suggesting that TET1 also prevents DNA methyltransferase activity at CpG-rich regions (Xu et al., 2011). On the other hand, TET3 CXXC domain binds to both non-CpG and CpG DNA oligos; additionally, the TET3 CXXC domain strongly binds to CmCGG (Xu et al., 2012). Indeed, TET1 primarily regulates 5hmC levels at gene promoters and transcription start sites (TSSs), whereas TET2 mainly regulates 5hmC levels in gene bodies. Interestingly, the TSS localization of TET1 is thought to promote transcriptional activation, supported by its genomic localization primarily at regions with high levels of histones modifications associated with permissive chromatin (Williams et al., 2011; Wu et al., 2011). TET3 ChIP-seq data in NPCs shows that TET3-binding sites also cluster close to TSSs, suggesting that TET1 and TET3 may have similar functions, despite their distinct temporal expression patterns (Li et al., 2016). Therefore, besides their functionally redundant roles in the generation of 5hmC, TET-family members also display distinct roles, in part because they are expressed in different cellular locations or at different developmental stages and regulated 5hmC levels at different genomic locations (Li et al., 2016).

All *Tet* transcripts are present in the brain, with *Tet3* being the most abundant, at least in the cerebellum, cortex, and hippocampus, followed by *Tet2* and *Tet1* (Szwagierczak et al., 2010). All TETs exhibit strong co-localization with the neuronal marker NeuN (Kaas et al., 2013; Li et al., 2014; Mi et al., 2015), suggesting that its abundance is mainly attributed to neuronal cells, which is in line with 5hmC

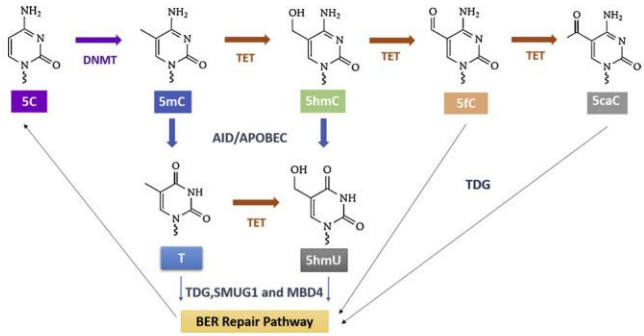

Fig. 1. Potential pathways for **TET-mediated active DNA demethylation cycle -** DNMTs convert unmodified C to 5mC. 5mC can be converted back to unmodified cytosine by TET mediated oxidation to 5hmC, 5fC and 5caC, followed by excision of 5fC or 5caC mediated by TDG coupled with BER. 5mC and 5hmC can be deaminated by AID/APOBEC, giving rise to T and 5hmU respectively, that are recognized by DNA glycosylases, producing an abasic site that is then repaired by the BER machinery. It was shown in mouse ES cells that TET enzymes can also convert T into 5hmU (Pfaffeneder et al., 2014). C, cytosine; 5-mC, 5-methylcytosine; 5-hmC, 5-hydroxymethylcytosine; 5fC, 5-formylcytosine; 5-caC, 5-carboxylcytosine; 5hmU, 5-hydroxymethyluracil; T, Thymine; DNMT, DNA methyltransferase; TET, Ten-eleven translocation enzyme; TDG, thymine DNA glycosylase; BER, base excision repair; AID/APOBEC, activation-induced cytidine deaminase/apolipoprotein B mRNA editing enzyme, catalytic polypeptide-like; SMUG1, strand-selective monofunctional uracil-DNA glycosylase 1; MBD4, methyl-CpG- binding domain protein 4.

Table 1
Phenotypes of full or conditional knockout (cKO) and knockdown (KD) mouse models of TET enzymes in neuronal plasticity and behavior.

Enzyme	Type of deletion	Region/Cell type	Phenotype	Molecular alterations	References
TET1	KO (*in vivo*)	Constitutive	Impairment in memory extinction; enhanced long-term depression (LTD)	Decreased expression of *Arc*, *Npas4*, *c-Fos*; hypermethylation of *Npas4* in the hippocampus and cortex	(Rudenko et al., 2013)
	KO (*in vivo*)	Constitutive	Impairment in spatial learning and short- term memory	Decreased expression and hypermethylation of *Gdi*, *Cpg4* and *Ngb* in TET1 KO NPCs.	(Zhang et al., 2013)
	KO (*in vivo*)	Constitutive	Enhancement in memory consolidation and long-term storage	Decreased expression of *Arc*, *Egr1*, *Npas4* and *c-Fos*; increased expression of *Creb1*, *Bdnf*, *Calcineurin*, *Cdk5*, *N4a2* in the hippocampus CA1 region.	(Kumar et al., 2015)
	KD (*in vivo*)	Dorsal Hippocampus	Enhancement of spatial memory for object location	No analyzes were performed	(Kumar et al., 2015)
	KD (*in vitro*)	Neurons	Increased mEPSC amplitudes	No analyzes were performed	(Yu et al., 2015)
TET2	cKO (*in vivo*)	Adult neural progenitor cells	Impairment of short and long-term learning and memory	No analyzes were performed	(Gontier et al., 2018)
	KD (*in vitro*)	Neurons	Increased mEPSC amplitudes	No analyzes were performed	(Yu et al., 2015)
TET3	KD (*in vivo*)	ILPF cortex	Impairment in fear extinction memory	Inhibition of the increase of expression and 5hmC gain of *Gephyrin* locus in the ILPFC after extinction training	(Li et al., 2014)
	KO (*in vivo; CRISPR-mediated*)	Constitutive (Tet3-mutant chimeras)	Increased mEPSC frequency in CA1 and cortex layer 2/3 neurons and reduced mIPSC frequency and amplitudes	Slight hypermethylation (and decrease in expression) of *Bdnf* IV, IX and *Wfdc2*	(Wang et al., 2017)
	KD (*in vitro*)	Neurons	Increased mEPSC amplitudes	Increased expression of *Glur1* and decreased expression and hypermethylation of *Bdnf* IV	(Yu et al., 2015)

enrichment in these cells (Szulwach et al., 2011); nevertheless, it remains unclear what are the levels of expression in other non-neuronal cells of the CNS. To date, only one report shows TET1 expression in the soma of glial fibrillary acidic protein (GFAP) positive cells, hence identified as astrocytes, in the adult mouse hippocampus (Kaas et al., 2013). Regarding oligodendrocytes, expression of all TET enzymes was detected in the corpus callosum, from embryonic development until P30 (Zhao et al., 2014). The expression from that moment until the adult stage remains to be investigated, as well as its expression in other brain regions.

Since 2011, many studies have shown the importance of TET enzymes in neuronal function, which are summarized in Table 1 and described in detail for each TET enzyme, in the following sections, organized by neurophysiological and behavioral findings.

2.1. TET1

TET1, the first enzyme described as being capable of catalyzing the conversion of 5mC into 5hmC (Tahiliani et al., 2009), is the best-studied TET family member in the brain.

Regarding **neurophysiology**, there are two main studies reporting how TET1 is regulated in basal physiology. Kaas and collaborators observed that *Tet1* transcript levels are downregulated by neuronal activity either *in vitro*, when primary hippocampal neurons were incubated with KCl, resulting in cellular depolarization, or *in vivo*, in the dorsal CA1 subregion, after flurothyl-induced seizures or after fear conditioning (Kaas et al., 2013). All these approaches resulted in a significant reduction in *Tet1* mRNA levels compared to controls, while the transcripts of *Tet2* and *Tet3* did not consistently respond to stimulation using any of these activity-inducing paradigms. On the other hand, Yu and collaborators did not observe changes in *Tet1* (and *Tet2*) transcript levels when hippocampal neurons in culture were treated with bicuculline, a $GABA_A$ receptor antagonist commonly used to induce a robust increase in neuronal firing and synaptic activity, or with Tetrodotoxin (TTX), which decreases global synaptic activity (Yu et al., 2015). Additionally, TET1 KO mice exhibited normal basal synaptic transmission and presynaptic excitability in hippocampal slices (Kumar et al., 2015; Rudenko et al., 2013).

In terms of synaptic plasticity in the Schaffer collateral-CA1 pathway, it was observed that long-term depression (LTD) was significantly increased in the TET1 KO mouse (Rudenko et al., 2013), whereas hippocampal long-term potentiation (LTP) remained normal (Kumar et al., 2015; Rudenko et al., 2013). Considering that LTD is regulated by AMPA receptor trafficking and *Arc* modulates the trafficking of AMPA-type glutamate receptors (AMPARs) (Clem and Huganir, 2010; Liu and Cull-Candy, 2000), the observed down-regulation of *Arc* (Rudenko et al., 2013) may affect proper function of various components of LTD machinery. Additionally, previous studies demonstrated a connection between LTD and memory extinction (Dalton et al., 2008; Kim et al., 2011; Ryu et al., 2008; Tsetsenis et al., 2011). Additionally, overexpression of either the catalytic active or inactive forms of TET1 peptide did not lead to any significant effects in LTP either (Kumar et al., 2015). In terms of basal electrophysiology findings, *in vitro* work showed that *Tet1* knockdown (KD) in primary hippocampal neurons leads to increased miniature excitatory post-synaptic current (mEPSC) amplitudes (Yu et al., 2015).

The TET1 KO mouse model was used to unravel a potential connection between TET1 protein function and **behavior/cognitive processes**. In terms of learning and memory, there are conflicting results (Rudenko et al., 2013; Zhang et al., 2013). Zhang and colleagues addressed the putative involvement of TET1 in neural plasticity using hippocampal-dependent cognitive tasks, such as spatial memory (Broadbent et al., 2004). Both WT and TET1 KO mutants exhibited similar escape latency and swim path to the visible platform, suggesting comparable vision and motivation between the two groups. However, when short term memory retention was tested (24 h after the 5-day

training), the mutant group showed significant deficiency in reaching the virtual platform, measured by both the platform crossing and the time spent in the target quadrant, indicating that *Tet1* deficiency can lead to **impairment in spatial learning and short-term memory.** The brain structure was analyzed but no obvious morphological or developmental brain abnormalities were observed (Zhang et al., 2013), similarly to what was observed by other authors (Rudenko et al., 2013). Considering adult neurogenesis implication in spatial learning and memory, a potential link between memory impairment and the lack of TET1 was further explored. Using Nestin-GFP transgenic mice, the authors observed that, when TET1 was ablated in neural precursor cells, the number of GFP-positive cells in the subgranular zone of the hippocampal dentate gyrus (DG) in adult mice was dramatically reduced, by 45%, compared to WT animals (Zhang et al., 2013). Analysis of gene expression and methylation changes in TET1 KO mice revealed decreased expression of a cohort of genes involved in neurogenesis, including *Galanin* (*Gal*), *Ng2* (*Cspg4*) and *Neuroglobin* (*Ngb*). Methylation analysis using gene-specific bisulfite sequencing showed that the promoter regions of these genes were hypermethylated, suggesting that TET1 positively regulates adult neurogenesis through the oxidation of 5mC to 5hmC in these genes (Zhang et al., 2013).

In contrast to the results by Zhang and collaborators, Rudenko and colleagues reported normal short-term memory and spatial learning, but impaired memory extinction of both contextual fear memory and spatial reference memory (Rudenko et al., 2013). The authors observed normal locomotor behavior and no changes in anxiety and depressive-like behaviors, as well as no difference was also observed in contextual learning and cued fear memory acquisition. However, regarding memory extinction, the authors reported impaired memory extinction in TET1 KO mice, both after contextual fear conditioning and for hippocampus-dependent spatial reference memory, using the Morris water maze (MWM) test. Several neuronal activity-regulated genes were found to be downregulated, namely *Arc*, *Npas4* and *c-Fos*, in the cortex and hippocampus. Hypermethylation of the *Npas4* promoter region was observed in the cortex and in the hippocampus of both naïve TET1 KO mice and after extinction training. *Npas4* is a transcription factor highly expressed in the brain which regulates the formation and maintenance of inhibitory synapses in response to excitatory synaptic activity; it was shown to be a key regulator of transcriptional programs involving neural activity-regulated genes and essential for contextual memory formation and regulation of cognitive and social functions (Coutellier et al., 2012; Ramamoorthi et al., 2011).

These results might indicate independent epigenetic programs being activated during memory acquisition *versus* memory extinction. Nonetheless, the discrepancy between TET1 role in spatial learning and memory could also be explained by the differences in the TET1 KO mouse models, with distinct exons being targeted (exon 4 in the study by Rudenko et al., resulting in an unstable truncated form; and exons 11–13 in the study by Zhang et al., which are part of the catalytic domain). Moreover, no other learning and memory tasks were used beyond MWM in the study by Zhang and colleagues, whereas Rudenko and colleagues used Pavlovian fear conditioning showing that TET1 mutant mice have normal memory acquisition.

Additionally, a curious finding was the observation of memory enhancement in TET1 KO animals, namely threat recognition learning, long-term memory and remote memory consolidation (Kumar et al., 2015). Consistent with a previous study (Rudenko et al., 2013), this group found normal threat memory acquisition and short-term fear memory in TET1 KO mice. However, an enhancement in memory consolidation and long-term storage was observed in TET1 KO, using contextual and cued fear conditioning tests. These are apparent opposing results when compared with Zhang and colleagues work, which showed an impairment in spatial learning (Zhang et al., 2013). Kumar and colleagues suggested that these might be attributed to the behavior test used since MWM and fear conditioning are both hippocampal-dependent tasks, but MWM may involve stronger and more aversive motivational factors than fear conditioning and occurs over many more training trials of longer duration (Kumar et al., 2015). These differences might account for differential susceptibilities to effects of TET1 knockout in the water maze *versus* fear conditioning behavioral tests.

Using a virally mediated knockdown of *Tet1* mRNA in the dorsal hippocampus, they also observed an enhancement in hippocampus-dependent long-term spatial memory for object location (Kumar et al., 2015). Zhang and colleagues reported that TET1 KO impairs hippocampal-dependent spatial short-term memory, using the MWM test (Zhang et al., 2013). Hence, distinct roles for TET1 in different memory types can explain these differences. At the molecular level, Kumar and colleagues also found that TET1 ablation resulted in altered expression of numerous neuronal activity-regulated genes, such as increased expression of *Bdnf* and decreased levels of *Arc*, *Fos* and *Npas4*, as previously observed by others (Rudenko et al., 2013). Interestingly, a compensatory upregulation of *Tet2* and *Tet3* was reported, together with increased transcript levels of other genes involved in the active DNA demethylation pathway, such as *Gadd45b*, *Smug*, *Apobec1* and *Tdg*. Intriguingly, a strong upregulation was also observed for DNA methyltransferases *Dnmt1*, *Dnmt3a* and *Dnmt3b*, suggesting coordination of the epigenetic regulators transcriptional network in the CNS (Kumar et al., 2015).

In addition to loss-of-function studies, the discovery that TET1 expression is downregulated in the dorsal CA1 of mice after fear learning motivated gain-of-function studies: TET1 overexpression (OE) in the dorsal hippocampus did not affect exploratory or anxiety-like behavior but impaired long-term, but not short-term, memory in the contextual fear conditioning (CFC) test (Kaas et al., 2013). This deficit in long-term memory formation was observed for both catalytically active and inactive forms of TET1, suggesting that TET1's role in memory formation is independent of its catalytic activity but may rely on an allosteric mechanism and contribute to explain non-redundancy between TET enzymes. Importantly, the authors found the same set of genes (*Fos*, *Nr4a2*, *Bdnf*, *Homer1*) upregulated by overexpression of TET1 and TET1m, suggesting that TET1 regulates the expression of these genes, at least in part independently of 5mC to 5hmC conversion, and that these genes might be responsible for the observed memory dysfunction. Another gain-of-function study has shown that overexpression of either the catalytically active or the catalytically inactive TET1 peptide did not lead to any significant effect on LTP compared with control, and basal synaptic transmission also remained constant (Kumar et al., 2015).

Additionally, TET1 overexpression, but not TET1m, led to an increase in 5hmC levels in the microdissected CA1 area, concomitant with a decrease in global 5mC levels, suggesting an increase in global 5mC to 5hmC conversion (Kaas et al., 2013). Furthermore, TET1 OE resulted in upregulation of many neuronal activity-related genes such as *c-Fos*, *Bdnf*, *Arc*, *Egr1* (Kaas et al., 2013), whereas TET1 KO resulted in downregulation of some of these genes (Rudenko et al., 2013). Therefore, considering the downregulation of Immediate Early Genes (IEGs) in TET1 KO mice and their upregulation in TET1 OE in hippocampal regions, these studies suggest that *Tet1* bidirectionally regulates IEGs levels. Similarly, Guo and collaborators performed overexpression of TET1, and TET1m, in the adult mouse dentate gyrus and observed that OE of TET1, but not TET1m, led to an increase in the levels of 5hmC by 43% (Guo et al., 2011). Concerning methylation levels at specific neuronal-genes, namely *Bdnf* and *Fgf1*, the authors reported that overexpression of TET1, but not TET1m, led to significant decreases in CpG methylation levels at promoter IX of *Bdnf* and brain-specific promoter of *Fgf1*. On the other hand, *Tet1* knockdown in the adult dentate gyrus completely abolished electroconvulsive stimulation (ECS)-induced demethylation of both *Bdnf*IX and *Fgf1B*, suggesting that *Tet1* is required for neuronal activity-induced, region-specific, active DNA demethylation and gene expression in the adult brain (Guo et al., 2011).

Together, these findings support that TET1 contributes to basal neuronal 5hmC levels, and this interferes with the regulation of

important neuronal regulatory genes. However, the behavioral effects of TET1 should still motivate further investigation, considering the discrepant results in short-term memory and spatial learning.

2.2. TET2

TET2 is the least characterized TET enzyme member in the brain, despite its high level of expression (Szwagierczak et al., 2010). Whilst brain defects have not been described in TET2 KO mouse model (Ko et al., 2011; Li et al., 2011), a behavioral characterization was missing.

Regarding **neurophysiology**, *in vitro* studies using hippocampal neurons did not show changes in *Tet2* mRNA levels after global synaptic activity increase or decrease, induced by bicuculline or tetrodotoxin, respectively. However, association of this enzyme with **basal** synaptic transmission has been observed since hippocampal neurons with decreased *Tet2* expression exhibited increased mEPSC, similarly to what was observed in *Tet1* KD (Yu et al., 2015).

Additionally, a role for TET2 in neurogenesis was firstly proposed by Hahn and collaborators, as the double knockdown of *Tet2* and *Tet3* in the mouse embryonic cortex led to defects in the differentiation of the cells migrating from the subventricular zone to the cortical plate (Hahn et al., 2013). More recently, another work using a TET2 KO mouse model showed that depletion of TET2 leads to increased adult neural stem cell proliferation, but reduced differentiation capacity *in vitro* and *in vivo* (Li et al., 2017). Mechanistically, the authors show that *Tet2* physically interacts with forkhead box O3 (*Foxoa3*) and regulates expression of genes related to neural stem cell proliferation. *Foxoa3* is a mammalian forkhead family member, well known to regulate gene expression and help preserve an intact pool of neural stem cells, at least in part by negatively regulating neuronal differentiation (Rafalski and Brunet, 2011). To overcome the limitations of a constitutive full knockout model, a more recent work used a conditional model ablating *Tet2* in adult Neural Precursor Cells (NPCs) and demonstrated that the specific deletion of this enzyme in adult NPCs is sufficient to impair the neurogenic process, translated by a significant decrease in the number of Doublecortin (Dcx)-positive newly-born neurons, Bromodeoxyuridne (BrdU)-positive cells and BrdU/NeuN-positive mature differentiated neurons (Gontier et al., 2018). The authors also observed that decreased levels of *Tet2* expression, achieved by shRNA injection in the hippocampal neurogenic niche, resulted in a significant decrease in the number of NPCs and newly-born neurons, as observed by conditional deletion in NPCs.

Additionally, for the first time, a **behavioral** evaluation was performed, showing that reducing *Tet2* levels in the hippocampus impairs cognitive function, namely hippocampal-dependent learning and memory which were assessed using radial arm water maze (RAWM) and contextual fear-conditioning (CFC) paradigms (Gontier et al., 2018). Both the animals presenting a global abrogation of TET2 in the Dentate Gyrus (known as the adult hippocampal neurogenic niche) and mice carrying a conditional deletion of TET2 in adult NPCs showed worse performance in finding the platform location during both short-term and long-term learning and memory probes. When measuring the freezing time after fear conditioning training, both TET2 ablation models showed decreased freezing time during contextual, but not cued, memory testing. Thus, TET2 decreased levels in the adult neurogenic niche or specifically in adult NPCs resulted in impaired long-term hippocampal-dependent spatial learning and memory and associative fear memory acquisition. Interestingly, the authors also observed that restoration of TET2 levels in the aged brain was sufficient to rescue age-related regenerative decline as observed by the increased number of NPCs and newly-born neurons, the similar learning capacity in RAWM performance and an increased freezing time during contextual memory test when comparing animals under this rescue with the control group (Gontier et al., 2018). These findings suggest an important role for TET2 in the regulation of neurogenesis and cognitive functions, and a key molecular mediator of neurogenic rejuvenation.

2.3. TET3

The most highly expressed TET enzyme member in the brain, TET3, was also described as an essential enzyme in neuronal differentiation, including maintenance of NPCs *in vitro* (Li et al., 2015) and *in vivo* during early neocortical development (Lv et al., 2014).

Regarding **neurophysiology**, TET3 was described as a synaptic activity sensor, since TET3 levels are sensible to neuronal activity, and this enzyme reacts to it, mediating homeostatic synaptic transmission (Yu et al., 2015). Synaptic activity bi-directionally regulates neuronal *Tet3* expression, and consequently *Tet3* controls glutamatergic synaptic transmission through regulation of target genes, namely glutamate receptor 1 (*GluR1*) levels (Yu et al., 2015). Neurons with *Tet3* knockdown exhibited substantially larger miniature glutamatergic excitatory post-synaptic current (mEPSC) amplitudes whereas *Tet3* overexpression decreased this parameter. It should be noted that although both *Tet1* and *Tet2* knockdowns also increase mEPSC amplitudes, the effects are less pronounced. Furthermore, when DNA demethylation was inhibited through the blocking of the two major components of the BER pathway, the poly (ADP-ribose) polymerase or the apurinic/apyrimidinic endonuclease, the mEPSC amplitudes were also increased, resembling the *Tet3* KD (Yu et al., 2015). These results suggest that excitatory synaptic transmission in neurons is regulated through DNA oxidation *via* TET and, subsequently, BER.

Additionally, it was shown that *Tet3* is required for homeostatic synaptic plasticity. Both *Tet3* KD and BER inhibition elevated mEPSC amplitudes linearly across the spectrum under basal conditions, which was comparable to the scaling-up effect induced by TTX treatment in normal neurons. Thus, downregulation of *Tet3* signaling appears to be sufficient to induce scaling-up. On the other hand, neurons over-expressing *Tet3* exhibited reduced mEPSC amplitudes linearly across the spectrum, resembling bicuculline-induced scaling-down in normal neurons. Hence, the authors suggested that global synaptic activity modulates *Tet3* expression and DNA demethylation activity, which in turn mediate homeostatic synaptic scaling-up or scaling-down (Yu et al., 2015).

A key cellular mechanism regulating both basal glutamatergic synaptic transmission and homeostatic scaling is the control of surface levels of glutamate receptors. Yu and colleagues have shown that *Tet3* regulates basal excitatory synaptic transmission *via* regulating surface *GluR1* levels (Yu et al., 2015). Also, *Tet3* knockdown was sufficient to elevate surface *GluR1* levels and prevented further changes induced by TTX or bicuculline treatments. Regulation of *Arc* levels appears to explain changes in surface *GluR1* levels following *Tet3* KD. Together, these results suggest that *Tet3* and active DNA demethylation signaling respond to changes in global synaptic activity to re-establish a responsive cellular state. Moreover, transcriptome analysis of *Tet3*-KD neurons revealed differential expression of genes involved in the synapse and synaptic transmission, suggesting an essential role for *Tet3* in regulating gene expression in response to changes in global synaptic activity. *Bdnf*, already described as undergoing active demethylation in depolarized neurons (Ma et al., 2009) and implicated in synaptic transmission and synaptic scaling (Rutherford et al., 1998), was hypermethylated at the promoter IV region in *Tet3* KD neurons, with a consequent decrease in its expression. Interestingly, whereas *Tet1*-deficient neurons exhibited hypermethylation at *Arc* and *Npas4* promoters (Rudenko et al., 2013), Tet3-KD neurons did not. No changes in methylation were observed at the *Arc* or *Npas4* promoter regions, suggesting that activity-induced expression of immediate early genes *Arc* and *Npas4* is mediated by the oxidative function of TET1, but not of TET3. A physical interaction between TET3 and *Bdnf IV* promoter region was described by the authors in neurons, using chromatin immunoprecipitation (ChIP)-PCR analysis (Yu et al., 2015).

A more recent paper used CRISPR-Cas9 technology, termed 2-cell embryo-CRISPR-Cas9 injection (2CC), to induce *in vivo Tet3* loss-of-function and recorded AMPAR-mediated miniature **excitatory** post-

synaptic currents (mEPSCs) from layer 2/3 pyramidal neurons of the primary somatosensory cortex of P14 chimeric mice and from hippocampal CA1 neurons (Wang et al., 2017). The authors observed that *Tet3*-mutant neurons had a significantly higher mEPSC frequency and a similar mEPSC amplitude in layer 2/3 neurons whereas in the hippocampus both the frequency and amplitudes were significantly increased, suggesting an important role of endogenous *Tet3* in negatively regulating excitatory synaptic transmission in young mice. These findings corroborated Yu and colleagues *in vitro* studies reporting the role of TET3 in the downregulation of excitatory synaptic transmission. Bisulfite sequencing analyses revealed slightly increased CpG methylation at the *Bdnf* IV, IX and *Wfdc2* promoter regions, consistent with Yu and colleagues, but not on the *Npas4* promoter-exon 1 junction or the *Fgf1G* and *Ndst1* promoter regions. Additionally, loss of TET3 function significantly reduced both the frequency and amplitude of $GABA_AR$-mediated **inhibitory** synaptic transmission, as measured by miniature inhibitory post-synaptic currents (mIPSCs) in the cortical layers 2/3 pyramidal neurons and hippocampal CA1 region, suggesting a promoting role of endogenous *Tet3* in regulating inhibitory synaptic transmission as well (Wang et al., 2017).

In vivo **behavioral** studies correlated *Tet3* mRNA expression levels in the hippocampus with neuronal activity after Contextual Fear Conditioning (CFC) behavioral test. The authors observed that *Tet3* mRNA transcripts, but not *Tet1* and *Tet2*, were upregulated after 30 min and 3 h, but returned to baseline after 24 h (Kremer et al., 2018). Importantly, *Tet3* expression was not modified by cold swim stress suggesting that the changes were specific to memory formation in CFC and were not related to the stress response elicited by fear conditioning. When the NMDA (N-methyl-D-aspartate) receptors were activated in primary hippocampal neurons, *Tet3* mRNA levels were upregulated, suggesting that NMDA receptor signaling increases *Tet3* transcription. Expression levels of *mir-29b* were also altered, being downregulated, after NMDA receptors stimulation indicating another target of this glutamate receptor. Transcriptional analysis in hippocampus 30 min after training showed that synaptic plasticity and genes related with memory, such as *Notch1*, *Creb1*, *Crebbp* and *Gadd45b* are sensitive to TET3 upregulation (Kremer et al., 2018).

Li and collaborators described upregulation of *Tet3* transcript levels, but not *Tet1* as reported by others (Guo et al., 2011; Zhang et al., 2013), in primary cortical neurons after 7 h and 10 h of KCl-induced depolarization (Li et al., 2014). Consistently, *Tet3* was also upregulated in the infralimbic prefrontal cortex (ILPFC) after fear extinction training. Moreover, *Tet3* knockdown in the ILPFC resulted in normal fear memory acquisition but impairment in fear extinction memory (Li et al., 2014). Genome-wide analyses revealed that 16% of genes with 5hmC gain after fear extinction training were associated with synaptic signaling. One example was *Gephyrin* gene, which anchors GABA receptors to the postsynaptic membrane and is directly involved in fear extinction, showing a gain of 5hmC accompanied by a 5mC decrease within an intron, 24 h post-extinction training. An increase in *Gephyrin* mRNA transcripts was also observed transiently 2 h after extinction training, together with an increase in TET3 occupancy surrounding the *Gephyrin* gene, suggesting that DNA methylation can be dynamically regulated after learning. The effect of extinction learning on TET3 occupancy at the *Gephyrin* locus, as well as the dynamic changes in the accumulation of 5hmC and 5mC, G*ephyrin* mRNA and associated effects on the chromatin landscape were completely blocked in the presence of *Tet3* shRNA (Li et al., 2014). Together, these results suggest that *Tet3* activity within the ILPFC is necessary for the learning-dependent accumulation of 5hmC and related chromatin modifications, which underpins rapid behavioral adaptation.

Overall, these studies suggest that TET3 has an important role in fear extinction memory, probably through modulation of synaptic genes. However, it is still unclear if TET3 influences other cognitive behaviors, such as memory and learning, and what are the mechanisms underlying the neuronal activity, mediated by this enzyme.

3. Conclusions and future directions

Since all three TET enzymes are present in the mammalian brain and share the capacity of oxidizing 5mC into 5hmC, a putative intermediate in the DNA demethylation process, their functions could be assumed to be mostly redundant. However, recent publications describing different effects of each TET knockout or knockdown in the brain physiology and development, have stirred the debate. As we have comprehended from the above-mentioned works, loss or gain-of-function of each of these individual isoenzymes produced singular findings, suggesting non-redundant functions for TET enzymes in the brain. Indeed, TET1 was implicated in a wide range of specific behaviors, such as spatial and fear learning, short-term and object location memories. TET2 was shown as an unequivocal player in controlling short and long-term spatial learning, as well as memory processes. TET3 enzyme was identified as a key enzyme to regulate fear extinction memory. Altogether, these studies have demonstrated that TET deficiencies produce significant changes in neuronal function. This is probably due to the critical role of TET enzymes in regulation of the epigenetic state of key regulatory regions, such as promoters, of neuronal activity-associated genes and its consequence on the transcription levels and gene functions.

Further studies using double and triple TET KO models could help increase our knowledge on the relative contribution and potential cooperation of the different TET enzymes. Also, considering the dynamic nature of DNA modifications in the nervous system, a temporal perspective on TET mediated activity throughout life is mandatory. Importantly, so far many of the studies were performed using full TET KO. Therefore, some phenotypes may result from the developmental roles of TET enzymes rather than dysregulation of the function of mature neurons. In the future, the conditional ablation of TET proteins in specific cell types and considering the development stage is needed.

Despite recent advances, a full understanding of how epigenetic modifications regulate neuronal physiology, plasticity and cognitive functions is still a matter of debate and require further investigation. Particularly, it would be of utmost importance to generate conditional knockouts for each TET enzyme in specific areas of the brain or types of neurons, for example. Additionally, it would be interesting to knockout or knockdown TET enzymes in the brain of specific models of diseases affecting the CNS, in order to investigate the possible contribution of these epigenetic players in disease onset, progression or even possible therapeutics. One very important technical breakthrough is the possibility of performing epigenetic editing of the genome, using CRISPR/Cas system. This would be a promising tool to manipulate neurons *in vitro* or brain cells *in vivo*, trying to modulate brain cognitive processes related to depression, anxiety, amongst others, possibly leading to the production of new chemical compounds that could target epigenetic pathways, looking for novel treatments for brain dysfunction.

Conflict of interest

The authors declare that they have no conflict of interest.

Acknowledgments

We thank the reviewers for their constructive comments that significantly improved this review.

The authors also wish to thank Patrícia Monteiro and Jorge Diogo Silva (ICVS, University of Minho) for helpful comments after critical reading the manuscript. This work was supported by National Funds through Portuguese Foundation for Science and Technology (FCT) fellowships (PD/BD/106049/2015 to C.A., IF/01079/2014 to L.P. and IF/00047/2012 and CEECIND/00371/2017 to C.J.M); FCT project grant (PTDC/BIA-BCM/121276/2010) to C.J.M; EpiGeneSys Small Collaborative project to L.P.; BIAL Foundation Grant427/14 to L.P.; Northern Portugal Regional Operational Programme (NORTE 2020),

under the Portugal 2020 Partnership Agreement, through the European Regional Development Fund (FEDER; NORTE-01-0145-FEDER-000013); FEDER funds, through the Competitiveness Factors Operational Programme (COMPETE), and National Funds, through the FCT (POCI-01-0145-FEDER-007038).

References

Azpurua, J., Eaton, B.A., 2015. Neuronal epigenetics and the aging synapse. Front. Cell. Neurosci. 9 208-208.

Bird, A., 2002. DNA methylation patterns and epigenetic memory. Genes Dev. 16, 6–21.

Branco, M.R., Ficz, G., Reik, W., 2011. Uncovering the role of 5-hydroxymethylcytosine in the epigenome. Nat. Rev. Genet. 13, 7–13.

Broadbent, N.J., Squire, L.R., Clark, R.E., 2004. Spatial memory, recognition memory, and the hippocampus. Proc. Natl. Acad. Sci. U. S. A. 101, 14515–14520.

Cadena-del-Castillo, C., Valdes-Quezada, C., Carmona-Aldana, F., Arias, C., Bermudez-Rattoni, F., Recillas-Targa, F., 2014. Age-dependent increment of hydroxymethylation in the brain cortex in the triple-transgenic mouse model of Alzheimer's disease. J. Alzheimers Dis. 41, 845–854.

Campbell, R.R., Wood, M.A., 2019. How the epigenome integrates information and reshapes the synapse. Nat. Rev. Neurosci. 20, 133–147.

Clem, R.L., Huganir, R.L., 2010. Calcium-permeable AMPA receptor dynamics mediate fear memory erasure. Science (New York, N.Y.) 330, 1108–1112.

Coutellier, L., Beraki, S., Ardestani, P.M., Saw, N.L., Shamloo, M., 2012. Npas4: a neuronal transcription factor with a key role in social and cognitive functions relevant to developmental disorders. PLoS One 7, e46604.

Dalton, G.L., Wang, Y.T., Floresco, S.B., Phillips, A.G., 2008. Disruption of AMPA receptor endocytosis impairs the extinction, but not acquisition of learned fear. Neuropsychopharmacology 33, 2416–2426.

Day, J.J., Sweatt, J.D., 2011. Epigenetic mechanisms in cognition. Neuron 70, 813–829.

Deaton, A.M., Bird, A., 2011. CpG islands and the regulation of transcription. Genes Dev. 25, 1010–1022.

Fasolino, M., Welsh, S.A., Zhou, Z., 2017. Chapter 4 – TET and 5hmC in neurodevelopment and the adult brain. In: Bredy, T.W. (Ed.), DNA Modifications in the Brain. Academic Press, San Diego, pp. 61–79.

Globisch, D., Munzel, M., Muller, M., Michalakis, S., Wagner, M., Koch, S., Bruckl, T., Biel, M., Carell, T., 2010. Tissue distribution of 5-hydroxymethylcytosine and search for active demethylation intermediates. PLoS One 5, 0015367.

Gontier, G., Iyer, M., Shea, J.M., Bieri, G., Wheatley, E.G., Ramalho-Santos, M., Villeda, S.A., 2018. Tet2 rescues age-related regenerative decline and enhances cognitive function in the adult mouse brain. Cell Rep. 22, 1974–1981.

Guo, J.U., Su, Y., Zhong, C., Ming, G.L., Song, H., 2011. Hydroxylation of 5-methylcytosine by TET1 promotes active DNA demethylation in the adult brain. Cell 145, 423–434.

Guo, J.U., Su, Y., Shin, J.H., Shin, J., Li, H., Xie, B., Zhong, C., Hu, S., Le, T., Fan, G., Zhu, H., Chang, Q., Gao, Y., Ming, G.L., Song, H., 2014. Distribution, recognition and regulation of non-CpG methylation in the adult mammalian brain. Nat. Neurosci. 17, 215–222.

Hahn, M.A., Qiu, R., Wu, X., Li, A.X., Zhang, H., Wang, J., Jui, J., Jin, S.G., Jiang, Y., Pfeifer, G.P., Lu, Q., 2013. Dynamics of 5-hydroxymethylcytosine and chromatin marks in Mammalian neurogenesis. Cell Rep. 3, 291–300.

Ito, S., D'Alessio, A.C., Taranova, O.V., Hong, K., Sowers, L.C., Zhang, Y., 2010. Role of Tet proteins in 5mC to 5hmC conversion, ES-cell self-renewal and inner cell mass specification. Nature 466, 1129–1133.

Ito, S., Shen, L., Dai, Q., Wu, S.C., Collins, L.B., Swenberg, J.A., He, C., Zhang, Y., 2011. Tet proteins can convert 5-methylcytosine to 5-formylcytosine and 5-carboxylcytosine. Science (New York, N.Y.) 333, 1300–1303.

Kaas, G.A., Zhong, C., Eason, D.E., Ross, D.L., Vachhani, R.V., Ming, G.L., King, J.R., Song, H., Sweatt, J.D., 2013. TET1 controls CNS 5-methylcytosine hydroxylation, active DNA demethylation, gene transcription, and memory formation. Neuron 79, 1086–1093.

Kawasaki, F., Beraldi, D., Hardisty, R.E., McInroy, G.R., van Delft, P., Balasubramanian, S., 2017. Genome-wide mapping of 5-hydroxymethyluracil in the eukaryote parasite Leishmania. Genome Biol. 18 23-23.

Kim, J.I., Lee, H.R., Sim, S.E., Baek, J., Yu, N.K., Choi, J.H., Ko, H.G., Lee, Y.S., Park, S.W., Kwak, C., Ahn, S.J., Choi, S.Y., Kim, H., Kim, K.H., Backx, P.H., Bradley, C.A., Kim, E., Jang, D.J., Lee, K., Kim, S.J., Zhuo, M., Collingridge, G.L., Kaang, B.K., 2011. PI3Kgamma is required for NMDA receptor-dependent long-term depression and behavioral flexibility. Nat. Neurosci. 14, 1447–1454.

Ko, M., Bandukwala, H.S., An, J., Lamperti, E.D., Thompson, E.C., Hastie, R., Tsangaratou, A., Rajewsky, K., Koralov, S.B., Rao, A., 2011. Ten-Eleven-Translocation 2 (TET2) negatively regulates homeostasis and differentiation of hematopoietic stem cells in mice. Proc. Natl. Acad. Sci. U. S. A. 108, 14566–14571.

Ko, M., An, J., Bandukwala, H.S., Chavez, L., Äijö, T., Pastor, W.A., Segal, M.F., Li, H., Koh, K.P., Lähdesmäki, H., Hogan, P.G., Aravind, L., Rao, A., 2013. Modulation of TET2 expression and 5-methylcytosine oxidation by the CXXC domain protein IDAX. Nature 497, 122–126.

Kohli, R.M., Zhang, Y., 2013. TET enzymes, TDG and the dynamics of DNA demethylation. Nature 502, 472–479.

Kremer, E.A., Gaur, N., Lee, M.A., Engmann, O., Bohacek, J., Mansuy, I.M., 2018. Interplay between TETs and microRNAs in the adult brain for memory formation. Sci. Rep. 8, 1678.

Kriaucionis, S., Heintz, N., 2009. The nuclear DNA base 5-hydroxymethylcytosine is present in Purkinje neurons and the brain. Science (New York, N.Y.) 324, 929–930.

Kumar, D., Aggarwal, M., Kaas, G.A., Lewis, J., Wang, J., Ross, D.L., Zhong, C., Kennedy, A., Song, H., Sweatt, J.D., 2015. Tet1 oxidase regulates neuronal gene transcription, active DNA hydroxy-methylation, object location memory, and threat recognition memory. Neuroepigenetics 4, 12–27.

Li, Z., Cai, X., Cai, C.L., Wang, J., Zhang, W., Petersen, B.E., Yang, F.C., Xu, M., 2011. Deletion of Tet2 in mice leads to dysregulated hematopoietic stem cells and subsequent development of myeloid malignancies. Blood 118, 4509–4518.

Li, X., Wei, W., Zhao, Q.Y., Widagdo, J., Baker-Andresen, D., Flavell, C.R., D'Alessio, A., Zhang, Y., Bredy, T.W., 2014. Neocortical Tet3-mediated accumulation of 5-hydroxymethylcytosine promotes rapid behavioral adaptation. Proc. Natl. Acad. Sci. U. S. A. 111, 7120–7125.

Li, T., Yang, D., Li, J., Tang, Y., Yang, J., Le, W., 2015. Critical role of Tet3 in neural progenitor cell maintenance and terminal differentiation. Mol. Neurobiol. 51, 142–154.

Li, X., Yue, X., Pastor, W.A., Lin, L., Georges, R., Chavez, L., Evans, S.M., Rao, A., 2016. Tet proteins influence the balance between neuroectodermal and mesodermal fate choice by inhibiting Wnt signaling. Proc. Natl. Acad. Sci. U. S. A. 113, E8267–E8276.

Li, X., Yao, B., Chen, L., Kang, Y., Li, Y., Cheng, Y., Li, L., Lin, L., Wang, Z., Wang, M., Pan, F., Dai, Q., Zhang, W., Wu, H., Shu, Q., Qin, Z., He, C., Xu, M., Jin, P., 2017. Ten-eleven translocation 2 interacts with forkhead box O3 and regulates adult neurogenesis. Nat. Commun. 8, 15903.

Liu, S.Q., Cull-Candy, S.G., 2000. Synaptic activity at calcium-permeable AMPA receptors induces a switch in receptor subtype. Nature 405, 454–458.

Liu, S., Wang, J., Su, Y., Guerrero, C., Zeng, Y., Mitra, D., Brooks, P.J., Fisher, D.E., Song, H., Wang, Y., 2013. Quantitative assessment of Tet-induced oxidation products of 5-methylcytosine in cellular and tissue DNA. Nucleic Acids Res. 41, 6421–6429.

Long, H.K., Blackledge, N.P., Klose, R.J., 2013. ZF-CxxC domain-containing proteins, CpG islands and the chromatin connection. Biochem. Soc. Trans. 41, 727–740.

Lv, X., Jiang, H., Liu, Y., Lei, X., Jiao, J., 2014. MicroRNA-15b promotes neurogenesis and inhibits neural progenitor proliferation by directly repressing TET3 during early neocortical development. EMBO Rep. 15, 1305–1314.

Ma, D.K., Jang, M.-H., Guo, J.U., Kitabatake, Y., Chang, M.-l., Pow-anpongkul, N., Flavell, R.A., Lu, B., Ming, G.-l., Song, H., 2009. Neuronal activity–induced Gadd45b promotes epigenetic DNA demethylation and adult neurogenesis. Science (New York, N.Y.) 323, 1074–1077.

Mi, Y., Gao, X., Dai, J., Ma, Y., Xu, L., Jin, W., 2015. A novel function of TET2 in CNS: sustaining neuronal survival. Int. J. Mol. Sci. 16, 21846–21857.

Munzel, M., Globisch, D., Bruckl, T., Wagner, M., Welzmiller, V., Michalakis, S., Muller, M., Biel, M., Carell, T., 2010. Quantification of the sixth DNA base hydroxymethylcytosine in the brain. Angew. Chem. Int. Ed. Engl. 49, 5375–5377.

Pastor, W.A., Aravind, L., Rao, A., 2013. TETonic shift: biological roles of TET proteins in DNA demethylation and transcription. Nat. Rev. Mol. Cell Biol. 14, 341–356.

Pfaffeneder, T., Spada, F., Wagner, M., Brandmayr, C., Laube, S.K., Eisen, D., Truss, M., Steinbacher, J., Hackner, B., Kotljarova, O., Schuermann, D., Michalakis, S., Kosmatchev, O., Schiesser, S., Steigenberger, B., Raddaoui, N., Kashiwazaki, G., Muller, U., Spruijt, C.G., Vermeulen, M., Leonhardt, H., Schar, P., Muller, M., Carell, T., 2014. Tet oxidizes thymine to 5-hydroxymethyluracil in mouse embryonic stem cell DNA. Nat. Chem. Biol. 10, 574–581.

Rafalski, V.A., Brunet, A., 2011. Energy metabolism in adult neural stem cell fate. Prog. Neurobiol. 93, 182–203.

Ramamoorthi, K., Fropf, R., Belfort, G.M., Fitzmaurice, H.L., McKinney, R.M., Neve, R.L., Otto, T., Lin, Y., 2011. Npas4 regulates a transcriptional program in CA3 required for contextual memory formation. Science (New York, N.Y.) 334, 1669–1675.

Rudenko, A., Dawlaty, M.M., Seo, J., Cheng, A.W., Meng, J., Le, T., Faull, K.F., Jaenisch, R., Tsai, L.H., 2013. Tet1 is critical for neuronal activity-regulated gene expression and memory extinction. Neuron 79, 1109–1122.

Rutherford, L.C., Nelson, S.B., Turrigiano, G.G., 1998. BDNF has opposite effects on the quantal amplitude of pyramidal neuron and interneuron excitatory synapses. Neuron 21, 521–530.

Ryu, J., Futai, K., Feliu, M., Weinberg, R., Sheng, M., 2008. Constitutively active Rap2 transgenic mice display fewer dendritic spines, reduced extracellular signal-regulated kinase signaling, enhanced long-term depression, and impaired spatial learning and fear extinction. J. Neurosci. 28, 8178–8188.

Shin, J., Ming, G.-l., Song, H., 2014. DNA modifications in the mammalian brain. Philos. Trans. Biol. Sci. 369, 20130512.

Smith, Z.D., Meissner, A., 2013. DNA methylation: roles in mammalian development. Nat. Rev. Genetics 14, 204–220.

Song, C.X., Szulwach, K.E., Fu, Y., Dai, Q., Yi, C., Li, X., Li, Y., Chen, C.H., Zhang, W., Jian, X., Wang, J., Zhang, L., Looney, T.J., Zhang, B., Godley, L.A., Hicks, L.M., Lahn, B.T., Jin, P., He, C., 2011. Selective chemical labeling reveals the genome-wide distribution of 5-hydroxymethylcytosine. Nat. Biotechnol. 29, 68–72.

Sweatt, J.D., 2013. The emerging field of neuroepigenetics. Neuron 80, 624–632.

Szulwach, K.E., Li, X., Li, Y., Song, C.-X., Wu, H., Dai, Q., Irier, H., Upadhyay, A.K., Gearing, M., Levey, A.I., Vasanthakumar, A., Godley, L.A., Chang, Q., Cheng, X., He, C., Jin, P., 2011. 5-hmC-mediated epigenetic dynamics during postnatal neurodevelopment and aging. Nat. Neurosci. 14, 1607–1616.

Szwagierczak, A., Bultmann, S., Schmidt, C.S., Spada, F., Leonhardt, H., 2010. Sensitive enzymatic quantification of 5-hydroxymethylcytosine in genomic DNA. Nucleic Acids Res. 38, e181.

Tahiliani, M., Koh, K.P., Shen, Y., Pastor, W.A., Bandukwala, H., Brudno, Y., Agarwal, S., Iyer, L.M., Liu, D.R., Aravind, L., Rao, A., 2009. Conversion of 5-methylcytosine to 5-Hydroxymethylcytosine in mammalian DNA by MLL partner TET1. Science (New York, N.Y.) 324, 930–935.

Tsetsenis, T., Younts, T.J., Chiu, C.Q., Kaeser, P.S., Castillo, P.E., Sudhof, T.C., 2011. Rab3B protein is required for long-term depression of hippocampal inhibitory

synapses and for normal reversal learning. Proc. Natl. Acad Sci. U. S. A. 108, 14300–14305.
Wang, L., Li, M.Y., Qu, C., Miao, W.Y., Yin, Q., Liao, J., Cao, H.T., Huang, M., Wang, K., Zuo, E., Peng, G., Zhang, S.X., Chen, G., Li, Q., Tang, K., Yu, Q., Li, Z., Wong, C.C., Xu, G., Jing, N., Yu, X., Li, J., 2017. CRISPR-Cas9-mediated genome editing in one blastomere of two-cell embryos reveals a novel Tet3 function in regulating neocortical development. Cell Res. 27, 815–829.
Williams, K., Christensen, J., Pedersen, M.T., Johansen, J.V., Cloos, P.A.C., Rappsilber, J., Helin, K., 2011. TET1 and hydroxymethylcytosine in transcription and DNA methylation fidelity. Nature 473, 343.
Wu, H., D'Alessio, A.C., Ito, S., Xia, K., Wang, Z., Cui, K., Zhao, K., Sun, Y.E., Zhang, Y., 2011. Dual functions of Tet1 in transcriptional regulation in mouse embryonic stem cells. Nature 473, 389–393.
Xu, Y., Wu, F., Tan, L., Kong, L., Xiong, L., Deng, J., Barbera, A.J., Zheng, L., Zhang, H., Huang, S., Min, J., Nicholson, T., Chen, T., Xu, G., Shi, Y., Zhang, K., Shi, Y.G., 2011. Genome-wide regulation of 5hmC, 5mC, and gene expression by Tet1 hydroxylase in mouse embryonic stem cells. Mol. Cell 42, 451–464.
Xu, Y., Xu, C., Kato, A., Tempel, W., Abreu, J.G., Bian, C., Hu, Y., Hu, D., Zhao, B., Cerovina, T., Diao, J., Wu, F., He, H.H., Cui, Q., Clark, E., Ma, C., Barbara, A., Veenstra, G.J., Xu, G., Kaiser, U.B., Liu, X.S., Sugrue, S.P., He, X., Min, J., Kato, Y., Shi, Y.G., 2012. Tet3 CXXC domain and dioxygenase activity cooperatively regulate key genes for Xenopus eye and neural development. Cell 151, 1200–1213.
Yu, H., Su, Y., Shin, J., Zhong, C., Guo, J.U., Weng, Y.L., Gao, F., Geschwind, D.H., Coppola, G., Ming, G.L., Song, H., 2015. Tet3 regulates synaptic transmission and homeostatic plasticity via DNA oxidation and repair. Nat. Neurosci. 18, 836–843.
Zhang, H., Zhang, X., Clark, E., Mulcahey, M., Huang, S., Shi, Y.G., 2010. TET1 is a DNA-binding protein that modulates DNA methylation and gene transcription via hydroxylation of 5-methylcytosine. Cell Res. 20, 1390–1393.
Zhang, R.R., Cui, Q.Y., Murai, K., Lim, Y.C., Smith, Z.D., Jin, S., Ye, P., Rosa, L., Lee, Y.K., Wu, H.P., Liu, W., Xu, Z.M., Yang, L., Ding, Y.Q., Tang, F., Meissner, A., Ding, C., Shi, Y., Xu, G.L., 2013. Tet1 regulates adult hippocampal neurogenesis and cognition. Cell Stem Cell 13, 237–245.
Zhao, X., Dai, J., Ma, Y., Mi, Y., Cui, D., Ju, G., Macklin, W.B., Jin, W., 2014. Dynamics of ten-eleven translocation hydroxylase family proteins and 5-hydroxymethylcytosine in oligodendrocyte differentiation. Glia 62, 914–926.

REPÚBLICA PORTUGUESA | AGRICULTURA, FLORESTAS E DESENVOLVIMENTO RURAL

dgav Direção Geral de Alimentação e Veterinária

Ex ma Senhora
Doutora Magda João Castelhano Carlos
Escola de Medicina/ Instituto de Investigação em Ciências da Vida e Saúde
Campus de Gualtar
4710 – 057 BRAGA - P

2017-03-01 007902

Nossa referência	Vossa referência	Vossa data
0421/000/000 /2017		

Assunto: **PROTEÇÃO DOS ANIMAIS UTILIZADOS PARA FINS EXPERIMENTAIS E/OU OUTROS FINS CIENTÍFICOS – PEDIDO DE AUTORIZAÇÃO PARA REALIZAÇÃO DE PROJECTO DE EXPERIMENTAÇÃO ANIMAL**

Na sequência do pedido efetuado por V. Exª no sentido de poder ser autorizada a realização do projeto experimental designado **"Mecanismos epigenéticos na cognição e comportamento"**, tendo como investigadoras responsáveis as Doutoras Luísa Pinto e Cristina Joana Moreira Marques, cabe-me informar que o mesmo foi avaliado de acordo com o Artigo 44º do Decreto-Lei nº 113/2013, de 7 de Agosto, relativo à "proteção dos animais utilizados para fins científicos".

Mais se informa V. Exª que o projeto em apreço recebeu uma **avaliação favorável** e foi **autorizado** de acordo com o nº 1, do Artigo 42º do mesmo diploma legislativo.

Para além disso, e dado existir uma classificação prospetiva de que os procedimentos a realizar aos animais se expressem em severidade incluída na categoria **Ligeiro**, é primordial fazer-se, no decorrer do projeto, uma adequada monitorização dos sinais de dor, sofrimento ou angústia dos animais envolvidos, por forma a poder fazer-se uma atualização sobre o nível de dor efetiva a que os mesmos possam ficar sujeitos, nomeadamente, se os animais poderão vir a demonstrar sofrimento enquadrável nas categorias Moderado ou Severo, o que, neste último caso, a acontecer, implicará a sujeição do projeto a uma avaliação retrospetiva de acordo com o artigo nº 45º do diploma legislativo atrás mencionado.

Finalmente, resta-me especificar, de acordo com o discriminado no nº 2, do Artigo 46º, do atrás referido Decreto-Lei, o seguinte:

- **O utilizador que realiza o projeto:** Senhor Diretor do Instituto de Investigação em Ciências da Vida e Saúde, da Escola de Ciências da Saúde, da Universidade do Minho;
- **A pessoa responsável pela execução global do projeto e pela sua conformidade com a autorização do mesmo:** Doutoras Luísa Pinto e Cristina Joana Moreira Marques;
- **O estabelecimento onde o projeto vai ser realizado:** Estabelecimento de utilização de animais (pequenos roedores), do IICVS, da Escola de Medicina, da Universidade do Minho;

Com os melhores cumprimentos,

P/O Diretor Geral

Fernando Bernardo

Graça Mariano
Subdiretora Geral

DBEA/APM